




5-2010

Systems Biology Approach to Identifying Host Interactive Pathways Modulating the Severity of Streptococcal Sepsis

Nourtan Fatty Abdeltawab
University of Tennessee Health Science Center

Follow this and additional works at: <https://dc.uthsc.edu/dissertations>

 Part of the [Biological Phenomena, Cell Phenomena, and Immunity Commons](#), [Genetic Processes Commons](#), and the [Medical Genetics Commons](#)

Recommended Citation

Abdeltawab, Nourtan Fatty , "Systems Biology Approach to Identifying Host Interactive Pathways Modulating the Severity of Streptococcal Sepsis" (2010). *Theses and Dissertations (ETD)*. Paper 5. <http://dx.doi.org/10.21007/etd.cghs.2010.0003>.

This Dissertation is brought to you for free and open access by the College of Graduate Health Sciences at UTHSC Digital Commons. It has been accepted for inclusion in Theses and Dissertations (ETD) by an authorized administrator of UTHSC Digital Commons. For more information, please contact jwelch30@uthsc.edu.

Systems Biology Approach to Identifying Host Interactive Pathways Modulating the Severity of Streptococcal Sepsis

Document Type

Dissertation

Degree Name

Doctor of Philosophy (Medical Science)

Program

Biological Science

Track

Genetics, Functional Genomics and Proteomics

Research Advisor

Malak Y. S. Kotb, Ph.D.

Committee

Linda M. Hendershot, Ph.D. Tony N. Marion, Ph.D. David R. Nelson, Ph.D. Robert W. Williams, Ph.D.

DOI

10.21007/etd.cghs.2010.0003

Comments

Two year embargo expired May 2012.

**SYSTEMS BIOLOGY APPROACH TO IDENTIFYING HOST INTERACTIVE
PATHWAYS MODULATING THE SEVERITY OF STREPTOCOCCAL SEPSIS**

A Dissertation
Presented for
The Graduate Studies Council
The University of Tennessee
Health Science Center

In Partial Fulfillment
Of the Requirements for the Degree
Doctor of Philosophy
From The University of Tennessee

By
Nourtan Fathy Abdeltawab
May 2010

Chapter 2 © 2007 by the Nature Publishing Group.
Chapter 3 © 2008 by Public Library of Science.
All other materials © 2010 by Nourtan Fathy Abdeltawab.
All rights reserved.

DEDICATION

To all my teachers, to whom I am forever indebted to, starting with my parents, and to my dissertation readers, I wish you would enjoy it as much as I did.

ACKNOWLEDGMENTS

I am grateful to everyone who helped me in the process of achieving my Ph.D. degree. To start with, I would like to express my deep gratitude to Dr. Malak Kotb, who is not only my mentor; but also a dear friend who I am privileged to have. I have enjoyed my journey in her laboratory with all its ups and downs. I cannot thank her enough for her heartfelt dedication as a mentor that was fundamental to my scientific development and maturation. I am forever grateful for her everlasting support; she has taught me priceless lessons in my scientific and social life.

I would like to thank my committee members; each and every member has been crucial towards my scientific development. Their critiques and suggestions towards better dissecting the mechanisms of the studied sepsis model have been tremendously constructive. I would like to especially thank Dr. Robert Williams and his research team with whom I enjoyed working closely as a collaborating student throughout my Ph.D. research project.

I would like to extend a special thanks to Dr. Kotb's research team, present and previous members, as with the extensive animal experiments done in this dissertation, I could not have ever done it on my own. While working with Dr. Kotb laboratory members, I have learned something valuable from each and every one of them. I would like to thank all my co-authors on my publications. I would like to extend a special thanks to Dr. William Taylor for sharing his experience with me during my gene expression analysis studies. I am forever grateful to Dr. Yan Jiao for our various collaboration studies that will result in multiple manuscripts to be soon published.

On a personal level, I would like to thank all my friends along this journey. There are too many to mention everyone, they all have been very supportive. I would like to especially thank Mrs. Sarah Rowe Hasty, who has been a great asset to my success; she is a living example of sincerity and devotion. She is a genuinely dedicated scientist that I enjoyed learning from and working with. I will always cherish the time we spent together whether in the lab or outside it, as she has been a wonderful second mother to me.

Words cannot express enough my deep gratefulness to my parents, my father, Prof. Dr. Fathy M. Abdeltawab and my mother, Prof. Dr. Maie F. Ali. They have been tremendously supportive throughout my Ph.D. journey. Last but not least, I would like to thank my brother, Amr and his beautiful wife Samah, and their cute daughter Rose, who lightens up my days with her cute playful giggles.

Finally, I am grateful to various funding agencies that supported this work. These agencies include Medical Research Service, Department of Veterans Affairs (Merit Award to M.K.), the U.S. Army Medical Research Acquisition Activity (W81XWH-05-1-0227 to M.K.), AI40198-06 grant from NIH, National Institute of Allergy and Infectious Diseases (NIAID, to M.K.). Development and maintenance of Gene Network and the BXD Colony is partly supported by INIA and Human Brain Project funded

jointly by the NIMH, NIDA, and NIAAA (P20-DA 21131, U01AA13499 to R.W.W.), NCI MMHCC (U01CA105417 to R.W.W.), and the Biomedical Informatics Research Network (BIRN), NCRR (U24 RR021760 to R.W.W.). Parts of this work were awarded ASM Student travel award, funded by Richard and Mary Finkelstein grants (ASM award to N.F.A.).

ABSTRACT

Clinical outcomes of infectious diseases are controlled by complex interactions between the host and the pathogen. Epidemiological, genetic and molecular studies in my mentor's laboratory provided evidence that in invasive Group A streptococcal (GAS) infections, genetic variations in both bacteria and patients influenced the severity of GAS sepsis. Allelic variations in class II human leukocyte antigens (HLA) contributed significantly to differences in the severity of group A streptococcal sepsis caused by the same virulent strain of the bacteria. HLA class II molecules present streptococcal superantigens (SAgs) to T cells, and variations in HLA class II molecules can strongly influence SAg responses. However, the bacteria produce a very large number of additional virulence factors that participate in the pathogenesis of this complex disease, and it is likely that host genes besides HLA class II molecules are also participating in modulating the severity of GAS sepsis. The main focus of this Ph.D. project was to identify additional host genes and pathways that may be modulating the severity of GAS sepsis.

To achieve this goal I applied a systems genetics approach, involving genome wide association studies (GWAS) of GAS sepsis in the Advanced Recombinant Inbred (ARI) panel of BXD mouse strains. We used this panel of ARI-BXD strains as a genetically diverse reference population to study differential severity of GAS sepsis as ARI-BXD strains diversity mimics the genetic diversity of human population. We assessed several traits associated with differential host responses to GAS sepsis, and analyzed variations in these traits in the context of mice genotypic variability, using genome-wide scans and the sophisticated analysis tools of WebQTL. This allowed us to map quantitative trait loci (QTL) associated with modulating susceptibility to severe GAS sepsis on chromosome (Chr) 2 and Chr X. The mapped QTLs strongly predicted disease severity (accounting for 25–30% of variance), and harbored highly polymorphic genes known to play important roles in innate immune responses. Based on linkage analyses, gene ontology, co-citation networks, and variations in gene expression, we identified interleukin 1 (IL1) and prostaglandin E (PGE) pathways as prime candidates associated with modulating the severity of GAS sepsis.

To further investigate mechanisms underlying differential host susceptibility, we analyzed genome-wide differential gene expression in blood and spleens of uninfected vs. infected mice belonging to highly resistant or susceptible BXD strains, at selected times post infection. Our transcriptional analyses revealed common pathways between susceptible and resistant strains associated with innate immune response, e.g. Interferon signaling pathway.

Since our data has pointed to a strong association of differential response to GAS with innate immune responses, we explored if differences in the numbers of relevant immune cells among the BXD strains played a role in their differential susceptibility to GAS. We found no significant differences in numbers or percentages of immune cell populations between susceptible and resistant strains under normal, uninfected

conditions. However, depletion of neutrophils and/or macrophages significantly increased the severity of GAS sepsis in both resistant and susceptible strains. Taken together, our data suggested that differences in mobilization and/or function of these cells between susceptible and resistant strains might play a role in modulating differential severity of GAS sepsis.

In conclusion, we found that variations in the severity of GAS sepsis have a strong genetic component that is complex and multigenic. Different combinations of genetic variants influenced the onset, progression, and severity of GAS sepsis and disease and ultimate outcome. Our overall approach of systems genetics, where we systematically dissected genetic, molecular, cellular and functional differences that may be associated with differential host susceptibility to GAS provided us with tremendous insight into disease mechanism. The knowledge gained can help the development of better diagnostics and means to predict disease severity based on a set of genetic and prognostic biomarkers to help customize patient care, to apply effective and more targeted therapeutic interventions and improve disease outcomes in septic patients.

TABLE OF CONTENTS

CHAPTER 1. INTRODUCTION	1
Pathogenesis Mechanisms of <i>Streptococcus pyogenes</i>	1
Streptococcal Arsenal of Virulence Factors	1
Streptococcal Sepsis as a Model of Host-pathogen Interactions	4
Infectious Diseases as Complex Traits that Require a Systems Approach to Better Understand Them.....	5
Systems Genetics Approach – Definition and Tools	6
Overview of Aims, Results, and Organization of the Dissertation.....	9
Aims of the Studies	9
Results and Organization of the Dissertation.....	10
CHAPTER 2. SUSCEPTIBILITY TO SEVERE STREPTOCOCCAL SEPSIS: USE OF A LARGE SET OF ISOGENIC MOUSE LINES TO STUDY GENETIC AND ENVIRONMENTAL FACTORS	12
Summary	12
Introduction.....	12
Results.....	14
Survival Scores Show Differential Susceptibility to Severe GAS Sepsis	14
Bacterial Loads in Blood and Organs Show Various Degrees of Bacteremia and Tissue Dissemination	14
Statistical Analysis Evaluates the Confounding Factors Affecting Mice Survival	16
Analysis of Covariates Underscores the Role of Genetic Background in Determining Animal Susceptibility to GAS	18
BXD Strains Exhibited Phenotype Variability Outside the Range of the Parental Strains	18
Controlled Time-course Experiments Show the Kinetics of Bacterial Spread and Confirm Results of Population-based Experiments	22
Preliminary Quantitative Trait Loci Mapping	22
Discussion	26
The Strength of the BXD Recombinant Inbred Population Model.....	26
The Complexity of the Phenotype	27
The Power of Statistical Analysis	28
The Preliminary Quantitative Trait Loci Mapping Results	28
Conclusion	29
Materials and Methods.....	29
Mice	29
Bacteria and Culture Media	30
Experimental Design and Infection Scheme.....	30
Design of Controlled Time-course Experiments	30

Bacterial Loads in Blood and Organs	31
Data Handling and Statistical Analysis.....	31
Preliminary Quantitative Trait Loci Mapping	31
CHAPTER 3. AN UNBIASED SYSTEMS GENETICS APPROACH TO MAPPING GENETIC LOCI MODULATING SUSCEPTIBILITY TO SEVERE STREPTOCOCCAL SEPSIS	32
Summary	32
Introduction.....	32
Results.....	33
Variable Susceptibility to Severe GAS Sepsis in Genetically Distinct Mice	33
Genome-wide Scans for Mapping GAS Susceptibility Quantitative Trait Loci	34
<i>In silico</i> Prediction of BXD Susceptibility to Severe GAS Sepsis	40
Mining for Candidate Genes and Pathways in Mapped Loci	44
Discussion.....	44
Materials and Methods.....	51
Mice	51
Experimental Design.....	52
Population-based experiments	52
Phenotype assessment experiments	52
Quantitative Trait Loci Mapping	52
Quantitative PCR Analysis for Target Genes Expression	53
Identification of Differentially Expressed Genes in the Mapped Interval and Bioinformatics Functional Pathways Analyses	53
Statistical Analysis.....	53
Web Site URL.....	54
CHAPTER 4. IDENTIFICATION OF SOLUBLE AND GENETIC BIOMARKERS ASSOCIATED WITH DIFFERENT OUTCOMES OF GAS SEPSIS REVEALS UNDERLYING MECHANISMS OF DIFFERENTIAL HOST SUSCEPTIBILITY	55
Summary	55
Results and Discussion	56
Comparison of Genome-wide Differential Expression in Blood between Susceptible and Resistant Strains at Selected Times Post Infection.....	56
Soluble Biomarkers Associated with Differential Susceptibility in Select Susceptible and Resistant Strains at Multiple Time Series Post-infection	72
Analysis of the Role of Prostaglandin at Early Stage of Infection	86
Conclusion	89
Materials and Methods.....	89
Bacteria and Infection Studies Using Mice	89
Experimental Design of Time Series Infection Studies.....	89
Processing of Blood and Spleen Samples and Purification of RNA	90

Microarray Platform and Design	90
Microarray Data Processing and Analysis.....	91
Identification of Differentially Expressed Genes and Functional Pathways Analyses.....	91
Cytokine Measurements and Analyses	91
Prostaglandin Studies.....	92
Statistical Analyses	92
CHAPTER 5. ANALYSIS OF CELLULAR POPULATIONS MODULATING DIFFERENTIAL RESPONSE TO SEVERE GAS SEPSIS.....	94
Summary.....	94
Results and Discussion	95
Profiling of Blood Cell Populations across Selected Resistant and Susceptible Strains Reveals Possible Migratory and Functional Differences Rather than Cellular Availability as a Possible Mechanism of Individual Variations in Susceptibility to Severe GAS Sepsis	95
Immunophenotyping Analyses of Cellular Population under Normal Physiological Conditions in Spleen of BXD Strains Revealed No Differences in Cellular Numbers or Relative Percentages among Susceptible and Resistant Strains.....	96
<i>In vivo</i> Manipulation of Cellular Populations in Susceptible and Resistant Strains: Depletion of Gr-1 ⁺ Cells and Macrophages Rendered Resistant Strains Susceptible.....	96
Conclusions.....	105
Materials and Methods.....	105
Experimental Design of Immunophenotyping Studies.....	105
Differential Blood Counts.....	107
Flow Cytometric Analyses of Splenocytes.....	107
Cellular Depletion Studies	107
Data Analysis and Statistical Analyses.....	108
CHAPTER 6. SUMMARY FUTURE DIRECTIONS AND CONCLUSIONS.....	109
Summary.....	109
Future Directions	113
Dissection of Migratory and Functional Differences of Immune Cell Populations between Susceptible and Resistant Strains	113
Analysis of Relationship of Prostaglandins and Modulation of Differential Response to GAS	114
Cytokine Profiling Associated with Susceptibility to GAS Sepsis.....	116
Analysis of the Role of Nod-like Receptors as a Candidate Pattern Recognition Receptor Associated with Modulation of Differential Response to GAS Sepsis	116
Concluding Remarks.....	117
LIST OF REFERENCES.....	118

APPENDIX A. PRIMER SEQUENCES USED FOR QPCR AND THE RELATIVE EXPRESSION LEVELS OF CANDIDATE GENES	136
APPENDIX B. LIST OF GENES AND TRANSCRIPTS IN THE MAPPED LOCI	141
APPENDIX C. POLYMORPHISM ANALYSIS OF GENES AND TRANSCRIPTS IN THE MAPPED LOCI	155
APPENDIX D. LIST OF PUBLISHED LOCI AND GENES ON CHROMOSOME 2 THAT ARE ASSOCIATED WITH DIFFERENTIAL SUSCEPTIBILITY TO INFECTIOUS DISEASES	163
VITA.....	165

LIST OF TABLES

Table 2-1.	Mouse strains used in the final analysis of this study	19
Table 2-2.	Analysis of Variance for Survival Index.....	19
Table 2-3.	Extent of invasiveness in time-course experiments, as measured by bacterial loads in spleen, liver, and lung.....	25
Table 3-1.	The relative expression levels of candidate genes post infection in resistant and susceptible strains expressed as ratio of post/pre infection in susceptible and resistant strains	45
Table 4-1.	Differentially expressed genes in peripheral blood of resistant and susceptible strains at 8 hrs post GAS infection.....	63
Table 4-2.	Differentially expressed genes in peripheral blood of resistant and susceptible strains at 12 hrs post GAS infection.....	70
Table 5-1.	Cell surface markers that were used to defines spleen immune cells populations characterized in the current study.....	108
Table A-1.	Primer sequences used in quantitative PCR assays for candidate genes.....	137
Table A-2.	Relative expression levels of candidate gene list expressed as mean fold difference between pre- and post-infection \pm standard deviation (SD) in selected resistant and susceptible strains.....	139
Table B-1.	Genes and their SNPs in mapped locus on Chr 2 between 22-34 Mb	142
Table B-2.	Genes and their SNPs in mapped locus on Chr 2 between 124-150 Mb.....	146
Table B-3.	Genes and their SNPs in mapped locus on Chr X between 50-100Mb ...	150
Table C-1.	SNP analysis of genes in mapped locus on Chr 2 between 22-34Mb.....	156
Table C-2.	SNP analysis of genes in mapped locus on Chr 2 between 125-150Mb.....	157
Table C-3.	SNP analysis of genes in mapped locus on Chr X between 50-100Mb...	160
Table D-1.	Diseases and mouse models associated with quantitative trait loci and genes located at Chromosome 2 loci mapped in current study.....	164

LIST OF FIGURES

Figure 1-1.	An overview of group A streptococcal main virulence factors.....	2
Figure 1-2.	Breeding scheme used for generation of RI strains of mice	7
Figure 2-1.	Distribution and correlation of survival scores and bacteremia indices.....	15
Figure 2-2.	Effect of non-genetic factors on the survival of BXD mice and their parental strains	17
Figure 2-3.	Differential susceptibility of BXD strains to invasive GAS	20
Figure 2-4.	Variation in bacteremia and spleen dissemination in different BXD strains	21
Figure 2-5.	Kinetics of bacterial dissemination in lung, liver, and spleen of six BXD strains.....	23
Figure 3-1.	Differential susceptibility to GAS sepsis among different BXD strains and their parental strains	35
Figure 3-2.	Genome-wide scan for mice susceptibility to GAS sepsis showing mapped QTL on Chr 2	38
Figure 3-3.	Recombinant inbred BXD strain distribution patterns at region of interest on Chr 2.....	41
Figure 3-4.	Patterns of differential gene expression levels of candidate genes post infection in susceptible and resistant strains	46
Figure 3-5.	Functional network of genes modulating GAS QTL	47
Figure 4-1.	Experimental design to test gene expression differences associated with differential susceptibility to severe GAS sepsis at selected stages of infection	57
Figure 4-2.	Pathways associated with differentially expressed genes at 8 hours post infection in peripheral blood of resistant and susceptible strains compared to uninfected (0hr) mice of respective strains	60
Figure 4-3.	Pathway analysis of differentially expressed genes at 12 hrs post infection in peripheral blood of resistant and susceptible strains compared to uninfected (0hr) mice of respective strains	67
Figure 4-4.	Pathways associated with differentially expressed genes in spleens of uninfected versus infected resistant and susceptible ARI-BXD strains at 36h post GAS infection	73
Figure 4-5.	TNF α plasma levels profiles across early time points post infection comparing selected highly susceptible and highly resistant ARI-BXD strains	75
Figure 4-6.	IL6 plasma levels profiles across early time points post infection comparing selected highly susceptible and highly resistant ARI-BXD strains	77

Figure 4-7.	IL10 plasma levels profiles across early time points post infection comparing selected highly susceptible and highly resistant ARI-BXD strains	79
Figure 4-8.	IFN γ plasma levels profiles across early time points post infection comparing selected highly susceptible and highly resistant ARI-BXD strains	82
Figure 4-9.	Comparison of ratios of anti-inflammatory to pro-inflammatory cytokines, comparing ratios of medians of IL 10/IFN γ plasma levels across early time points post infection in selected highly susceptible and highly resistant ARI-BXD strains	84
Figure 4-10.	Analysis of prostaglandin role at early stages of severe GAS sepsis.....	88
Figure 5-1	Differential blood count of selected susceptible and resistant BXD strains	97
Figure 5-2.	Diagram showing a scheme for flow cytometric analysis of immune cell populations in spleen employed in the current study	99
Figure 5-3.	Immunophenotyping of spleen cellular populations in selected resistant and susceptible BXD strains	101
Figure 5-4.	Depletion of Gr-1+ cells in selected resistant and susceptible BXD strains shows reversal of survival in response to GAS sepsis.....	103
Figure 5-5.	Kinetics of neutrophils and monocytes at early time points post GAS infection.....	104
Figure 5-6.	Comparison of the kinetics of neutrophils and monocytes numbers in susceptible versus resistant strains during the first 2 hours post GAS infection	106

CHAPTER 1. INTRODUCTION

Pathogenesis Mechanisms of *Streptococcus pyogenes*

Streptococcus pyogenes is an important human pathogen that can cause a wide spectrum of diseases with varying degrees of severity (reviewed in [Cunningham, 2000; Kotb *et al.*, 2003]). These diseases range from mild sore throat or skin infections to severe and often deadly ones, such as streptococcal toxic shock syndrome (STSS) and necrotizing fasciitis (NF), known as flesh-eating disease, giving the bacteria its nickname as the flesh-eating bacteria. Certain individuals develop post-streptococcal non-suppurative sequelae that include glomeronephritis, acute rheumatic fever, post-streptococcal arthritis, and neurological disorders collectively known as pediatric autoimmune neuropsychiatric disorders associated with streptococcal infections (PANDAS).

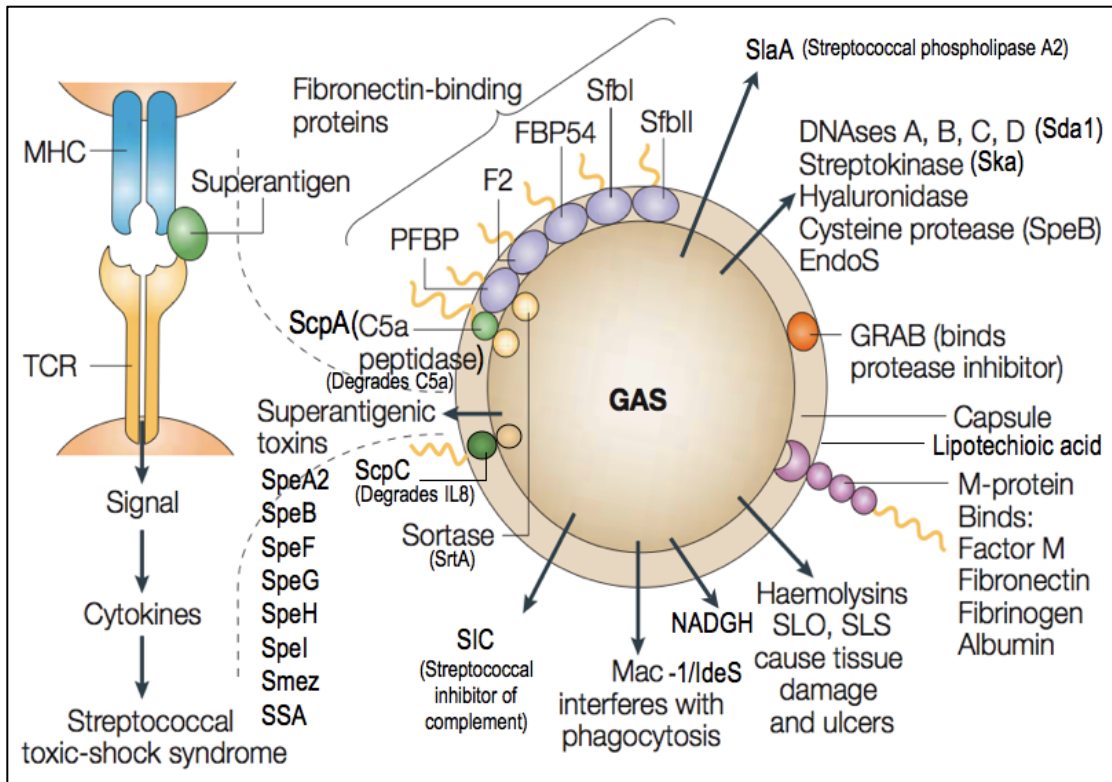
The wide range of diseases associated with *Streptococcus pyogenes* infections and their varying degrees of severity has intrigued us and other researchers to study the basis for the variable outcomes of the infection. Research groups have long debated over which is more vital towards the final outcome of streptococcal diseases, the bacteria or the host, with evidence supporting each side. Lately, it has become evident that interactions between host factors, which are influenced by their genetic background, and environmental factors, and the bacterial arsenal of virulence factors shape the final outcome of group A streptococcal (GAS) infection. I will briefly review the bacteria virulence factors and then elaborate on host genes associated with modulating the susceptibility to infectious diseases and sepsis.

Streptococcal Arsenal of Virulence Factors

Streptococcus pyogenes expresses multiple virulence factors that are tailored to their human host. Not all of these factors are expressed at the same time as *Streptococcus pyogenes* (also known as (GAS)) senses its environment and accordingly restructures its community to where mutants that are best fit for specific host environment are selected. These mutants have distinct genetic expression patterns. Examples of GAS virulence factors are shown in Figure 1-1. Some virulence factors are secreted and others are surface bound, of note, superantigens (SAGs), which are a large group of secreted proteins (exotoxins) and are associated with severe GAS sepsis and STSS. GAS produces virulence factors that specifically impair host mechanisms of bacterial killing; for example, GAS interferes with host signals for neutrophil chemotaxis, migration and function. Streptococcal chemokine protease A (ScpA), also known as the complement 5a (C5a) peptidase, degrades host C5a an important chemoattractant. Meanwhile, streptococcal chemokine protease C (ScpC), also known as interleukin 8 (IL8) degrading enzyme, degrades host IL8 thus impairing one of neutrophil chemotaxis factors (Sjolinder *et al.*, 2008; Gleich-Theurer *et al.*, 2009). Streptococcal inhibitor of complement (SIC) inhibits complement membrane attack complex and was also recently associated with inhibition of several of the human innate immune machinery namely, lysozyme, secretory

Figure 1-1. An overview of group A streptococcal main virulence factors.

GAS displays multiple virulence factors depending on site and stage of infection, shown are selected virulence factors. Each of these virulence factors has been tailored to counteract one or more of the host defenses. For example, ScpA (streptococcal chemokine protease A, also known as C5a peptidase) degrades host C5a, and ScpC (streptococcal chemokine protease C) degrades interleukin 8 (IL8), with a net result of hindering the recruitment of neutrophils to site of infection (Hidalgo-Grass et al., 2006; Sjolinder et al., 2008; Zinkernagel et al., 2008). Streptococcal inhibitor of complement (SIC) as its name suggests, inhibits complement membrane attack complex and was also recently associated with inhibition of four more proteins of the human innate immune machinery namely, lysozyme, secretory leukocyte proteinase inhibitor, human α -defensin 1 and LL-37 (Johansson et al., 2008; Minami et al., 2009). M protein binds and counteracts host's counter-regulatory factors e.g. host fibronectin. Streptokinase (Ska) degrades human plasminogen into plasmin thereby, dissolving blood clots. EndoS, endoglycosidase S; FBP54, fibronectin-binding protein 54; Mac, Mac1-like protein; MHC, major histocompatibility complex; PFBP, pyogenes fibronectin-binding protein; Sfb, streptococcal fibronectin-binding protein; SlaA, streptococcal phospholipase A2; cytotoxins streptolysin O (SLO) and streptolysin S (SLS); Spe, streptococcal pyogenic exotoxin (aka superantigens (SAGs)); Smez, streptococcal mitogenic exotoxin Z; SSA, streptococcal superantigen A; GRAB, G-related α 2-macroglobulin-binding protein; NADGH, Nicotine adenine dinucleotide (NAD) glycohydrolase; and TCR, T-cell receptor. Source: Adapted with permission. Mitchell, T.J. (2003) The pathogenesis of streptococcal infections: from tooth decay to meningitis. *Nat Rev Microbiol* 1: 219-230.



leukocyte proteinase inhibitor, human α -defensin 1 and LL-37 (Johansson *et al.*, 2008; Minami *et al.*, 2009). Another example of GAS interfering with neutrophil killing mechanisms is Sda1, a potent DNase produced by M1T1 (GAS strain under study). Sda1 dissolves neutrophil extracellular traps (NETs), which are DNA filaments produced by neutrophils and contain histones and antimicrobial peptides, allowing the bacteria to escape the entrapment and on mechanism of killing by neutrophil (Aziz *et al.*, 2004b; Buchanan *et al.*, 2006; Walker *et al.*, 2007).

According to site and stage of infection, GAS virulence factor genes are turned on or off to survive the host immune response and adapt to its environment. How the bacterium does that is not completely understood, but it is postulated that according to the environmental pressure, GAS selects for the most-fit mutants, sacrificing even the wild type. This has been shown in several recent studies by our group and others (Buchanan *et al.*, 2006; Walker *et al.*, 2007) and reviewed by (Aziz and Kotb, 2008; Bessen, 2009)

In the studies discussed in this dissertation, I used a hypervirulent clonal GAS strain, designated M1T1. This hypervirulent M1T1 clonal strain, along with M3, M18, and M28 strains, has been associated with the resurgence of the severe GAS sepsis in the 1980s (Johnson *et al.*, 1992; Hoge *et al.*, 1993). M1 and M3 GAS strains have displayed highest associations with severe GAS sepsis (STSS) and NF (Hauser *et al.*, 1991; Johnson *et al.*, 1992). Our research focus has been on the M1T1 strain, which has been consistently isolated over the past 20 years from patients with both noninvasive and invasive disease displaying varying degrees of severity (Chatellier *et al.*, 2000; Johnson *et al.*, 2002; Ikebe *et al.*, 2007). The hypervirulence of this strain is believed to be due to the acquisition of virulence factors through horizontal gene transfer, recombination and mutations (reviewed in [Aziz and Kotb, 2008]).

Streptococcal Sepsis as a Model of Host-pathogen Interactions

In studies presented in this dissertation, our focus was to determine the basis for differential host susceptibility to one of the most severe GAS invasive diseases, streptococcal toxic shock syndrome (STSS). STSS is an invasive disease of GAS, where bacteria reach an otherwise sterile site in the body, e.g. blood, and the patient has hypotension, plus two or more of the following clinical symptoms that are indicative of multiple organ failure: renal impairment, coagulopathy, hepatic involvement or respiratory distress. A STSS case is classified as probable if GAS is isolated from a non-sterile site or fluid, e.g. throat, and the patient displays hypotension and two or more of the above-mentioned symptoms (Lappin and Ferguson, 2009).

The pathophysiology of STSS has multiple aspects and is associated with host interactions and response to the bacterial arsenal of virulence factors including superantigens (SAGs). The Kotb research group has found, through epidemiological studies, that the severity of GAS sepsis is associated with allelic variations in human leukocyte antigen (HLA) class II (Kotb *et al.*, 2002). Patients with GAS sepsis expressing HLA class II (DR15/DQ6) haplotype were protected from severe GAS sepsis, whereas

those with HLA class II (DR14/DQ5) haplotype were at high risk for developing severe and often fatal forms of the disease (Kotb *et al.*, 2002; Norrby-Teglund *et al.*, 2002; Nooh *et al.*, 2007). Ensuing studies, *in vitro* and *in vivo*, dissected the molecular mechanisms underlying these differential responses and helped to dissect the role of GAS SAg in severe GAS sepsis and their interactions with HLA-II (Kotb *et al.*, 2002; Norrby-Teglund *et al.*, 2002; Welcher *et al.*, 2002; Kotb *et al.*, 2003; Kotb, 2004; Nooh *et al.*, 2007).

Whereas HLA-II allelic variations clearly influenced disease severity, it was clear that other host factors must also be participating in the pathogenesis of GAS sepsis because different inbred mice that do not express HLA-II were also found to display differential susceptibility to GAS sepsis (Medina *et al.*, 2001). This observation was interesting because mice are normally less susceptible to GAS SAg because they have an inherent poorer affinity of MHC-II to GAS SAg. Therefore, other bacterial virulence factors, other than SAg, and hence other host factors, other than HLA-II, are also likely to modulate differential severity to GAS sepsis. Moreover, the bacteria produce a number of additional, important virulence factors that must also participate in the pathogenesis of GAS sepsis. The overall aim of my study was to identify additional host factors modulating susceptibility to severe GAS sepsis and to identify host genes and pathways involved in this disease (Aziz *et al.*, 2007; Abdeltawab *et al.*, 2008).

Infectious Diseases as Complex Traits that Require a Systems Approach to Better Understand Them

It is now established that infectious diseases are a manifestation of complex traits modulated by the interaction of host factors and genetic background with the pathogen virulence factors and other environmental factors. Complex interactions between the pathogen virulence factors and host immune-related genetic makeup determine the progression and outcomes of the infection. Host genetic variations modulating differential response to infectious diseases have long been studied (Hornef *et al.*, 2002; Fortin *et al.*, 2007; Carvalho *et al.*, 2009; Chai *et al.*, 2009; Deghmane *et al.*, 2009; Ko *et al.*, 2009; Zhang *et al.*, 2009a). Variations in host response can be attributed to variations in pathogen recognition, prior exposure and preexisting immunity, immune regulation and/or quantitative differences in the immune response mounted to the infectious agents (reviewed in [Frank, 2002]). Variation in host recognition of pathogens and their virulence components can arise from a number of factors, including variations in many immune genes, including genes encoding pattern recognition receptors (PRR), and major histocompatibility complex (MHC) molecules. Also, variations in genes involved in immune regulation can strongly affect the host response to the infection. An added level of host immune response variability arises from polymorphisms of key immune-related genes.

Two main approaches have been employed to identify host genetic polymorphisms associated with infectious diseases. The first approach is to examine a candidate gene or genes for polymorphisms and analyze the distribution of these polymorphisms in patients or infected subjects vs. a normal group. The hypotheses are usually based on plausible associations based on the mechanism of diseases studied and

prior reports in the literature. The second approach employed is genome-wide association studies (GWAS). In GWAS no assumptions are made as to which gene might be involved and a scan of associations of phenotype with genotypes is performed. Such approaches have been widely applied in animal models and moving forward with using human subjects, as more projects like the human haplotype map (HapMap) (Frazer *et al.*, 2007) and the Wellcome Trust Case Control Consortium (2007) are establishing genomic repositories for case-control studies of common diseases.

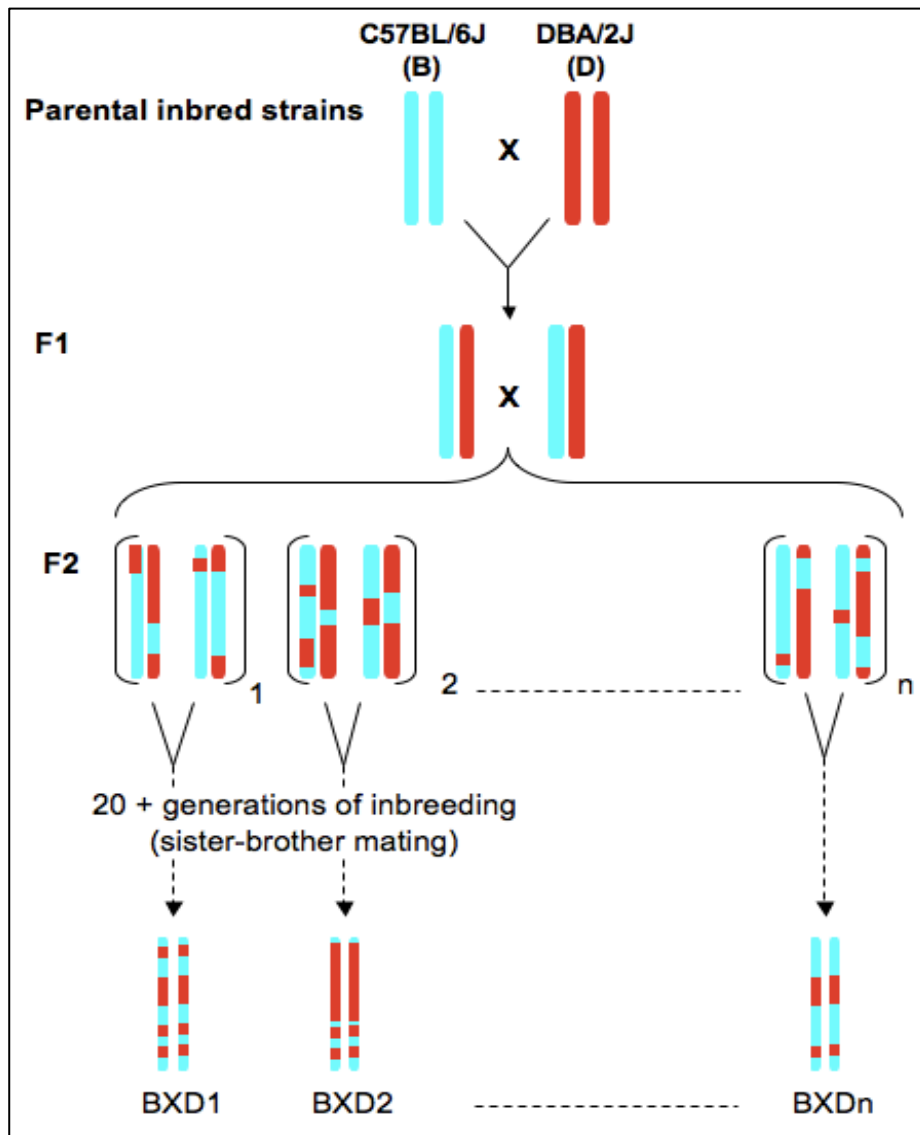
Systems Genetics Approach – Definition and Tools

Systems genetics is an approach that studies the effects of multiple genes on modulating disease phenotypes. Instead of the classical one gene, one disease approach, systems genetics attributes variations in phenotypes of a trait to a network of genes or loci that are in turn affected by environmental conditions (Sieberts and Schadt, 2007). Instead of looking at one gene, systems genetics explores one or more quantitative trait loci (QTL) associated with a given disease or complex trait. QTLs are regions within the genome whose genetic variation modulates quantitatively a phenotype characteristic of the particular trait under study (Lynch and Walsh, 1998). Determining the association between variations in specific disease phenotypes or a trait, with variations in genotypes of a reference population can be used to locate a QTL. One of the methods used for mapping QTLs associated with complex traits is genetic markers-trait association. Genetic markers associated with certain loci can be inherited in linkage disequilibrium. Generating populations with linked loci in disequilibrium is achieved through either crosses between inbred lines, or use of the out-bred populations. In this study we used recombinant inbred mouse strains that are fully genotyped as a genetic reference population for mapping QTLs.

Recombinant inbred (RI) and advanced RI (ARI) mice are a genetically diverse, segregating reference population that affords a powerful tool for systems genetics approaches (Williams *et al.*, 2001; Peirce *et al.*, 2004; Tsaih *et al.*, 2005). RI and ARI strains have been successfully used to map quantitative trait loci (QTLs) associated with various phenotypes and diseases (Hardy *et al.*, 2001; Grizzle *et al.*, 2002; Chesler *et al.*, 2005; Miyairi *et al.*, 2007; Abdeltawab *et al.*, 2008). RI and ARI strains of mice are the progeny of two ancestral inbred strains. For example, BXD strains are progeny of mating C57Bl/6J (B6) and DBA/2J (D2). B6 was mated with D2 to give F1 mice; all F1 progeny are identical, yet heterozygous, with one allele from the B6 parent (*B*) and the other from the D2 parent (*D*). Those F1 hybrids were then crossed to generate an F2 progeny, each with random patterns of recombination. Pairs of F2 mice were designated as “parents” of an RI line, and are then sib-mated for > 20 generations to achieve homozygosity for each genetically distinct RI line (Figure 1-2). This breeding strategy accumulates recombinations and random assortment of polymorphic loci. The breeding scheme used for generation of ARI strains is slightly different from RI strains and was adopted to increase recombination events per ARI strain, resulting in roughly double the number of recombinations per strain compared to a conventional RI strain (Williams *et al.*, 2001; Tsaih *et al.*, 2005; Shifman *et al.*, 2006). ARI breeding scheme involves random mating

Figure 1-2. Breeding scheme used for generation of RI strains of mice.

BXD strains are an example of recombinant inbred mice strains (RI). In this Figure, a scheme of crossing C57Bl/6J (B6 carrying B allele) female to a DBA/2J (D2 carrying D allele) male is shown. A representative one chromosome is shown. The parental strains chromosomes are homozygous and when crossed, their F1 progeny are identical and each chromosome pair is heterozygous carrying BD alleles. F1 mice are crossed to generate F2 progeny with random recombinations. Randomly assigned F2 pairs are designated as parents for a BXD strain, and are sib-mated for ≥ 20 generations to achieve homozygosity. Advanced RI (ARI) strains are bred using a slightly different scheme, where at the F2 stage, mice are randomly mated till generation 9 or 11 (according to the adopted breeding scheme (Peirce et al., 2004)) avoiding sib mating and even cousin mating to increase the number of recombinations and diversity of the genetic pool. There are currently > 80 ARI-BXD strains available for genome-wide association studies.



of F2 mice till generation 9 or 11 avoiding sib mating and even cousin mating to increase the recombinations and hence diversity of the genetic pool. After reaching generation 9 or 11, pairs of mice are set as parental for a designated BXD strain and are sib mated for ~20 generations or until each chromosome become homozygous (Peirce *et al.*, 2004). The net result in both cases is a mosaic chromosomal pattern of both ancestral parents, B6 and D2.

In the studies presented in this dissertation, we used the BXD panel of RI and ARI strains. We had found that parental strains of BXD mice, B6 and D2 strains, showed differential response to GAS severe sepsis. We found that D2 were susceptible to severe GAS sepsis showing high mortality and bacterial loads in blood while B6 were relatively resistant. This differential response of the BXD ancestral strains to GAS sepsis motivated us to use ARI-BXD strains to parse out genes associated with differential response to GAS sepsis. Figure 1-2 shows the breeding scheme used to generate the BXD RI panel (explained above). The BXD strains are derived from B6 and D2 strains and consisting of homozygous, inbred lines, each of which is genetically distinct. There are now more than 80 BXD strains. Each strain is a clone, as the recombinations become fixed after approximately 20 generations of sib mating, so each strain is renewable and the number of mice that can be tested per strain can be infinite with high reproducibility of results. This is in contrast to using F2 crosses, which have recombinations and have been used in mapping studies, however, F2 crosses recombinations are random, and therefore, it may be not possible to reproduce results obtained using these mice. In contrast, each BXD strain has a unique set of recombinations different from the other BXD strains and is renewable, where we can test the same BXD strain several times ($n = \infty$) with highly reproducible results. The high number of recombinations of each ARI-BXD strain makes these strains genetically diverse, thus mimicking the genetic diversity of the human population (Williams *et al.*, 2001; Churchill, 2007; Peters *et al.*, 2007). The use of BXD strains as a reference population is facilitated by the fact that BXD strains have been heavily genotyped with approximately 580,000 SNP and microsatellite markers (Churchill and Doerge, 1994; Shifman *et al.*, 2006). In addition, the genomes of the B6 and D2 parental strains have been fully sequenced with 4.5 million SNPs, 450,000 indels, copy number variants, and inversions, facilitating the dissection of mapped genetic loci. All taken together makes the BXD panel of ARI strains a very powerful tool as a genetically diverse reference population for genome-wide association studies.

Overview of Aims, Results, and Organization of the Dissertation

Aims of the Studies

The overall aim of this dissertation was to analyze the role played by host immunogenetic variability in influencing differential susceptibility to severe GAS sepsis. To accomplish this overall aim, we first wanted to discover loci associated with differential genetic susceptibility to severe GAS sepsis. This was done by performing genome-wide scans for mapping QTLs associated with differential survival of a panel of recombinant inbred (RI) mice. These scans revealed multiple QTLs on mouse

chromosomes (Chr) 2 and X. Next, steps were taken to fine tune and explore additional and interactive QTLs modulating severity of GAS sepsis. We fine-tuned the mapped QTLs to narrow down the list of candidate genes at mapped QTLs. To narrow down the candidate genes within individual mapped QTLs, we used additional BXD RI strains; chosen based on strains haplotypes also known as strain distribution patterns (SDP) of all BXD in the region of the mapped QTLs.

We then applied bioinformatics tools including linkage, gene ontology, co-citation networks, polymorphism analyses and pathway analyses to prioritize our candidate genes list. Next we aimed to identify genes and pathways modulating host response to GAS sepsis and validate those specific genes. This was accomplished by multiple approaches. We first compared the gene expression profiles of resistant and susceptible strains pre- and post- infection and validated differentially expressed gene identified with quantitative real time PCR analyses that revealed multiple pathways involved in modulating differential susceptibility to GAS sepsis. We then validated these pathways by studying the kinetics of soluble biomarkers, both cytokines and lipid mediators, associated with these pathways. We then aimed to analyze the cellular populations modulating differential response to severe sepsis and identify cellular mechanisms of differential response to severe GAS sepsis. The results of the studies are outline below including organization of the dissertation.

To identify correlates for survival, we explored additional independent and/or interactive traits associated with severity of GAS sepsis. Accordingly, we assessed variations in the number of bacteria in blood as well as dissemination of bacteria to various organs. Interestingly, both traits mapped to the same QTLs on Chr 2 associated with modulating survival but not with the one on Chr X. Additionally we found that there were interactions (epistatic effects) between two mapped QTLs on Chr 2. We also found interactions between Chr 2 QTLs and the Chr X QTL.

Results and Organization of the Dissertation

In Chapter 2 of this dissertation, I will discuss the establishment of the mouse model of GAS sepsis where we analyzed genetic, environmental and non-genetic covariates that might be contributing to the measured phenotypes. We standardized our model so that the observed phenotypes were mainly due to genetic differences of the strains (heritability) rather than any of the underlying covariates. The covariates studied included mice age, sex, and body weight, in addition to bacterial inoculate. This study is crucial, as phenotypes associated with complex traits can be affected by interactions with environment and/or other covariates, thus masking the actual gene networks associated with the trait under study. Chapter 2 was published as a peer-reviewed manuscript: Aziz, R.K., Kansal, R., Abdeltawab, N.F., Rowe, S.L., Su, Y., Carrigan, D., Nooh, M.M., Attia, R.R., Brannen, C., Gardner, L.A. *et al* (2007) Susceptibility to severe Streptococcal sepsis: use of a large set of isogenic mouse lines to study genetic & environmental factors. *Genes Immun.* 8(5): 404–415.

In the next chapter (Chapter 3), I will present how we analyzed disease phenotypes in the context of the mice genotypes which mapped two quantitative trait loci (QTLs) on Chromosome (Chr) 2. One QTL, between 22–35 Mb, that strongly predicts disease severity and accounts for 25%–30% of variance (calculated using hereditary tests) was highly significant (likelihood ratio statistic (LRS) 34.2 i.e. $P < 0.0000001$). We also mapped disease severity to a second QTL on Chr 2 (LRS 12 $P < 0.001$). Both QTLs harbor several polymorphic genes known to regulate immune responses to bacterial infections. Candidate genes within these QTLs were evaluated using multiple parameters that included linkage, gene ontology, and variation in gene expression. We identified interleukin 1 (IL1) and prostaglandin E synthases pathways as key networks involved in modulating GAS sepsis severity. Chapter 3 was published as a peer-reviewed manuscript: Abdeltawab, N., Aziz, R.K., Kansal, R.K., Rowe, S., Su, Y., Gardner, L.A., Brannen, C., Nooh, M., Attia, R., Abdelsamed, H. *et al.* (2008). An Unbiased Systems Genetics Approach to Mapping Genetic Loci Modulating Susceptibility to Severe Streptococcal Sepsis. *PLoS Pathog.* 4(4):e1000042.

In Chapter 4, I will present our attempts to identify molecular and soluble biomarkers associated with differential susceptibility at multiple stages of infection. I explored changes in the genome-wide expression levels, where we examined differential gene expression at early stages of infection in resistant and susceptible strains and compared it to late stages of infection. In addition, we sought to examine patterns of cytokines, as soluble biomarkers, associated with late and early stages. Chapter 4 is a manuscript in preparation: Abdeltawab, NF, Kansal, R, Mukandan, S., Bangar, H., Aronoff, D., Senn, T., Jordan, M., Williams, RW, & Kotb, M. Genomic & soluble biomarkers associated with different outcomes of Group A streptococcal sepsis reveal underlying mechanisms of differential host susceptibility.

Next, in Chapter 5 we wanted to examine the role of these genes and pathways at the cellular level. We immunophenotyped selected resistant and susceptible BXD strains where we examined and characterized the relative percentages of blood and spleen cellular populations at normal uninfected selected resistant and susceptible strains. We concluded that migratory and functional differences rather than cellular availability might be a possible mechanism of resistance. Subsequently, we wanted to dissect and confirm the cellular response in our model by depleting neutrophils, which are known to be associated with susceptibility to GAS infection. We blocked Gr-1 receptors, which are receptors expressed on the surface of neutrophils and some populations of monocytes and dendritic cells, this rendered resistant strains susceptible. This led us to more experiments on analyzing the role of neutrophils and the associated host pathways modulating this response. Chapter 5 is a manuscript in preparation: Abdeltawab, NF, Bangar, H., Kansal, R., Williams, RW, & Kotb, M. Host-pathogen interactions in Group A streptococcal sepsis: role of macrophages & neutrophils.

Finally, I will discuss and summarize the results of the studies done in this dissertation in Chapter 6, in addition to future directions of this project.

CHAPTER 2. SUSCEPTIBILITY TO SEVERE STREPTOCOCCAL SEPSIS: USE OF A LARGE SET OF ISOGENIC MOUSE LINES TO STUDY GENETIC AND ENVIRONMENTAL FACTORS*

Summary

Variation in responses to pathogens is influenced by exposure history, environment, and the host's genetic status. We recently demonstrated that HLA class II allelic differences are a major determinant of the severity of invasive group A streptococcal (GAS) sepsis in humans. While in-depth controlled molecular studies on populations of genetically well-characterized humans are not feasible, it is now possible to exploit genetically diverse panels of recombinant inbred (RI) BXD mice to define genetic and environmental risk factors. Our goal in this study was to standardize the model and identify genetic and nongenetic covariates influencing invasive infection outcomes. Despite having common ancestors, the various BXD strains (n strains = 33, n individuals = 445) showed marked differences in survival. Mice from all strains developed bacteremia but exhibited considerable differences in disease severity, bacterial dissemination, and mortality rates. Bacteremia and survival showed the expected negative correlation. Among nongenetic factors, age—but not sex or weight—was a significant predictor of survival ($p = 0.0005$). To minimize nongenetic variability, we limited further analyses to mice ages 40–120 days and calculated a corrected relative survival index (cRSI) that reflects the number of days an animal survived post-infection normalized to all significant covariates. Genetic background (strain) was the most significant factor determining susceptibility ($p \leq 0.0001$), thus underscoring the strong effect of host genetic variation in determining susceptibility to severe GAS sepsis. This model offers powerful unbiased forward genetics to map specific quantitative trait loci and networks of pathways modulating the severity of GAS sepsis.

Introduction

There is now overwhelming evidence that specific genetic factors influence a host's susceptibility or immunity to many infectious agents, and modulate severity and outcome of infectious diseases (reviewed in [Skamene, 1983; Roy and Malo, 2002; Frodsham and Hill, 2004; Kotb, 2004]). Infection with group A streptococcus (GAS or *Streptococcus pyogenes*) represents an ideal model for studying effects of host genetics on disease. This human pathogen causes a wide variety of conditions ranging from sore throat to invasive life-threatening diseases (reviewed in [Cunningham, 2000]), and the same strain of pathogen leads to different outcomes in different individuals (Chatellier *et al.*, 2000). Our laboratory provided direct evidence that the highly polymorphic human

* Source: Reprinted with permission. Aziz, R.K., Kansal, R., Abdeltawab, N.F., Rowe, S.L., Su, Y., Carrigan, D., Nooh, M.M., *et al.* (2007) Susceptibility to severe Streptococcal sepsis: use of a large set of isogenic mouse lines to study genetic and environmental factors. *Genes Immun* 8: 404-415.

leukocyte antigen (HLA) genes confer high risk or protection in rheumatic heart disease (Guedez *et al.*, 1999) as well as in streptococcal toxic shock (STSS) and necrotizing fasciitis (NF) (Kotb *et al.*, 2002; Kotb *et al.*, 2003). In GAS sepsis, allelic variation in HLA class II molecules plays a major role in modulating infection severity, primarily because they serve as binding and signaling receptors for superantigens (Kotb, 1992; Kotb, 1995), which are the primary trigger of the severe inflammatory responses that can lead to organ failure and shock (Norrby-Teglund *et al.*, 2001; Proft *et al.*, 2003).

To systematically identify additional gene variants that modulate susceptibility to severe GAS sepsis and to elucidate how they influence disease outcome, we sought a robust experimental model of the disease with attributes that incorporate roughly the same level of genetic variation as that of human populations. Small numbers of conventional inbred mouse strains have been used previously to study differential susceptibility to GAS infection (Medina *et al.*, 2001; Goldmann *et al.*, 2003, 2004b); however, these models are limited in their genetic variability and cannot be used to map modifier loci. HLA transgenic mice are appropriate models for GAS sepsis (Nooh *et al.*, 2007) but these too are generated on the genetic background of conventional inbred laboratory strains.

The genetically diverse mouse reference population of recombinant inbred (RI) strains, which can be likened to an immortal population of human monozygotic twins, is an ideal model for our studies. RI strains are generated by the crossing of two inbred strains followed by ≥ 20 consecutive generations mating among siblings (Bailey, 1971; Taylor, 1978). These types of strains are frequently used for studying genetic variation and mapping quantitative trait loci (QTL) influencing disease (Peirce *et al.*, 2004; Chesler *et al.*, 2005). The BXD strains were used recently to study variation in the pathogenicity of bovine spongiform encephalopathy and to uncover genes modulating anthrax and pox lethality (Benjamin *et al.*, 1986; Melvold *et al.*, 1990; Watters *et al.*, 2001). Among the different panels of RI strains, we selected the BXD set produced from an intercross of C57BL/6J and DBA/2J. The parental strains are known to differ in response to many pathogens (Plant and Glynn, 1976; Anthony *et al.*, 1989; Boyartchuk *et al.*, 2001; Mahler *et al.*, 2002). The other notable advantage of this particular panel of RI strains is that both parental strains have been sequenced (Waterston *et al.*, 2002). This makes it possible to use reverse genetic methods to test modifier genes (Williams, 2006). We have 80 BXD strains that are being extensively phenotyped and genotyped.

As a first step in exploiting the BXD strains to study the genetics of GAS susceptibility, we have studied the influence of differences in sex, age, body weight, inoculum titer, and genetic factors on disease development. Our main objective has been to develop a protocol that can be applied uniformly across the entire BXD set of 80. Our second objective has been to measure heritability and evaluate prospects of mapping modifier loci. We show the genetic and nongenetic factors that determine whether a mouse is protected from or susceptible severe GAS sepsis, we evaluate the contribution of each of these factors using multivariate analysis, and we discuss the proper measures that should be followed to design experiments using this novel and promising mouse

model in other infectious disease and for elucidating the complex events of host-pathogen interactions.

Results

The main purpose of this study was to adapt and standardize the BXD RI model to investigate the genetic and molecular mechanisms associated with susceptibility to severe invasive GAS sepsis, to determine the nongenetic environmental factors affecting the model, and to test whether the genetic variations among these mice would affect the progression and severity of invasive GAS disease. We used 717 mice in the study: 218 mice in the preliminary phase, 445 for the initial statistical analysis, 307 of which were selected for the final analysis as detailed below, and 54 for the time-course experiments.

Survival Scores Show Differential Susceptibility to Severe GAS Sepsis

To assess the phenotype ‘susceptibility or resistance of mice to severe GAS sepsis,’ we calculated a survival score for each animal as a quantitative trait: among 445 mice tested in six experiments, a notable variability was observed in survival scores measured as days post-infection. Interestingly, the distribution of the survival scores was not normal but multimodal, showing three groups (Figure 2-1-A), the largest of which represented animals ($n = 208$) that died early (in less than 2.5 days). Another group included an intermediate population ($n = 125$) that survived between 2.5 and 4.5 days and the third group ($n = 112$) survived for more than 5 days and up to the entire 7-day observation period. This pattern of survival was highly reproducible and predictable from one experiment to another with slight variability in the boundaries separating the three clusters in each experiment.

Bacterial Loads in Blood and Organs Show Various Degrees of Bacteremia and Tissue Dissemination

The bacterial load in blood (calculated as ‘bacteremia index,’ $BI = \log \text{CFU/ml}$ blood sampled 24 h post-infection) was measured for 396 of 445 mice used in six experiments.* In contrast to the survival scores, bacterial load followed a normal distribution (Figure 2-1-B). With the exception of a few mice ($n = 6$) whose blood was sterile (possibly due to injection failure), all mice had bacteremia with counts ranging from 125 CFU/ml ($BI = 2.097$) to 1.72×10^9 CFU/ml ($BI = 9.236$), the mean $BI \pm SE$ was 5.2 ± 0.07 reflecting a highly symmetrical distribution. Correlation analysis showed an inverse relation between survival scores and BI. The Pearson product moment-correlation factor of -0.430 (Figure 2-1-C) indicates that the BI accounts for 20 – 30 % of variance in mortality.

* In some cases, mice died before their blood was sampled and in other cases, the bacteria were too numerous to be counted by the plate dilution technique.

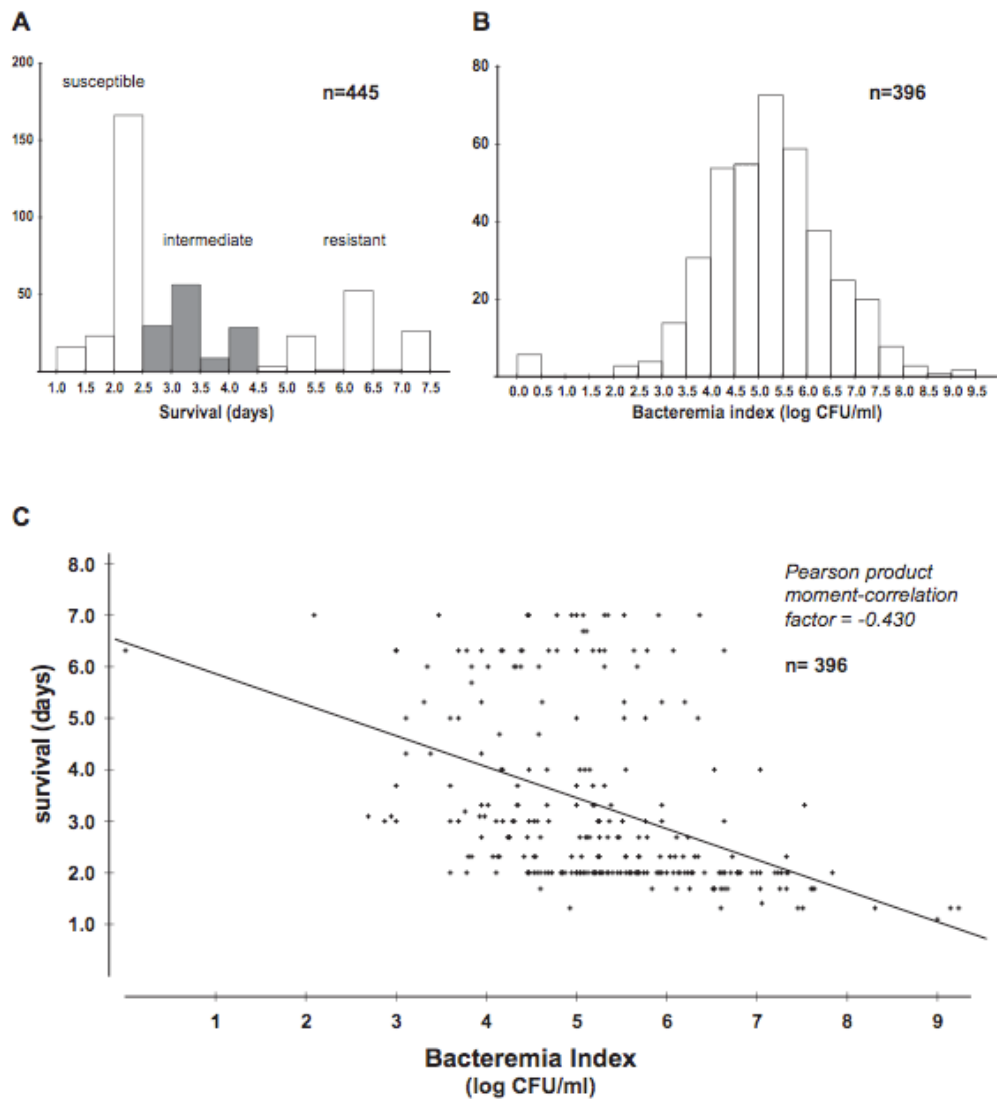


Figure 2-1. Distribution and correlation of survival scores and bacteremia indices.

Histograms showing the frequencies of survival scores (A) and log CFU/ml blood, or bacteremia indices, BI (B). A. The distribution of the survival scores of 445 animals from six experiments was multimodal, showing three clusters representing a susceptible, an intermediate, and a resistant population. Bars representing the intermediate population are shaded in grey. B. The distribution of BI for 396 was unimodal and symmetric, with the exception of six animals having sterile blood (leftmost bar). C. A scatter plot showing the negative correlation between survival scores and BI. Pearson product-moment correlation factor is indicated.

In addition to counting bacteria in blood, in some experiments we determined the bacterial dissemination in different systemic organs (mainly spleen, but also liver and lung) to estimate invasiveness of the disease. Among 335 mice with confirmed bacteremia, only 14 had sterile spleens while the remaining mice had bacterial counts ranging from 10² to 3x10¹⁰ CFU/spleen, with a median count of 1.3x10⁸ CFU/spleen. Bacterial loads in liver and lung were determined for 77 mice, and the median counts were 3.16x10⁹ CFU/liver and 2x10⁹ CFU/lung, with a wide range of variation.

Statistical Analysis Evaluates the Confounding Factors Affecting Mice Survival

The variability in animal mortality and extent of bacteremia is not surprising and matches that reported in human infection (Davies *et al.*, 1996; Basma *et al.*, 1999; Muller *et al.*, 2003) and in mice strains (Medina *et al.*, 2001). However, in this particular set of experiments, it was necessary to determine whether this variability reflects genetic differences between different BXD strains or is it mere biological variability caused by confounding factors like sex, body weight, animal age, or experiment-to-experiment variability (due in part to differences in inoculum size or other experimental error). The large number of animals used and the availability of replenishable inbred BXD lines made such analysis possible and efficient.

First, we examined the effect of inoculum size. In preliminary experiments, we conducted a dose-response study in which we exposed animals to bacterial inocula ranging from 10⁵ to 10⁸ CFU/ml to find an optimal dose that would kill animals rapidly but would also discriminate between susceptible and resistant strains (data not shown). We chose an inoculum size of 10⁷ CFU/ml because it showed clear differences between the parental strains (C57BL/6J and DBA/2J). However, because it is difficult to reproduce the inoculum titer in every experiment, and because precise counts could only be determined after injection, it was important to examine whether the inter-experimental differences in inoculum size had an effect on survival. Slight variation in inoculum size had an insignificant effect on survival ($r^2 = 0.1\%$, $p = 0.533$) Figure 2-2-A.

We tested whether sex had an effect on survival. Male mice ($n = 235$) had a mean survival of 3.49 ± 0.12 days and a median of 3 days, slightly higher than female mice ($n = 206$) that had a mean of 3.25 ± 0.12 days and a median of 2.3 days. This difference did not achieve statistical significance ($p = 0.153$) Figure 2-2-B.

Subsequently, we tested the effect of animal body weight and age on survival, and each of the two factors, independently, showed positive association with survival scores (Figure 2-2-C and 2-2-D). Whereas weight had a correlation of 0.29, age has a stronger correlation (factor = 0.44). It is noteworthy that weight was directly proportional with animal age between the ages of 40–120 days. Based on these findings, we decided to use animals in the age range of 40–120 days and to correct for age effects using a General Linear Model (GLM).

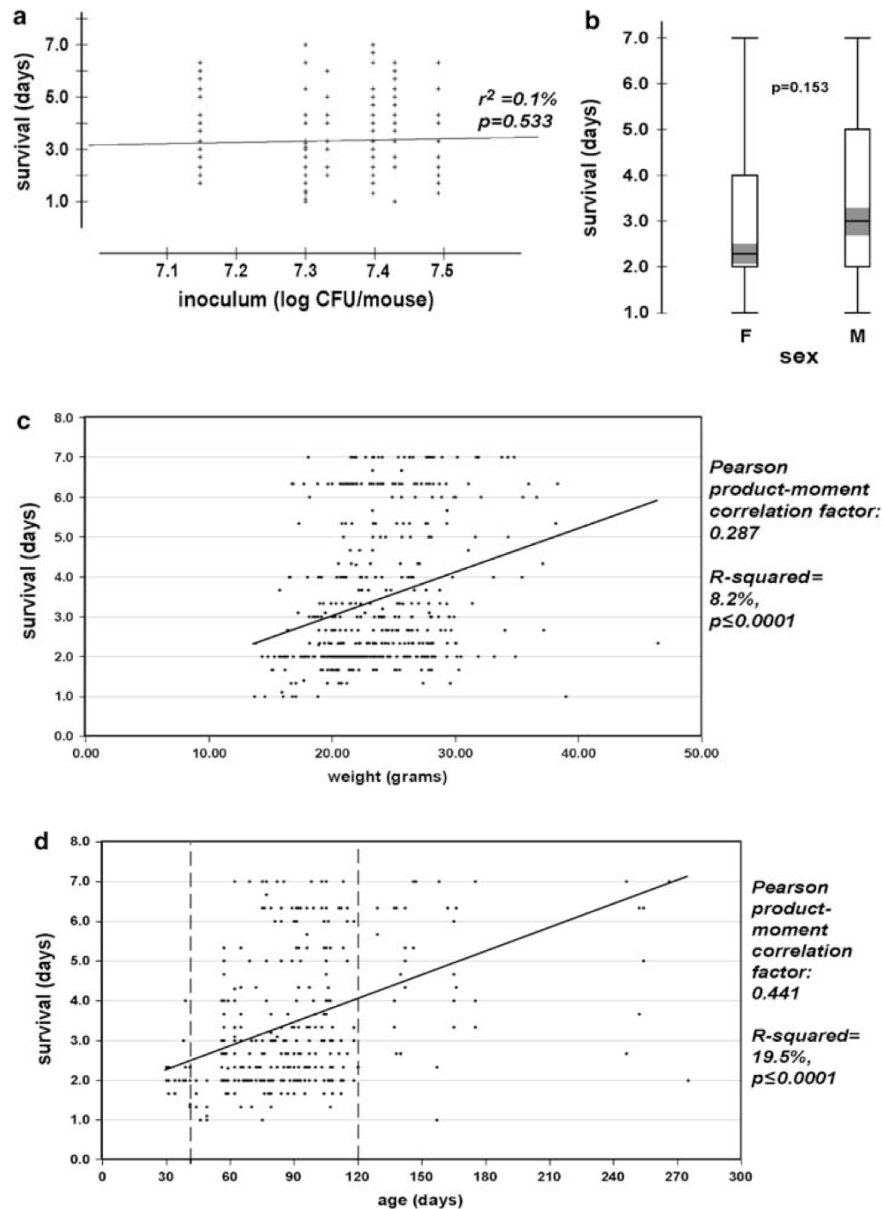


Figure 2-2. Effect of non-genetic factors on the survival of BXD mice and their parental strains.

Scatter plots showing the effect of the inoculum size (A), the mice body weight (C), and their age (D) on their survival. The effects of these confounding factors were evaluated by linear regression and Pearson product-moment correlation analyses, and the values of r^2 and correlation factors are shown when necessary. B. Box plots of animal sex versus animal survival in days post-infection. The significance of the effect of sex was tested by the student-t test, and the p-value is shown. D. Vertical dashed lines show the range of animals selected for further analysis.

Analysis of Covariates Underscores the Role of Genetic Background in Determining Animal Susceptibility to GAS

Having determined the effect of several major cofactors on survival scores, we set out to determine the complex interaction between these covariates and the genetic factor (i.e., the mouse strain). At this stage of the analysis, we filtered our data set to exclude mice that were outside the 40–120 days age range (see above) and we selected BXD strains that had been used in at least two experiments. Table 2-1 lists mice selected for final analysis. We took advantage of the multimodal distribution of survival scores detailed above (see Figure 2-1-A) to define a survival index (SI): animals were given a score ranging from 0.25 to 3, with increments of 0.25 (0.25 for most susceptible and 3.0 for most resistant). The use of SI was superior to survival scores as it normalized the data across experiments and minimized the unavoidable experiment-to-experiment variance in survival scores caused by slight differences in inoculum size and other systematic sources of error.

Finally, we performed GLM analysis of covariates using ordinary least squares ANOVA to determine the relative effect of covariates, including mouse strain, on survival (Table 2-2). This analysis revealed that strain was the most significant predictor ($p \leq 0.0001$), followed by age ($p = 0.0005$), and weight ($p = 0.02$). As shown in Figure 2-2-B, sex remained an insignificant factor in the final analysis (Table 2-2). From the GLM, we estimate the main effect attributable to strain (a measure of heritability) to be 25–30% (42.21/152.44, see Table 2-2). This GLM analysis was not only helpful in assessing effects of several factors, but it also allowed us to generate a corrected relative survival index (cRSI), which was used to compare the strains and determine their relative susceptibility—correcting for differences in age and weight (Figure 2-3).

BXD Strains Exhibited Phenotype Variability Outside the Range of the Parental Strains

The comparison of cRSI values between different strains (Figure 2-3) reveals the stark effect that the genetic background plays in predicting how long a mouse will survive after being exposed to a high dose of GAS. Some strains have very low mean cRSI (e.g., BXD66, BXD97, and BXD61) and are highly susceptible, whereas others are almost completely resistant (e.g., BXD87, BXD92, and BXD69). The difference between the cRSI values of parental strains, shown on the two extreme sides of the bar chart (Figure 2-3), was more modest than the variation displayed by the different BXD strains. This finding underscores the complexity of the trait we are measuring (susceptibility/resistance) and highlights the fact that the survival phenotype is modulated by multiple loci.

Following the same method of building a GLM for covariate analysis, we corrected the BI and the log CFU/spleen by calculating the coefficients that express the contribution of ‘mouse strain’ as a predictor for BI and for spleen dissemination (Figure 2-4). As shown with the inverse correlation between survival score and BI (Figure 2-1-C), most strains that were judged susceptible based on their cRSI (e.g. BXD60,

Table 2-1. Mouse strains used in the final analysis of this study.

Strain	N	Age (Mean ± SE)	Body Weight (Mean ± SE)
C57BL/6J	11	75.55 ± 3.76	21.98 ± 0.90
DBA/2J	12	88.92 ± 3.79	23.74 ± 0.59
BXD43	11	91.45 ± 5.05	23.92 ± 0.77
BXD44	11	75.09 ± 7.96	22.67 ± 1.88
BXD45	20	80.00 ± 4.48	24.10 ± 0.72
BXD51	16	74.00 ± 4.39	23.32 ± 0.89
BXD60	13	68.38 ± 6.31	24.28 ± 1.63
BXD61	9	57.67 ± 0.53	20.13 ± 0.64
BXD62	14	62.14 ± 2.26	20.70 ± 0.71
BXD64	12	96.67 ± 2.38	22.46 ± 0.77
BXD66	7	90.57 ± 6.30	23.66 ± 1.19
BXD69	14	73.93 ± 5.63	21.48 ± 0.70
BXD70	17	82.00 ± 4.83	24.11 ± 0.81
BXD73	14	86.14 ± 2.01	22.40 ± 1.24
BXD74	14	77.00 ± 7.14	21.53 ± 0.97
BXD75	22	74.36 ± 4.16	23.69 ± 0.74
BXD85	16	78.69 ± 4.97	26.72 ± 1.42
BXD87	8	89.00 ± 3.78	19.50 ± 0.74
BXD89	23	87.22 ± 4.48	23.71 ± 0.56
BXD90	17	83.71 ± 5.09	27.40 ± 0.81
BXD92	14	81.86 ± 1.82	27.48 ± 1.66
BXD97	12	98.33 ± 4.24	26.68 ± 1.09
Total Cases	307	80.33 ± 1.123	23.66 ± 0.240

Table 2-2. Analysis of Variance for Survival Index.

Source	df*	Sums of Squares	Mean Square	F-ratio	Probability
Const	1	937.56	937.56	2911.80	≤ 0.0001
Wt	1	1.73	1.73	5.37	0.0212
Sex	1	0.19	0.19	0.58	0.4452
Age	1	3.97	3.97	12.32	0.0005
Strain	21	42.21	2.01	6.24	≤ 0.0001
Error	282	90.80	0.32		
Total	306	152.44			

* df: Number of degrees of freedom.

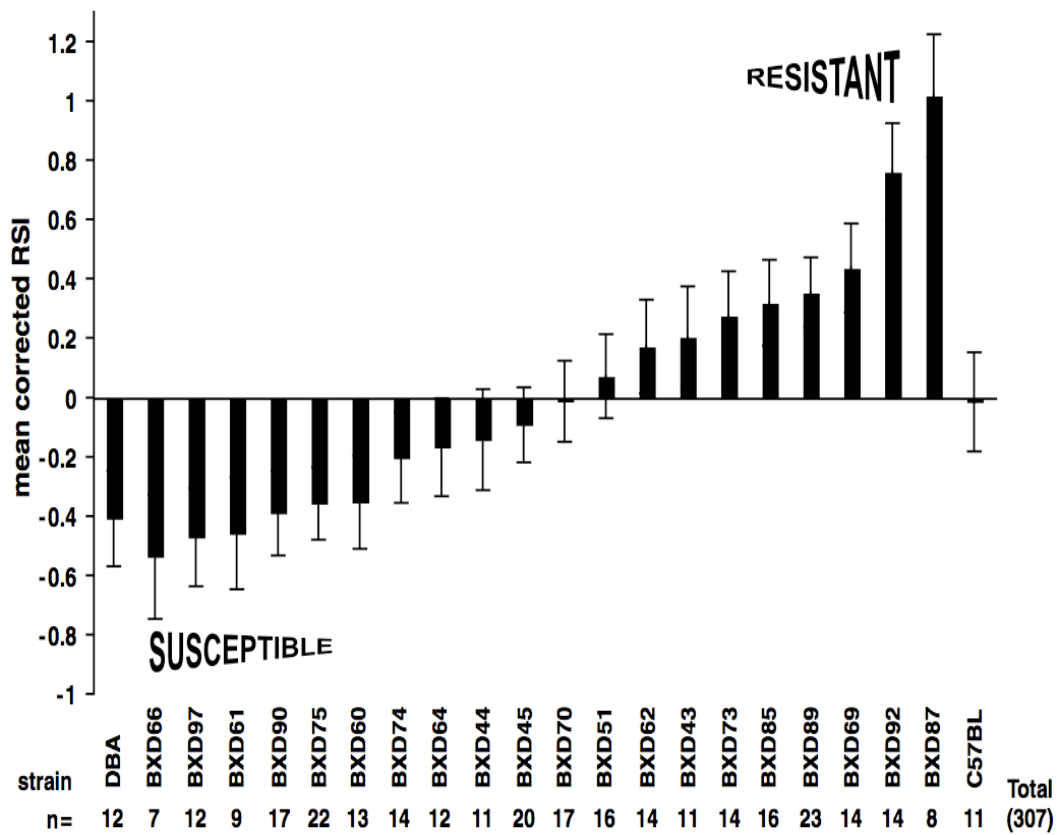


Figure 2-3. Differential susceptibility of BXD strains to invasive GAS.

A bar chart showing the mean values of corrected relative survival indices (cRSI) for different BXD strains, arranged in ascending order. Parental strains (C57Bl/6J and DBA/2J) are shown on the two extremities of the X-axis. Error bars represent the standard errors of the means. The total number of animals (n) used per strain is indicated.

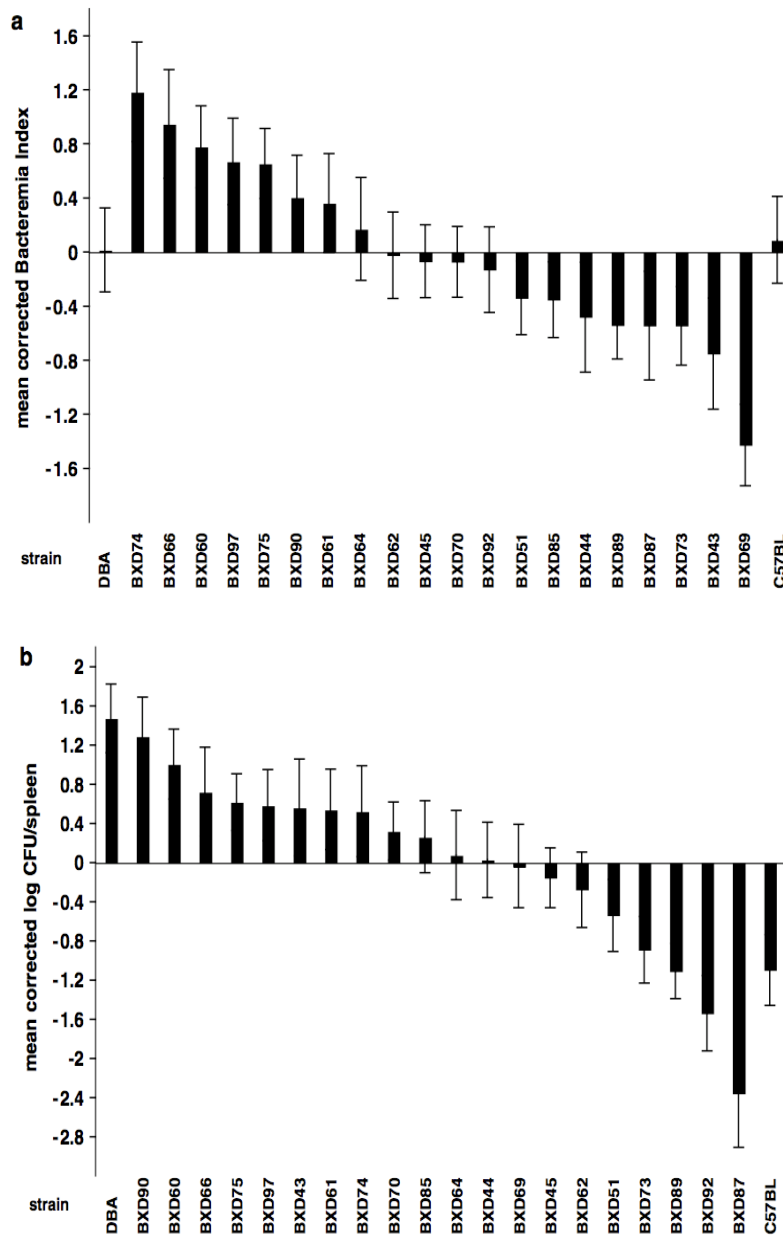


Figure 2-4. Variation in bacteremia and spleen dissemination in different BXD strains.

Bar chart showing the mean values of corrected bacteremia indices, cBI, (A) and corrected loc CFU/spleen (B) for different BXD strains, arranged in ascending order. Parental strains (C57Bl/6J and DBA/2J) are shown on the two extremities of the X-axis. Error bars represent the standard errors of the means.

BXD66, and BXD75) had higher cBIs, and vice versa (e.g. BXD69 and BXD73). However, there were exceptions, e.g., BXD44 had a negative cRSI and a negative cBI as well, and BXD92 was one of the most resistant strains but showed intermediate, rather than low, bacteremia (Figure 2-4-A). Additionally, when examining the bacterial dissemination in spleens of different strains (Figure 2-4-B), most susceptible strains had high dissemination and vice versa, again with exceptions, e.g. BXD69. Conversely, the parental strains were this time clearly on two sides of the spectrum, with DBA/2J having the highest spleen dissemination and C57BL/6J having one of the lowest values. Collectively, the data suggest the existence of different mechanisms leading to mortality.

Controlled Time-course Experiments Show the Kinetics of Bacterial Spread and Confirm Results of Population-based Experiments

Having generated data with large number of mice and with strong statistics, we moved to confirm the population-based study through time-course experiments that would clarify the kinetics of bacterial dissemination or clearance in the early hours of infection. In one representative experiment, we selected animals from six strains predicted to have the following descending order of susceptibility BXD61, BXD60, BXD51, BXD73, BXD89, BXD69 (Figure 2-3-A) and we infected them with the same dose of bacteria, then sacrificed three mice per strain at 18 h, 36 h, and 60 h. Overall, the results were as expected: All mice developed bacteremia, and their organs (spleen, lung, and liver) were positive for bacterial dissemination, but the kinetics of bacterial dissemination/ clearance were quite different. Strains BXD60 and BXD61, predicted as the most susceptible in this experiment, behaved as expected with highest bacterial loads in their spleens and highest rate of bacterial invasiveness, estimated from the slopes of bacterial dissemination in their organs over time (Figure 2-5 and Table 2-3). BXD69 was the most resistant strain to bacterial dissemination, with the lowest bacterial loads in organs and a tendency to clear bacteria rapidly (note the negative slopes in Figure 2-5-B and 2-5-C); this behavior matches its rank as having one of the lowest cRSI (Figure 2-3) and cBI (Figure 2-4-A). A similar pattern was displayed by BXD51, an intermediate strain that tends to have lower bacterial counts in blood and spleen (Figure 2-4). More interesting, however, was the behavior of BXD73 and BXD89 strains, both of which are resistant strains that showed delayed bacterial clearance in the first 60 h. While BXD73 had bacterial dissemination in organs an order of magnitude lower than BXD60 and BXD61, BXD89's counts seemed to follow the pattern of a susceptible rather than a resistant strain. This underscores the dissociation between the speed of bacterial dissemination and animal mortality as separate traits. A possible explanation is that BXD89 has an attenuated immune system that may delay bacterial clearance but that does not harm the host.

Preliminary Quantitative Trait Loci Mapping

To provide accurate QTL mapping, we are conducting a more extensive study with more strains and more mice per strain. However, with the current number of strains

Figure 2-5. Kinetics of bacterial dissemination in lung, liver, and spleen of six BXD strains.

Scatter plots of the bacterial dissemination during the first 60 h of an active infection in spleens (A), livers (B), and lungs (C) of mice from 6 strains with different susceptibility to GAS sepsis. Color regression lines indicate the rate and extent of change in log CFU bacteria/organ versus time for each strain.

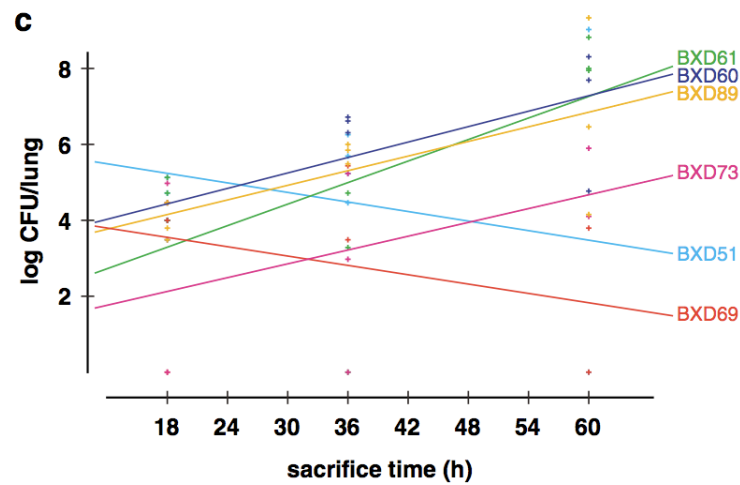
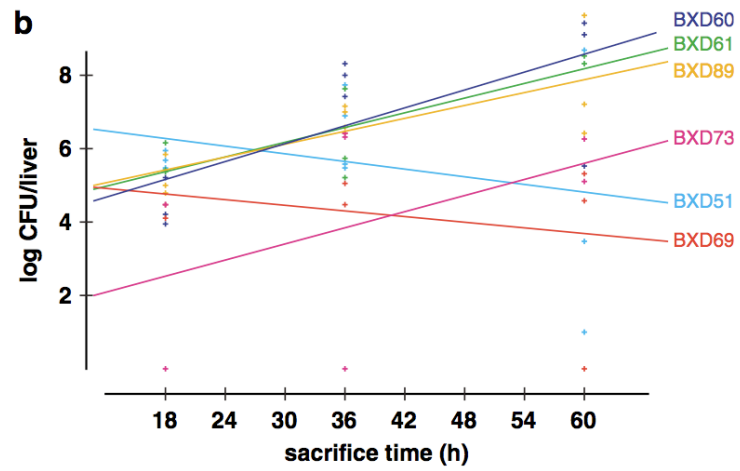
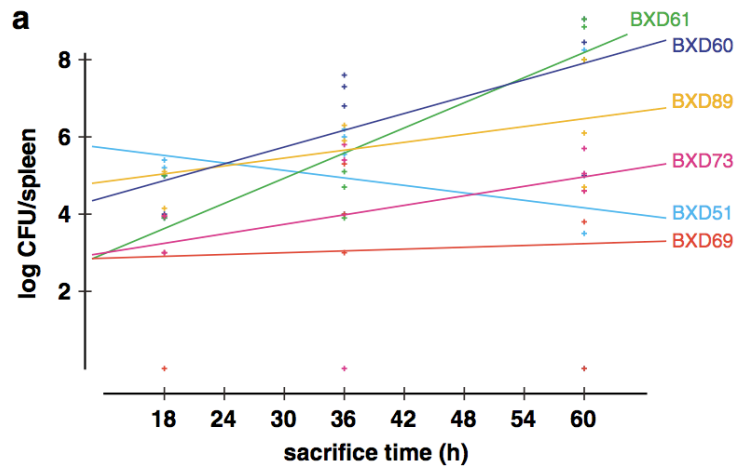


Table 2-3. Extent of invasiveness in time-course experiments, as measured by bacterial loads in spleen, liver, and lung.

Strain	Mean ± SE Log CFU/Spleen			Regression	
	18h	36h	60h	r²	p
BXD51	5.19 ± 0.12	5.44 ± 0.50	3.91 ± 2.39	6.80%	0.466
BXD60	4.29 ± 0.35	7.22 ± 0.24	7.50 ± 1.26	47.90%	0.039
BXD61	4.26 ± 0.37	4.57 ± 0.35	8.64 ± 0.32	81.40%	0.001
BXD69	2.31 ± 1.19	4.10 ± 0.67	2.79 ± 1.41	0.60%	0.84
BXD73	3.48 ± 0.48	3.74 ± 1.87	5.11 ± 0.32	14.60%	0.35
BXD89	4.78 ± 0.31	6.16 ± 0.13	6.27 ± 0.96	29.50%	0.131

Strain	Mean ± SE Log CFU/Liver			Regression	
	18h	36h	60h	r²	p
BXD51	5.71 ± 0.13	6.43 ± 0.54	4.06 ± 2.53	9.60%	0.385
BXD60	4.45 ± 0.39	7.92 ± 0.26	8.03 ± 1.25	49.00%	0.036
BXD61	5.64 ± 0.27	6.20 ± 0.74	8.39 ± 0.06	72.70%	0.004
BXD69	4.22 ± 0.13	5.31 ± 0.58	3.31 ± 1.67	6.80%	0.499
BXD73	2.24 ± 2.24	4.24 ± 2.12	5.49 ± 0.38	23.80%	0.22
BXD89	5.21 ± 0.33	6.92 ± 0.16	7.74 ± 0.96	56.50%	0.02

Strain	Mean ± SE Log CFU/Lung			Regression	
	18h	36h	60h	r²	p
BXD51	4.60 ± 0.33	5.43 ± 0.38	3.01 ± 3.01	7.00%	0.46
BXD60	3.97 ± 0.28	6.55 ± 0.13	6.93 ± 1.09	52.20%	0.028
BXD61	4.62 ± 0.33	2.68 ± 1.40	8.26 ± 0.29	39.00%	0.072
BXD69	2.83 ± 1.42	4.13 ± 0.65	1.26 ± 1.26	12.70%	0.346
BXD73	2.50 ± 2.50	2.74 ± 1.52	5.01 ± 0.90	19.10%	0.327
BXD89	3.90 ± 0.28	5.77 ± 0.16	6.66 ± 1.50	42.00%	0.059

and mice we used the WebQTL tools on the GeneNetwork web site (<http://www.genenetwork.org>) and were able to exclude certain sites that could have possibly contributed to the modulation of GAS sepsis severity. For example, our human genetic association studies in patients with severe GAS sepsis revealed a strong association with HLA class II haplotypes (Kotb *et al.*, 2002). It was therefore interesting to determine whether any QTLs map to the H2 locus. Although the parental strains differed in their H2 types (the C57/BL6 mice are H2-b while the DBA/2J mice are H2-d), we could not find any hint for significant QTLs in the H2 region on chromosome 17. Instead, our preliminary mapping results suggest two significant QTLs on chromosome 2 that we are currently verifying and fine-tuning using additional mice and strains. The insignificant contribution of the mice H2 locus was not entirely surprising because the HLA class II association in humans is related to the role of these molecules in presenting GAS superantigens to T-cells. While superantigens play a crucial role in the human disease and in HLA-transgenic mice (Nooh *et al.*, 2007), they have little contribution in the BXD mouse model because GAS superantigens are poorly presented by mouse H2.

Discussion

The Strength of the BXD Recombinant Inbred Population Model

Clinical and epidemiological observations provide evidence of strong differences in human susceptibility to GAS infections and the severity and outcomes of diseases caused by the same strain of bacteria (Hoge *et al.*, 1993; Davies *et al.*, 1996; Kaul *et al.*, 1997; Johnson *et al.*, 2002; Kotb, 2004). For example, we have previously demonstrated a dominant effect of HLA class II allelic polymorphisms in severe GAS sepsis (Kotb *et al.*, 2002; Kotb *et al.*, 2003). We also provided biological confirmation of these associations with HLA both *in vitro* (Kotb *et al.*, 2002; Norrby-Teglund *et al.*, 2002) and *in vivo* (Nooh *et al.*, 2007). Despite this strong association with HLA class II polymorphic alleles, we realize that sepsis is a complex disease affected by multiple interactive pathways. To identify additional pathways and polymorphisms contributing to the stark difference in the severity of GAS sepsis, we explored several animal models that may be suitable for this genetic study. While non-human primates represent an alternative to study human GAS infections (Virtaneva *et al.*, 2003; Virtaneva *et al.*, 2005), their use in immunogenetic population studies is expensive and impractical due to their slow breeding pattern and small progeny, high cost, and ethical issues. Meanwhile, regular laboratory mice, which share ~85% gene content with humans (Jackson, 2001), are not sensitive to invasive GAS infections (Miethke *et al.*, 1992; Welcher *et al.*, 2002) just as certain human populations are not good models for certain human diseases because of their genetic resistance. This natural resistance of mice to severe GAS sepsis can be overcome by the use of high infectious doses, less resistant strains, or transgenic mice carrying human HLA class II (Nooh *et al.*, 2007) or human plasminogen (Sun *et al.*, 2004; Cole *et al.*, 2006).

Despite this, successful attempts were made with standard inbred mouse lines, e.g., BALB/c, C3H/HeN, and CBA/J, C57BL/10 (Medina *et al.*, 2001), and DBA/2 and

C57BL/6 (Kansal and Kotb, submitted); whereas these studies were quite informative, conventional mouse models are limited in their genetic pool, and thus one may miss important genotype-trait relations. Our choice was thus to use one of the genetically diversified mouse reference populations generated by the international Complex Trait Consortium (CTC). The CTC strategy, known as the Collaborative Cross (CC), is to construct a very large set of RI strains from a genetically diverse set generated by intercrossing conventional inbred mice (Vogel, 2003; Churchill *et al.*, 2004; Peirce *et al.*, 2004).

RI strains are an ideal resource for systems biology research as they provide a reproducible, highly varied, and diversified yet controlled set of genetic backgrounds for functional genomics, QTL mapping, and identification of interactive gene networks modulating disease phenotype (Valdar *et al.*, 2006). Being inbred, RI strains are perpetually renewable, and have many advantages over F2 or backcross populations. Experiments performed with RI mice can be repeated in different laboratories and at different times with expected reproducibility. This adds high statistical power. Because the ancestral parents are fully sequenced, the genotyped RI strains afford a powerful tool for identifying genes within QTLs and are particularly useful for mapping multiple and epistatic genetic effects underlying complex phenotypes, including those seen in infectious diseases (Caron *et al.*, 2002; Churchill *et al.*, 2004; Peirce *et al.*, 2004; Ouburg *et al.*, 2005; Roy *et al.*, 2006).

Among the different RI sets of mice, we found the BXD panel more suitable for us than other series (e.g., the AXB set) as the BXD series is much larger, almost 3-times more than used in any other series of experiments and because both parental strains (C57BL/6J and DBA/2J) have been fully sequenced (Waterston *et al.*, 2002), and have been shown to differ in their response to many pathogens (Hormaeche, 1979b, a; Mitsos *et al.*, 2000; Boyartchuk *et al.*, 2001; Boyartchuk and Dietrich, 2002; Mitsos *et al.*, 2003), including GAS (Kansal and Kotb, personal communication).

The Complexity of the Phenotype

Susceptibility to a particular bacterial infection and disease severity are complex phenotypes likely to be contributed by more than one genetic factor, and by networks and pathways modulated by gene products. Our attempt to attribute one or two sets of genetic loci that predispose mice to or protect them from certain infections could be misleading if we fail to take the complexity of the phenotype into consideration. In this study, we explored the response of a panel of 20 BXD RI mice (plus the two parental strains) to infection with the same dose of GAS and monitored them over a week post-infection. To quantify the animals' susceptibility to GAS and the severity of sepsis, we measured three variables: animal survival, bacteremia, and dissemination in systemic organs (spleen, liver, and lung). Our results provide solid evidence of the complexity of our phenotype. One manifestation of this complexity is that BXD strains exhibited a much wider range of variability in survival (Figure 2-3) and bacteremia (Figure 2-4-A) than the parental strains; yet, the two ancestral strains were on the two extreme sides of the panel of bacterial dissemination in spleen (Figure 2-4-B). This behavior is likely a result of the

random assortment of many polymorphic loci that accentuate resistance or susceptibility to infection depending on the pattern by which they are inherited from the parental strains to the offspring. Another consequence of the trait complexity is that the different strains did not show identical patterns for the different measured variables (Figures 2-3 and 2-4). There was a significant correlation between survival and bacteremia (Figure 2-1-C), but it only explained 25% of the variance. Differences in the kinetics of bacterial dissemination to organs of BXD strains in the first 60 h of disease (Figure 2-5 and Table 2-3) highlights the uniqueness of each strain, and shows the importance of following the course of infection at multiple time points.

Our analysis indicates that bacteremia and dissemination to organs were major predictors of disease severity and mortality; however, it is likely that other factors contribute to mortality including severe toxicity and inflammatory responses in blood and organs.

The Power of Statistical Analysis

A major part of our study was dedicated to the optimization and standardization of this novel mouse model. We conducted preliminary experiments to optimize the inoculum size and volume, the number of mice to be used per strain, and the best randomization scheme for injecting mice and recording the data. Subsequently we generated a large data set from 445 mice, and we used this data set to estimate the effect of independent confounding factors like sex, age, body weight, and inoculum size (Figure 2-2) as well as the combined effects of these covariates (Table 2-2). As a result of these analyses, we filtered our data set, bringing the number of analyzed cases to 307, after excluding animals from strains that were tested only once, and those that did not fall in the age range where age and weight were colinear. The analysis of covariates also helped us to estimate the contribution of each factor in predicting susceptibility to the severe form of GAS sepsis therein allowing us to correct the measurable traits (SI, BI, and Log CFU/spleen) for significant covariates. Correction for age, for example, was a vital alternative to age-matching all animals, which is not feasible because the breeding scheme of 20 strains cannot be synchronized practically. The ability to use a large number of strains and to repeat experiments using the same strains added power to the statistical analysis. Combining the genetic diversity of the RI strains with statistical analysis allowed the dissection of many factors contributing to infection phenotype using relatively small numbers of animals and a large number of strains.

The Preliminary Quantitative Trait Loci Mapping Results

It is rather risky to attempt to identify QTLs using only 20 BXD strains, and this was not the intention of this study, which focused on developing the model and identifying significant covariates affecting the severity of GAS sepsis. Nonetheless, we were able to exclude plausible regions as major contributors to GAS sepsis severity. For example, we can comfortably exclude any contribution from the H2 region on chromosome 17. Although our previous studies showed strong association with HLA

class II genes (Kotb *et al.*, 2002; Nooh *et al.*, 2007), it was not surprising that the mouse H2 allelic variation does not contribute to GAS sepsis severity because the mouse H2 molecules are very poor presenters of GAS superantigens that are pivotal in mediating the pathogenesis of the human disease. The BXD model allows us now to map QTLs and identify additional bacterial virulence strategies involved in the pathogenesis of sepsis. The latter are usually masked by the overwhelming effects of superantigens in human studies and the HLA-transgenic mouse model (Kotb *et al.*, 2002; Nooh *et al.*, 2007). Preliminary mapping studies pointed to two regions on mouse chromosome 2, which harbor many genes of relevance to immune modulation. Ongoing studies using additional strains are expected to confirm and narrow down these QTLs.

Conclusion

The BXD RI strains afforded a good model for the analysis of traits that contribute to severe GAS sepsis. The genetic diversity of these strains exaggerates or suppresses traits seen in the parental strains. Having standardized the model and set major criteria for selecting the animals to be used and analyzed, we will continue generating data by using more BXD strains and bioinformatics tools to map QTLs and determine the genetic basis for the large differences in disease susceptibility among these animals. Mapping QTLs is likely to identify gene variants (polymorphisms, SNPs, or mutations) that underlie the remarkable individual differences that are a hallmark of host-GAS interactions; however, our long-term goal is to generate a disease roadmap by revealing the networks involved in these inter-strain differences.

Materials and Methods

Mice

The BXD strains are completely inbred strains generated by repeated mating between siblings starting from F2 intercross progeny between C57BL/6J and DBA/2J (Taylor, 1978; Taylor *et al.*, 1999; Williams *et al.*, 2001; Peirce *et al.*, 2004). In this study, we used 717 mice belonging to a set of 33 BXD strains along with the parental strains, C57BL/6J (B6) and DBA/2J (D2). Among these mice, 218 were used in the preliminary experiments for optimization of inoculum size and experimental conditions, 445 were used in the population-based experiments, and 54 were used in the controlled time-course experiments. The animals chosen for final statistical analysis of the population-based experiments ($n = 307$) were those that satisfied all the conditions determined in the study (see Results) and that belonged to a BXD strain that was used in at least two experiments.

The animals were mated and housed in a pathogen-free colony on hardwood chip bedding in microisolator cages at the VA Medical Center and the University of Tennessee Health Science Center, Memphis, TN. They were maintained on a 12 h light-dark cycle, in a room kept at 23 °C with 50–60% relative humidity and were given tap

water and sterile irradiated rodent chow (Harlan Teklad, Madison, WI) ad libitum. All protocols were approved by the Institutional Animal Care and use Committees of Veterans Affairs Medical Center and The University of Tennessee.

Bacteria and Culture Media

We used the clinical isolate, GAS-5448 (Kansal *et al.*, 2000), representative of the clonal MIT1 strain that has globally disseminated since the mid 1980s and was associated with severe and non-severe GAS infections (Chatellier *et al.*, 2000; Aziz *et al.*, 2005). The bacteria were incubated in Todd Hewitt Broth (DIFCO, Detroit, MI) supplied with 1.5% of yeast extract (DIFCO, Detroit, MI), or THY, for 17 h, washed twice with sterile phosphate-buffered saline solution, PBS (GIBCO, Carlsband, CA), then diluted to the final inoculum size with sterile PBS. The original isolate had been aliquoted in THY stocks containing 15% glycerol (Sigma, Saint Louis, MO) at -80°C . Before each use, the bacteria were spread on blood agar plates (Becton Dickenson, Franklin Lakes, NJ) for colony isolation and sterility checking.

Experimental Design and Infection Scheme

Before the start of each experiment, we randomized animals to avoid bias in the order of injection, weighing, or sampling. We kept males and females in different cages. Animals were infected via the tail vein injection with a $2 \pm 1 \times 10^7$ CFU/mouse (unless otherwise stated). Twenty-four hours post-infection, blood was sampled for bacteremia: 20 ml was drawn from the tail vein and diluted 10-fold in sterile saline (SS). During the observation period (7 days), animals were weighed twice a day (8:00 a.m., 4:00 p.m.) and checked for survival three times a day (8:00 a.m., 4:00 p.m., and at midnight). We dissected spleens, livers, and lungs from mice that were sacrificed at specified time points, as well as animals that expired prior to sacrifice, and we homogenized these tissues using a rotor stator homogenizer (Omni International, Marietta, GA) in SS, and a sample was used to estimate bacterial loads.

Design of Controlled Time-course Experiments

Time-course experiments were designed to investigate the kinetics of bacterial dissemination in the early stages of the infection. These experiments were performed following the same procedure as the population-based experiments (see experimental design and infection scheme), except that equal numbers of animals belonging to each strain (typically 3 animals per strain per time point) were sampled for blood, spleen, liver, and lung at 18 h, 36 h, and 60 h post-infection. Regardless of the specified sampling time, all animals were bled through the tail vein (20-50 μl) for determination of bacteremia at 18 h. At each time point, the animals were dissected, and their organs (spleens, livers, and lungs) were homogenized in 10 ml SS each.

Bacterial Loads in Blood and Organs

To determine bacterial loads in blood and organ homogenates, we diluted 10 ml of either sample (tail vein blood or homogenate) serially (up to 10^{-7}) and plated 10 ml of each dilution (as well as the original sample) on the surface of blood agar plates (Becton Dickinson, Franklin Lakes, NJ). After 24 h incubation, all plates were counted, and the number of colony forming units (CFU) per ml or per organ was calculated (CFU/organ = CFU/ml homogenate x 10).

Data Handling and Statistical Analysis

Results were recorded three times daily (or whenever an animal died). Data were reviewed for accuracy and consistency at the end of every experiment by a different set of investigators. We dedicated a considerable amount of time to data recording, error checking, and filtration after each experiment. Mice lost due to factors unrelated to infection were flagged in the database and excluded from the final analysis. We performed all primary calculations and sorting operations using simple features and functions of Microsoft Excel. Excel files were later exported to Data Desk (version 6.2) software (Data Description, Inc., Ithaca, NY; www.datadesk.com), which we used for all statistical analyses and tests, including clustering, correlation analysis, linear regression, multiple regression, and general linear model (GLM) analysis by ordinary least squares analysis of variance (OLS ANOVA).

Preliminary Quantitative Trait Loci Mapping

For QTL mapping, we used the web-based complex trait analysis platform, WebQTL (Wang *et al.*, 2003) available on the GeneNetwork web site (<http://www.genenetwork.org>). WebQTL evaluates potential QTL at regular intervals and estimates the significance at each location with a graphical representation of the likelihood ratio statistics (LRS).

CHAPTER 3. AN UNBIASED SYSTEMS GENETICS APPROACH TO MAPPING GENETIC LOCI MODULATING SUSCEPTIBILITY TO SEVERE STREPTOCOCCAL SEPSIS*

Summary

Striking individual differences in severity of group A streptococcal (GAS) sepsis have been noted, even among patients infected with the same bacterial strain. We had provided evidence that HLA class II allelic variation contributes significantly to differences in systemic disease severity by modulating host responses to streptococcal superantigens. Inasmuch as the bacteria produce additional virulence factors that participate in the pathogenesis of this complex disease, we sought to identify additional gene networks modulating GAS sepsis. Accordingly, we applied a systems genetics approach using a panel of advanced recombinant inbred mice. By analyzing disease phenotypes in the context of mice genotypes we identified a highly significant quantitative trait locus (QTL) on Chromosome 2 between 22–34 Mb that strongly predicts disease severity, accounting for 25–30% of variance. This QTL harbors several polymorphic genes known to regulate immune responses to bacterial infections. We evaluated candidate genes within this QTL using multiple parameters that included linkage, gene ontology, variation in gene expression, co-citation networks, and biological relevance, and identified interleukin1 alpha and prostaglandin E synthases pathways as key networks involved in modulating GAS sepsis severity. The association of GAS sepsis with multiple pathways underscores the complexity of traits modulating GAS sepsis and provides a powerful approach for analyzing interactive traits affecting outcomes of other infectious diseases.

Introduction

Infectious diseases, like most human diseases, are modulated by complex traits. Susceptibility and clinical outcomes of infections are often a manifestation of interactions between the host's complex traits and the pathogen's virulence components. Identification of genes and molecular networks that influence host responses to infectious agents can provide a disease road map that would focus the discovery of effective diagnostics and therapeutics.

Group A streptococci (GAS) are classified on the basis of surface M protein antigens into more than 100 serotypes, but recent studies showed a high degree of diversification within a serotype that is driven primarily by horizontal gene transfer (Aziz *et al.*, 2005; Sumbly *et al.*, 2005; Walker *et al.*, 2007). It is widely believed that such events are responsible for the emergence of highly virulent strains in the 1980s, including a hypervirulent MIT1 clonal strain, coinciding with the resurgence of severe invasive

* Source: Reprinted with permission. Abdeltawab, N.F., Aziz, R.K., Kansal, R., Rowe, S.L., Su, Y., Gardner, L., Brannen, C., *et al.* (2008) An unbiased systems genetics approach to mapping genetic loci modulating susceptibility to severe streptococcal sepsis. *PLoS Pathog* 4: e1000042.

GAS infections associated with streptococcal toxic shock syndrome (STSS) and necrotizing fasciitis (NF), also known as the “flesh eating” disease (Low *et al.*, 1997). We showed that this hypervirulent MIT1 clinical strain can cause sore throat or mild bacteremia and erysipelas in some patients, while in others it can cause STSS and NF (Chatellier *et al.*, 2000). These findings suggested a strong role for host factors in modulating the outcome of infection by this highly virulent strain. Indeed, we found that allelic variations in host HLA class II haplotypes are associated with markedly different outcomes of GAS sepsis in humans (Kotb *et al.*, 2002; Kotb *et al.*, 2003). We confirmed these associations using HLA transgenic mice that were expressing different HLA class II alleles (Nooh *et al.*, 2007). Inasmuch as STSS pathogenesis is largely mediated by streptococcal superantigens (Strep SAg), and because HLA class II molecules serve as SAg receptors, such an association was expected. However, GAS is rich in many other virulence factors, and we believe that some of those virulence factors, beside SAg, may also interact with additional host factors to modulate host responses to GAS infections.

To identify additional host factors involved in GAS severity we needed an approach that allowed us to uncover the effect of interactions between complex, polymorphic genetic traits that may modulate sepsis outcomes. Previous animal models for GAS sepsis included various regular conventional inbred mouse strains (Medina *et al.*, 2001; Goldmann *et al.*, 2004b), congenic strains (Goldmann *et al.*, 2005a), and HLA transgenic mice (Welcher *et al.*, 2002; Nooh *et al.*, 2007). These models confirmed that host genetic variability can have a strong effect on infection outcome. Despite their significant utility, these mouse models do not offer the genetic diversity that is characteristic of the human population.

In this study, we used a panel of advanced recombinant inbred (ARI) mice as a genetically diverse, segregating reference population that affords a powerful tool for systems genetics approaches. Recombinant inbred (RI) strains have been successfully used to map quantitative trait loci (QTLs) associated with various phenotypes and diseases (Hardy *et al.*, 2001; Rosen and Williams, 2001; Grizzle *et al.*, 2002; Peirce *et al.*, 2003; Chesler *et al.*, 2005; Mountz *et al.*, 2005; Aziz *et al.*, 2007; Miyairi *et al.*, 2007). We used the BXD panel of ARI mice derived from C57BL/6J (B6) and DBA/2J (D2) strains and consisting of homozygous, inbred BXD lines, each of which is genetically distinct. Using this genetically diverse BXD panel, we mapped QTLs modulating GAS sepsis severity, and identified candidate genes within these QTLs that were parsed into pathways likely to modulate the severity of this complex infectious disease.

Results

Variable Susceptibility to Severe GAS Sepsis in Genetically Distinct Mice

Our initial studies (Aziz *et al.*, 2007) demonstrated that there is considerable variability among BXD strains with respect to susceptibility to severe GAS sepsis. To quantify differences among strains in this study, we used three main quantitative traits, namely animal survival, bacteremia, and bacterial dissemination to spleen.

We infected mice ($n = 5\text{--}26$ mice per strain), belonging to 32 strains (30 different BXD strains and their parental strains, B6 and D2), intravenously (i.v.) with the same bacterial dose ($2 \pm 1.5 \times 10^7$ CFU/mouse). Survival was expressed as normalized corrected relative survival indices (cRSI) calculated for each of the 32 strains as detailed in materials and methods. We observed significant difference in relative susceptibility to GAS sepsis across the BXD panel ($P \leq 0.0001$), Figure 3-1-A. This wide range of susceptibility across the various strains, together with the finding that some of the strains showed phenotypes considerably more exaggerated than the parental strains (B6 and D2), is an illustration of how different combination of polymorphic genes can manifest quite differently according to the overall genetic context.

Similarly, we determined bacterial load in blood (log CFU/ml blood), 24 h post-infection and found considerable variation across the strains. In general there was an inverse correlation between mice survival and extent of bacteremia ($r = -0.471$, $P \leq 0.0001$, $R^2 = 22.2\%$), Figure 3-1-B. Bacterial dissemination to spleen also varied across the strains, showing a stronger inverse correlation with mice survival ($r = -0.717$, $P \leq 0.0001$, $R^2 = 51.4\%$), Figure 3-1-C.

Although these inverse correlations between mice survival and bacterial load in blood and spleen made biological sense because it is anticipated that susceptible strains would have higher bacterial load than in resistant strains, there were several exceptions. For example, although strains BXD44 and BXD45 are ranked susceptible based on their survival, they showed low bacterial load in blood and spleen. Similarly, BXD43 and BXD85 strains, which are ranked resistant, had a high bacterial load in their spleen. Another interesting observation was that, in general, susceptible strains survival was better correlated with bacterial load in blood and spleen than resistant strains. Together, these findings confirm that there is more than one mechanism modulating differential susceptibility or resistance to severe GAS sepsis (Aziz *et al.*, 2007).

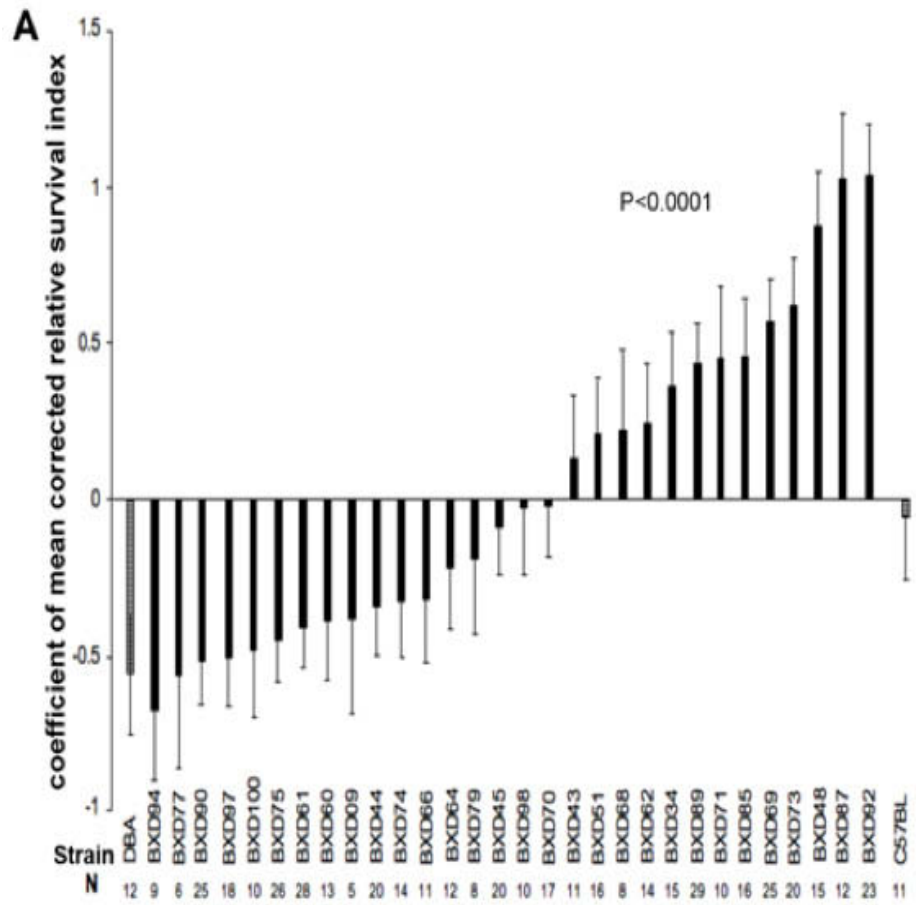
Genome-wide Scans for Mapping GAS Susceptibility Quantitative Trait Loci

We used bioinformatics tools available through Gene Network (GN) to link measured phenotypes to strains genotypes. Each of the quantified phenotypes was analyzed in the context of the studied mice genotypes and single nucleotide polymorphism (SNPs) using 3795 SNPs and microsatellite markers for BXD strains. Significant QTLs modulating survival, bacteremia 24 h post-infection and bacterial dissemination to spleen mapped to mouse Chromosome (Chr) 2.

The strongest QTL modulating mouse survival (cRSI) mapped to mouse Chr 2 between 22–34 Mb, with an likelihood ratio statistic (LRS) of 34.2 ($P \leq 0.0000001$), Figure 3-2-A. A second less significant QTL was also mapped on the same chromosome between 125–150 Mb with an LRS of 12 ($P \leq 0.001$), and a third QTL on Chr X, Figure 3-2-A. The QTLs for bacteremia and bacterial dissemination to spleen overlapped with

Figure 3-1. Differential susceptibility to GAS sepsis among different BXD strains and their parental strains.

(A) Rank-ordered bar chart of survival expressed as mean values of coefficient of mean corrected relative survival indices (cRSI) across 30 different BXD strains and their parental strains (DBA/2J and C57Bl/6J). N = 489 belonging to 32 strains; number of mice used per strain is indicated. (B) Bar chart of GAS bacteremia expressed as coefficient of mean values of corrected log blood CFUs 24 h post injection (corrected log CFU/ml blood). (C) Bar chart of GAS dissemination to spleen expressed as coefficient of corrected bacterial load in spleen (log CFU/spleen). B and C Strains are ordered by their corrected relative survival indices with the parental strains at the two extremes of the X-axis. Error bars represent the standard errors of the means. Statistical test is two-way ANOVA (with correction to covariates) $P \leq 0.0001$.



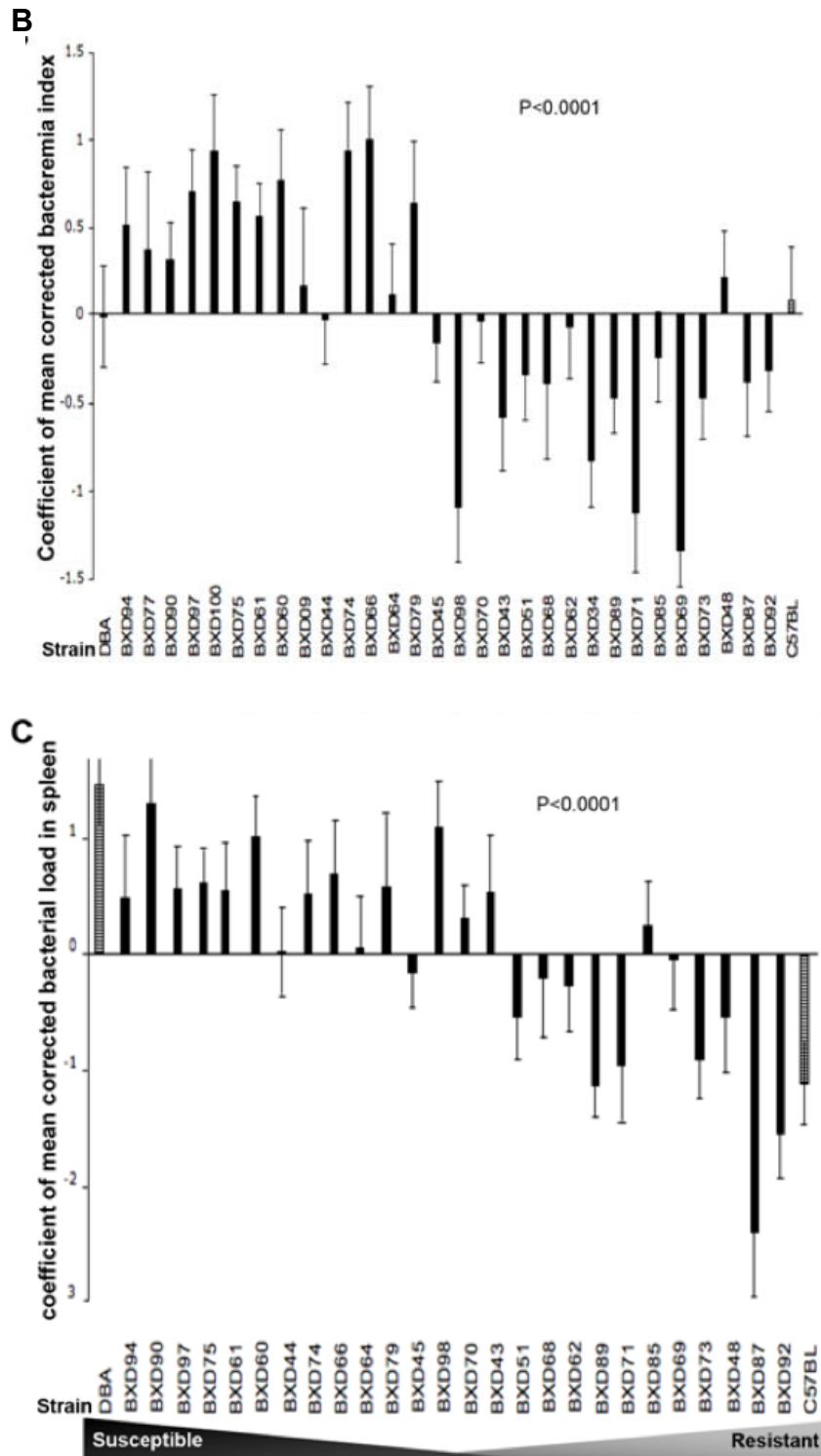
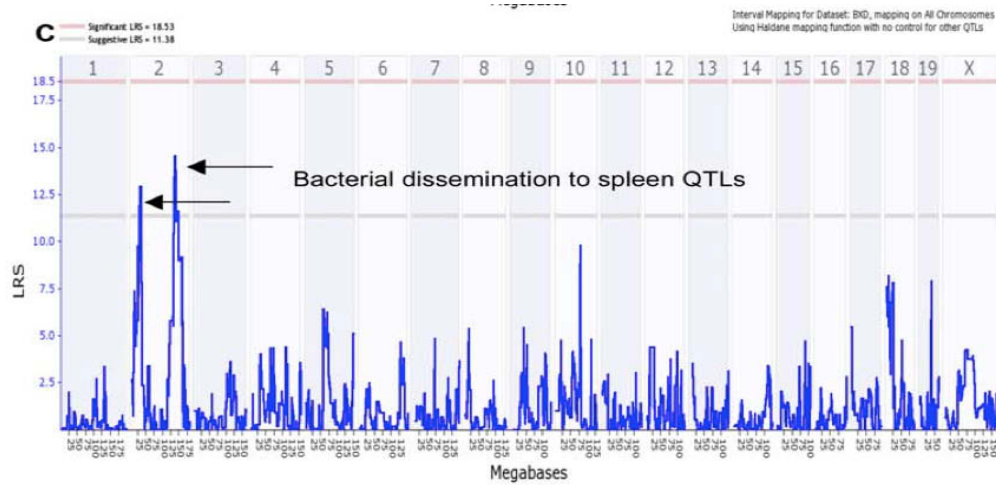
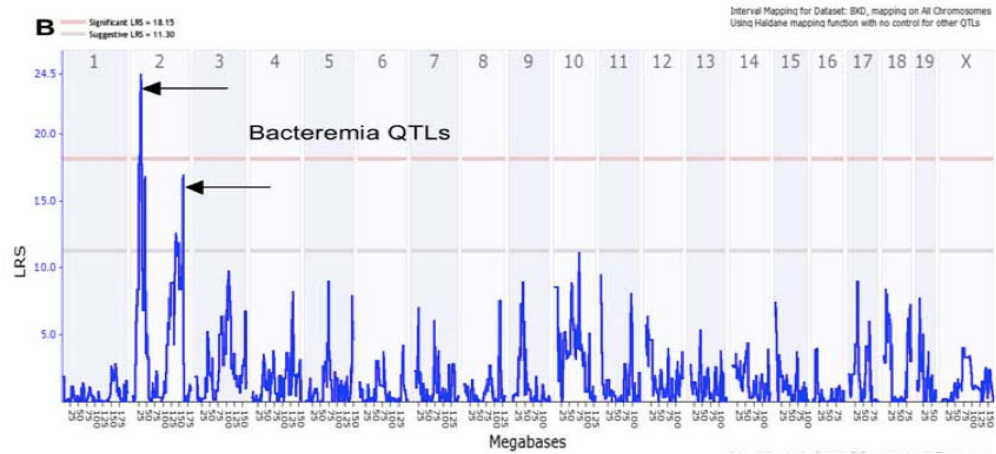
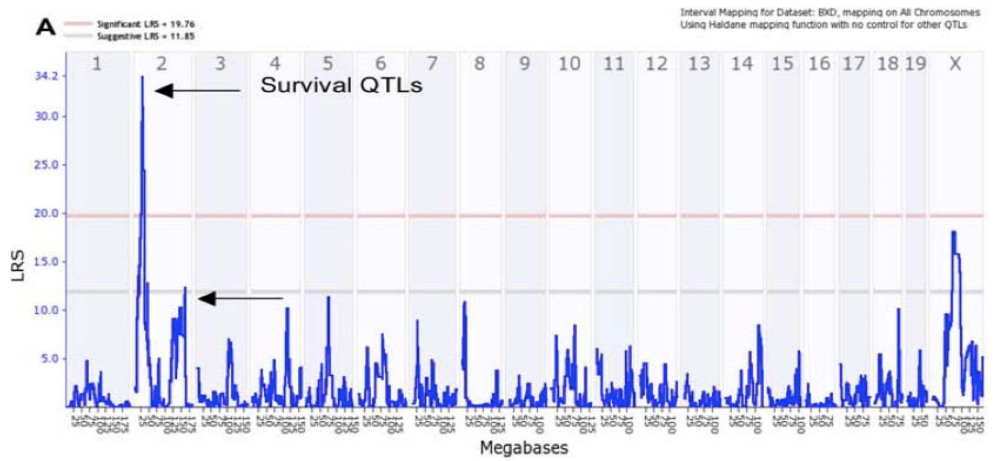


Figure 3-1. (Continued).

Figure 3-2. Genome-wide scan for mice susceptibility to GAS sepsis showing mapped QTL on Chr 2.

Interval mapping of survival (expressed as corrected relative survival index, cRSI), showing a significant QTL (based on 1000 permutation tests) on Chr 2 between 22–34 Mb with LRS of 34.2 ($P \leq 0.0000001$), and a suggestive QTL between 125–150 Mb with LRS of 12 ($P \leq 0.001$). (B) Whole genome interval mapping of GAS bacteremia using bacterial load 24 h post injection expressed as corrected log CFU/ml blood, showing two QTLs on Chr 2: first QTL between 22–34 Mb with LRS of 24.5 ($P \leq 0.00001$) and a second with LRS of 17 ($P \leq 0.0001$) between 125–150 Mb. (C) Whole genome mapping of GAS sepsis using tissue dissemination of GAS expressed as corrected log CFU/spleen with QTL between 125–150 Mb with LRS of 15 ($P \leq 0.0001$). Red line indicates significant LRS, while grey line indicates suggestive LRS. Upper x-axis shows mouse chromosomes, and lower x-axis shows physical map in mega bases, y-axis represents linkage in LRS score.



those for survival, with slight difference in significance. The first QTL modulating bacteremia mapped to Chr 2 between 22–34 Mb with an LRS of 24.5 ($P \leq 0.00001$), Figure 3-2-B. The second QTL mapped to the same chromosome between 125–150 Mb with an LRS of 17 ($P \leq 0.0001$), Figure 3-2-B. A QTL modulating bacterial dissemination to spleen also mapped to Chr 2 between 125–150 Mb with LRS of 15 ($P \leq 0.001$), Figure 3-2-C.

To further investigate and narrow down the mapped region on Chr 2, we resorted to haplotype maps of BXD strains to select additional strains that may be informative in validating, and further confirming mapped QTLs.

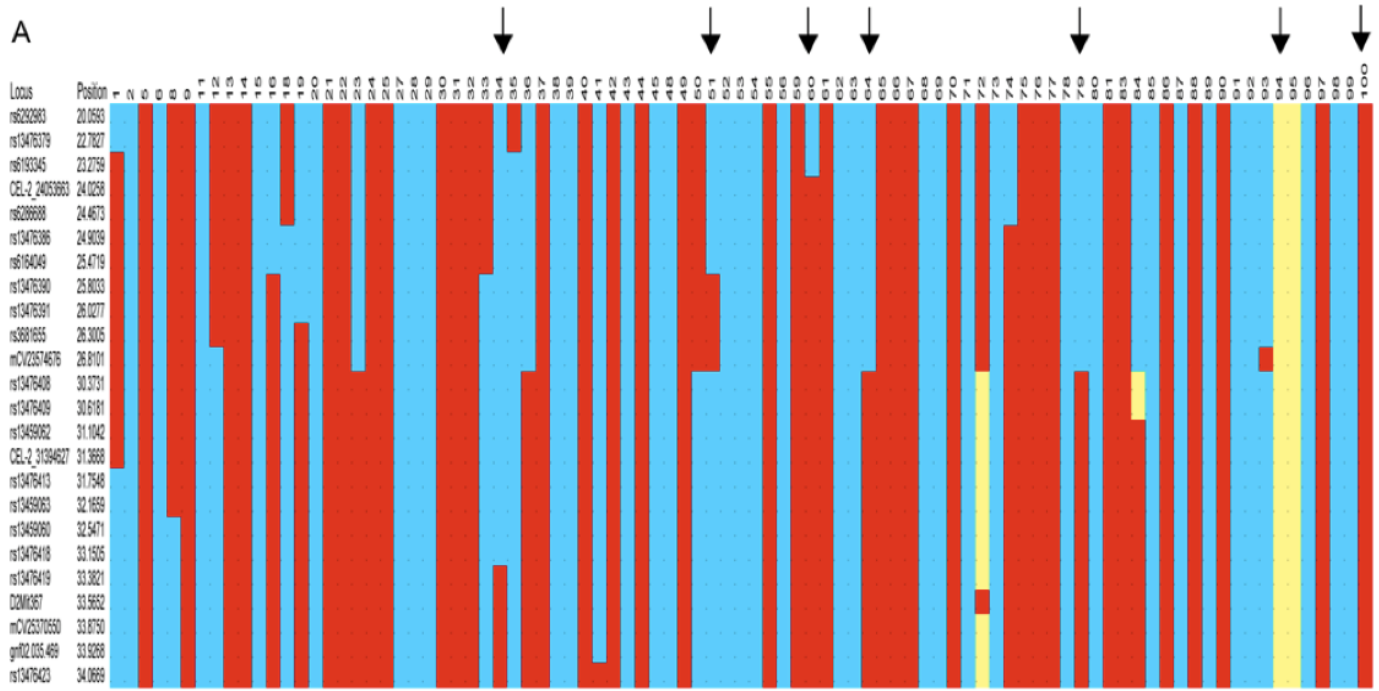
***In silico* Prediction of BXD Susceptibility to Severe GAS Sepsis**

Our mapped QTLs directed us to select more strains for survival experiments based on differences in their haplotypes within the QTLs. For example, we selected BXD100 with a *D* haplotype at Chr 2 between 22–34 Mb region, Figure 3-3-A, and found it to be susceptible. Similarly, we tested BXD87 with a *B* haplotype in the same region and this strain as predicted, exhibited a resistant phenotype. To further narrow down the mapped QTLs, we chose strains with breakage in the mapped interval, i.e. with recombination at Chr 2 region 22–34 Mb for further survival testing (Figure 3-3-A). BXD34 with a *B* haplotype at Chr 2 between 24–33.15 Mb region was resistant, while BXD60 with a *B* haplotype at Chr 2 between 20–23.27 Mb region was susceptible, Figure 3-1-A and 3-3-A. This narrowed down the relevant susceptibility region to Chr 2 between 23.27–33.15 Mb. Using more strains with recombination at this narrowed region, we found BXD51, 64, and 79 to be quite interesting as they showed intermediate resistance suggesting that genes at this region are candidate modulators of the mapped QTL, Figure 3-3-B. Another interesting strain was BXD94 that we found susceptible to infection, yet has a heterozygous genotyping, suggesting that *D* allele exhibited dominance, Figure 3-3-B.

Similarly, we inspected haplotypes of studied BXD strains at the second QTL between 125–150 Mb (Figure 3-3-C), the majority of susceptible strains had *D* alleles, while resistant strains had *B* alleles with some exceptions, for example BXD77 is a susceptible strain, yet had *B* alleles. It was interesting to find that the susceptible strain BXD44 had *B* alleles at this QTL (Figure 3-3-C), suggesting that observed lower bacterial load in blood compared to other susceptible strains (Figure 3-1-B) might be modulated by *B* allele in the second QTL. Meanwhile, BXD48, a resistant strain, has a breakage at 135.9 Mb (Figure 3-3-C) with *D* alleles suggesting that its relatively higher bacterial load in blood (Figure 3-1-B) might be modulated by the second QTL. Collectively, these findings suggest that both loci modulate different observed phenotypes of GAS sepsis severity.

Figure 3-3. Recombinant inbred BXD strain distribution patterns at region of interest on Chr 2.

(A) Haplotype maps of the first QTL on Chr 2 between 20–34 Mb showing available BXD strains. Haplotype maps were used for *in silico* selection of strains for survival studies based on the strain distribution patterns, where B allele (blue bars) inherited from the resistant parent C57Bl/6J and D alleles from the susceptible parent DBA/2J, beige bars indicate strains that are heterozygous at this region, resembling an F1. Arrows indicate BXD strains 34, 51, 60, 64, 79, 94, and 100. Recombinant inbred BXD strain distribution patterns at region of interest on Chr 2. (B) Haplotype maps of the first QTL region on Chr 2 between 20–34 Mb across BXD strains used in the population-based survival experiments showing the pattern of alleles inherited from each parent at region of interest on Chr 2. The different BXD strains are rank-ordered according to their susceptibility to GAS sepsis from susceptible to more resistant. Resistant strains show a pattern of accumulation of alleles inherited from resistant parent (B) C57Bl/6J (blue bars) while the susceptible strains show a pattern of alleles from susceptible parent (D) DBA/2J (red bars), with the exception of BXD94 strain, heterozygous (beige bars) at the QTL region. (C) Haplotype maps of the second QTL region on Chr 2 between 125–150 Mb across BXD strains used in the population-based survival experiments showing the pattern of alleles inherited from each parent at region of interest on Chr 2. The different BXD strains are rank-ordered according to their susceptibility to GAS sepsis from susceptible to more resistant. BXD genotype data set can be downloaded from www.genenetwork.org/genotypes/BXD.geno.



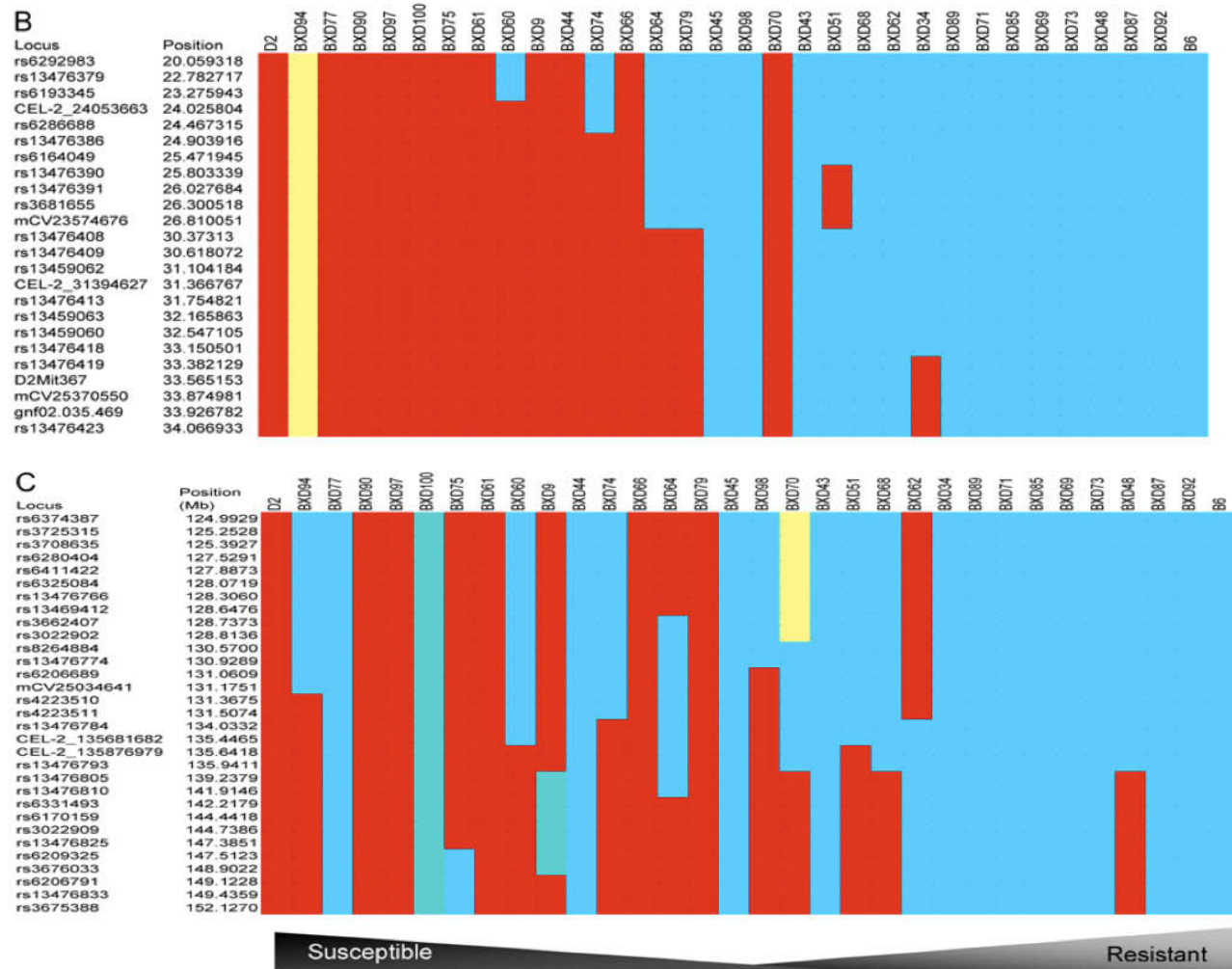


Figure 3-3. (Continued).

Mining for Candidate Genes and Pathways in Mapped Loci

Based on our *in silico* strain selection and QTL validation by experimental assessment, we evaluated candidate genes within the mapped QTLs, taking into account linkage, gene ontology analyses, co-citation networks, and biological relevance. To categorize genes and transcripts in the mapped QTLs into functional pathways, we performed functional analyses using Ingenuity Pathways Analysis (IPA) (www.ingenuity.com). We parsed our genes into 50 functional networks; the most relevant networks involved those associated with immune response, cell signaling, cellular assembly and organization, and lipid metabolism. From these interrelated pathways, we selected 37 representative genes to study their role in GAS susceptibility QTL by quantitative analysis of their expression levels in selected resistant and susceptible strains (groups) pre- and post-infection (Appendix A. Table A-1).

We found that 28 out of a representative 37 genes were differentially expressed post-infection (Appendix A. Table A-2), of those 14 genes were down regulated in the resistant group while up regulated in the susceptible group post-infection. Nine genes were down regulated in both groups post-infection, and five were up regulated in both groups post-infection (Appendix A. Table A-2). Fourteen of the 28 differentially expressed genes showed significant change post-infection in both resistant and susceptible strains (Table 3-1 and Figure 3-4). In general, susceptible strains showed an increase in the relative expression levels post-infection (19 genes) of both pro and anti-inflammatory genes, e.g. interleukin1 alpha (*Il1 α*), and IL1 receptor antagonist (*Il1rn*) respectively. By contrast, in the resistant BXD strains, most of the tested genes showed a decrease (23 genes) in expression levels post-infection with few exceptions (five genes) e.g. TNF receptor associated factor 1 (*Trafi1*) (Figure 3-4 and Appendix A. Table A-2). Differentially expressed genes were associated with both innate and early adaptive immune response. Among those associated with early immune response, *Il1a*, *Il1rn*, prostaglandin E synthase (*Ptges*), and *Ptges2* were up regulated in susceptible strains, whereas their levels decreased in resistant strains. Several of the differentially expressed genes show polymorphisms as SNPs between the parental strains B6 and D2, suggesting that these polymorphic genes modulate differential response to infection (Appendix C). The differential expression of IL1 α was confirmed at the protein level (data not shown).

We parsed the differentially expressed genes into pathways, using IPA, IL1 and prostaglandins were key early response molecules modulating susceptibility to severe GAS sepsis in two of the mapped networks, which are shown merged in Figure 3-5. The first network ($P < 10^{-27}$) comprised of genes related to lipid metabolism and innate immunity, e.g. *Il1a*, *Il1rn*, *Ptges*, while the second network ($P < 0.01$) contained genes modulating nucleic acid metabolism, energy production and host responses to injury e.g. Ectonucleoside triphosphate diphosphohydrolase 2 (*Entpd2*) (Figure 3-5).

Discussion

It has been established that networks of multiple pathways, rather than a single gene, modulate traits and affect susceptibility and outcomes of virtually all diseases. The

Table 3-1. The relative expression levels of candidate genes post infection in resistant and susceptible strains expressed as ratio of post/pre infection in susceptible and resistant strains.

Gene ID	Gene	Resistant Strains	P-value ^a	Susceptible Strains	P-value
Genes down regulated in resistant group while up regulated in susceptible group					
<i>Anapc2</i>	Anaphase promoting complex subunit 2	0.551	0.022 *	1.475	0.509
<i>Il1α</i>	Interleukin 1 a	0.739	0.010 *	44.525	0.062 †
<i>Il1rn</i>	Interleukin 1receptor antagonist	0.851	0.680	54.687	0.221
<i>Ptges</i>	Prostaglandin E synthase	0.417	0.001 *	6.363	0.028 *
<i>Ptges2</i>	Prostaglandin E synthase 2	0.913	0.774	1.456	0.005 *
<i>Sh2d3c</i>	SH2 domain containing 3C	0.162	0.055 †	1.009	0.980
Genes down regulated in both resistant group and susceptible groups					
<i>Entpd2</i>	Ectonucleoside triphosphate diphosphohydrolase 2	0.359	0.010 *	0.654	0.064 †
<i>Edf1</i>	Endothelial differentiation-related factor 1	0.349	0.095 †	0.470	0.014 *
<i>Garnl3</i>	GTPase activating RANGAP domain-like 3	0.601	0.142	0.674	0.070 †
<i>Nfatc2</i>	Nuclear factor of activated t-cells, cytoplasmic, calcineurin-dependent 2	0.178	0.095 †	0.693	0.208
<i>Phpt1</i>	Phosphohistidine phosphatase 1	0.229	0.077 †	0.714	0.233
<i>Psm5</i>	Proteasome (prosome, macropain) 26S subunit, non-ATPase 5	0.644	0.006 *	0.963	0.652
<i>Ppp2r4</i>	Protein phosphatase 2A regulatory subunit B	0.902	0.256	0.734	0.091 †
Genes up regulated in both resistant group and susceptible group					
<i>Traf1</i>	TNF receptor associated factor 1	1.826	0.300	5.995	0.066 †

^a Significance based on t-test, * P < 0.05, † P = 0.06–0.08

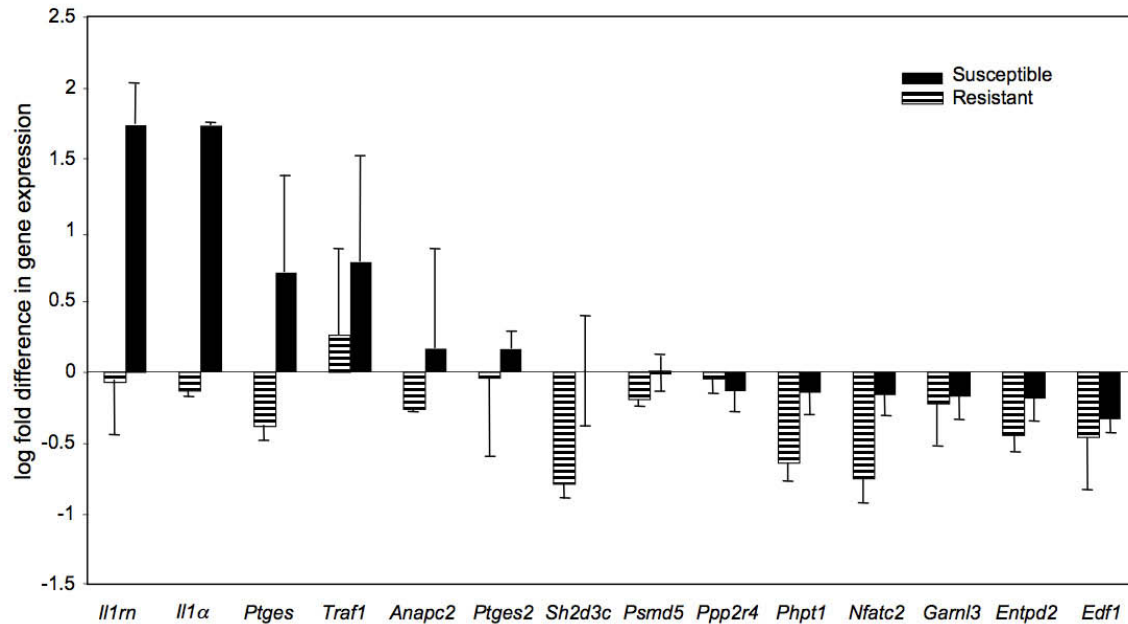


Figure 3-4. Patterns of differential gene expression levels of candidate genes post infection in susceptible and resistant strains.

Quantitative PCR results showing levels of gene expression of 14 genes with significant ($P = 0.05-0.08$) change post-infection in susceptible and resistant strains, expressed as Log_{10} fold differences in gene expression level post-infection. Genes are grouped to three groups, a) genes up regulated in susceptible strains post-infection and decreased in resistant strains post-infection, b) genes down regulated in both susceptible and resistant strains post-infection, and c) genes up regulated in both susceptible and resistant strains post-infection. Susceptible strains are represented as solid black bars, we used two highly susceptible strains BXD61 and BXD90, and resistant strains as dashed bars, we used two highly resistant strains BXD 73 and BXD87. The bars represent 2–4 biological replicates run in three technical replicates each and significance is based on t-test. *Anapc2*, anaphase promoting complex subunit 2; *Entpd2*, ectonucleoside triphosphate diphosphohydrolase 2; *Edf1*, endothelial differentiation-related factor 1; *Garnl3*, GTPase activating RANGAP domain-like 3; *Il1a*, interleukin 1 alpha; *Il1rn*, interleukin 1 receptor antagonist; *Nfatc2*, nuclear factor of activated t-cells, cytoplasmic, calcineurin-dependent 2; *Phpt1*, phosphohistidine phosphatase 1; *Ptges*, prostaglandin E synthase; *Ptges2*, prostaglandin E synthase 2; *Psm5*, proteasome (prosome, macropain) 26S subunit, non-ATPase 5; *Ppp2r4*, Protein phosphatase 2A regulatory subunit B; *Sh2d3c*, SH2 domain containing 3C; *Traf1*, TNF alpha receptor associated factor.

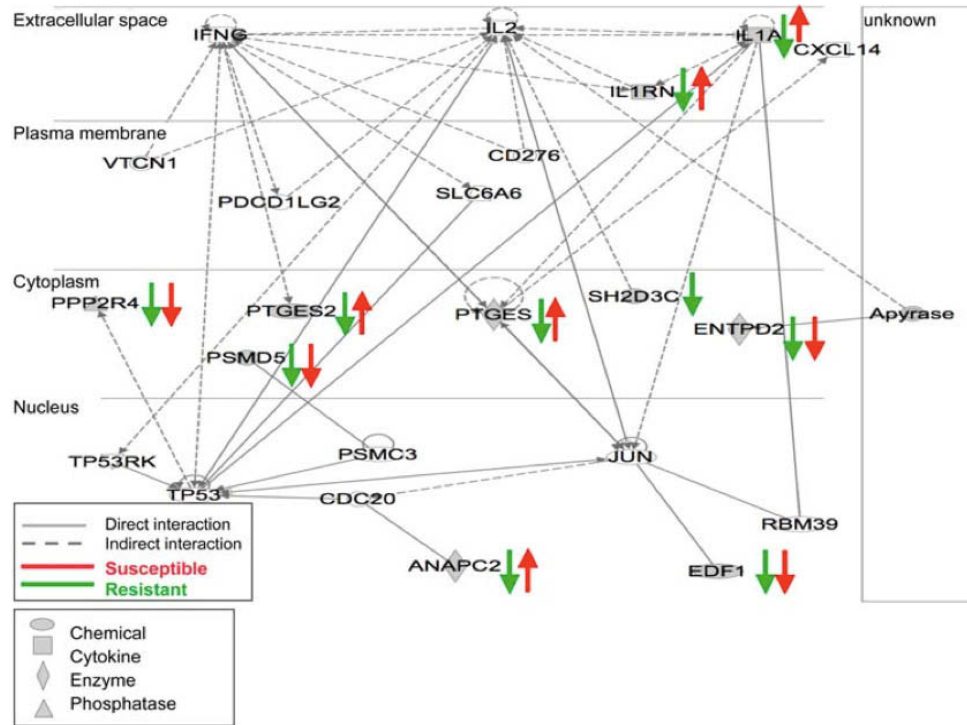


Figure 3-5. Functional network of genes modulating GAS QTL.

Graphical representation of the molecular relationships between differentially expressed genes, showing the central role of IL1, IL1rn, PTGES, and PTGES2 in modulating response to GAS sepsis and their indirect interactions with IFN γ and IL2 networks in modulating bacterial sepsis. Genes are represented as nodes, and the biological relationship between two nodes is represented as line, solid lines represent direct interactions, dashed lines represent indirect interactions. Oval shapes represent chemical or drug, squares represent cytokines, diamond shapes represent enzymes, concentric circles represent group of family, and triangles represent phosphatases. Blue lines and arrows represent expression levels of resistant strains, while red lines and arrows represent susceptible strains expression levels. Apyrase, ATP diphosphohydorlase; ANAPC2, anaphase promoting complex subunit 2; CDC20 cell division cycle homolog 20; CXCL14, chemokine (c-x-c motif) ligand 14; ENTPD2, ectonucleoside triphosphate diphosphohydrolase 2; EDF1, endothelial differentiation-related factor 1; JUN jun oncogene; IL1A, interleukin 1 alpha; IL1RN, interleukin 1receptor antagonist; IFNG interferon gamma; IL2 interleukin2; PDCD1LG2, programmed cell death ligand 2; PTGES, prostaglandin E synthase; PTGES2, prostaglandin E synthase 2; PSMC3 proteasome (prosome, macropain) 26S subunit ATPase 3; PSMD5, proteasome (prosome, macropain) 26S subunit, non-ATPase 5; PPP2R4, protein phosphatase 2A regulatory subunit B; RBM39, RNA binding protein 39; SH2D3C, SH2 domain containing 3C; SLC6A6, solute carrier family 6; TP53 tumor protein p53; TP53RK, TP53 regulating kinase; VTCN1, V-set domain containing T cell activation inhibitor 1.

ARI strains used in this study afford one of the best unbiased forward genetics approaches to determine how different combinations of polymorphic genes interact to shape disease phenotypes. Using ARI-BXD panel as a genetically diverse reference population, we were able to map QTLs modulating specific phenotypes associated with severe GAS sepsis.

GAS causes a wide range of diseases depending on multiple factors including site and route of infection, interplay of the pathogen virulence factors with host immune defenses that are affected by the host immune status and difference in the genetic makeup of the host (Kotb *et al.*, 2002). Thus, these bacteria represent a good model to explore the impact of host complex traits on susceptibility to infections. Previous studies have shown that host-pathogen interactions modulate the severity of GAS sepsis (Chatellier *et al.*, 2000; Medina *et al.*, 2001; Kotb *et al.*, 2002; Goldmann *et al.*, 2004b), and we found that patients with GAS sepsis expressing HLA class II DRB1*15/DQB1*06 (DR15/DQ6) haplotype are protected from severe GAS sepsis, whereas those with HLA class II DRB1*14/DQB1*05 (DR14/DQ5) haplotype are at high risk for developing severe and often fatal forms of the disease (Kotb *et al.*, 2002). The strong association between disease severity and HLA class II allelic polymorphism is primarily related to the differential ability of HLA class II alleles to present SAgS to T cells, where presentation of Strep SAgS by the protective HLA class II alleles results in a significantly attenuated response as compared to their presentation by the neutral or high-risk alleles (Kotb *et al.*, 2002; Norrby-Teglund *et al.*, 2002; Nooh *et al.*, 2007). While this association made perfect biological sense based on the known central role of SAgS in the human disease, mice are not susceptible to SAgS due to an inherent lower affinity of mouse MHC class II molecules to GAS SAgS. The role of GAS SAgS can be well investigated in HLA class II transgenic mice as others and we have reported (Leder *et al.*, 1998; Andersen *et al.*, 1999; Welcher *et al.*, 2002; Nooh *et al.*, 2007). However, due to the overwhelming response to SAgS in these mice, it is difficult to use them to dissect host response to other GAS virulence factors in the disease process. For this reason, our present ARI mouse model of sepsis is ideal for identifying host genetic variations, besides the MHC class II antigens, that may also contribute to differences in GAS sepsis severity.

We invested time and effort to standardize the GAS infection model using a large number of BXD mice ($n = 717$) and this allowed us to optimize infection dose and identify significant covariates (e.g. age and sex) needed to be accounted for in our final analysis (Aziz *et al.*, 2007). Although GAS strains can vary considerably with regards to virulence, we showed that the same virulent strain could cause diseases with starkly different severity in humans (Chatellier *et al.*, 2000; Kotb *et al.*, 2002). The strain used in this study is a hypervirulent derivative of the MIT1 clonal strain that emerged in the 1980s at the same time that the severe forms of the invasive GAS infections resurged (Kazmi *et al.*, 2001; Aziz *et al.*, 2004a; Buchanan *et al.*, 2006; Walker *et al.*, 2007). Initial studies (Aziz *et al.*, 2007) identified an optimal infection dose of $2 \pm 1 \times 10^7$ CFU/mouse, and indicated the need to use mice with an age range of 40–120 days for linear correlation with survival. In addition, these pilot studies determined that sex has insignificant effect in this GAS sepsis model (Aziz *et al.*, 2007) and revealed a stark variation among various BXD strains used with respect to their susceptibility to severe

sepsis. However, precise mapping of QTLs required that we study more BXD strains and include more mice per BXD strain to obtain statistical power.

With a total of 30 BXD strains and an average of 15 mice per strain, we mapped QTLs on Chr 2 that modulate severity to GAS sepsis, measured by comparing mice survival post-infection, bacterial load in blood, and bacterial dissemination to spleen across the BXD strains. Inasmuch as the BXD strains are heavily genotyped with more than 3600 genomic markers, identifying QTLs is relatively straightforward. The mapped QTLs on Chr 2 harbor a relatively large number of candidate genes associated with various functional networks and signaling pathways including nuclear factor- κ B (NF- κ B) and p38 mitogen activated protein kinases (MAPK) pathways, proliferation of immune cells, and eicosanoid signaling. Such output is typical of unbiased genome-wide analysis studies, and required further analyses to determine which of these genes are the key modulators of the studied trait.

To narrow down the gene list to a handful of genes that can be experimentally validated, we used multiple methods including linkage, gene ontology, and differential gene expression analyses. Our quantitative PCR analysis of 37 representative candidate genes showed that 28 genes were differentially expressed in selected susceptible and resistant strains post-infection. These differentially expressed genes fell into three main categories, genes associated with innate and adaptive immune response, and genes associated with apoptosis. Differentially expressed genes associated with innate immune response were both pro- and anti-inflammatory as well as adaptive immune response genes associated with T and B cell proliferation and differentiation, cell signaling and antigen processing and presentation.

Differentially expressed genes associated with innate immune response were either related to pro- or anti-inflammatory responses. Both pro- and anti-inflammatory associated genes were up-regulated in the selected susceptible strains post-infection, and this is in agreement with a recent study by Goldmann, *et al.* (2007) who showed a mixed pro- and anti-inflammatory response belonging to M1 and M2 macrophage phenotypes in response to GAS infection. This increase in both pro- and anti-inflammatory response could be attributed to homeostatic mechanisms where, for example, the increase in *Il1* levels in the susceptible strains was accompanied by an increase in its endogenous antagonist *Il1rn*. This was not the case in the resistant strains that showed decreased levels of expression of pro- and anti-inflammatory related genes both pre- and post-infection. These findings suggest that susceptibility to GAS sepsis is associated with an overzealous innate immune response as observed in susceptible BXD strains only. These results mirror previous findings in humans, where association of exaggerated inflammatory responses, including IL1, with susceptibility to GAS sepsis was detected (Norrby-Teglund *et al.*, 2000; Norrby-Teglund and Kotb, 2000; Kotb *et al.*, 2002). However, unlike what we found in this mouse model, human responses are dominated by high levels of IFN γ and TNF β , presumably because the human disease is driven primarily by SAGs (Norrby-Teglund *et al.*, 1997; Norrby-Teglund *et al.*, 2000).

In general, differentially expressed genes associated with early adaptive immune

responses showed a pattern of decrease in expression levels in both susceptible and resistant strains with the exception of anaphase promoting complex subunit 2 (*Anapc2*) that was slightly increased in susceptible strains post-infection (Figure 3-5). By contrast, several genes associated with pro- and anti-apoptotic response were differentially expressed in the selected susceptible and resistant strains post-infection (Figure 3-5). Apoptosis in streptococcal pathogenesis is affected by interacting factors including, context of infection (Marriott and Dockrell, 2006), cells undergoing apoptosis (Kobayashi *et al.*, 2003; Nakagawa *et al.*, 2004; Miyoshi-Akiyama *et al.*, 2005), for example, apoptosis aids in the clearing of infection if macrophages are undergoing apoptosis, while it would be harmful to the host if lymphocytes are undergoing apoptosis. Other factors include, whether the bacteria is internalized or extracellular (Cywes Bentley *et al.*, 2005) and accordingly the type of apoptosis pathways activated (Klenk *et al.*, 2005). In our murine GAS sepsis model, we have measured expression levels in whole spleens, which involved the response of various cells including macrophages, T and B lymphocytes, dendritic and endothelial cells etc. Consequently, we expected to observe a mixed response; however, in our ongoing studies, we are examining possible alterations in splenic population profiles post-infection in the various BXD strains to determine which cell types are responsible for the major differences in cytokine levels seen post-infection and to dissect the role of different cell populations in this GAS sepsis model.

Another interesting observation was that the relative expression level of genes measured in the selected resistant strains showed a pattern of decrease post-infection, with the exception of five genes, heat shock 70KDa protein 5 (*Hspa5*), *Traf1*, *Traf2*, Notch gene homolog 1 (*Notch1*), and signal-regulatory protein alpha (*Sirpa*). It is worthy to note the link between these genes, as they are involved directly and indirectly with activation of early adaptive response. *Hspa5* is an Hsp70, which is associated with cytoprotection, anti-apoptosis, and anti-inflammation (Kiang and Tsokos, 1998; Yenari *et al.*, 2005; Kim *et al.*, 2006), and has been associated with immune response to sepsis (Kustanova *et al.*, 2006; Singleton and Wischmeyer, 2006). *Notch1* has been associated with the signaling involved in regulation of lymphocytes development and activation to effector cells (Minato and Yasutomo, 2005), natural killer cells development (van den Brandt *et al.*, 2004; Garcia-Peydro *et al.*, 2006; Rolink *et al.*, 2006) and recently *Notch1* was associated with macrophage activation (Monsalve *et al.*, 2006). We took into consideration in our experimental design that stress might alter the expression of stress related genes especially heat shock proteins and chemokines, therefore, we subjected control mice to the same stress as infected mice by injecting control mice with saline, so that any change in expression levels would be accounted to GAS sepsis.

Among the differentially expressed genes, four genes, *Il1*, *Il1rn*, *Ptges*, and *Ptges2*, showed marked up regulation in susceptible strains, while they showed no change or slight decrease in levels in resistant strains post-infection (Figure 3-5). Increase in expression of *Ptges* and *Ptges2* genes is induced by the increased levels of *Il1* (Bream *et al.*, 2000), which is an indirect effect of the activation of IFN γ (Figure 3-5). *Ptges* and *Ptges2* are prostaglandin synthases for the lipid inflammatory mediators PGE₂, which along with platelet activating factor and leukotrienes; mediate vasodilatation in the early response to inflammation (Harris *et al.*, 2002; Mosca *et al.*, 2007). Vasodilatation in turn

leads to hypotension, a hallmark of STSS. Although the role of prostaglandins in inflammation and immune response has long been studied, their role in the immune response to infectious diseases has been lately pursued (Ruiz *et al.*, 1998; Maloney *et al.*, 2000; Smith *et al.*, 2002; Chen *et al.*, 2004; Jobin *et al.*, 2006; Woolard *et al.*, 2007). Increased production of prostaglandins has been associated with various Gram positive bacterial infections including *Streptococcus suis* (Jobin *et al.*, 2006), group B streptococcal (Maloney *et al.*, 2000), and GAS skin infections (Ruiz *et al.*, 1998).

In conclusion, our holistic approach of studying the genetic basis of differential susceptibility to GAS sepsis revealed loci on Chr 2 that harbor major immune modulators. In the present study, we examined the interactions of pathogen multiple virulence factors with the host immune system in an *in vivo* model of sepsis using a genetically diverse reference population. This shed light on a network of host genes modulating variation in GAS severity, which includes cytokines, pro- and anti-inflammatory mediators, and genes associated with apoptosis and early adaptive immune response. Our ongoing detailed studies to identify interactive molecular pathways contributing to the complex trait of GAS sepsis will undoubtedly help us dissect the various mechanisms by which the host interacts with the bacteria *in vivo*, resulting in resistance or increased susceptibility to severe GAS sepsis.

Materials and Methods

Mice

We generated the BXD advanced recombinant inbred (ARI) mice at UTHSC by crossing B6 and D2 mice to generate F1 hybrids, which were crossed to generate F2 progeny, each with random patterns of recombination. Random crossing of F2 mice generated F3 and so on, till F11 generation, after which we designated pairs of F11 hybrids as parents of each BXD line, and inbred them by sib mating for >20 generations to achieve homozygosity for each genetically distinct BXD line. This breeding scheme was done to increase recombination events resulting in roughly double the number of recombinations per strain compared to conventional RI strains (Williams *et al.*, 2001; Peirce *et al.*, 2004).

The genomes of the B6 and D2 parental strains have been sequenced and a database of their SNPs is available at the Gene Network (GN) web site (www.genenetwork.org/webqtl/snpBrowser.py). Simple sequence length polymorphism (SSLP) markers were typed for all BXD RI strains as previously described (Williams *et al.*, 2001). The BXD progeny is genotyped at 13377 SNPs and microsatellite markers (Shifman *et al.*, 2006), a selected subset of 3795 SNPs and microsatellite markers used by GN BXD genotype dataset for mapping traits, can be downloaded at www.genenetwork.org/genotypes/BXD.geno.

We recently standardized the model of BXD ARI mice for use in GAS infection studies (Aziz *et al.*, 2007). In the current study, a total of 696 mice were used, from

which 183 flagged mice were excluded based on predetermined criteria as previously detailed in (Aziz *et al.*, 2007). All procedures involving mouse tissues were approved by the institutional animal care and use committee at the UTHSC.

Experimental Design

Population-based experiments

Groups of 5–26 mice from a total of 30 BXD lines and their parental strains (B6 and D2) were injected via tail vein with $2 \pm 1.5 \times 10^7$ CFU/mouse of a hypervirulent form of the clinical isolate GAS 5448 (M1T1) (Chatellier *et al.*, 2000; Aziz *et al.*, 2004a; Aziz *et al.*, 2004b) as detailed previously (Aziz *et al.*, 2007). Mortality and weight loss were recorded every 8 h for the ensuing 6 days. To normalize across experiments, we inspected survival days distribution clusters for each experiment and determined multimodal distribution and boundaries of each cluster for a total of three clusters: susceptible, intermediate, and resistant. Survival days within each cluster were then converted into a survival index ranging from 0.25–1, 1.25–2, and 2.25–3 for susceptible, intermediate, and resistant clusters respectively. The survival index was assigned to each mouse irrespective of its strain. Indices for each strain, across experiments were then corrected for significant covariates (age, sex, body weight, and inocula) using multiple regression analyses.

Phenotype assessment experiments

We designed experiments for the assessment of survival, bacteremia, and bacterial dissemination to spleen. We assessed relative mice survival and bacteremia in the same experiment. We measured bacteremia as CFU/ml by culturing serial dilutions of blood drawn from mice tails 24 h post-injection. We determined bacterial load in spleen by homogenizing spleens of expired mice using tissue homogenizer, TH (Omni International, Marietta, GA). Each tissue homogenate was serially diluted 10 folds to 10^{-6} fold, and each dilution was cultured for determination of bacterial load in spleens (CFU/ml) that was then normalized to spleen weight and expressed as CFU/spleen.

Quantitative Trait Loci Mapping

We performed QTL mapping using web-based complex trait analysis available on the GN website and the mapping module which analyzes phenotypes in context of mouse genotypic differences. Interval mapping evaluates potential QTL at regular intervals and estimates the significance at each location using 1000 permutation tests (Churchill and Doerge, 1994). We performed three sets of analyses using strain means for the following three variables: (1) corrected relative survival index, described earlier, (2) log bacterial load in blood 24 h post injection, and (3) log bacterial load in spleen at expiration.

Quantitative PCR Analysis for Target Genes Expression

We investigated the differential expression of target genes in spleen of infected vs. control PBS-injected mice at selected time points; we selected strains based on their susceptibility, BXD61 and 90 representing susceptible strains, and BXD73 and 87, representing resistant strains. We performed 2–3 biological replicates of each set of paired susceptible and resistant ($n = 6–8$ per strain). Mice were sacrificed 40 h post i.v. injection with $2 \pm 1.5 \times 10^7$ CFU/mouse of clinical isolate GAS 5448 (MIT1) and RNA from individual mice was extracted from spleens. Bacteremia was determined as described above. We isolated RNA using RNA-STAT 60 method and when necessary, we purified RNA samples using RNeasy mini kit clean up columns (Qiagen, Valencia, CA). We pooled RNA samples per strain with A260/280 ratios ≥ 1.8 for cDNA synthesis with SuperScript III reverse transcriptase kit (Invitrogen, Carlsbad CA) using oligo dT primers. We designed real time PCR assays, hydrolysis probes, and gene specific primers that span long introns to distinguish cDNA from genomic DNA using primer design online software universal probe library (UPL) at www.roche-applied-science.com/sis/rtPCR/upl/index.jsp. We performed quantitative TaqMan PCR on light cycler LC480 (Roche Applied Science, Indianapolis, IN). We used the mouse housekeeping gene, hypoxanthine guanine phosphoribosyl transferase (*Hprt1*) as an endogenous control to which we normalized gene expression data. Primer sequences are listed in Appendix A Table A-1. Samples were analyzed in triplicates for each of 2–4 biological replicates. We used delta delta Ct (threshold cycle) method for calculating relative expression levels expressed as fold differences between pre- and post-infection values for each gene analyzed. Student t-test was used to assess statistical significance.

Identification of Differentially Expressed Genes in the Mapped Interval and Bioinformatics Functional Pathways Analyses

We generated functional analyses of genes within the QTLs using Ingenuity pathways analysis (IPA) (www.ingenuity.com). Each data set containing gene identifiers was uploaded into the online application, and each gene was overlaid onto a molecular network developed from information contained in the ingenuity pathways database. Networks of genes were then generated based on their connectivity, and we chose the top 50 significant networks. The significance of the association between the data set and the pathways was measured in two ways: (1) the ratio of the number of genes from the data set that map to the pathway divided by the total number of genes that map to the pathway; and (2) by Fischer's exact test with $P < 0.001$.

Statistical Analysis

We used the DataDesk 6.2 (www.datadesk.com) to calculate mean survival indices, corrected survival indices, and correlation coefficients. Covariates association was evaluated for significant associations by Spearman correlation as described previously (Aziz *et al.*, 2007). Fischer exact test was used to analyze association of the analyzed differentially expressed genes with specific pathways.

Web Site URL

Our data sets stored in WebQTL can be found at Gene Network (www.genenetwork.org) under BXD published phenotypes record ID 10836.

CHAPTER 4. IDENTIFICATION OF SOLUBLE AND GENETIC BIOMARKERS ASSOCIATED WITH DIFFERENT OUTCOMES OF GAS SEPSIS REVEALS UNDERLYING MECHANISMS OF DIFFERENTIAL HOST SUSCEPTIBILITY

Summary

Individuals infected with the same group A streptococcal (GAS) strain can develop starkly different disease progression and outcomes. My mentor's laboratory have shown that the same GAS strain can cause a wide range of diseases, from mild bacteremia and erysipelas to streptococcal toxic shock syndrome (STSS) and necrotizing fasciitis (NF) (Chatellier *et al.*, 2000). Difference in disease severity was associated with differences in the profile and magnitude of cytokine responses, where overzealous inflammatory cytokine responses, triggered mainly by streptococcal superantigens (SAGs), were associated with severe disease, including STSS and NF (Norrby-Teglund *et al.*, 2000). Our group has found that HLA class II allelic variations contributed to the differences in cytokine responses in these patients, where individuals with DR14/DQ5 HLA class II haplotypes, produced high levels of inflammatory cytokines and were at risk of developing severe systemic disease and STSS. Whereas, we found that patients who had DR15/DQ6 haplotype mounted moderate cytokine responses and experienced mild sepsis and/or cellulitis (Kotb *et al.*, 2002; Norrby-Teglund *et al.*, 2002).

The HLA-II association was related to interactions of GAS SAGs with the host where GAS SAGs forced interactions of HLA-II on antigen presenting cells and T cell receptors on T helper cells stimulating both types of cells to mount cytokine responses which differed based on HLA-II alleles as described above. However, GAS is rich in many other virulence factors that are likely to engage other host defense mechanisms. Indeed, we have recently shown that additional host factors, other than HLA- II, are modulating host differential responses to GAS infections. Employing genome-wide association studies, we mapped differential susceptibility to severe GAS sepsis to QTLs on mouse Chr 2 and X (Abdeltawab *et al.*, 2008). We found that within these QTLs most significant association with differential susceptibility to GAS sepsis was that of interleukin 1 and prostaglandin E pathways. We validated our results based on genome-wide association studies (GWAS) using multiple bioinformatics tools and quantitative gene expression analyses (as detailed in chapter 3). However, we aimed to perform genome-wide expression analyses to study patterns associated with differential responses to GAS sepsis at early stages of infection. In the current chapter, we aimed to further dissect the mechanisms of the discovered pathways (discussed in chapter 3) and how they are associated with differential susceptibility. In the studies covered in this chapter, in addition to analyzing genome wide (GW) gene expression patterns, we also analyzed soluble biomarkers that are associated with pathways identified by both GW mapping and GW expression analyses.

Results and Discussion

Comparison of Genome-wide Differential Expression in Blood between Susceptible and Resistant Strains at Selected Times Post Infection

In studies outlined in this dissertation, our overall aim was to investigate mechanisms underlying differential response to GAS sepsis. We employed genome-wide association studies (GWAS) adopting systems genetics approach as discussed in chapters 2 and 3. Using these genome-wide association studies, we identified interleukin 1 and prostaglandin pathways as candidate pathways associated with modulation of differential susceptibility to severe GAS sepsis (chapter 3 and Abdeltawab *et al.* 2008). In this chapter, we sought to characterize and further dissect genetic and soluble biomarkers associated with differential susceptibility to GAS sepsis. To do so, we first aimed to characterize differential gene expression patterns associated with differential susceptibility to GAS sepsis. We compared global gene expression differences (genetic biomarkers) and differences in a selected set of cytokines associated with sepsis (soluble biomarkers) between uninfected vs. infected mice of selected highly resistant and highly susceptible strains at 8, 12, and 24 hours post infection.

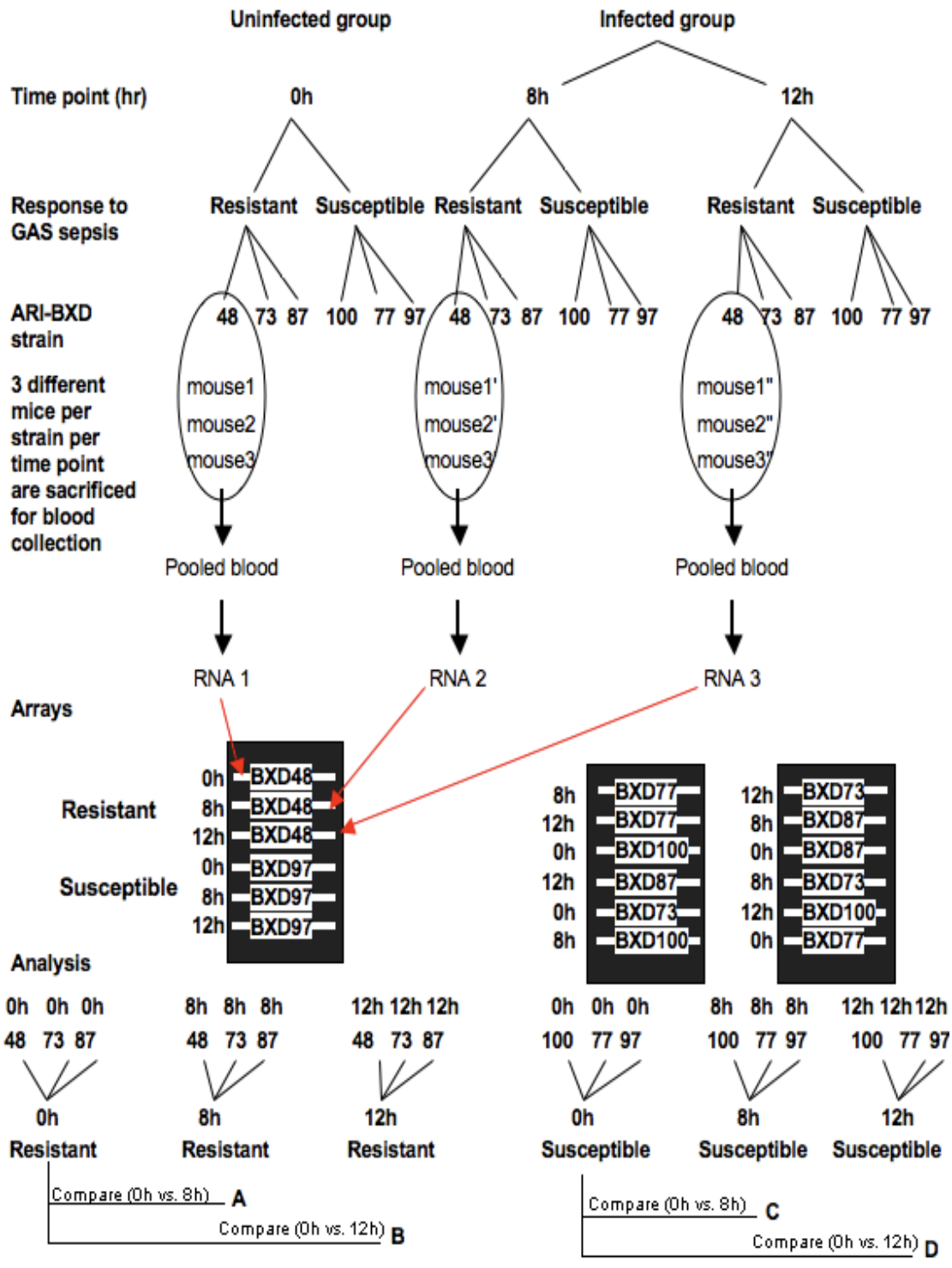
In our global gene expression analyses, we aimed to profile patterns associated with differential susceptibility to severe GAS sepsis. To achieve this aim, we compared infected mice at different stages of infection (8 and 12 hours post GAS infection) to uninfected group of mice (0hrs) (experimental design illustrated in Figure 4-1). We used groups of ARI-BXD strains that displayed marked differences in response to severe GAS sepsis as characterized in studies outlined in chapters 2 and 3 of this dissertation and Aziz *et al.* 2007 and Abdeltawab *et al.* 2008. We designed our experiments so that there were multiple levels of replication. First at the level of ARI-BXD strains used, we selected three highly susceptible ARI-BXD strains (BXD97, 100, and 77)* to represent the most susceptible side of strains (see gradient of differential susceptibility in Figure 3-1). Similarly for the resistant group, we chose to use three most resistant ARI-BXD strains (BXD48, 73, 87)†. In doing so, there were replicas on the level of both susceptible and resistant groups, instead of one strain representing the susceptible group; we collected data from three extremely susceptible strains and similarly for resistant strains as illustrated in Figure 4-1. Within each of these selected representative six strains, we collected and pooled blood from three mice per strain. Each pool of blood represented one strain at a selected time point; this represented biological replica (3 mice per strain). To guard against effects of stress due to multiple bleedings of the same mouse, we used three different sets of mice (3 different mice per set) to analyze each of the studied time points whether pre infection or at different stages of infection (Figure 4-1).

* According to our studies outlined in chapter 3 as illustrated in Figure 3-1, BXD94 and BXD90 are among the extremely susceptible strains; however we did not use BXD94 and BXD90 as BXD94 is now extinct, while BXD90 has been recently difficult to breed in our hands.

† Similarly for resistant strains, we used strains that exhibit extreme resistance as illustrated in Figure 3-1 (BXD48, BXD73 and BXD87), however, we did not use BXD92 which is also extremely resistant as it has become extinct.

Figure 4-1. Experimental design to test gene expression differences associated with differential susceptibility to severe GAS sepsis at selected stages of infection.

Illustration of experimental design used for the assessment of patterns of differential gene expression in blood associated with differential susceptibility to GAS sepsis at early stages of infection (8 and 12 hours post infection). We selected mice belonging to highly resistant strains (BXD48, 73 and 87) and highly susceptible strains (BXD100, 97 and 77). Strains were chosen based on our previous differential susceptibility results detailed in chapter 3 of this dissertation. At each time point, 0 h representing uninfected mice and 8 and 12 hours post infection, we sacrificed three mice per strain and collected blood that was later pooled per strain, representing certain strain at a certain time point (e.g. BXD48 in the illustration, where RNA1 represents BXD48 0 h and RNA2 represents BXD48 8h, each RNA sample was prepared from pooled blood of 3 mice). The same design was repeated for each and every strain. We extracted RNA from these pooled blood samples and hybridized purified high quality RNA to Illumina WG-6 V2.0 mouse arrays (see methods for details of arrays processing). We compared differentially expressed genes in the resistant group (as a whole) at 8 and 12 hours post infection to uninfected mice, and obtained a list of differentially expressed genes, denoted as A and B for resistant strains at 8 and 12 h respectively. Similarly, gene lists C and D for susceptible strains at 8 and 12 hours respectively as shown. We then parsed these differentially expressed gene lists associated with resistance and those with susceptibility into pathways. These pathways are shown in Figures 4-2 and 4-3, and methods used to generate these pathways are detailed in methods section.



We adopted the design (illustrated in Figure 4-1) to allow us to investigate patterns of differentially expressed genes associated with differential susceptibility to severe GAS sepsis. In addition we wanted to investigate stage-specific differential gene expression patterns associated with differential susceptibility.

We chose blood for our current analyses of early stage of infection as our genome-wide association studies revealed association of differential susceptibility to the innate immune cells, neutrophils and monocytes. In addition, blood is the main organ that mounts the first line of defense to this blood borne pathogen. Nonetheless, we also collected data for differentially expressed genes in the spleens of above-mentioned selected highly susceptible and highly resistant strains at multiple times post infection representing different stages of infection. We chose to also investigate genome-wide differential gene expression in the spleen due to the spleen role as one of the main secondary lymphoid tissues involved in clearance of extracellular blood borne bacteria. In future studies to be performed in the laboratory, we plan to also investigate differential gene expression in lungs of these differentially susceptible and resistant strains, as the lung is one of the main organs involved in the severe outcome of GAS sepsis associated with high mortality in clinical settings manifested by acute respiratory distress syndrome.

In our genome-wide differential gene expression analyses of blood, we aimed to analyze stage-specific patterns of resistant strains and susceptible strains compared to their uninfected control (Figure 4-1). For example gene expression levels at 8 hours post infection from three resistant strains compared to 0 hr (uninfected mice) of the same strains. Similarly for susceptible strains at 8 hours vs. 0 hours and also we performed similar analyses for 12hrs compared to 0 hrs for both resistant and susceptible groups (Figure 4-1). However, our current design allows us to analyze the data we generated in multiple ways asking different questions. For instance, we can ask the question of what are the patterns of different mechanisms of resistance by comparing the sets of differentially expressed genes of each of the tested three resistant strains, and similarly for susceptible strains. Another question we would like to address is: what are the differences in gene expression in blood cells between susceptible and resistant group pre-infection (0h). This will help us address the question of possible predisposition to severe sepsis prior to GAS infection.

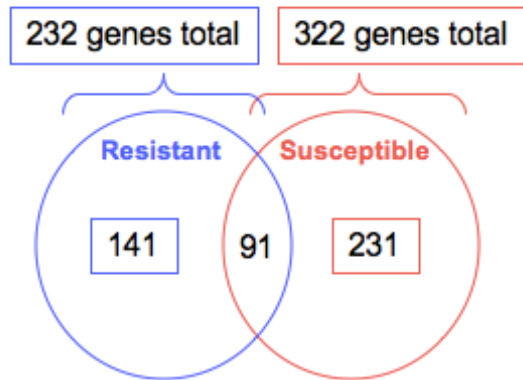
We compared global gene expression in blood at 8 hours vs. 0 hours and found that 232 genes were differentially expressed in resistant strains, while 322 genes were differentially expressed in blood cells of susceptible strains (Figure 4-1, 4-2 and Table 4-1). Comparing these two differentially expressed gene lists, we found that there were 91 genes that were shared (common) between differentially expressed gene sets of susceptible and resistant strains (Figure 4-2). These shared genes fell into multiple pathways, including interferon signaling and interferon regulatory factor activation pathway. Both pathways were upregulated in both susceptible and resistant strains (Figure 4-2 and Table 4-1). However, there were quantitative differences between susceptible and resistant strains in this upregulation (Table 4-1). For example, interferon induced protein with tetratricopeptide repeats 3 (Ifit3) was upregulated at 8 h vs. 0 h in

Figure 4-2. Pathways associated with differentially expressed genes at 8 hours post infection in peripheral blood of resistant and susceptible strains compared to uninfected (0hr) mice of respective strains.

Panel A. Venn diagram of differentially expressed genes in blood of resistant and susceptible strains, showing common (shared) and unique genes. Resistant strains had 232 genes differentially expressed within these, 141 genes were unique to resistant strains while 91 genes were shared with susceptible strains. A total of 322 genes were differentially expressed in susceptible strains within these genes, 231 genes were unique to susceptible strains. These lists of differentially expressed genes were parsed into pathways using ingenuity pathway analysis tool (IPA) as detailed in methods section. Shown are the most significant pathways. We parsed common (shared) differentially expressed genes in both resistant and susceptible strains into pathways shown in panel B. The significant pathways associated with genes that are differentially expressed only in resistant strains are shown in panel C, while those associated only with susceptible strains are shown in panel D. Whether the genes within a pathway are up or down regulated is denoted in words and as arrows beside each pathway. The x-axis displays significance in $(-\log(p\text{-value}))$ where the higher the number (the longer the blue bar) the more likely the association of the differentially expressed genes with the noted pathways is not by chance, this significance is also expressed as p-values on each bar. For each pathway we calculated a ratio (orange squares, and decimal number associated with it), the ratio is the number of differentially expressed genes divided by total number of molecules in the specified pathway.

A Venn diagram of differentially expressed genes at 8 h post infection in blood of resistant and susceptible strains, showing common (shared) and unique genes

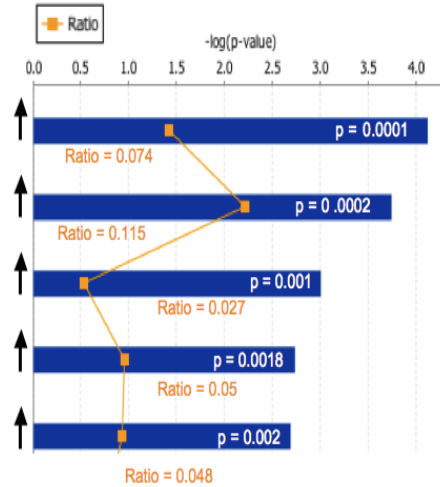
Differentially expressed genes in **resistant(R)** / **susceptible(S)** strains at 8 hrs vs. uninfected (0h) mice



B Pathways of differentially expressed genes shared (common) between resistant and susceptible strains at 8 h post infection

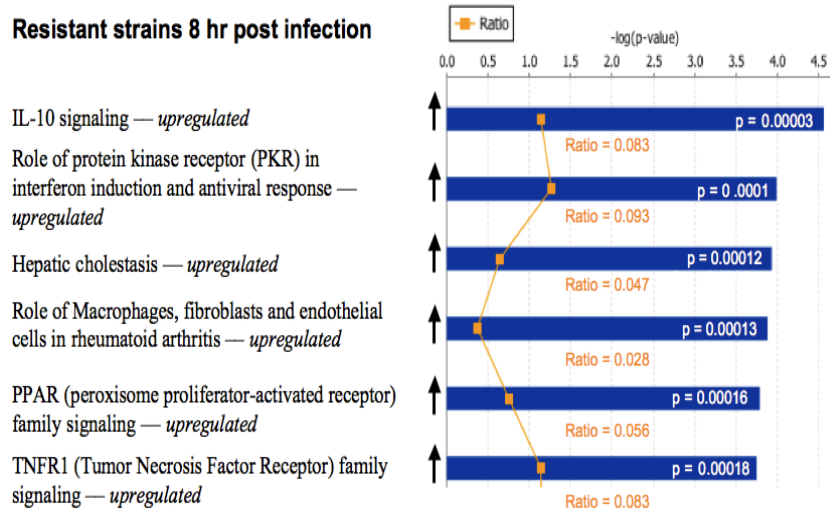
Common pathways 8 hr post infection

- Activation of interferon regulatory factor (IRF) family by cytosolic pattern recognition receptors — *upregulated*
- Interferon signaling — *upregulated*
- Protein ubiquitination pathway — *upregulated*
- Death receptor signaling — *upregulated*
- Induction of apoptosis — *upregulated*



C Pathways of differentially expressed genes associated with resistant strains at 8 h post infection

Resistant strains 8 hr post infection



D Pathways of differentially expressed genes associated only with susceptible strains at 8 h post infection

Susceptible strains 8 hr post infection

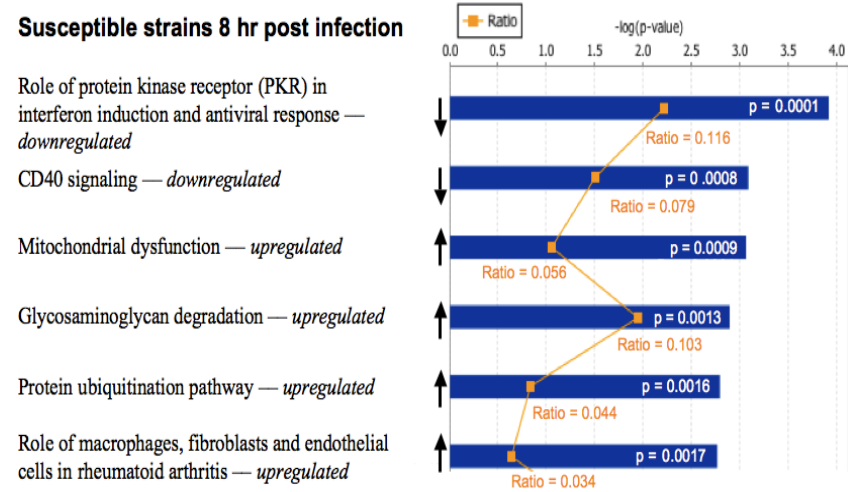


Figure 4-2. (Continued).

Table 4-1. Differentially expressed genes in peripheral blood of resistant and susceptible strains at 8 hrs post GAS infection.

Pathways and Genes/Transcripts	Gene/Transcript Description	Fold Change	
		Susceptible	Resistant
Top pathways associated with differentially expressed genes shared between susceptible and resistant strains			
Interferon signaling and activation of IRF by cytosolic pattern recognition receptors			
<i>Ifit3</i>	Interferon-induced protein with tetratricopeptide repeats 3 (Ifit3)	19.83	29.42
<i>Ifit2</i>	Interferon-induced protein with tetratricopeptide repeats 2 (Ifit2)	5.58	9.57
<i>Stat2</i>	Signal transducer and activator of transcription 2 (Stat2)	4.04	3.42
<i>Zbp1</i>	Z-DNA binding protein 1 (Zbp1)	4.13	3.93
<i>Dhx58</i>	DEXH (Asp-Glu-X-His) box polypeptide 58 (Dhx58)	8.50	8.79
<i>Oas1</i> γ	2'-5' oligoadenylate synthetase 1G (Oas1 gamma)	12.14	11.48
Top pathway associated with differentially expressed genes in resistant strains (8h vs. 0h)			
IL10 signaling			
<i>Arg2</i>	Arginase, type II		3.78
<i>Ikbke</i>	Inhibitor of kappa light polypeptide gene enhancer in B-cells, kinase epsilon		3.79
<i>Il1b</i>	Interleukin 1, beta		5.99
<i>Il1rn</i>	Interleukin 1 receptor antagonist		9.49
<i>Tnf</i>	Tumor necrosis factor (TNF superfamily, member 2)		4.63
<i>Jun</i>	Jun oncogene (Jun)		2.23

Table 4-1 (Continued).

Pathways and Genes/Transcripts	Gene/Transcript Description	Fold Change	
		Susceptible	Resistant
Top pathway associated with differentially expressed genes in susceptible strains (8h vs. 0h)		-2.03	
Role of PKR in Interferon induction		-2.53	
<i>Ikkγ</i>	Inhibitor of kappa light polypeptide gene enhancer in B-cells, kinase gamma		
<i>Map2k3</i>	Mitogen-activated protein kinase kinase 3		

susceptible group by ~20 folds vs. 29 folds in resistant group (Table 4-1). Similarly other quantitative differences between susceptible and resistant group were observed. However, we didn't observe this quantitative difference between resistant and susceptible group at 12 hours post-infection (Table 4-1 and 4-2). Further studies, which are beyond the scope of this dissertation, are needed to elucidate if and how these observed quantitative differences relate to differential susceptibility to GAS sepsis.

Among the top pathways (pathways with highest significance) associated with differentially expressed genes in resistant strains (8 vs. 0 hours) was IL10 signaling pathway (Figure 4-2 and Table 4-1). We found that most of the differentially expressed genes in IL10 signaling pathway were upregulated (Table 4-1). Of note was the upregulation of arginase II (Arg II) in resistant strains at 8 h post infection (Table 4-1). Arg II and nitric oxide synthase (NOS) compete for the same arginine pool with the production of L-ornithine or nitric oxide (NO) respectively. Therefore, upregulation of Arg II in resistant strains might reflect a plausible mechanism of resistance, where upregulation of Arg II might regulate the production of NO in endothelial cells by decreasing the bio availability of arginine. This suggested that resistant strains might be upregulating Arg II to control a possible over production of NO. Over production of NO can lead to an increase in vascular permeability and leakage, leading to increase loss of fluids from vascular vessels, leading to hypotension which leads to shock, and consequently STSS.

In addition, association of upregulation of IL10 signaling pathway with resistance (Figure 4-2) suggested that resistance might be initiated early on in infection with known involvement of IL10 signaling pathway in induction of tissue repair and its immunomodulatory responses. However, in our analyses, we did not find upregulation of IL10 gene itself upregulated; although its signaling pathway was upregulated. In addition to IL10 signaling pathway, multiple pathways associated with tissue development, cell proliferation, activation of macrophages, pattern recognition activation were associated with resistance (Figure 4-2). We also found that pathways associated with bacterial killing and reactive oxygen species (ROS) production were among pathways associated with differentially expressed genes in resistant strains only. It seems contradictory that we found that resistant strains had upregulation of both Arg II (associated with regulation of NO production) and ROS production pathways. However, it might be that these resistant strains exert an active suppression of over production of such ROS but not ROS production per se. Since overproduction of NO is associated with tissue damage and shock, resistant strains guard against these deleterious effects by using up arginine pools (Arg II upregulation), meanwhile adequate production of ROS is induced to control the bacterial infection.

In susceptible strains, we found that 231 genes were differentially expressed at 8 h post infection compared to 0 h (Figure 4-1 list C and 4-2). The top pathways associated with these differentially expressed genes were role of protein kinase receptor (PKR) interferon induction and CD40 signaling. Most of the differentially expressed genes belonging to both pathways were downregulated. This observed downregulation of PKR induced interferon signaling in susceptible strains at 8 hrs is in contrast to resistant strains

that manifested upregulation of the same pathway at same time point. CD40 signaling pathway is involved in a multitude of immune responses ranging from induction of pro-inflammatory cytokines to activation of cell survival and was associated in the production of IL1 and IL8 from vascular endothelial cells, in addition, it is involved in the induction of prostaglandin endoperoxide synthase 2 (*Ptgs2*) and subsequent production of PGE2 (Elgueta *et al.*, 2009). The observed downregulation of genes associated with CD40 signaling and PKR induction of interferon signaling in susceptible strains might be associated with the lack of mounting appropriate response to GAS infection.

Next, we examined differential gene expression patterns at 12 hours post infection; we found that 380 genes were differentially expressed in resistant strains at 12 h compared to uninfected mice, out of which 268 genes were unique to resistant strains and 112 genes were shared with susceptible strains (Figure 4-3). Again similar to 8 h, the shared (common) differentially expressed genes between resistant and susceptible strains (112 genes) fell into pathways that included interferon signaling. However, the quantitative differences between susceptible and resistant strains were more towards higher levels in susceptible than resistant strains, while the reverse was true at 8h, e.g. *Ifit3* levels at 8 vs. 12 hrs (common genes Table 4-1 and 4-2). The 268 genes differentially expressed in resistant strains only, fell into interferon signaling pathway and activation of interferon signaling by pattern recognition receptors and PKR signaling. We observed this upregulation of genes associated with interferon signaling at both 8 and 12 hours in both susceptible and resistant strains however, the mechanism of induction was different and there was a down regulation of PKR induced interferon signaling in susceptible strains at 8 h. Further detailed studies might help in elucidating the details of mechanisms of interferon in modulating differential susceptibility.

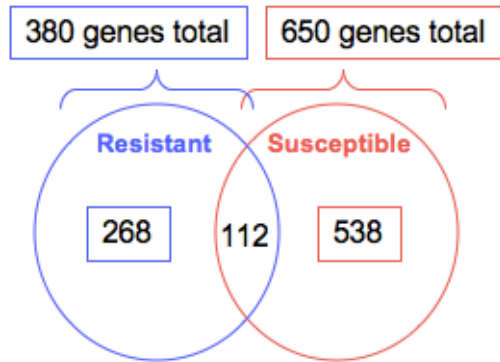
Meanwhile, pathways associated with differentially expressed genes in the blood of susceptible strains at 12h post infection were mainly associated with induction of mitochondrial enzymes, induction of apoptosis and oxidative phosphorylation. Genes within these pathways were upregulated; this upregulation of mitochondrial pathways might be associated with bacterial induced mitochondrial injury and bioenergetic failure thus leading to sepsis-associated multiple organ failure. This is further supported by our finding that in susceptible strains mitochondrial oxidative phosphorylation enzymes e.g. NADH dehydrogenase and succinate dehydrogenase were upregulated at both 8 and 12 h post infection (Figure 4-2, 4-3 and Table 4-2), suggesting that mitochondrial oxidative phosphorylation is upregulated to counteract the ROS produced. Furthermore, mitochondrial apoptosis related enzymes e.g. caspase 8 and cytochrome C-1, as well as pathways associated with induction of apoptosis were upregulated in only the susceptible strains at 12h (Figure 4-3 and Table 4-2). This simultaneous upregulation of electron transport chain (ETC) enzymes and mitochondrial-induced apoptosis signaling could be explained in terms of possible positive feedback between the cascades of oxidative phosphorylation provided by ETC to enhance apoptotic pathway. This fits with a recent report that showed that GAS can induce mitochondrial permeability leading to bioenergetic and redox damage. Thus evading host immune defense and causing inflammatory programmed cell death in monocytes (Goldmann 2009). Furthermore, it results have been recently reported that GAS streptolysin S and O virulence factors

Figure 4-3. Pathway analysis of differentially expressed genes at 12 hrs post infection in peripheral blood of resistant and susceptible strains compared to uninfected (0hr) mice of respective strains.

Panel A. Venn diagram of differentially expressed genes in blood of resistant and susceptible strains, showing common (shared) and unique genes. Resistant strains had 380 genes differentially expressed within these, 268 genes were unique to resistant strains while 112 genes were shared with susceptible strains. A total of 650 genes were differentially expressed in susceptible strains within these genes, 538 genes were unique to susceptible strains. These lists of differentially expressed genes were parsed into pathways using ingenuity pathway analysis tool (IPA) as detailed in methods section. Shown are the most significant pathways. We parsed common (shared) differentially expressed genes in both resistant and susceptible strains into pathways shown in panel B. The significant pathways associated with genes that are differentially expressed only in resistant strains are shown in panel C, while those associated only with susceptible strains are shown in panel D. Whether the genes within a pathway are up or down regulated is denoted in words and as arrows beside each pathway. The x-axis displays significance in $(-\log(p\text{-value}))$ where the higher the number (the longer the blue bar) the more likely the association of the differentially expressed genes with the noted pathways is not by chance, this significance is also expressed as p-values on each bar. For each pathway we calculated a ratio (orange squares, and decimal number associated with it), the ratio is the number of differentially expressed genes divided by total number of molecules in the specified pathway.

A Venn diagram of differentially expressed genes at 12 h post infection in blood of resistant and susceptible strains, showing common (shared) and unique genes

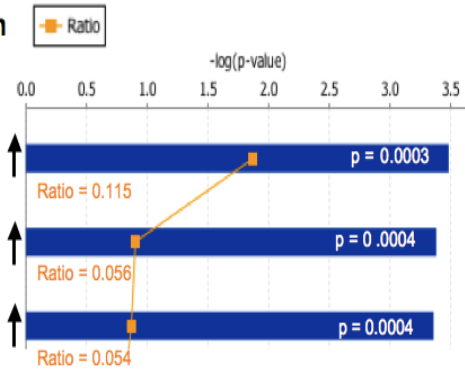
Differentially expressed genes in **resistant(R)** / **susceptible(S)** strains at 12 hrs vs. uninfected (0h) mice



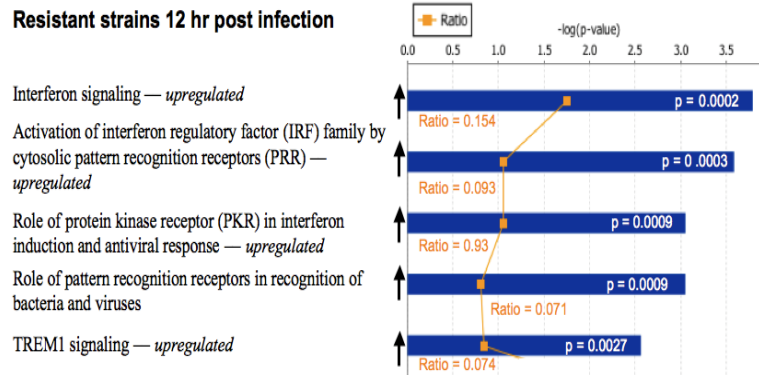
B Pathways of differentially expressed genes shared (common) between resistant and susceptible strains at 12 h post infection

Common pathways 12 hr post infection

- Interferon signaling — *upregulated*
- Liver X receptor / Retinoid X receptor (LXR/RXR) activation — *upregulated*
- Communication between innate and adaptive immune cells — *upregulated*



C Pathways of differentially expressed genes associated with resistant strains at 12 h post infection



D Pathways of differentially expressed genes associated only with susceptible strains at 12 h post infection

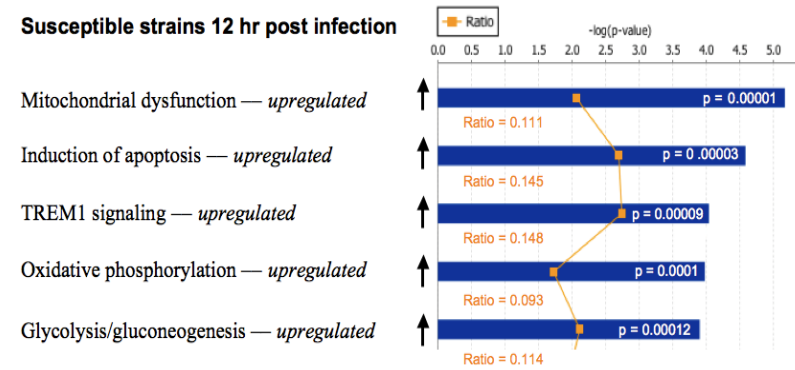


Figure 4-3. (Continued).

Table 4-2. Differentially expressed genes in peripheral blood of resistant and susceptible strains at 12 hrs post GAS infection.

Pathways and Genes/Transcripts	Gene/Transcript Description	Fold Change	
		Susceptible	Resistant
Top pathways associated with differentially expressed genes shared between susceptible and resistant strains			
Interferon signaling and LXR/RXR signaling pathways			
<i>Ifit3</i>	Interferon-induced protein with tetratricopeptide repeats 3 (Ifit3)	22.93	22.31
<i>Tap1</i>	Transporter 1, ATP-binding cassette, sub-family B (MDR/TAP)	4.21	2.78
<i>Oas1γ</i>	2'-5' oligoadenylate synthetase 1G (Oas1 gamma)	15.54	11.54
<i>Il18</i>	Interleukin 18	6.84	5.03
<i>Il1rn</i>	Interleukin 1 receptor antagonist, transcript variant 1	5.41	5.75
<i>Nr1h3</i>	Nuclear receptor subfamily 1, group H, member 3	17.61	15.80
<i>Tlr4</i>	Toll-like receptor 4	2.59	2.67
Top pathway associated with differentially expressed genes in resistant strains (12h vs. 0h)			
Interferon signaling pathway			
<i>Stat1</i>	Signal transducer and activator of transcription 1		4.00
<i>Stat2</i>	Signal transducer and activator of transcription 2		2.82
Top pathway associated with differentially expressed genes in susceptible strains (12h vs. 0h)			
Mitochondrial dysfunction			
<i>App</i>	Amyloid beta (A4) precursor protein	8.51	
<i>Casp8</i>	Caspase 8, apoptosis-related cysteine peptidase	2.84	
<i>Cyc1</i>	Cytochrome c-1	2.61	

Table 4-2 (Continued).

Pathways and Genes/Transcripts	Gene/Transcript Description	Fold Change	
		Susceptible	Resistant
<i>Htra2</i>	HtrA serine peptidase 2	4.17	
<i>Ndufa8</i>	NADH dehydrogenase (ubiquinone) 1 alpha subcomplex 8, 19 kDa	3.96	
<i>Ndufa9</i>	NADH dehydrogenase (ubiquinone) 1 alpha subcomplex 9, 39 kDa	3.91	
<i>Ndufs2</i>	NADH dehydrogenase (ubiquinone) Fe-S protein 2, 49 kDa	2.45	
<i>Ndufs3</i>	NADH dehydrogenase (ubiquinone) Fe-S protein 3, 30 kDa	2.98	
<i>Ndufs7</i>	NADH dehydrogenase (ubiquinone) Fe-S protein 7, 20 kDa	2.45	
<i>Ndufs8</i>	NADH dehydrogenase (ubiquinone) Fe-S protein 8, 23 kDa	2.76	
<i>Sdhb</i>	Succinate dehydrogenase complex, subunit B, iron sulfur (Ip)	3.39	
<i>Sdhc</i>	Succinate dehydrogenase complex, subunit C	2.24	
<i>Uqcrc1</i>	Ubiquinol-cytochrome c reductase core protein 1	2.92	
<i>Xdh</i>	Xanthine dehydrogenase	6.20	

specifically interfere with killing mechanisms by induction of mitochondrial dysfunction (Aikawa *et al.*, 2010). Nonetheless, these previous studies did not elucidate the exact mechanisms and role of mitochondrial dysfunction in modulating severity of GAS sepsis. Therefore, more detailed studies with more time points focusing on the role of mitochondrial dysfunction in inducing multiple organ failure are required to further elucidate our results.

In general, our global gene expression studies comparing differential gene expression in blood of infected vs. uninfected susceptible and resistant strains at multiple times post infection gave us insight into some aspects of how the host might be modulating differential immune response to GAS sepsis. Our data suggested that the involvement of multiple pathways in modulating differential susceptibility, where starting as early as 8h post infection, IL10 signaling pathways were upregulated only in resistant strains. In addition, pathways associated with bacterial killing and resolution of infection were triggered in resistant strains at that early stage. It was noteworthy that genes and pathways involved in macrophage and neutrophils killing mechanisms were also associated with these discovered pathways.

Next, we analyzed change in gene expression in spleen at 8, 12, 16, 24 and 36h post infection following the same design as blood microarrays studies detailed in Figure 4-1. However, we chose to start by analyzing the 36 h post infection differential gene expression arrays, to investigate immune response after allowing enough time for the bacteria to disseminate to the spleen. Analysis of the differentially expressed genes in spleens of resistant and susceptible ARI-BXD strains revealed the engagement of the same pathways suggested by the systems genetics genome-wide association studies. These pathways encompass many of the genes located within all 3 survival QTLs, including the one on Chr X. In those studies, we infected susceptible and resistant ARI-BXD strains with MIT1 GAS, uninfected control mice from the same strains were injected with saline. The data revealed significant changes in the expression of highly relevant genes in both susceptible and resistant mice, both pre- and post infection (Figure 4-4). Many of those genes are located within our 3 mapped QTLs (e.g. *Il1 α* , *Il1 β* , and *Il1rn*) on Chr 2, in addition to *Irf1* on Chr X. These genes and pathways are likely to contribute to the pathogenesis and differential severity of GAS sepsis. However, this spleen microarray data is very preliminary, with further analyses and more samples needed to be done for obtaining a clearer picture of mechanisms of differential susceptibility.

Soluble Biomarkers Associated with Differential Susceptibility in Select Susceptible and Resistant Strains at Multiple Time Series Post-infection

Next, we wanted to dissect soluble biomarkers associated with differential response. Therefore, we aimed to analyze the kinetics of selected cytokines levels in plasma of uninfected vs. infected resistant and susceptible strains at selected time points post infection. We analyzed differences in the levels of selected cytokines that are known to be associated with modulation of differential severity of GAS sepsis and were associated with differential gene expression analyses detailed in the first section of

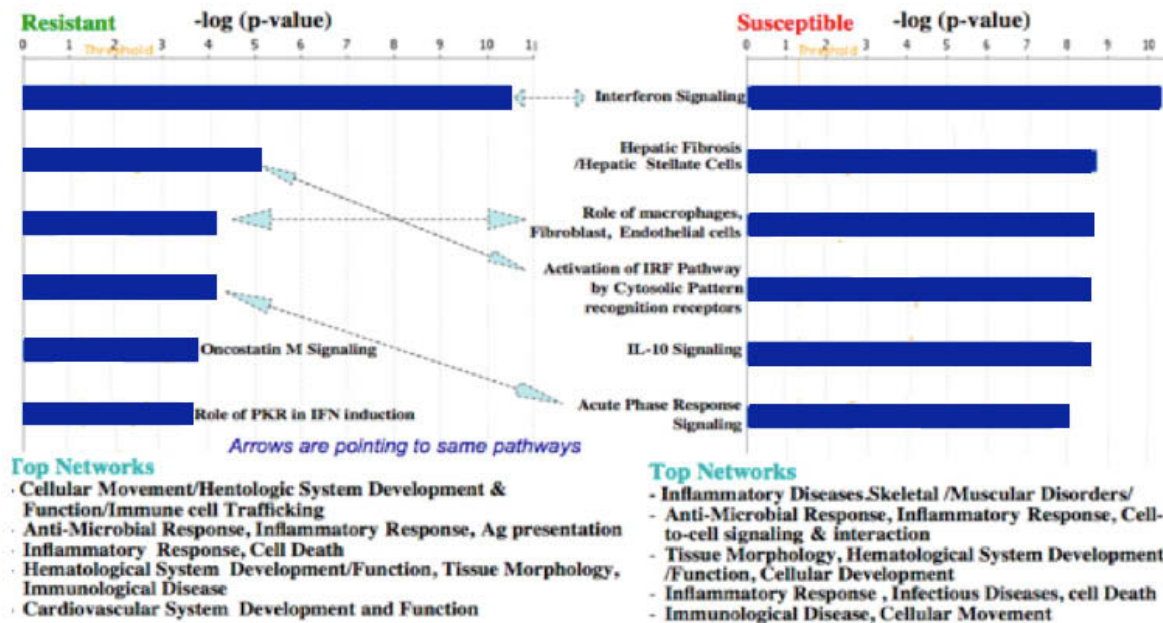


Figure 4-4. Pathways associated with differentially expressed genes in spleens of uninfected versus infected resistant and susceptible ARI-BXD strains at 36h post GAS infection.*

We infected selected highly susceptible and highly resistant ARI-BXD strains (n = 3–4 strains in each group, 3–5 mice per strain per time point) with M1T1 GAS strain. In parallel, a control group of mice was injected with saline. Differentially expressed genes in spleen at 36h post infection were parsed into pathways, shown are the most significant pathways in resistant and susceptible group. The x-axis displays significance in (–log (P-value)) where the higher the number the more likely the association is not by chance. Matching pathways shown were connected with arrows in light blue.

* Data represented in this Figure is preliminary, as we are planning to do more analysis as well as more time points that we have already collected samples, these samples represent earlier stages of infection. We are continuing to analyze these data to elucidate mechanisms associated with differential response.

Chapter 4. We investigated selected pro-inflammatory cytokines, interleukin 6 (IL-6), interferon gamma (IFN γ) and tumor necrosis factor alpha (TNF α) and anti-inflammatory cytokine, IL10 at selected time points post-infection (0, 8, 12 and 24 hours).

We first aimed to analyze stage specific differences within each group, i.e. susceptible group at different time points post infection and similarly resistant group. We found that in susceptible strains TNF α showed significant increase in plasma levels at 8 hours post infection, followed by a drop in plasma levels at 12 hours to almost the same levels as “zero” or uninfected control mice, then no changes at 24 h from 12 h (Figure 4-5-A)*. This might suggest that there might be a possible early induction of acute systemic sepsis manifested by the observed high systemic levels of TNF α at 8 hours in susceptible strains only. As for the resistant strains studied, we found that levels of TNF α significantly increase in the plasma only at 24 h post infection (compared to uninfected mice) (Figure 4-5-B). This might suggest that the release of TNF α at that stage of infection is more beneficial and induces appropriate response to resolve infection as these strains are protected against sepsis. However, on comparing TNF α levels in resistant vs. susceptible group at each of studied stages of infection, there were trends of differences but none reached significant (Figure 4-5-C).

For IL6 both susceptible and resistant strains showed significant increase in plasma levels at 12 and 24 hours post infection in comparison to 0 h (uninfected controls) (Figure 4-6-A and 4-6-B). However, the levels of IL6 in susceptible strains at 24 hours post infection were almost double that of resistant strains, yet it didn't reach statistical significance differences due to the spread of data points (Figure 4-6- C). Collectively, TNF α and IL6 pro-inflammatory cytokines and crucial mediators of systemic sepsis didn't show differences in the levels between susceptible and resistant strains. However, we realize that this might due to assessing plasma levels of these cytokines, which does not reflect the actual producing cells; therefore, we plan to perform intracellular cytokine staining, where we can determine which cells are producing these cytokines at the studied stages of infection and hence draw a more definitive conclusion. Yet, our results indicate that at these early time points, systemic levels of IL6 and TNF α do not differ between susceptible and resistant strains at the selected time points.

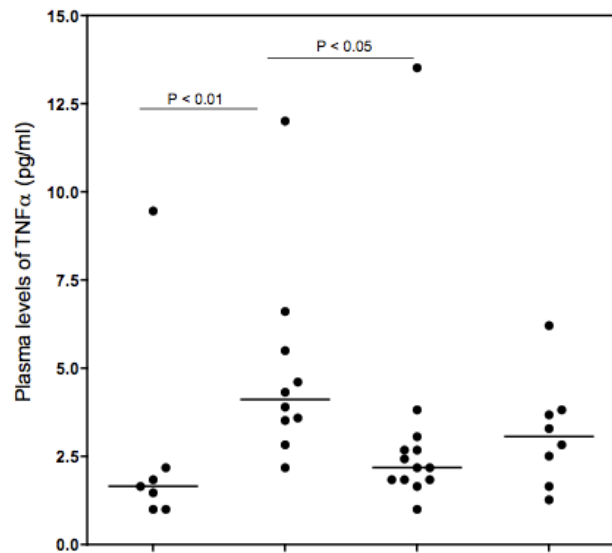
Next we looked at levels of anti-inflammatory cytokine IL10 in susceptible and resistant strains at multiple stages of infection. We found that both susceptible and resistant strains showed significantly high levels at 8 and 12 hours post-infection (Figure 4-7-A and 4-7-B). However, levels of IL10 were 2-3 folds higher in resistant strains than susceptible strains; indeed comparing susceptible to resistant strains, showed that higher levels of IL10 were associated with resistant strains at as early as 8 and 12 hours post

* The analyzed data shown in Figures 4-5 to 4-9 are representative of susceptible and resistant groups, where 2 mice per strain per time point were analyzed, with the exception of: a) susceptible group, where we used 4 mice at 8 h and 12h for BXD 97 and for BXD77 we used 4 and 6 mice at 12 and 24 h respectively b) Resistant group, we used 4 mice at 8, 12 and 24 h of BXD87 and one mouse at 8 hours of BXD48. We collected far more plasma samples that are to be assayed. All other data shown is for 2 mice per strain (3 strains used) per time point (4 time points analyzed).

Figure 4-5. TNF α plasma levels profiles across early time points post infection comparing selected highly susceptible and highly resistant ARI-BXD strains.

We infected three highly susceptible ARI-BXD strains (BXD100, 77 and 97) and three highly resistant ARI-BXD strains (BXD48, 73 and 87) with 2×10^7 CFU/mouse of hypervirulent MIT1 GAS strain, design of study is similar to microarray studies shown in Figure 4-1, further details of cytokine measurements in methods section. We sacrificed and collected plasma for a set of mice per strain at each time point post infection, 8, 12, and 24 hours, therefore, there were no multiple bleedings of any of the mice used. In parallel, a control group of uninfected mice were used for collection of plasma for estimating normal levels of TNF α in these selected strains. (A). Comparison of medians of levels of TNF α in susceptible mice showed that levels of TNF α increased significantly at 8 hours post-infection, then significantly drop back to almost the zero levels at 12 hours post infection. Panel (B). Resistant strains showed significant increase in levels of TNF α only at 24 hours post-infection. Panel C. We compared TNF α plasma levels in susceptible (red dots) vs. resistant (blue dots) groups at the analyzed time points. There were differences in levels of TNF α but none reached statistical significance based on Mann-Whitney test. We applied Kruskal-wallis test to assess statistical significance of differences in levels of TNF α between and across time points (stages of infection) (panels A and B). In general a p value of < 0.05 was considered significant.

A Susceptible strains



B Resistant strains

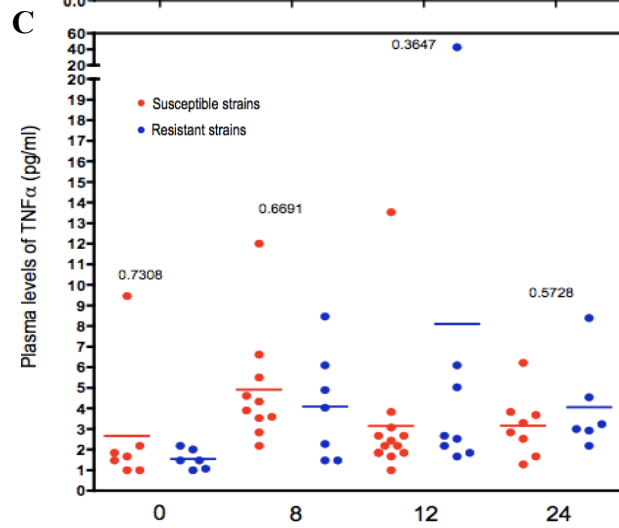
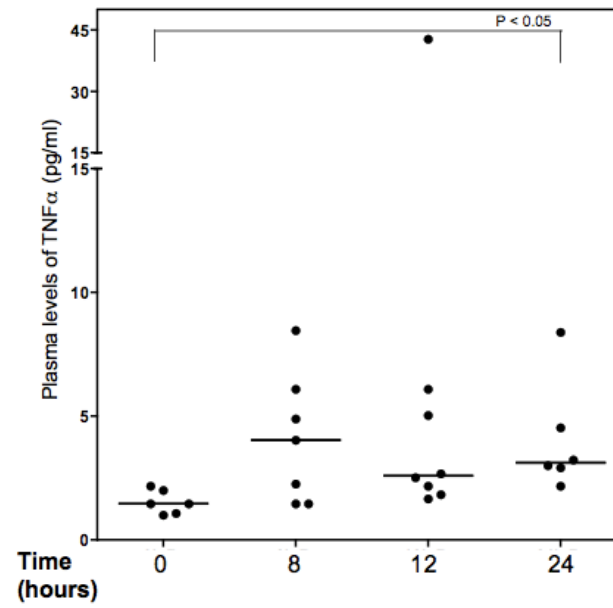
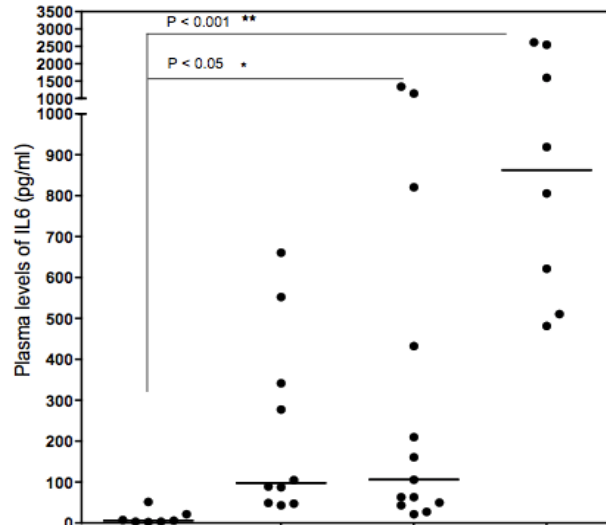


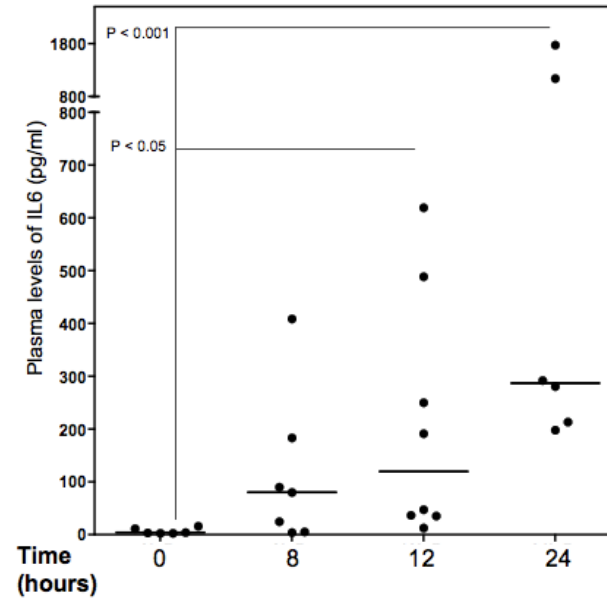
Figure 4-6. IL6 plasma levels profiles across early time points post infection comparing selected highly susceptible and highly resistant ARI-BXD strains.

We infected three highly susceptible ARI-BXD strains (BXD100, 77 and 97) and three highly resistant ARI-BXD strains (BXD48, 73 and 87) with 2×10^7 CFU/mouse of hypervirulent MIT1 GAS strain. We sacrificed and collected plasma for a set of mice per strain at each time point post infection, 8, 12, and 24 hours, therefore, there were no multiple bleedings of any of the mice used. In parallel, a control group of uninfected mice were used for collection of plasma for estimating normal levels of IL6 in these selected strains. (A). Comparison of medians of levels of IL6 in susceptible mice showed that levels of IL6 increased significantly at 12 and 24 hours post-infection compared to pre-infection (zero hour). Panel B. Similarly, resistant strains showed significant increase in levels of IL6 12 and 24 hours post-infection, however, the maximum value and hence the range of IL6 levels was higher and wider in susceptible strains, up to 3500 pg/ml vs. 1800 pg/ml in resistant strains. Panel C. We compared IL6 plasma levels in susceptible (red dots) vs. resistant (blue dots) groups at the analyzed time points. There were differences in levels of IL6 but none reached statistical significance based on Mann-Whitney test. We applied Kruskal-wallis test to assess statistical significance of differences in levels of IL6 between and across time points (stages of infection) (panels A and B). In general a p-value of < 0.05 was considered significant. (For number of samples analyzed please refer to page 65 footnote).

A Susceptible strains



B Resistant strains



C

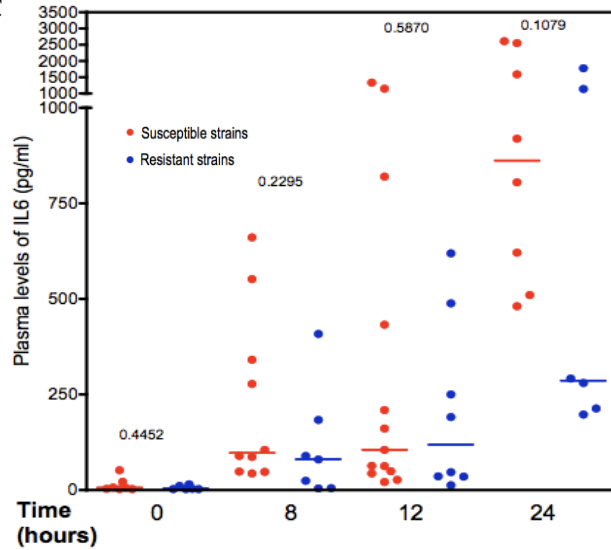
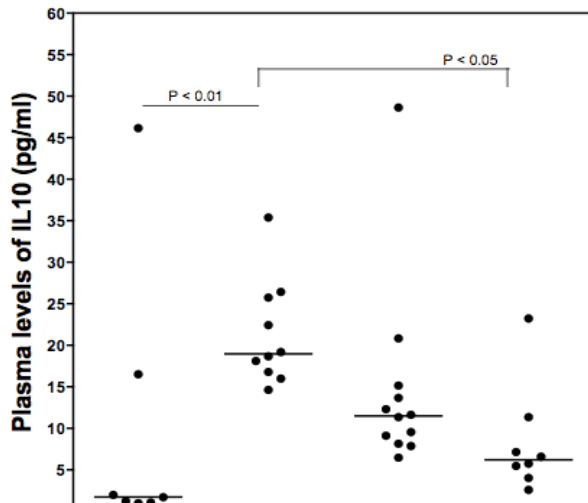


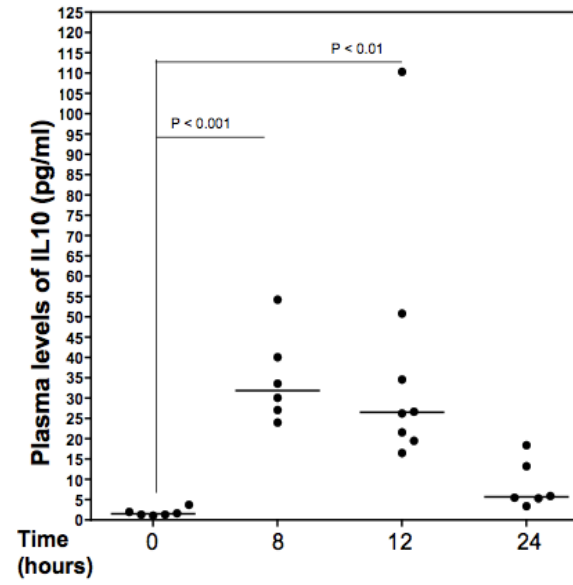
Figure 4-7. IL10 plasma levels profiles across early time points post infection comparing selected highly susceptible and highly resistant ARI-BXD strains.

We infected three highly susceptible ARI-BXD strains (BXD100, 77 and 97) and three highly resistant ARI-BXD strains (BXD48, 73 and 87) with 2×10^7 CFU/mouse of hypervirulent MIT1 GAS strain. We sacrificed and collected plasma for a set of mice per strain at each time point post infection, 8, 12, and 24 hours, therefore, there were no multiple bleedings of any of the mice used. In parallel, a control group of uninfected mice were used for collection of plasma for estimating normal levels of IL10 in these selected strains. (A). Comparison of medians of levels of IL10 in susceptible mice showed that levels of IL10 increased significantly at 8 hours post-infection compared to pre-infection (zero hour), then dropped at 12 and 24 hours with significant drop at 24 to almost same as “zero” hour. Panel B. Similarly, resistant strains showed significant increase in levels of IL10 at 8 hours post infection, with a drop at 12 and 24 hours post-infection, however, levels at 12 hours were still significantly higher than zero hour. In addition, in general the resistant strains had higher levels of IL10 levels than the susceptible strains. Panel C. We compared IL10 plasma levels in susceptible (red dots) vs. resistant (blue dots) groups at the selected analyzed time points. We found that IL10 levels were significantly higher in plasma of resistant strains at early time points (8 and 12 hours) however, at 24 hours post infection both susceptible and resistant strains IL10 levels dropped and no statistical differences between their levels. Significance between susceptible and resistant strains IL10 levels were calculated based on Mann-Whitney test. We applied Kruskal-wallis test to assess statistical significance of differences in levels of IL10 between and across time points (stages of infection) (panels A and B). In general a p-value of < 0.05 was considered significant. (For number of samples analyzed please refer to page 65 footnote).

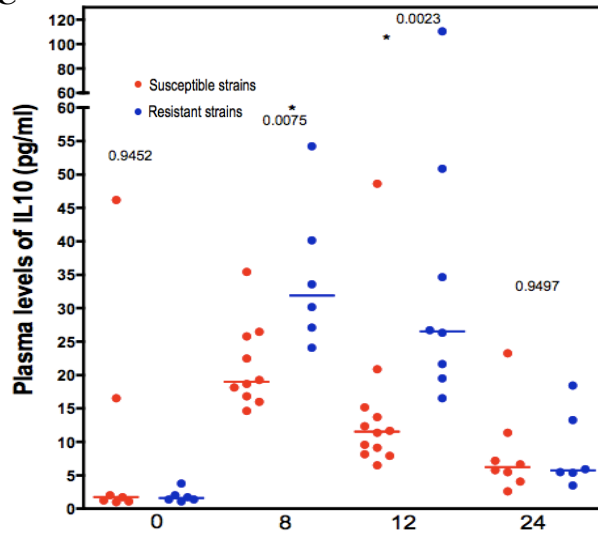
A Susceptible strains



B Resistant strains



C



infection (Figure 4-7-C). The association of higher levels of anti-inflammatory IL10 suggested that an active immunosuppressive of the cytokine avalanche might be the mechanism of resistance and protection against sepsis. While highly susceptible strains had lower levels of IL10 suggesting an unchecked cytokine response was associated with higher severity of sepsis.

IFN γ was significantly higher in susceptible strains at 24 hours post infection; however, in resistant strains there were no significant increase in levels of IFN γ (Figure 4-8-A and 4-8-B). Comparing levels of IFN γ resistant to susceptible strains, again 24 hours susceptible strains had higher levels, this being a biologically relevant time point for IFN γ actions. (Figure 4-8-C) Collectively, results from pro-inflammatory cytokines, IL6, TNF α and IFN γ , showed increase in levels in susceptible across time points suggested that systemic acute response in susceptible strains. However, these increase were also seen in resistant strains (Figures 4-5, 4-6, and 4-8 panels A and B), yet we postulated that the increase in these pro-inflammatory cytokines was neutralized or modulated by anti-inflammatory cytokines in resistant strains. Therefore, we compared anti- to pro- inflammatory cytokines ratios, as shown in Figure 4-9 comparing IL10/IFN γ ratios. This comparison revealed that resistant strains had higher levels of IL10/IFN γ ratio at all time points post infection and even at 0 h prior to infection. Collectively, our data suggest that susceptibility to severe GAS sepsis is mainly associated with unchecked production of pro-inflammatory cytokines and mediators at early time points. Meanwhile, protected mice are better able to down regulate excessive inflammatory responses and hence are protected against STSS. Our cytokine profiling analyses validated the pathways discovered through our transcriptome profiling of blood cells from the mice at different time points post infection in addition to our GWAS mapping results.

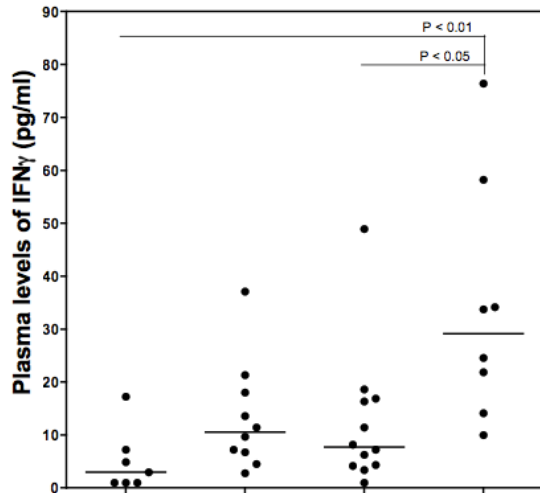
Moreover, our findings outlined in chapters 3 and 4 of this dissertation are in concordance to the clinical disease data; where our recent human *ex vivo* data showed that IL10 exerts active suppression of exaggerated immune responses in individuals carrying protective HLA-II alleles (DR15/DQ6) (Nooh and Kotb in press). Whereas individuals carrying the STSS high-risk alleles (DR14/DQ5) mounted significantly lower levels of IL10 and higher levels of IFN γ (Nooh and Kotb in press). Further validation was done by the addition of exogenous rIL10 to PBMCs isolated from individuals carrying high-risk HLA-II alleles (DR14/DQ5) decreased SAg-induced T cell proliferation and cytokine responses (Nooh and Kotb in press). Moreover, the association of higher levels of IL10 with protection from sepsis was also observed in our human transcriptome profiles of patients with severe vs. non-severe GAS sepsis (Kanasal and Kotb in final preparation).

Collectively, our murine *in vivo* and *in vitro* data with our human *ex vivo* data support our hypothesis that resistance (protection) is actively exerted by the production of the anti-inflammatory immunomodulatory IL10. In addition, IL10 is highly regulated and can be produced by a number of innate immune cells, including dendritic cells, macrophages, and most recently it has been shown to be produced by neutrophils (Saraiva and O'Garra, 2010). We observed that IL10 in plasma was detected at a rather early stage of the infection (8 and 12). Therefore, it is likely that innate immune cells are producing IL10. Interestingly, recent reports indicated that neutrophils can exert

Figure 4-8. IFN γ plasma levels profiles across early time points post infection comparing selected highly susceptible and highly resistant ARI-BXD strains.

We infected three highly susceptible ARI-BXD strains (BXD100, 77 and 97) and three highly resistant ARI-BXD strains (BXD48, 73 and 87) with 2×10^7 CFU/mouse of hypervirulent MIT1 GAS strain. We sacrificed and collected plasma for a set of mice per strain at each time point post infection, 8, 12, and 24 hours, therefore, there were no multiple bleedings of any of the mice used. In parallel, a control group of uninfected mice were used for collection of plasma for estimating normal levels of IFN γ in these selected strains. (A). Comparison of medians of levels of IFN γ in susceptible mice showed that levels of IFN γ increased significantly only at 24 hours post-infection compared to pre-infection (zero hour). In addition, levels at 24 hours were significantly higher than 12 hours post infection. Panel B. Resistant strains showed increase in levels of IFN γ post-infection, however, none reached statistical significance. Panel C. We compared IFN γ plasma levels in susceptible (red dots) vs. resistant (blue dots) groups at the analyzed time points. There were significant differences in levels of IFN γ between resistant and susceptible strains only at 24 hours, which is the biologically relevant time point for IFN γ actions. Statistical significance comparing resistant to susceptible groups was based on Mann-Whitney test. We applied Kruskal-wallis test to assess statistical significance of differences in levels of IFN γ between and across time points (stages of infection) analyzed (panels A and B). In general a p-value of < 0.05 was considered significant. (For number of samples analyzed please refer to page 65 footnote).

A Susceptible strains



B Resistant strains

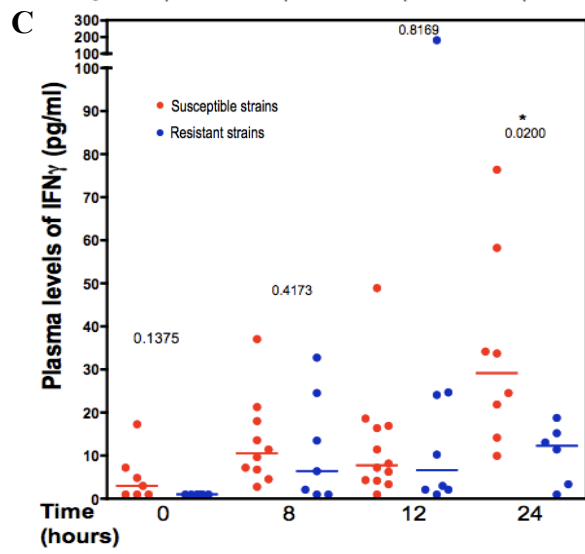
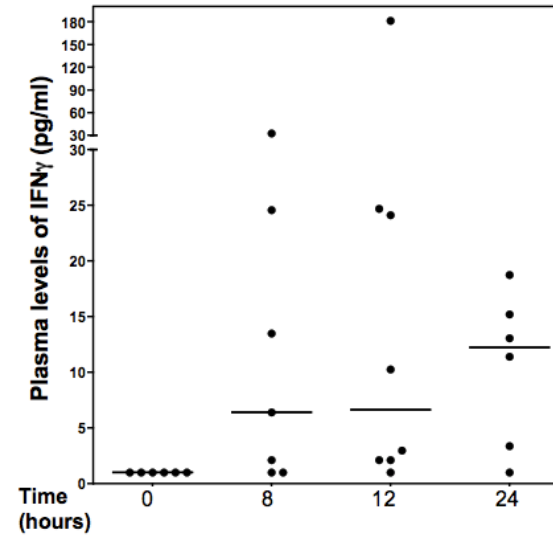
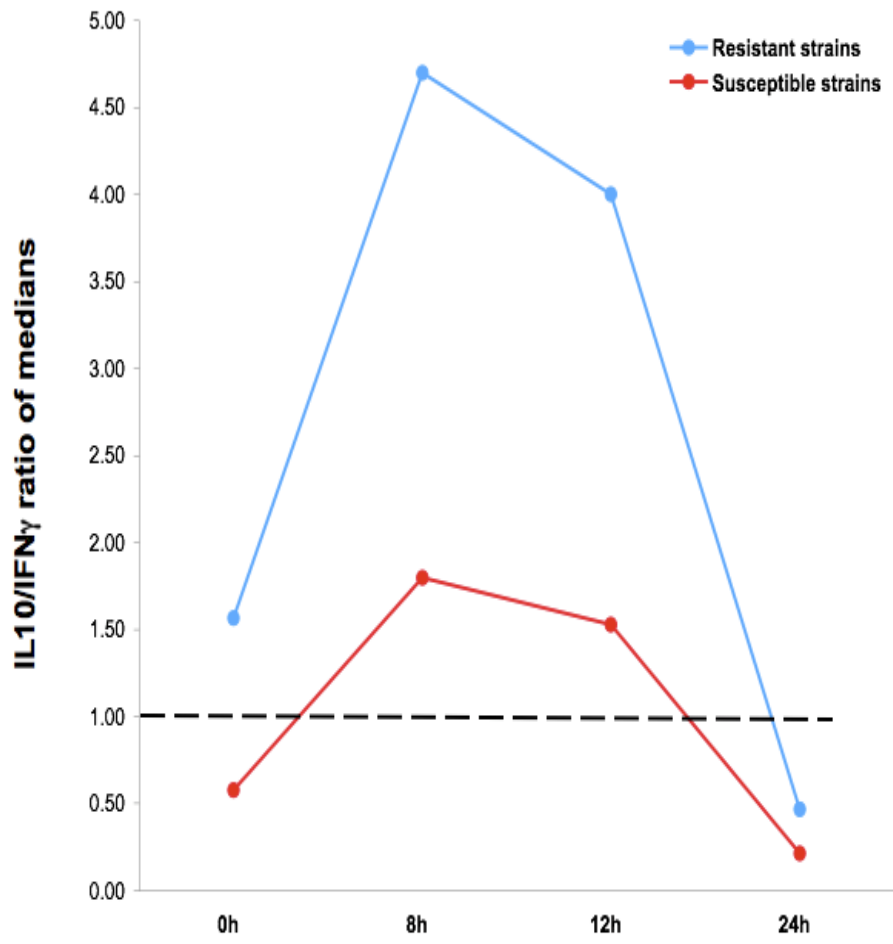


Figure 4-9. Comparison of ratios of anti-inflammatory to pro-inflammatory cytokines, comparing ratios of medians of IL10/IFN γ plasma levels across early time points post infection in selected highly susceptible and highly resistant ARI-BXD strains.

We infected three highly susceptible ARI-BXD strains (BXD100, 77 and 97) and three highly resistant ARI-BXD strains (BXD48, 73 and 87) with 2×10^7 CFU/mouse of hypervirulent MIT1 GAS strain. We sacrificed and collected plasma for a set of mice per strain at each time point post infection, 8, 12, and 24 hours, therefore, there were no multiple bleedings of any of the mice used. In parallel, a control group of uninfected mice were used for collection of plasma for estimating normal levels of IL10 and IFN γ in these selected strains. Data for individual cytokines were shown in Figures 4-7 and 4-8. Shown here are data from Figures 4-7 and 4-8 reanalyzed where medians of each cytokine at each time point was calculated and ratio of medians of IL10/IFN γ was calculated. Resistant group showed higher ratio of IL10/IFN γ than susceptible group at all the compared time points, indicating that anti-inflammatory levels are governing the immune response in resistant strains, adjusting the pro-inflammatory levels to appropriate levels and keeping the pro-inflammatory cytokines in check. Higher levels of IL10 were generally associated with protection, where we postulate that uncontrolled pro-inflammatory cytokine avalanche leads to sepsis in the current studied GAS sepsis model. (For number of samples analyzed please refer to materials and methods section).



immunomodulatory effects by secreting IL10 (Cassatella *et al.*, 2009; Zhang *et al.*, 2009b). These findings are interesting as it agrees with our hypothesis of IL10 exerting active suppression of exaggerated immune responses and hence high levels of IL10 are associated with protection. More detailed studies to support or refute this hypothesis are needed, with further dissection of the causal agent and modulator of IL10 levels, which we hypothesized to be PGE2 as discussed in the next section. In conclusion, the association of GAS sepsis severity with cytokines exerting their effects temporally underscores the complexity of traits modulating severe GAS sepsis.

Analysis of the Role of Prostaglandin at Early Stage of Infection

The QTLs we mapped to Chr 2 have several immune-related genes that are polymorphic and made biological sense. We narrowed down our QTLs using multiple bioinformatics tools including linkage analyses, gene ontology analyses, and polymorphism analyses; at this point we had a candidate gene list that we parsed into pathways. The resultant pathways were validated by selecting key genes in each pathway and validating differential levels in susceptible and resistant strains post infection (as detailed in chapter 3). Real time PCR analyses associated differential susceptibility with two main pathways, IL1 and prostaglandin E pathways (Abdeltawab *et al.* 2008 and chapter 3 in this dissertation). In this section of the dissertation, I am going to focus on studies we performed to find prostaglandins association with differential susceptibility to GAS sepsis.

There are a total of five prostaglandins genes located either within our two main mapped QTLs on Chr 2 or located in their proximity. These genes were differentially expressed in our quantitative PCR analyses, however, we didn't detect these differences in our array data at the time points we selected. The five prostaglandin genes in our QTL include, prostaglandin D2 synthase (*Ptgds*), Chr 2 (25.28 Mb), which is a polymorphic (see Appendix C) gene encoding a lipocalin-type prostaglandin. Over expression of *Ptgds* in lung was associated with better outcomes in bacterial pneumonia model (Joo *et al.*, 2007). Two other prostaglandins are located in the proximity of mapped QTLs, prostaglandin-endoperoxide synthase 1 (*Cox-1*) (Chr 2 (36.05 Mb)) and prostaglandin I2 (*Ptgis*) aka prostacyclin (Chr 2 (166.89 Mb)). Prostacyclin has immunoregulatory properties similar to PGE2, with immunosuppressive actions on macrophage in infectious diseases (Aronoff *et al.*, 2007). Of particular interest are prostaglandin E synthases 1 (*Ptges*) and 2 (*Ptges2*), on Chr 2, at 30.71 and 32.21Mb, respectively. These two genes were quite interesting as we found that increased expression levels of *Ptges* and *Ptges2* were associated with increased susceptibility to GAS sepsis (chapter 3 in this dissertation and (Abdeltawab *et al.*, 2008). Although following Occam's razor principle one would postulate that one gene within these QTLs might be the modulator of the differential susceptibility observed. In addition, it might be that the co-existence of these immune-related genes is by chance since the QTL is huge (~10Mb in size) allowing co-existence of multiple immune-related genes. However, we found that these candidate genes were polymorphic (Appendix C), in addition, pathway analyses revealed that these mapped genes act together, moreover, our QTL acts as cis-acting QTL.

Based on our QTL analyses and our quantitative gene expression analyses and literature associated with other infectious diseases, we hypothesized that exaggerated production of prostaglandins E2 (PGE2), the product of PTGES, in susceptible strains might predispose them to severe response to GAS. Meanwhile, controlled amounts of PGE2 in resistant strains could modulate a balanced response. To test our hypothesis, we aimed to quantify PGE2 levels in susceptible and resistant strains at early time points post infection that are more relevant to the quick responses mounted by PGE2. Being a lipid mediator, PGE2 can exert its actions within few minutes post infection and is crucial in the first 24 hours of infection (reviewed in [Harris *et al.*, 2002; Bos *et al.*, 2004; Sakata *et al.*, 2010]). Therefore, we investigated the levels of PGE2 at 30 minutes intervals after infecting susceptible and resistant strains with the hypervirulent M1T1 GAS strain. We sacrificed 4 mice per strain at each time point, examining the first 2 hours in 30 minutes intervals (30, 60, 90 and 120 minutes) following infection (Figure 4-10). We found that susceptible strains had significantly higher PGE2 levels compared to resistant mice, especially during the first 60 min post-infection (Figure 4-10). This suggested that our hypothesis is valid and matched our real time PCR expression data of *Ptges* and *Ptges2*, our mapped QTL, and the association between increased levels of PGE2 and severe of GAS sepsis. Further studies to elucidate the mechanism of action are undergone in the laboratory.

Our finding that higher levels of PGE2 association with severe GAS sepsis along with our finding its synthases in our mapped QTL in our GWAS (Chapter 3, Appendix A and Abdeltawab *et al.* 2008). These synthases are polymorphic (Appendix C) and their levels are differential expressed as observed in our qPCR results (Chapter 3 and Abdeltawab *et al.* 2008). Collectively this led us to believe that PGE2 is an excellent candidate modulator of differential susceptibility, however, the mechanism of modulation needs further studies especially that PGE2 mechanism of action is complicated by the fact that it acts as a Janus mediator. PGE2 can act as pro-inflammatory mediator inducing IL6 production and causing vasodilatation and vascular leakage in inflammatory responses (reviewed in [Harris *et al.*, 2002; Bos *et al.*, 2004; Sakata *et al.*, 2010]). Both events are crucial in GAS sepsis severity. In addition, PGE2 can act as an immunosuppressive, reducing neutrophil migration and bacterial killing by macrophages, by blocking production of reactive oxygen intermediates (ROI) (Sakata *et al.* 2010).

Moreover, it has been debated whether PGE2 promotes Th1 or Th2 responses, however, recent studies show that PGE2 activates its EP2 and EP4 receptors, and promotes Th1 differentiation and Th17 expansion (Yao *et al.*, 2009) However, the two faces of PGE2 are not mutually exclusive, as PGE2 actions depend on multiple factors, including the cells it is exerting its actions on, stage of infection, receptors being activated and nature of the activation signal, and more importantly the concentration of PGE2. Where studies have shown that if the fine balance of this mediator is disturbed it can lead to pathological consequences. For example alterations in the amounts of PGE2 are associated with high risk of infection with HIV, cancer, and malnutrition (Lima *et al.*, 2006; Anstead *et al.*, 2009; Greenhough *et al.*, 2009).

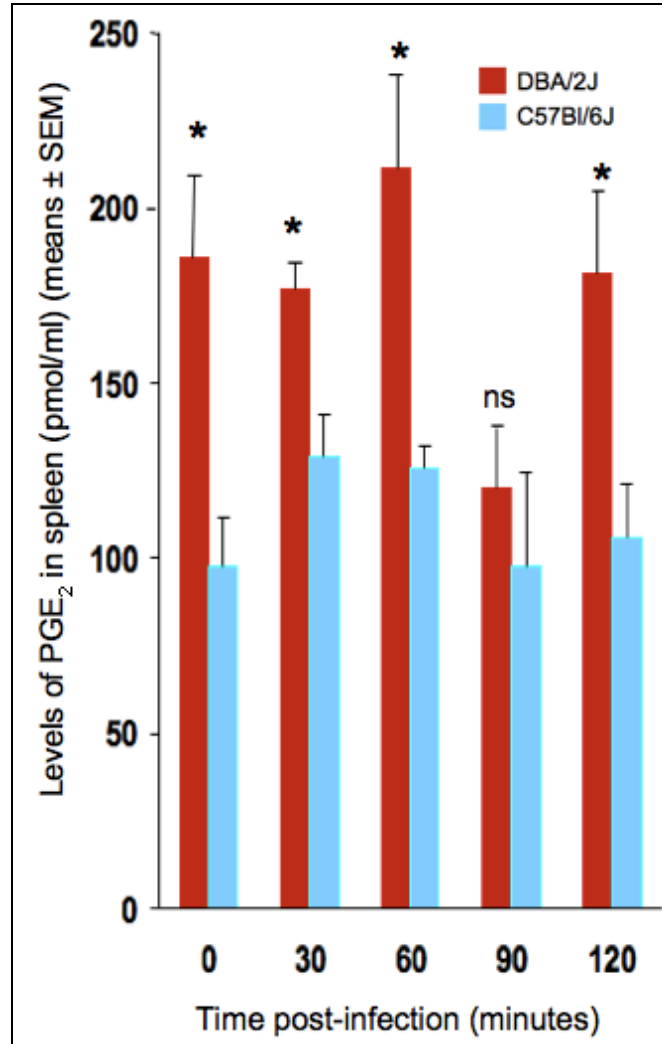


Figure 4-10. Analysis of prostaglandin role at early stages of severe GAS sepsis.

Higher levels of PGE₂ in susceptible strains at all examined stages of infection were observed. We used the parental strains of BXD panel, C57Bl/6J (B6) and DBA/2J (D2), (n = 4 mice per strain per time point). The time points examined were, 0, 30, 60, 90 and 120 minutes post infection. Data shows that D2 (the susceptible parental strain) has higher levels of PGE₂ compared to B6 even before infection (0hr). Following infection with GAS (2×10^7 CFU), D2 PGE₂ levels remained high throughout the observed 120 min following infection except for a drop at 90 min. Meanwhile, B6 seemed to maintain a steady level of PGE₂ with a trend of slight increase at 30-60 min then back to starting levels at 90-120 min.

Excitingly, studies have shown that PGE2 can inhibit production of IL10 from T cells, and to exacerbate Th17 mediated inflammation (Boniface *et al.*, 2009; Yao *et al.*, 2009). In the studies outlined in this dissertation we have shown that susceptibility and poor outcome of sepsis were associated with higher levels of PGE2 (Figure 4-10), and IFN γ (Figure 4-8) and lower levels of IL10 (Figure 4-7). Therefore, we hypothesize that PGE2 can act as a “switch”, where in susceptible strains PGE2 can inhibit IL10 production, and increase IFN γ levels, thereby promoting Th17 mediated inflammation. Meanwhile, we believe that in resistant strains PGE2 is produced in controlled levels, allowing Th1 and Th17 polarization and subsequent containment of infection. We are even more interested in this interactive role of PGE2 and IL10 as our recent *in vitro* human studies showed that IL10 mediates protection against severe GAS sepsis (discussed above). In addition, our mouse genome-wide expression pathway analyses identified IL10 pathways to be upregulated in resistant strains at early time points (8h) (Figure 4-2) associating high levels of IL10 with resistance to GAS sepsis and better outcomes of infection.

Conclusion

Our genome-wide transcriptional analyses of infected vs. uninfected resistant and susceptible strains revealed differentially expressed genes that belong to innate immune response pathways that matched our mapped QTLs pathways. Moreover, our analyses of secreted soluble biomarkers (cytokines and prostaglandins) at the studied time points validated the pathways identified through GWAS and GW expression analyses. This shows the power of the systems genetics approach in identifying disease mechanisms, biomarkers and pathways that are associated with differential susceptibility to severe GAS sepsis. Importantly our pathway discovered in mouse matched our findings from clinical studies. This showed that pathways to pathways comparisons between mouse and human can be more readily translated than comparing gene to gene.

Materials and Methods

Bacteria and Infection Studies Using Mice

We used hypervirulent MIT1 GAS strain clinical isolate GAS 5448 (Chatellier *et al.*, 2000). Bacterial culture and inoculum used in infection studies were prepared as detailed previously (Aziz *et al.*, 2007). The institutional animal care and use committee (IACUC) at the University of Cincinnati, OH approved all procedures involving mice and mice tissues described in current study.

Experimental Design of Time Series Infection Studies

To study the kinetics of cytokines and differential gene expression post GAS sepsis, we designed time course (series) experiments. In these experiments, we infected a

group of mice belonging to selected highly resistant and highly susceptible ARI-BXD strains and sacrificed the mice at selected time points post infection. In parallel, we injected saline to control group of mice belonging to those selected strains as above. At each time point, we sacrificed the mice, collected blood, using cardiac puncture procedure, and harvested spleens. Blood was used to isolate plasma for cytokine analyses and reconstituted blood (with nuclease-free saline) and preserved blood in RNALater for blood RNA purification at a later stage. Harvested spleens were immediately homogenized in RLT buffer and frozen at -80°C till further purification of spleen RNA.

Processing of Blood and Spleen Samples and Purification of RNA

We investigated the global gene expression in spleen and blood of infected vs. control groups of mice at selected time points. We selected highly susceptible strains (BXD97, BXD100, and BXD77) and highly resistant strains (BXD87, BXD48, and BXD73) for our analyses. We performed 2–3 biological replicates (experiments) for each selected highly susceptible and highly resistant strains, $n = 3$ mice per strain per time point (Figure 4-1). Data represents 7 different experiments with the use of the same strains overlapping multiple cohorts and comparing expression from same strain used in different experiments. We isolated spleen RNA using RNeasy mini (Qiagen, Valencia, CA) and isolated blood RNA using Mouse RiboPure kit (Ambion, Austin, Texas) according to manufacturer's protocol. We pooled RNA samples per strain using RNA samples that passed our quality control testing of integrity and purity as detailed below. Globin mRNA was removed from all blood RNA using GlobinClear kit (Ambion). All RNA samples (blood and spleen) were treated for removal of DNA contamination and RNA was further purified by re-precipitation using ethanol precipitation. All RNA samples were checked for RNA purity and integrity. RNA purity was evaluated using the 260/280 and 260/230 absorbance ratios; RNA samples with 260/280 and 260/230 values of ≥ 1.8 were chosen. Further, RNA integrity was assessed using 1% RNA denaturing agarose gels. We required clear sharp bands of 18S and 28S rRNA for all samples compared to a control RNA sample to ensure intactness of RNA.

Microarray Platform and Design

We used Illumina mouse GW-6 v2.0 BeadChip; probes cover more than 45,200 transcripts per sample, targeting genes and known alternative splice variants. The probes content is derived from the NCBI Reference Sequence (RefSeq) (Build 36, Release 22), supplemented with probes derived from the Mouse Exonic Evidence Based Oligonucleotide (MEEBO) set, as well as exemplar protein-coding sequences described in the RIKEN FANTOM2 database.

We used RNA samples that passed quality control as detailed above and of concentration ≥ 50 ng/ul for cRNA synthesis using Illumina TotalPrep RNA amplification kit (Ambion) according to manufacturer protocol. The basic outline of the procedure involves reverse transcription of RNA to synthesize cDNA using oligo (dT) primer, followed by *in vitro* transcription of purified dsDNA to synthesize amplified biotinylated

cRNA (aRNA). We evaluated purified labeled cRNA using same methods as mentioned above for RNA samples. cRNA samples of good quality were then used to hybridize to Illumina mouseWG-6 v2.0 according to Illumina standard protocols.

This data set consists of arrays processed in four batches or groups, where groups of 2, 4, 1, and 4 beadchips were scanned at a time. Samples from seven different ARI-BXD strains were compared at 5 time points (0, 8, 12, 16 and 24 hours post infection) belonging to two different tissues, blood and spleen. A single operator processed all arrays using illumina protocol for hybridization, washing and scanning. All samples in a group were labeled on one day and chips were scanned using BeadArray Reader.

Microarray Data Processing and Analysis

Pooled RNA samples from blood and spleens (n = 60 samples) were processed using a total of 10 Illumina mouseWG-6 BeadChips. All chips passed quality control and error checking. This data set was extracted and processed using the Bead Studio 3. We applied 75th percentile normalization to all the samples and the resulting expression values were analyzed for statistical significance of differences between susceptible and resistant strains at different time points in the studied tissues.

Identification of Differentially Expressed Genes and Functional Pathways Analyses

We performed functional analyses of differentially expressed genes from our genome-wide transcriptome analyses using Ingenuity pathways analysis (IPA) (www.ingenuity.com). Each data set containing gene identifiers was uploaded into the online application, and each gene was overlaid onto a molecular network developed from information contained in the ingenuity pathways database. We chose IPA most significant “Canonical Pathways”, which are pathways identified from the Ingenuity Pathways Analysis library of pathways to be most significant to the data set. The Canonical Pathways are displayed as y-axis in bar charts; x-axis displays the significance in ($-\log(P\text{-value})$) where the higher the number the more likely the association is not by chance. In addition a ratio is calculated for each pathway, which is the number of differentially expressed genes divided by total number of molecules in this pathway. Therefore, taller bars have more genes associated with the Canonical Pathway than shorter bars. The significance of the association between the dataset and the pathways was measured in two ways: (1) the ratio (described above) and (2) by Fisher’s exact test with $P < 0.001$.

Cytokine Measurements and Analyses

We studied the kinetics of plasma cytokine production in selected highly resistant and susceptible strains. Groups of 3–5 mice per strain per time point from selected highly susceptible and highly resistant ARI-BXD strains, which were infected with $2 \pm 1.5 \times 10^7$ CFU/mouse of a hypervirulent MIT1 GAS strain. In parallel, a control group of

uninfected mice were used for collection of plasma for estimating normal levels of cytokines in these selected ARI-BXD strains. We euthanized mice and collected blood using cardiac puncture procedure into heparin-coated tubes. We separated plasma from individual mice, added protease inhibitor cocktail to each plasma sample and stored samples at -20°C till further use. We measured cytokines levels in plasma of representative 2 mice per strain of highly resistant (BXD48, 73 and 87) and highly susceptible strains (BXD100, 77 and 97), with exceptions where we assayed more samples from some strains as indicated in footnote of Figure 4-5. We analyzed data collected for time points 8, 12, and 24 hours post-infection. We used a multiplex cytokine ELISA kit from Millipore (Billerica, MA) to detect 4 cytokines: interleukin 6 (IL6), IL10, tumor necrosis factor alpha (TNF α), and gamma interferon IFN γ . The analyzed data shown in Figures 4-5 to 4-9 are representative of susceptible and resistant groups, where 2 mice per strain (mentioned above) per time point were analyzed, with the exception of BXD 97 at 8 and 12h we used 4 mice and for BXD77 we used 4 and 6 mice at 12 and 24 h respectively, and BXD87 at 8, 12 and 24 h 4 mice were used and one mouse at 8 hours of BXD48. We collected far more plasma samples that are to be assayed. All other data shown in Figures 4-5 to 4-9 are for 2 mice per strain (3 strains used) per time point (4 time points analyzed).

Prostaglandin Studies

We selected parental strains for studying the role of prostaglandins in modulating differential susceptibility to infection. Mice (6-8 weeks-old mice of DBA/2J susceptible parent strain and the C57Bl/6J resistant parent strain) were purchased from The Jackson Laboratory (Bar Harbor, Maine). To test the effect of prostaglandins on differential responses to GAS sepsis, we studied early systemic prostaglandin E₂ (PGE₂) production (within the first 2 hours of infection) in 30 minute intervals (30, 60, 90 and 120 minutes) following inoculation. We infected mice with 2×10^7 CFU/mouse of the hypervirulent M1T1 GAS strain, and sacrificed 4 mice per strain per time point. Bacterial suspensions used for infection of mice were prepared as detailed in Aziz *et al.* (2007). We collected blood using a standard cardiac puncture procedure and dissected the spleens and homogenized them using a tissue homogenizer, TH (Omni International, Marietta, GA) in 2 ml of PBS. Tissue homogenates were stored frozen at -20°C and sent on dry ice to the University of Michigan, Ann Arbor, MI. The homogenates were thawed then centrifuged at high speed (13,000 RPM) for 5 min to remove particulates. PGE₂ levels were quantified in spleen homogenate supernatants using an enzyme-linked immunosorbent assay (ELISA) PGE₂ kit according to the manufacturer's instructions (Assay Designs, Ann Arbor, Michigan).

Statistical Analyses

We used ANOVA and t unpaired test to assess significance of differentially expressed genes in either resistant or susceptible group at a given stage of infection compared to its uninfected control group, using GeneSpring GX 11.0 (Agilent technologies, Inc.). Normalization of microarray data is detailed above.

We used Kolmogorov-Smirnov test to assess normal distribution of our cytokine data, we found that our cytokine data was not normally distributed, and since the number of samples in some of the tested groups was less than 10, we didn't apply any normalization methods. Since our data showed that samples had non-normal distribution, we applied the non-parametric tests detailed below To assess statistical significance of differences in levels of different cytokines across time points analyzed we used Kruskal-Wallis test. We evaluated the statistical significance of levels of a given cytokine at a given time point in resistant vs. susceptible strains by using Mann-Whitney test. In all the statistical tests we performed, a P-value less than 0.05 was considered significant. All data was analyzed using GraphPad Prism (La Jolla, CA).

CHAPTER 5. ANALYSIS OF CELLULAR POPULATIONS MODULATING DIFFERENTIAL RESPONSE TO SEVERE GAS SEPSIS

Summary

We have previously mapped quantitative trait loci (QTLs) associated with differential susceptibility to severe GAS sepsis using advanced recombinant inbred (ARI) ARI-BXD strains (Abdeltawab *et al.*, 2008). We narrowed down these QTLs and parsed candidate genes into pathways associated with severity to GAS sepsis. We then compared pathways discovered through *in vivo* genome-wide association studies with those discovered through genome-wide transcriptome analyses and found that they matched quite well and even more interestingly, some of these pathways were interacting with each other. Subsequently, we aimed to explore the role of the key genes in those discovered pathways in modulating differential host responses to GAS sepsis (covered in Chapter 4).

In this chapter, we examined the cellular differences between resistant and susceptible strains to help us further elucidate cellular mechanisms underlying the differentially expressed candidate genes in modulating the differential susceptibility to GAS sepsis. To achieve this, we first aimed to examine and characterize differences in immune cell populations of blood and spleen of selected resistant and susceptible strains under normal physiological conditions and found that there were no significant differences between the susceptible and resistant strains with respect to the numbers and percentages of examined immune cells in both blood and spleen. This suggested that inherent variations in percentages of immune cell population among the immunophenotyped BXD strains were not linked to their differential susceptibility to severe GAS sepsis. Accordingly, we aimed to examine the hypothesis that migratory and functional differences rather than cellular availability might be a possible mechanism of resistance.

Subsequently, we aimed to examine the possibility that differences in cellular responses may account for the differential susceptibility to GAS sepsis in our mouse model. Specifically, we wanted to test the hypothesis that effective innate responses in the early stages of infection is directly associated with resolution of GAS infection, and better outcome of GAS sepsis. We based our hypothesis on studies from our group and other groups that showed that neutrophils (Voyich *et al.*, 2004; Buchanan *et al.*, 2006; Nilsson *et al.*, 2006; Soehnlein *et al.*, 2008a; Navarini *et al.*, 2009), macrophages (Goldmann *et al.*, 2004a; Thulin *et al.*, 2006; Goldmann *et al.*, 2009), NK cells (Goldmann *et al.*, 2005b; Takahashi *et al.*, 2007) and dendritic cells (Loof *et al.*, 2008; Cortes and Wessels, 2009; Yong *et al.*, 2009), each play an important role in streptococcal infections according to the site and the stage of infection. We started our cellular dissection by examining the role of neutrophils in differential susceptibility to GAS sepsis. Neutrophils are dominant cells in circulation and thus mediate early innate immune response. It has been shown that recruitment, migratory and functional defects in neutrophils result in increased mortality post bacterial infection (reviewed in [Nauseef, 2007]).

To examine the likely contribution of neutrophils in modulating differential susceptibility in our GAS sepsis model, we first depleted neutrophils and assessed how this may affect infection outcomes in susceptible vs. resistant ARI-BXD strains. We depleted neutrophils using anti-mouse Ly-6G and Ly-6C (RB6-8C5) (Czuprynski *et al.*, 1994) 24h prior to infection and found that this rendered resistant BXD strains susceptible. This was associated with an increased bacterial load in depleted mice vs. control mice. The reversal of phenotype of resistant strains, while susceptibility was exaggerated in susceptible strains, confirmed the key role of neutrophils in controlling GAS sepsis.

We also depleted macrophages using clodronate liposome (Van Rooijen and Sanders, 1994) in susceptible and resistant strains and found similar results with reversal of phenotype of resistant strains and exaggerated susceptibility of the susceptible strains. These results demonstrate the important role of both neutrophils and macrophages in modulating differential host responses in GAS sepsis. We also examined the kinetics of neutrophils and macrophages in the first 24 h post infection and found no significant differences between susceptible and resistant BXD strains. However, peripheral blood monocytes were significantly higher in susceptible strain at 16h post infection further showing that even higher numbers of monocytes did not contribute to better outcome of sepsis.

The above data suggested that the numbers of neutrophils and macrophages are not the determinant of the outcome of infection as susceptible strains had an equal or higher numbers of these cells as the resistant strains. Collectively, our data suggest that functional and/or migratory differences in these cells play an important role in modulating differential susceptibility.

Results and Discussion

Profiling of Blood Cell Populations across Selected Resistant and Susceptible Strains Reveals Possible Migratory and Functional Differences Rather than Cellular Availability as a Possible Mechanism of Individual Variations in Susceptibility to Severe GAS Sepsis

Homeostasis is a dynamic system regulated by complex interactions between environmental and genetic factors. Blood cellular percentages, platelet counts and erythroid traits have been associated with several QTLs using both inbred and BXD strains (Chen and Harrison, 2002; Peters *et al.*, 2005; Ferreira *et al.*, 2009) GAS has multiple virulence factors that affect and interfere with host homeostasis, for example, interruption of coagulation system (Tapper and Herwald, 2000; Frick *et al.*, 2007), as one of the causes of pathogenesis.

The parental strains of the BXD panel, C57Bl/6J and DBA/2J, show significant differences in numbers and percentages of lymphocytes and granulocytes populations in blood (Chen and Harrison, 2002; Kile *et al.*, 2003; Petkova *et al.*, 2008). Therefore, we

wanted to examine if observed differential susceptibility to GAS sepsis was due to differences in availability of immune cells. Hence, we aimed to explore differences in the percentages of immune cells in the blood of selected highly resistant and highly susceptible ARI-BXD strains prior to infection and/or any manipulation. Using complete blood counts (CBC), we profiled five immune cells populations in blood (neutrophils, monocytes, lymphocytes, eosinophils and basophils) of highly susceptible strains (BXD100, BXD90, BXD75) and highly resistant strains (BXD73, BXD87 and BXD69), Figures 5-1 and 5-2.

We found no significant differences between resistant and susceptible strains indicating that differences in response to GAS sepsis is not due to differences in cellular populations of susceptible strains vs. resistant strains. We also found that each strain irrespective of its susceptibility had a unique percentage of different immune cell populations, for example, neutrophil percentages (NE %) was variable among susceptible strains ranging from 23–37 % while in resistant strains it ranged from 14.7–27 %. Showing no significant differences between resistant and susceptible groups, indicating that variability in number of cells is irrespective of their differential susceptibility, and that differential response to GAS sepsis is not related to inherent differences in these immune cells numbers.

Immunophenotyping Analyses of Cellular Population under Normal Physiological Conditions in Spleen of BXD Strains Revealed No Differences in Cellular Numbers or Relative Percentages among Susceptible and Resistant Strains

We immunophenotyped spleen cellular populations in selected resistant and susceptible BXD strains. The spleen as a blood filtering lymphoid organ, is involved in mounting immune responses to extracellular blood borne pathogens such as GAS (Mebius and Kraal, 2005). We wanted to examine if there were any inherent differences in number of immune cells in spleen due to strains variability. We found no significant differences in the analyzed immune cell populations in spleen among highly susceptible and highly resistant strains under normal physiological conditions (Figure 5-3).

Altogether, these data illustrated how different combinations of polymorphic genes and recombinations, can result in a different manifestation from the ancestral parent of these strains. However, in the current study, variations in numbers of immune cells in both spleen and blood of selected highly resistant and susceptible strains were not linked to differential susceptibility to severe GAS sepsis. Our data suggest that possible migratory and functional differences rather than cellular availability as a possible mechanism of differential susceptibility to severe GAS sepsis.

***In vivo* Manipulation of Cellular Populations in Susceptible and Resistant Strains: Depletion of Gr-1⁺ Cells and Macrophages Rendered Resistant Strains Susceptible**

To this extent we have established that the numbers of immune cells at physiological state were not different between examined highly resistant and susceptible

Figure 5-1. Differential blood count of selected susceptible and resistant BXD strains.

We used 4–8 mice per sex, per strain, 8–12 weeks-old. The data show no significant differences between resistant and susceptible strains. Since there were significant differences in NE% between sexes of same strain (BXD69), we are showing males separate from females for all the results. LY lymphocytes, NE neutrophils, MO monocytes, BA basophiles, EO eosinophils. Significance based on Student t-test $p < 0.01$.

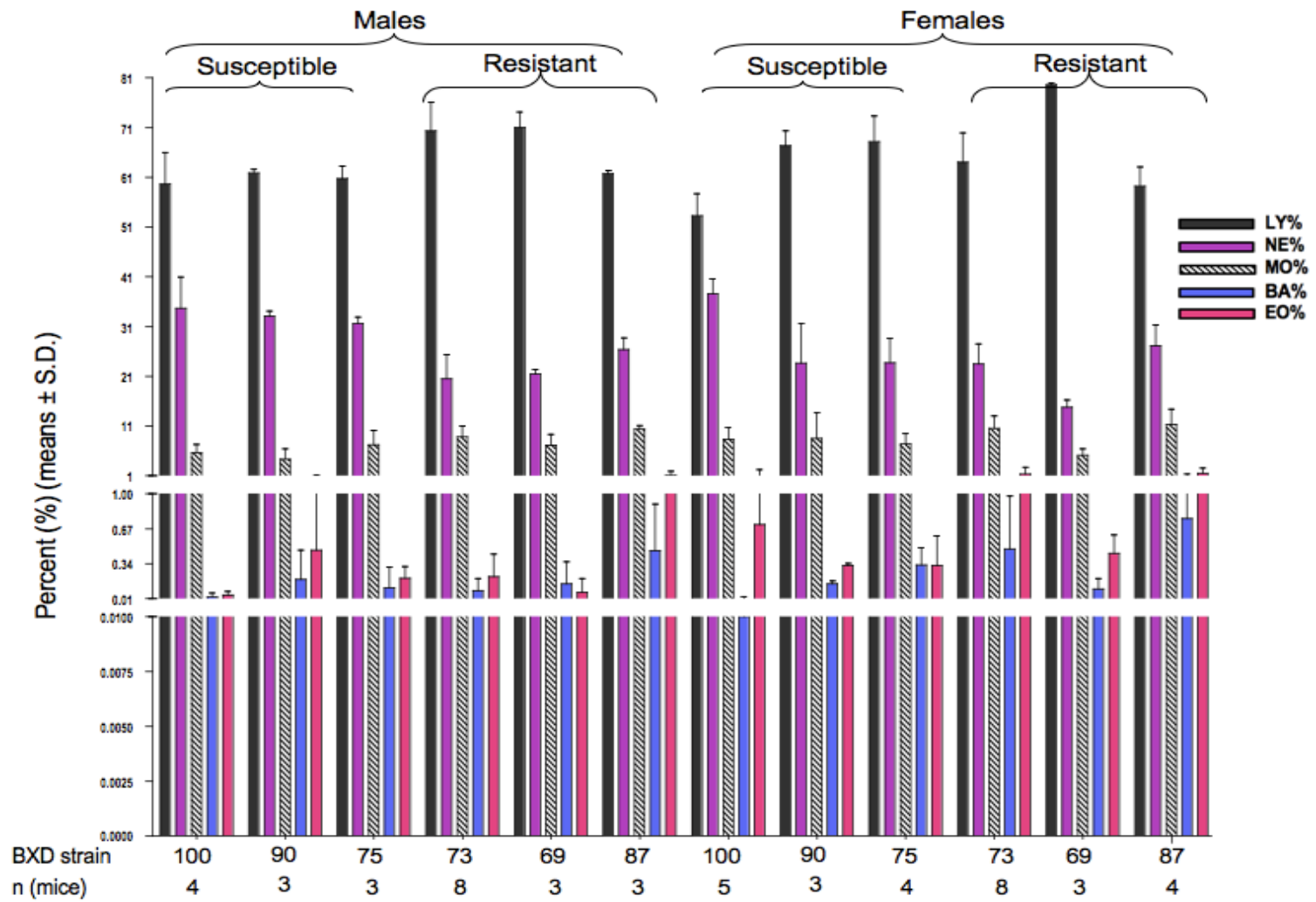
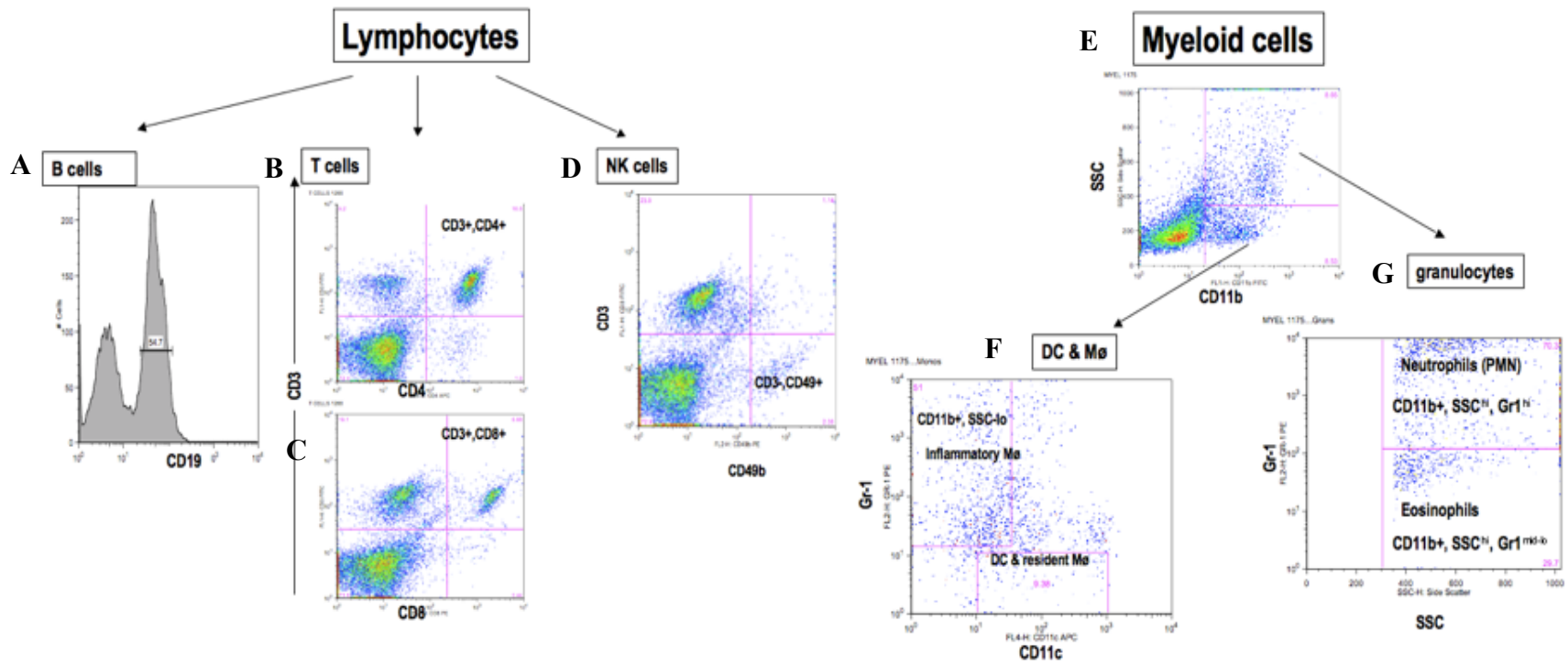


Figure 5-2. Diagram showing a scheme for flow cytometric analysis of immune cell populations in spleen employed in the current study.

We used CD19-FITC to characterize total B cells in spleens (panel A). To characterize main subpopulations of T lymphocytes, we used a mixture of CD3-FITC, CD8-PE and CD4-APC, we defined CD3⁺, CD4⁺ as T helper cells (panel B), and CD3⁺ CD8⁺ as T cytotoxic cells (panel C). Natural killer cells were gated as CD3⁻, CD49b⁺, where CD49b is a pan NK cells marker that is expressed on both parental strains NK cells. We differentiated between granulocytes and macrophages based on granularity (side scatter (SSC)) and CD11b staining as shown in panel E, where we gated on CD11b⁺ with high granularity and designated this as total granulocytes (panel G) while CD11b⁺ cells with lower granularity (SSC_{lo}) were assigned a separate gate and designated as macrophages (panel F). Macrophages were then categorized based on their Gr-1 and CD11c expression into resident and inflammatory macrophages (M \emptyset) as shown in panel F. Total granulocytes population (panel G) were then analyzed based on their Gr-1 and SSC into neutrophils and eosinophils as indicated in panel G.



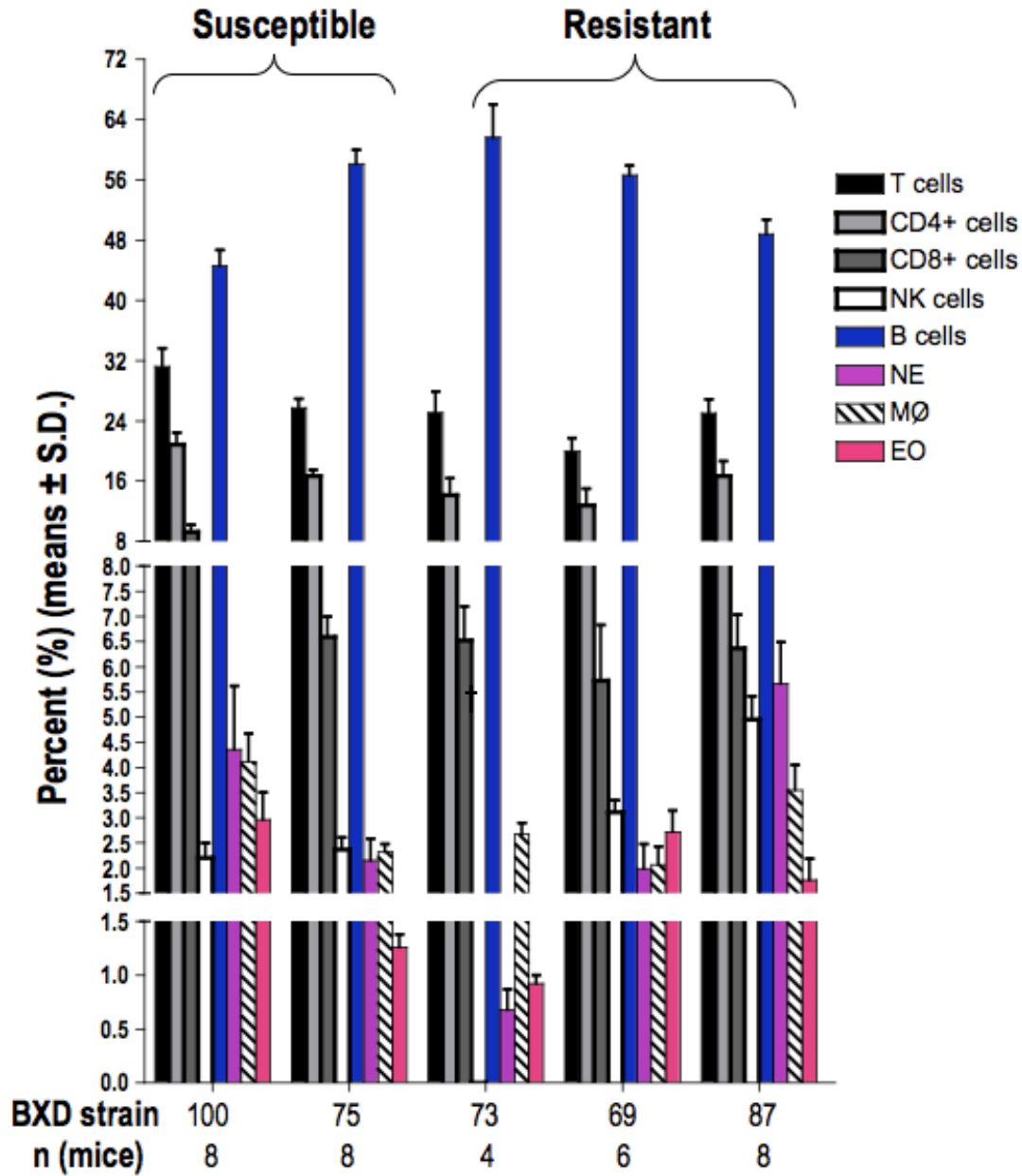


Figure 5-3. Immunophenotyping of spleen cellular populations in selected resistant and susceptible BXD strains.

We used 3–8 mice per sex per strain; age 8–12 weeks old. There were no significant differences in any of the analyzed cellular populations due to sex; therefore, data shown in this Figure represents pooled males and females per strain. There were no significant differences ($P \leq 0.01$) between resistant and susceptible strains when comparing different immune cell populations in spleen. NE neutrophils, Mø macrophages, EO eosinophils, and NK natural killer cells. † NK cells were not analyzed for BXD73.

strains. Therefore, migratory and/or functional differences rather than cellular availability may possibly account for the differential susceptibility to severe GAS sepsis. Therefore, we aimed to dissect the role of neutrophils and macrophage in differential susceptibility to severe GAS sepsis. We selected neutrophils (PMNs) and macrophages as our genome-wide association studies and our transcriptome analyses suggested key roles for these two cell populations in modulating severe GAS sepsis (Abdeltawab *et al.*, 2008).

Neutrophils and macrophages play an important role in modulating host responses to GAS sepsis (Goldmann *et al.*, 2004a; Voyich *et al.*, 2004; Medina and Lengeling, 2005). To dissect the role of these cells, we examined the effect of depleting them *in vivo* on differential mice susceptibility to severe GAS sepsis. We selected highly susceptible strains (BXD100 and BXD77) and highly resistant strains (BXD48 and BXD69) to test the effect of depleting Gr-1⁺ cells on GAS sepsis severity and outcomes (Figure 5-4).

Two days prior to the infection, we quantified the PMNs in all mice, and then at 24 hours prior to the infection, we injected a group of mice i.v. with 200 µg of anti-mouse Ly-6G and Ly-6C (RB6-8C5) antibody (Ab) which depletes Gr1⁺ cells within 12-24 hours. This depletion only lasts for 48h at which point PMNs are replenished by the bone marrow. In parallel, we injected a matching control group with isotypic control Ab (purified rat anti-mouse IgG2b κ). To verify neutrophil depletion in the (RB6-8C5) Ab treated group, we measured CBC/differential blood counts.

We then infected both groups with 10⁷ CFU/mouse of hypervirulent MIT1 GAS strain, and monitored their survival every 2 hours for the first 44 hours then every 8h till day 6 post infection, when all surviving mice were sacrificed. We found that the Gr-1 depleted resistant mice were rendered susceptible; indicating the key role of Gr-1 cells (PMNs and monocytes) in host defense against GAS sepsis. We found similar results when we depleted macrophages using clodronate liposomes. Both studies emphasize the role played by neutrophils and macrophages in resistance to severe GAS sepsis. Our results indicated that the first 24 hours of infection are crucial in determining the outcome of infection and the fate of the mice whether the mice will survive or succumb to the infection. This conclusion is based on the finding that despite the fact that PMNs are replenished at 48 hours post depletion and are increased in numbers this did not help anymore in fighting the infection (Figure 5-4). Our results are in concordance with (Goldmann *et al.*, 2004b) where depletion of macrophages prior to or during the first 24 h of infection affected mice susceptibility and that depletion of macrophages 48 hours post infection had no effect on mice survival. Therefore, our next step was to examine the kinetics of cellular populations in blood in the first 24 hours of infection in highly susceptible and resistant strains.

To examine the kinetics of neutrophils and monocytes in blood post infection, we measured percentages of these cells in susceptible and resistant strains at 8, 12 and 16 h post infection. We found no significant differences between resistant and susceptible strains (Figure 5-5). We also examined if there were any differences in further earlier time points of infection (2 hours) at intervals of 30 minutes, and we again found that there were no significant differences in numbers or percentages of neutrophils between

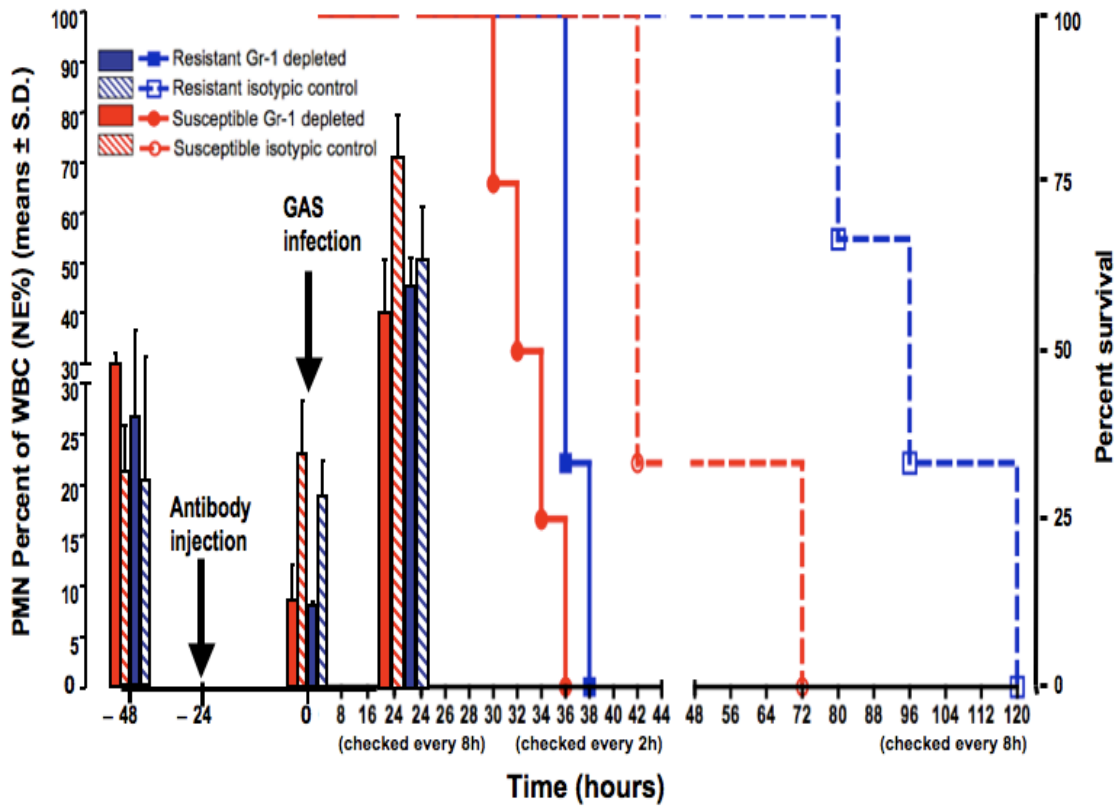


Figure 5-4. Depletion of Gr-1⁺ cells in selected resistant and susceptible BXD strains shows reversal of survival in response to GAS sepsis.

Summary of Gr-1⁺ depletion studies showing survival curves as percent survival on the right hand side, where depleted group are in solid lines and control group injected with isotypic control in dashed lines. Resistant strains were rendered susceptible, indicating the beneficiary effect of NEUTROPHILs in modulating host response to severe GAS sepsis. The bar graphs on the left represent percentage of neutrophils pre antibody injection, 24 hours post antibody injection and 24h post infection with GAS.

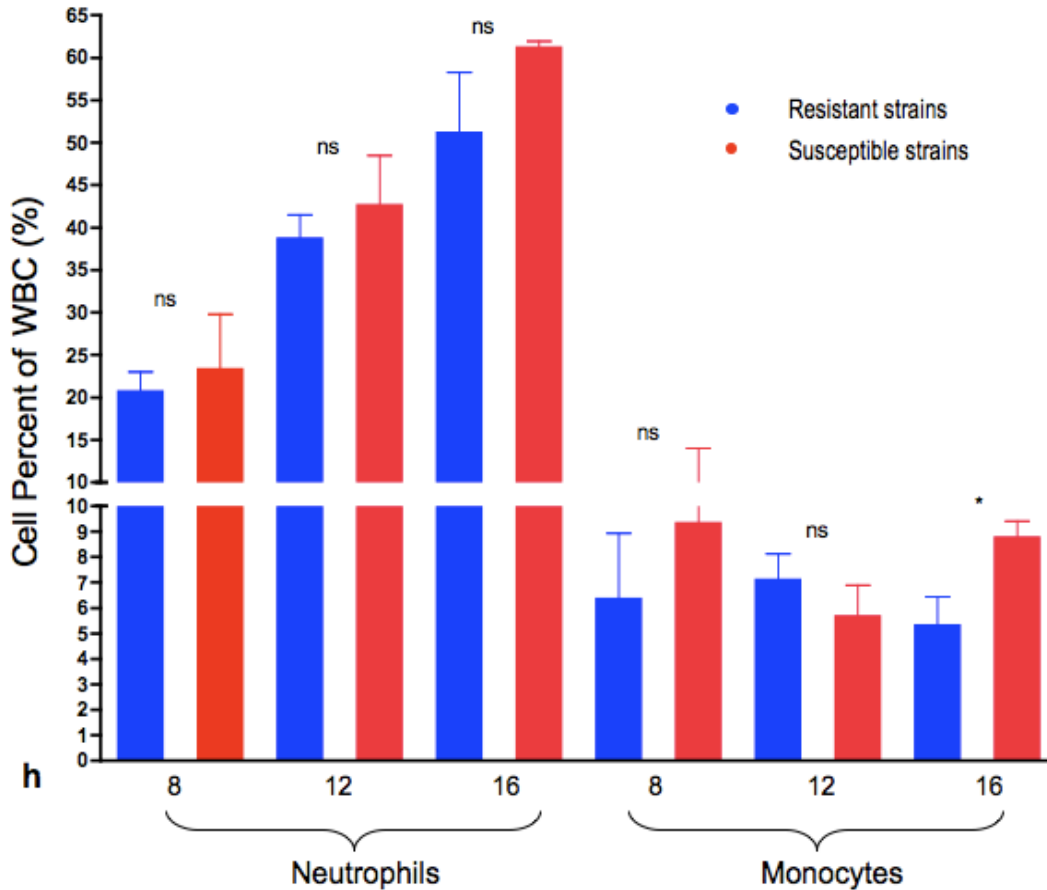


Figure 5-5. Kinetics of neutrophils and monocytes at early time points post GAS infection.

Susceptible and resistant strains were infected with 2×10^7 CFU/mouse of MIT1 hypervirulent GAS strain. We collected blood from 3–4 mice per strain per time point and evaluated percentages of neutrophils and monocytes at selected time points post infection. There were no significant differences in percentages of neutrophil at examined time points between susceptible strains compared to resistant ones. Interestingly, monocytes were higher at 16 h post infection in susceptible strains. Significance was calculated using on Student’s t-test, with $p \leq 0.05$ considered significant.

resistant and susceptible strains at 30–90 minutes post infection. However, at 120 minutes (2h) post infection susceptible strains had significantly higher numbers of neutrophils (Figure 5-6).

Conclusions

In this chapter, we found that there were no significant quantitative differences in the number of immune cells in blood and spleens of resistant and susceptible strains under normal physiological conditions. This led us to investigate if neutrophils and macrophages play a role in modulating differential response in GAS sepsis. We found that depletion of both cell types prior to, or within 24 h of GAS infection rendered resistant strains susceptible. We then examined the kinetics of neutrophils and monocytes post infection in susceptible and resistant strains and found no significant differences in numbers post infection. This suggested that numbers of neutrophils and monocytes available may not be a major determinant factors of the outcome of infection as susceptible and resistant strains had an equivalent numbers of these cells. Together our data suggest that functional differences in these cells may play an important role in modulating differential susceptibility.

This led us to initiate studies analyzing the role of neutrophils and pattern recognition receptors, NOD like receptor family (NLR) and in particular Nlrp3 (Craven *et al.*, 2009; Harder *et al.*, 2009; Munoz-Planillo *et al.*, 2009), in modulating differential response to bacterial sepsis. This work along with further *in vitro* functional assays are being planned and outlined and will be a future direction for the project after completion of the current dissertation.

Materials and Methods

Experimental Design of Immunophenotyping Studies

To characterize the main immune cell populations in blood and spleen of BXD strains displaying differential susceptibility to GAS sepsis, we selected highly resistant strains (BXD73, BXD69, and BXD87) and highly susceptible strains (BXD100, BXD90, and BXD75). We collected blood and harvested spleens from 8–16 mice per strain, 8–12 weeks-old, age-matched males and females at physiological conditions. Where the mice were housed in a pathogen-free colony in autoclaved pressurized individual ventilation (PIV) cages (4 mice/cage) at the University of Cincinnati, Cincinnati, OH. The mice used in the immunophenotyping studies were maintained on a 12 hours light dark cycle, and were fed ad libitum sterile irradiated rodent chow (Harlan Teklad, Madison, WI). All procedures involving mice were approved by the institutional animal care and use committee (IACUC) at the University of Cincinnati.

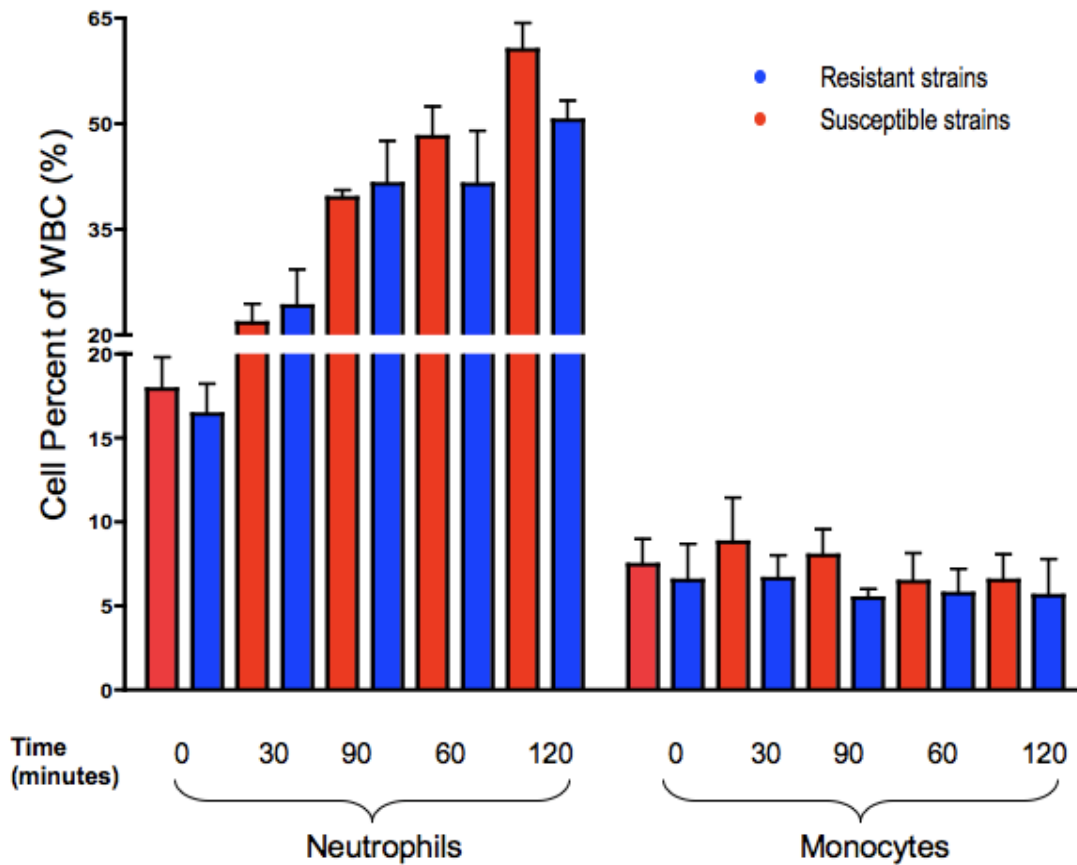


Figure 5-6. Comparison of the kinetics of neutrophils and monocytes numbers in susceptible versus resistant strains during the first 2 hours post GAS infection.

Susceptible and resistant strains were infected with 2×10^7 CFU/mouse of MIT1 hypervirulent GAS strain. We collected blood from 3–4 mice per strain per time point and evaluated percentages of neutrophils and monocytes at selected time points post infection. There were no significant differences in percentages of neutrophil at examined time points. Significance was calculated using on Student’s t-test, with $p \leq 0.05$ considered significant.

Differential Blood Counts

We measured numbers and percentage of different immune cells populations in blood using automated complete blood counts (CBC) with differentials. We euthanized age-matched (8–12 weeks-old) mice ($n = 4-8$ mice/sex/strain) and collected their blood using cardiac puncture immediately into 0.5 M K_2EDTA coated tubes. We performed CBC with differentials using Hemavet 950 automated hematology analyzer (Drew Scientific Inc, Oxford CT). We collected data for 5 immune cell populations: lymphocytes, monocytes, eosinophils, basophiles and neutrophils across selected susceptible and resistant ARI-BXD strains.

Flow Cytometric Analyses of Splenocytes

We used flow cytometric analysis to inspect percentages of different immune cell populations in spleens. We harvested spleens from 8–16 mice/strain, age-matched (8–12 weeks-old) males and females belonging to the above-mentioned BXD strains. We prepared single cell suspension of splenocytes using cell strainer method using a nylon mesh 70 μm (BD Biosciences, San Jose, CA). During the following procedures, splenocytes were kept on ice at all possible times. Cell suspensions were pelleted by centrifugation at 400 xg for 5 minutes at room temperature. We discarded the supernatants and lysed RBCs using 1X RBC lysis buffer (eBioscience, Inc, San Diego, CA). We washed the cells twice with FACS buffer (phosphate buffered saline (PBS), 2% fetal bovine serum (FBS) and 2 mM EDTA), and resuspended the cells in 10 ml of FACS buffer. We counted the splenocytes single cell suspensions using hemocytometer and brought the samples to a concentration of 10^7 cells/ml in FACS buffer.

We stained 10⁶ cells with the following anti-mouse antibodies, CD19-FITC, CD3-FITC, CD8-PE, CD4-APC, CD49b-PE, CD11b-FITC, CD11c-APC, Gr-1-PE (Ly-6G and Ly-6C, RB6-8C5), and corresponding isotype controls (BD Biosciences, San Jose, CA). Cell populations and cell surface markers used to identify these populations are listed in Table 5-1. Data acquisition and preliminary analysis were done using BD CellQuest Pro on a BD FACSCalibur flow cytometer (BD Biosciences). Detailed flow cytometric analyses were done using FlowJo software (Tree Star, Inc, Ashland, OR). We used single color staining for CD19, and staining was analyzed using single histogram statistics (Figure 5-1). We performed 2-color staining for NK cells (CD3 and CD49b), we chose CD49b as an NK cell marker as it is a pan NK cells marker that is expressed on both parental strains (B6 and D2) NK cells. We used 3-color staining for T cells (CD3, CD4 and CD8) and myeloid cells (Gr-1, CD11b and CD11c). Figure 5-1 shows scheme of analysis of different cell populations.

Cellular Depletion Studies

We used anti-mouse Ly-6G and Ly-6C (RB6-8C5) antibody (Ab) for depletion of Gr1⁺ cells. We injected 8 weeks-old males belonging to highly susceptible and highly

Table 5-1. Cell surface markers that were used to define spleen immune cells populations characterized in the current study.

Cell Population	Cell Surface Markers Used to Define the Cell Population
T cytotoxic cells (Tc cells)	CD3 ⁺ , CD8 ⁺
T helper cells (Th cells)	CD3 ⁺ , CD4 ⁺
B lymphocytes (B cells)	CD19 ⁺
Natural killer cells (NK cells)	CD3 ⁻ , CD49b ⁺
Neutrophil granulocytes, leukocyte (PMNs)	CD11b ⁺ , SSC ^{hi} , Gr-1 ^{hi}
Eosinophils (EO)	CD11b ⁺ , SSC ^{hi} , Gr-1 ^{mid-low}
Resident macrophage (Mø) & dendritic cells (DC)	CD11b ⁺ , SSC ^{low} , Gr-1 ⁻ , CD11c ⁺

resistant strains with 200 ug/mouse of RB6-8C5 Ab (iv tail) injections (Czuprynski *et al.*, 1994). In parallel, we injected a control group of mice with 200 ug/mouse of isotypic control Ab of purified rat anti-mouse IgG2b κ . We confirmed depletion by measuring neutrophils in blood 24 hours post Ab injections. We infected control group and Gr-1⁺ depleted group with 107 CFU/mouse of hypervirulent MIT1 GAS strain. Bacterial suspensions used for infection of mice were prepared as detailed in (Aziz *et al.*, 2007). We monitored mice survival every 2 hours for the first 44 hours until all depleted mice expired and then every 8h till day 6 post infection when all surviving mice were sacrificed. Similarly, we depleted monocytes and tissue macrophages using iv tail injection of clodronate-loaded liposomes (CLLs) as previously described in (Van Rooijen and Sanders, 1994). We followed same design for infection as above where control group were injected with PBS-loaded liposomes.

Data Analysis and Statistical Analyses

We used FlowJo software (Tree Star, Inc, Ashland, OR) for analysis of flow cytometry data. Statistical analysis and graphical presentation of flow cytometry and CBC/differential data was done in GraphPad Prism (GraphPad Software, La Jolla, CA). For granulocyte depletion studies, survival fractions were estimated using Kaplan-Meier method and curves generated were compared using log rank test. In various experiments, statistical significance was based on Student's t-test, a P-value of ≤ 0.01 was considered significant.

CHAPTER 6. SUMMARY FUTURE DIRECTIONS AND CONCLUSIONS

Summary

In the studies outlined in this dissertation, we aimed to delineate host genetic factors modulating differential susceptibility to severe GAS sepsis.

Our laboratory has previously found an association between variations in host HLA-II alleles and the severity of disease outcomes. These findings were based on extensive epidemiological studies, which were initiated based on two important findings. First, the isolation of genetically identical GAS strains from both severe and non-severe cases of GAS sepsis underscored the role of host variation in modulating outcome of infection (Chatellier *et al.*, 2000). Secondly, subsequent studies showed that there were variations in the magnitude of inflammatory responses elicited by the same GAS superantigens (SAGs) and that this correlated with the severity of GAS sepsis outcomes (Norrby-Teglund *et al.*, 2000). Because SAGs are presented to T cells by HLA-II molecules, they hypothesized that host HLA-II allelic variations could be modulating the observed differential response to the same GAS isolate (Chatellier *et al.*, 2000).

Therefore, extensive epidemiological studies were undertaken to determine the distribution of HLA-II haplotypes among patients with varying degrees of invasive GAS infections. Kotb *et al.* (2002) found associations between certain HLA-II haplotypes and high risk for STSS and that other haplotypes were associated with protection from STSS and/or NF (Kotb *et al.*, 2002; Kotb *et al.*, 2003). These breakthrough studies were then taken a step further to study mechanisms of interactions of the ternary complex of HLA-II–SAGs–TCR *in vivo* and *in vitro*. Validation and dissection of the role of in HLA-II variation in GAS sepsis were conducted using HLA-tg mice and bare lymphocyte syndrome (BLS) cell lines expressing either high risk or protective HLA-II alleles (Nooh *et al.*, 2007). The intriguing HLA-II studies in our laboratory are providing us with new exciting mechanistic data each day.

Despite the strong association between severity of GAS sepsis and host HLA-II polymorphism, GAS sepsis is a complex trait disease, affected by multiple interacting mechanisms. This elusive bacterium is rich in many other virulence factors, beside SAGs, of which may interact with additional host factors, other than HLA-II, to modulate disease outcomes. Therefore, we saw a great potential in adopting a systems approach to explore additional host factors modulating the severity of GAS sepsis.

A systems genetics approach is a hypothesis-free approach made feasible due to the coupling of powerful genetic and bioinformatics tools (Morahan and Williams, 2007; Chesler *et al.*, 2008). As detailed in the introductory chapter of this dissertation, ARI-BXD strains, which were used as a genetic reference population in our studies, are a well-defined, genetically diverse mouse population. These strains are well defined as they are heavily genotyped and their ancestral parents are fully sequenced (Williams *et al.*, 2001; Peirce *et al.*, 2004; Shifman *et al.*, 2006). This coupled with statistical analyses tools offered by the WebQTL platform (Wang *et al.*, 2003; Peirce *et al.*, 2008) provides

researchers, like myself, a great advantage of allowing us to easily link our measured traits of interest with mice genotypes and map genetic loci associated with observed differential response. The ARI-BXD strains, being genetically diverse, offer a huge advantage of having a vast genetic pool for mapping studies. This is in contrast to common inbred mice whose genetic pool is limited, thus in using ARI-BXD we are trying to mimic the genetic diversity of the human population.

Systems genetics approaches are novel in GAS sepsis field, and have just been recently employed in other infectious diseases (Hardy *et al.*, 2001; Miyairi *et al.*, 2007). To take advantage of such approaches, we first aimed to carefully account for and to take into consideration any non-genetic or environmental variations that might affect mice differential response to GAS sepsis. Our analyses revealed that among the various cofactors, age was the only significant cofactor that confounded differential response to GAS sepsis (Aziz *et al.*, 2007). This was predictable based on known effects of aging on innate immune responses (Gomez *et al.*, 2008) and in particular on those relating to sepsis (Turnbull *et al.*, 2009). Interestingly, a recent study has dissected such age-related differences in immune responses in relation to severe GAS sepsis in mice (Goldmann *et al.*, 2010). Based on our studies, we standardized an age range for our mice to be between 40 to 120 days that reflects differential response and in later studies of dissecting the mechanisms of differential susceptibility we used age range of 60 to 90 days.

We then mapped disease-associated traits of survival, bacteremia, and bacterial dissemination to organs to 2 QTLs on Chr 2. The survival phenotype also mapped to an additional QTL on Chr X (Abdeltawab *et al.*, 2008). Excitingly, we had a strong cis-acting QTL and the genes within these QTLs were polymorphic and associated with immune response pathways which made biological sense. We then narrowed down our QTLs using multiple bioinformatics tools including linkage analyses, SNP polymorphism, gene ontology, and pathway analyses. We then validated selected key genes within our candidate pathways by comparing gene expression levels (qPCR) in selected infected vs. uninfected highly resistant and highly susceptible BXD strains.

Collectively our data suggested the involvement of two key pathways of IL1 and prostaglandins in modulating differential susceptibility to GAS sepsis (Abdeltawab *et al.*, 2008). For the survival phenotype, we found that genes within all 3 QTLs (two on Chr 2 and one on Chr X) fell in the same or interactive pathways. In addition the QTL on Chr X also harbors genes likely to be involved in host-mediated pathogenesis (e.g. thrombosis, and coagulation). However, to further embrace our unbiased approach of systems genetics and to dissect mechanisms of differential susceptibility to severe GAS sepsis, we sought to compare genome-wide (GW) differential gene expression associated with differential response at different stages of infection. We designed these experiments so that we can gain insight into the dynamics of the host immune response during the infection. We compared GW differential gene expression of infected vs. uninfected mice of highly resistant and susceptible strains at selected times post infection.

We aimed to explore the basis of how mice react differently based on their genetic differences, which modulated the outcome of infection into the observed differential

susceptibility. In addition, we aimed to delineate stages of the infection at which divergence in response between susceptible and resistant strains occurs, i.e. stage at which their fates are being decided. We were excited to find that the same or interacting pathways were also pulled out with this GW transcriptome analysis approach (Chapter 4 in this dissertation). Moreover, we found that certain pathways were associated with certain times post infection i.e. infection stage-specific. This was exemplified by changes in the IL10 signaling pathways, which were only seen in resistant strains only at 8 h post infection (in blood as studied “organ”). This will help us tremendously in understanding the molecular mechanisms underlying each stage of the infection. To add to the excitement, IL10 cytokine levels correlated with protection from disease severity, as IL10 levels were significantly higher in resistant strains ($p < 0.01$) at early times post infection. Interestingly, we found significant differences between susceptible and resistant strains only in levels of IL10 and IFN γ and at certain times post infection corresponding with the expected time and role of each cytokine in sepsis modulation. The levels of IL10 were significantly higher in resistant strains starting at 8 h but showed no differences at 24 h. This suggests that IL10 may play an active role in regulating immune response within the early stage of the infection.

This becomes exceedingly exciting, when taken together with our *in vitro* HLA-II studies which showed that the protective HLA-II alleles induce high levels of IL10 production, suggesting an active suppression as mechanism of protection against STSS. Further support was achieved via *in vitro* studies, where adding exogenous r-IL10 to PBMCs isolated from individuals expressing high-risk HLA alleles decreased their SAg-induced proliferative and cytokine responses. Meanwhile, adding anti-IL10 to PBMCs isolated from individuals expressing protective HLA alleles increased their SAg-induced responses (Nooh and Kotb in press). The IL10 story gets even far more exciting with our microarray data on tissue samples from patients with severe and non severe GAS sepsis, which showed the IL10 signaling pathways as top differentially expressed pathways associated with disease outcomes (Kansal and Kotb in final preparation).

To further add to all the above exciting results, and to shape a bigger picture, our prostaglandin studies revealed that high levels of PGE2 were associated with increased severity of sepsis in inverse correlation with IL10 levels (chapter 4 in this dissertation). This is in agreement with previous studies showing that PGE2 can down regulate the production of IL10 and drives immune cellular responses towards an exaggerated Th17 inflammatory response (Boniface *et al.*, 2009; Yao *et al.*, 2009). However, it has been shown that PGE2 effects are affected by its concentration, type of cells it is acting upon, status of the relevant receptors activated and the site and stage of infection (Bos *et al.*, 2004; Tober *et al.*, 2007; Sakata *et al.* 2010.). Therefore, it seems that a very fine balance of its concentration is required for an effective immune response. This led us to formulate our hypothesis that PGE2 acts as a suppressor of IL10 production in susceptible strains, where at high concentrations of PGE2, IL10 will be inhibited and Th17 inflammation ensues with severe sepsis as an outcome. To test this hypothesis at a cellular mechanism level, we first wanted to profile cellular population percentages across resistant and susceptible strains under physiological conditions. In doing so, we wanted to account for any quantitative differences in number of immune cells of resistant vs. susceptible strains

prior to infection that might affect their differential response. We immunophenotyped cells from blood and spleen of selected highly resistant and highly susceptible strains and found no quantitative differences between these strains under normal physiological conditions. Furthermore, there were no significant differences in number of neutrophils post infection at selected times post infection.

Our finding of no significant differences in numbers of immune cells between susceptible and resistant strains was very interesting, as it has been previously noted that both qualitative and quantitative differences in neutrophils affect outcomes of infection (Nauseef, 2007). However, an interesting recent study showed that in severe bacterial infections including GAS infection, high bacterial loads induced depletion of bone marrow neutrophils, as it triggered TLR2 activation leading to over-activation of immune response mechanisms and blocking of recruitment of neutrophils to infectious abscess, as bone marrow became depleted of neutrophils (exhausted bone marrow) (Navarini *et al.*, 2009).

Our data continue to point to the important role played by neutrophils and macrophages in modulating the severity and outcomes of GAS sepsis. GAS has developed specific mechanisms to evade killing by these two cellular populations. For example, studies have shown invasive GAS strains to specifically develop mechanisms to evade PMN killing. For example, GAS produces virulence factors that specifically impair PMN chemotaxis, migration and function. C5a peptidase (ScpA) degrades host C5a while IL8 degrading enzyme (ScpC) degrades host IL8 and thus impairing neutrophil chemotaxis (Sjolinder *et al.*, 2008; Gleich-Theurer *et al.*, 2009). Another example of GAS interfering with PMN killing mechanisms is Sda1, a potent DNase produced by M1T1 (GAS strain under study). Sda1 dissolves neutrophil extracellular traps (NETs) allowing the bacteria to escape the entrapment and killing by PMN (Aziz *et al.*, 2004b; Buchanan *et al.*, 2006; Walker *et al.*, 2007). Studies analyzing the role of macrophages in modulating differential susceptibility to GAS, using transcriptome analyses of GAS infected macrophages; found that GAS stimulates an “unusual” macrophage response. As the transcriptional profiles were a mix of pro and anti-inflammatory response, including profiles characteristic of both M1 and M2 macrophages (Goldmann *et al.*, 2007). Nonetheless, PMN and macrophages are in constant interplay, where in GAS sepsis, PMN release antimicrobial LL37 and heparin binding protein (HBP), thereby increasing the extravasations of inflammatory monocytes (Soehnlein *et al.*, 2008b). Put together with our results, we can hypothesize that functional and/or migratory differences in neutrophils and/or monocytes between susceptible and resistant strains might modulate their differential response to GAS sepsis.

In conclusion, we aimed to determine host immunogenetic factors modulating differential host responses to GAS sepsis. To accomplish this aim, we employed systems genetics approaches to study the genetic and molecular basis of host-pathogen interactions leading to differential responses to GAS severe sepsis. We assessed variations in traits associated with severity of GAS sepsis across a genetically diverse reference population (ARI-BXD strains). We then performed genome-wide association scans (GWAS), mapping differential susceptibility to QTLs on mouse Chr 2 and X.

Combining genome-wide differential gene expression analyses with GWAS, and further biomarker and cellular validations, indicated that PGE2 pathways and IL10 signaling pathways modulate differential responses to GAS sepsis. In addition, our data suggested that prostaglandin itself might act as a key modulator, controlling a network of genes involved in innate immune response to GAS sepsis. We also showed using transcriptome analyses and soluble biomarker analyses, that pathways involving activation of IL10 signaling and IL10 high levels were associated with resistance to infection. Our contribution to the vertical growth of the GAS sepsis field is that we highlighted interactions of prostaglandins and IL10 with networks of candidate genes affect host differential susceptibility to severe GAS sepsis. Our future studies will be focused on further dissecting the molecular mechanisms of the differential susceptibility, these are outlined below.

Future Directions

Studies outlined in this dissertation have answered the original questions we asked, and raised other questions for follow up in future studies. I would like to believe that my studies helped in setting the foundation for future studies to answer some of the raised questions. I believe that with the knowledge we gained from my studies and the tools we are currently acquiring, answers to some of the raised questions are very plausible in the near future. However, some questions might remain as open-ended questions, which I hope we will someday answer to help us reach the laboratory mission of moving from bench side to bedside and finding better therapeutics that take into account individual variations and that incorporate the information generated to develop more targeted interventions for this aggressive disease.

Dissection of Migratory and Functional Differences of Immune Cell Populations between Susceptible and Resistant Strains

Our results strongly suggested that migratory and/or functional differences in neutrophils and/or monocytes between resistant and susceptible strains are governing differential response to GAS sepsis, as there were no significant differences in numbers of immune cells of blood and spleen of differentially susceptible strains. Moreover, comparison of neutrophil counts in susceptible and resistant strains post infection showed no association with differential susceptibility. Studies of various GAS virulence factors showed that several affect neutrophil recruitment, migration, and killing mechanisms (Buchanan *et al.*, 2006; Nilsson *et al.*, 2006; Sjolinder *et al.*, 2008; Sumbly *et al.*, 2008; Zinkernagel *et al.*, 2008; Lin *et al.*, 2009; Alexander *et al.*, 2010). Although these studies gave us insight into how the bacteria affect neutrophil killing mechanisms, however, the focus of these studies was to dissect bacterial virulence factors rather than to investigate differences in host neutrophils killing mechanisms that can vary between resistant and susceptible individuals.

I believe that studies to test our hypothesis of differences in migratory and functional properties of PMNs and macrophage as a means of host differential

susceptibility to GAS sepsis will give us great insight into mechanisms involved in differential susceptibility to severe sepsis. To compare differences in functionality of these cells, we will select highly susceptible and highly resistant BXD strains and isolate neutrophils from blood and macrophages from peritoneum, spleen and bone marrow. Then we will compare differences in phagocytic capacities, and production of reactive oxygen species (ROS) and reactive nitrogen species (RNS). In addition, we will measure effective bacterial killing by neutrophils/macrophages isolated from susceptible vs. resistant mouse strains, as it has been shown that although phagocytosized, GAS can survive intracellularly in APCs including neutrophils and monocytes (Medina *et al.*, 2003a; Medina *et al.*, 2003b; Staali *et al.*, 2006; Thulin *et al.*, 2006).

Based on the mapped QTLs and genes associated with GAS severity as well as our present neutrophil depletion studies, we are tempted to believe that the neutrophils/macrophages of the resistant strains will have a better bactericidal activity compared to the susceptible strains. In case we fail to observe expected differences in their *in vitro* function, an alternate approach would be to test if there are differences in the migration of these cells from lymphoid organs to periphery or vice versa following infection. We will use several *in vivo* and *in vitro* methods to study neutrophil migration.

For studying *in vivo* migration of neutrophils, we will use mouse air pouch technique. Air pouches will be formed on the back of susceptible and resistant BXD mice by subcutaneous injection of sterile air. Mice will then be infected intravenously with GAS and sacrificed at 1-4h post infection. The cells migrated in the pouches will be collected in sterile PBS, and counted with a hemocytometer. Leukocyte subpopulations will be distinguished by flow cytometry. Other studies have shown that neutrophils accounted for 80-95% of accumulated cells (Ben Yebdri *et al.*, 2009; Hattori *et al.*, 2010; Heissig *et al.*, 2010). *In vitro* neutrophil transmigration assay will be carried out in a Boyden chamber system. These studies should give us insight into the cellular mechanisms modulating susceptible and resistant strains differential susceptibility to GAS sepsis.

Analysis of Relationship of Prostaglandins and Modulation of Differential Response to GAS

PGE2 acts as a fast acting, delicately balanced lipid mediator that can act as either an immunosuppressor or immunoactivator depending on PGE2: a) concentration, b) cells it is activating, c) combination of receptors being activated, d) nature of activation signal and e) stage of infection (Bos *et al.*, 2004; Tober *et al.*, 2007; Sakata *et al.*, 2010). PGE2 as an immunosuppressor promotes inflammation, induces IL6 and causes vasodilatation, and vascular leakage; it can also reduce PMN migration and bacterial killing by macrophages, by blocking production of reactive oxygen intermediates (ROI) (Aronoff *et al.*, 2004; White *et al.*, 2005; Nakayama *et al.*, 2006; Huang *et al.*, 2007; Serezani *et al.*, 2007). However, recent studies have shown that it can be a regulator of that immune inflammation (immunoactivator) by activation of Th1 differentiation and Th17 expansion (Boniface *et al.*, 2009; Yao *et al.*, 2009; Sakata *et al.*, 2010).

If the fine balance of this mediator is disrupted, it can lead to serious pathological consequences. For example alterations in the amounts of PGE2 are associated with high risk of infection with HIV, cancer, and malnutrition (Lima *et al.*, 2006; Anstead *et al.*, 2009; Greenhough *et al.*, 2009). In promoting Th1 differentiation, PGE2 induces the production of IFN γ and via its EP4 receptor; PGE2 inhibits production of IL10 exacerbating Th17 mediated inflammation (Boniface *et al.*, 2009; Yao *et al.*, 2009). Excitingly, the outlined studies in this dissertation showed that susceptible strains had higher levels of PGE2, and IFN γ and low levels of IL10 while the reverse was true for resistant strains. Therefore, we hypothesize that PGE2 can act as a “switch”, wherein susceptible strains PGE2 inhibits IL10 production, and increase IFN γ , exacerbating Th17 mediated inflammation. Meanwhile, in resistant strains, PGE2 is produced at controlled levels, allowing Th1 and Th17 polarization and subsequent containment of infection. We are even more interested in this interactive role of PGE2 and IL10 as our studies in the HLA-tg mice have shown that IL10 mediates protection against severe GAS sepsis. In addition, our genome-wide expression pathway analyses identified IL10 pathways being up regulated in resistant strains at early time points (8h) associating high levels of IL10 with resistance to GAS sepsis and better outcomes of infection.

A likely applicable hypothesis is that PGE2 modulates differential susceptibility on more than one level, by inhibiting IL10 production, increasing IFN γ levels, promoting Th17 expansion but into exaggerated response and subsequent altering of neutrophils and/or macrophages recruitment and functionality. However, further studies are needed to dissect its role in each of these levels, therefore as a future direction of the work presented herein, follow up studies dissecting the role of PGE2 in relation to IL10 in modulating differential susceptibility would be quite interesting.

For these studies, to further explore the role of PGE2, one approach is to use knockout mice of receptors relevant to PGE2 immune actions. PGE2 has four receptors, prostanoid E receptor (EP) 1 through 4 (Narumiya *et al.*, 1999; Breyer *et al.*, 2001). EP2 and EP4 receptors are heavily involved in inflammatory and immune responses, migration of antigen presenting cells (APC) and in cancer research (Kobayashi and Narumiya, 2002; Greenhough *et al.*, 2009). A large body of research on prostaglandins associates the net action of PGE2 with the balance by which PGE2 activates “receptor pairs”. For example, in blood pressure regulation, PGE2 can activate EP2/EP4 (leading to vasodilatation) or EP1/EP3 (leading to vasoconstriction), depending on the balance it can shift to one action or the other (Zhang *et al.*, 2000).

Therefore, it would be interesting to test knockout mice of EP2 and EP4 receptors, which are involved in inflammatory and immune responses. We have two knockout mice already in line for future studies on the role of PGE2, these are microsomal prostaglandin E synthase 1 (mPGES1) and EP2 KO mice, which were made in DBA/1J and B6 backgrounds respectively. In our ongoing collaboration with Dr. Aronoff, of Univ. Michigan, we would like to determine how PGE2 might modulate disease severity. I predict that EP2-KO mice would be resistant (as resistant as B6 or more), but the main focus is to determine the mechanism of resistance, through functional

assays, including phagocytosis, production of ROI, and bacterial killing (clearing of bacteria) as detailed above.

Cytokine Profiling Associated with Susceptibility to GAS Sepsis

We have measured levels of selected cytokines in selected resistant and susceptible strains and found that IL10 is a promising candidate modulator of severity of sepsis as it was associated with differential response to GAS sepsis. I believe that a carefully designed study can be initiated using levels of IL10 at 8 h and/or 12h, as both time points had the highest correlation with disease severity (Figure 4-4), across BXD strains and map differential responses due to cytokine level differences. We have previously used survival, bacteremia and bacterial load in spleen as traits to map differential severity of GAS sepsis and all these traits mapped to Chr 2 QTLs (Abdeltawab *et al.*, 2008). However, we have found that survival was the only trait that mapped a QTL to Chr X. This suggested that genes within this QTL might be primarily engaged in host-mediated pathogenesis, which we found true when we inspected this QTL closely (data not shown).

Therefore, we are hoping that cytokine data will reveal QTLs associated with modulation of cytokine response in GAS sepsis. We postulate that this might be a totally different QTL, as it is known that complex interacting regulatory mechanisms govern cytokine production in sepsis (reviewed in [Cohen, 2002; Rittirsch *et al.*, 2008]). In addition, IL10 is of particular interest due to results shown in this dissertation, where it is correlated with better outcome of sepsis and is in inverse relation to PGE2 levels, another mediator that can be used for mapping.

The association of GAS sepsis severity with multiple cytokines exerting their effects temporally underscores the complexity of traits modulating severe GAS sepsis and emphasizes the importance of the time of administration of appropriate cytokine intervention to aid in the prevention of shock in severe GAS sepsis.

Analysis of the Role of Nod-like Receptors as a Candidate Pattern Recognition Receptor Associated with Modulation of Differential Response to GAS Sepsis

It has been recently found that Streptolysin O (SLO) produced by GAS (Harder *et al.*, 2009) and hemolysin produced by *Staphylococcus aureus* (Craven *et al.*, 2009) activate nucleotide-binding domain (NOD) like receptor (NLR) pyrin domain containing 3 (NLRP3) inflammasome, indicating that GAS activation of the inflammasome was independent of TLR signaling. NLRP3 inflammasome is involved in the regulation of caspase-1, which in turn regulates the processing and secretion of IL1 cytokine family including IL1 β and IL18, which are both parts of the pathways modulating susceptibility to GAS sepsis which were found by both our genome-wide mapping and transcriptional studies. NLR family acts as a pattern recognition mediating cytoplasmic recognition of bacterial products (Ting *et al.*, 2008; Ye and Ting, 2008). It will be particularly interesting to study the role of the inflammasome in our current GAS model given the growing connections and pointers that it might be associated with signaling pathways

modulating observed differential response. We have started collaboration with Dr. Jenny Ting, at UNC, where I will pursue this project as part of the immediate future directions of my studies. In these studies we are going to use knockout mice of Nlrp3 and ASC (Apoptosis-associated speck-like protein containing a CARD, also known as PYCARD), both mediators have been associated with modulation of NLRP3 inflammasome (reviewed [Cassel *et al.*, 2009; Lamkanfi and Kanneganti, 2010]).

Concluding Remarks

The studies presented in this dissertation have helped shed some light on host mechanisms of differential susceptibility to GAS sepsis. We were the first to find an association between differential susceptibility to GAS sepsis and QTLs on mouse Chr 2 and X. Some studies have found associations between genes or QTLs on Chr 2 and susceptibility to other infectious diseases (Appendix D), however none were for differential susceptibility to GAS sepsis. We validated our mapped QTLs and parsed the genes within those QTLs into pathways. This allowed us to explore plausible mechanisms of differential susceptibility. The data suggested that prostaglandin might act as a key modulator, controlling a network of genes involved in innate immune response to GAS sepsis. In addition, pathways involving activation of IL10 production and signaling (including PGE2) are likely to be associated with resistance to infection. Despite differences between mouse and human immune systems (Mestas and Hughes, 2004), our results match beautifully with results obtained from human patients and its validation using *in vivo* humanized HLA-tg mice. This demonstrates the strength of the systems genetics approach employed and how comparisons of pathways rather than genes can help us translate our findings from mouse to human.

LIST OF REFERENCES

Wellcome Trust Case Control Consortium. (2007) Genome-wide association study of 14,000 cases of seven common diseases and 3,000 shared controls. *Nature* **447**: 661-678.

Abdeltawab, N.F., Aziz, R.K., Kansal, R., Rowe, S.L., Su, Y., Gardner, L., Brannen, C., *et al.* (2008) An unbiased systems genetics approach to mapping genetic loci modulating susceptibility to severe streptococcal sepsis. *PLoS Pathog* **4**: e1000042.

Aikawa, C., Nozawa, T., Maruyama, F., Tsumoto, K., Hamada, S., and Nakagawa, I. (2010) Reactive oxygen species induced by *Streptococcus pyogenes* invasion trigger apoptotic cell death in infected epithelial cells. *Cell Microbiol* **12**: 814-830.

Alexander, L.E., Maisey, H.C., Timmer, A.M., Rooijackers, S.H., Gallo, R.L., von Kockritz-Blickwede, M., and Nizet, V. (2010) MIT1 group A streptococcal pili promote epithelial colonization but diminish systemic virulence through neutrophil extracellular entrapment. *J Mol Med* **88**: 371-381.

Andersen, P.S., Lavoie, P.M., Sekaly, R.P., Churchill, H., Kranz, D.M., Schlievert, P.M., Karjalainen, K., *et al.* (1999) Role of the T cell receptor alpha chain in stabilizing TCR-superantigen-MHC class II complexes. *Immunity* **10**: 473-483.

Anstead, G.M., Zhang, Q., and Melby, P.C. (2009) Malnutrition promotes prostaglandin over leukotriene production and dysregulates eicosanoid-cytokine crosstalk in activated resident macrophages. *Prostaglandins Leukot Essent Fatty Acids* **81**: 41-51.

Anthony, L.S., Ghadirian, E., Nestel, F.P., and Kongshavn, P.A. (1989) The requirement for gamma interferon in resistance of mice to experimental tularemia. *Microb Pathog* **7**: 421-428.

Aronoff, D.M., Canetti, C., and Peters-Golden, M. (2004) Prostaglandin E2 inhibits alveolar macrophage phagocytosis through an E-prostanoid 2 receptor-mediated increase in intracellular cyclic AMP. *J Immunol* **173**: 559-565.

Aronoff, D.M., Peres, C.M., Serezani, C.H., Ballinger, M.N., Carstens, J.K., Coleman, N., Moore, B.B., *et al.* (2007) Synthetic prostacyclin analogs differentially regulate macrophage function via distinct analog-receptor binding specificities. *J Immunol* **178**: 1628-1634.

Aziz, R.K., Pabst, M.J., Jeng, A., Kansal, R., Low, D.E., Nizet, V., and Kotb, M. (2004a) Invasive MIT1 group A *Streptococcus* undergoes a phase-shift in vivo to prevent proteolytic degradation of multiple virulence factors by SpeB. *Mol Microbiol* **51**: 123-134.

Aziz, R.K., Ismail, S.A., Park, H.W., and Kotb, M. (2004b) Post-proteomic identification of a novel phage-encoded streptodornase, Sda1, in invasive MIT1 *Streptococcus pyogenes*. *Mol Microbiol* **54**: 184-197.

- Aziz, R.K., Edwards, R.A., Taylor, W.W., Low, D.E., McGeer, A., and Kotb, M. (2005) Mosaic prophages with horizontally acquired genes account for the emergence and diversification of the globally disseminated MIT1 clone of *Streptococcus pyogenes*. *J Bacteriol* **187**: 3311-3318.
- Aziz, R.K., Kansal, R., Abdeltawab, N.F., Rowe, S.L., Su, Y., Carrigan, D., Nooh, M.M., *et al.* (2007) Susceptibility to severe Streptococcal sepsis: use of a large set of isogenic mouse lines to study genetic and environmental factors. *Genes Immun* **8**: 404-415.
- Aziz, R.K., and Kotb, M. (2008) Rise and persistence of global MIT1 clone of *Streptococcus pyogenes*. *Emerg Infect Dis* **14**: 1511-1517.
- Bailey, D.W. (1971) Recombinant-inbred strains. An aid to finding identity, linkage, and function of histocompatibility and other genes. *Transplantation* **11**: 325-327.
- Basma, H., Norrby-Teglund, A., Guedez, Y., McGeer, A., Low, D.E., El-Ahmedy, O., Schwartz, B., *et al.* (1999) Risk factors in the pathogenesis of invasive group A streptococcal infections: role of protective humoral immunity. *Infect Immun* **67**: 1871-1877.
- Ben Yebdri, F., Kukulski, F., Tremblay, A., and Sevigny, J. (2009) Concomitant activation of P2Y(2) and P2Y(6) receptors on monocytes is required for TLR1/2-induced neutrophil migration by regulating IL-8 secretion. *Eur J Immunol* **39**: 2885-2894.
- Benjamin, W.H., Jr., Turnbough, C.L., Jr., Posey, B.S., and Briles, D.E. (1986) *Salmonella typhimurium* virulence genes necessary to exploit the Itys/s genotype of the mouse. *Infect Immun* **51**: 872-878.
- Bernstein-Hanley, I., Balsara, Z.R., Ulmer, W., Coers, J., Starnbach, M.N., and Dietrich, W.F. (2006) Genetic analysis of susceptibility to *Chlamydia trachomatis* in mouse. *Genes Immun* **7**: 122-129.
- Bessen, D.E. (2009) Population biology of the human restricted pathogen, *Streptococcus pyogenes*. *Infect Genet Evol* **9**: 581-593.
- Boniface, K., Bak-Jensen, K.S., Li, Y., Blumenschein, W.M., McGeachy, M.J., McClanahan, T.K., McKenzie, B.S., *et al.* (2009) Prostaglandin E2 regulates Th17 cell differentiation and function through cyclic AMP and EP2/EP4 receptor signaling. *J Exp Med* **206**: 535-548.
- Bos, C.L., Richel, D.J., Ritsema, T., Peppelenbosch, M.P., and Versteeg, H.H. (2004) Prostanoids and prostanoid receptors in signal transduction. *Int J Biochem Cell Biol* **36**: 1187-1205.
- Boyartchuk, V., and Dietrich, W. (2002) Genetic dissection of host immune response. *Genes Immun* **3**: 119-122.

- Boyartchuk, V.L., Broman, K.W., Mosher, R.E., D'Orazio, S.E., Starnbach, M.N., and Dietrich, W.F. (2001) Multigenic control of *Listeria monocytogenes* susceptibility in mice. *Nat Genet* **27**: 259-260.
- Bream, J.H., Carrington, M., O'Toole, S., Dean, M., Gerrard, B., Shin, H.D., Kosack, D., *et al.* (2000) Polymorphisms of the human IFNG gene noncoding regions. *Immunogenetics* **51**: 50-58.
- Breyer, R.M., Bagdassarian, C.K., Myers, S.A., and Breyer, M.D. (2001) Prostanoid receptors: subtypes and signaling. *Annu Rev Pharmacol Toxicol* **41**: 661-690.
- Buchanan, J.T., Simpson, A.J., Aziz, R.K., Liu, G.Y., Kristian, S.A., Kotb, M., Feramisco, J., *et al.* (2006) DNase expression allows the pathogen group A *Streptococcus* to escape killing in neutrophil extracellular traps. *Curr Biol* **16**: 396-400.
- Caron, J., Loredó-Osti, J.C., Laroche, L., Skamene, E., Morgan, K., and Malo, D. (2002) Identification of genetic loci controlling bacterial clearance in experimental *Salmonella* enteritidis infection: an unexpected role of Nramp1 (Slc11a1) in the persistence of infection in mice. *Genes Immun* **3**: 196-204.
- Carvalho, A., Cunha, C., Pasqualotto, A.C., Pitzurra, L., Denning, D.W., and Romani, L. (2009) Genetic variability of innate immunity impacts human susceptibility to fungal diseases. *Int J Infect Dis*.
- Cassatella, M.A., Locati, M., and Mantovani, A. (2009) Never underestimate the power of a neutrophil. *Immunity* **31**: 698-700.
- Cassel, S.L., Joly, S., and Sutterwala, F.S. (2009) The NLRP3 inflammasome: a sensor of immune danger signals. *Semin Immunol* **21**: 194-198.
- Chai, L.Y., Netea, M.G., Vonk, A.G., and Kullberg, B.J. (2009) Fungal strategies for overcoming host innate immune response. *Med Mycol* **47**: 227-236.
- Chatellier, S., Ihendyane, N., Kansal, R.G., Khambaty, F., Basma, H., Norrby-Teglund, A., Low, D.E., *et al.* (2000) Genetic relatedness and superantigen expression in group A streptococcus serotype M1 isolates from patients with severe and nonsevere invasive diseases. *Infect Immun* **68**: 3523-3534.
- Chen, B.C., Chang, Y.S., Kang, J.C., Hsu, M.J., Sheu, J.R., Chen, T.L., Teng, C.M., *et al.* (2004) Peptidoglycan induces nuclear factor-kappaB activation and cyclooxygenase-2 expression via Ras, Raf-1, and ERK in RAW 264.7 macrophages. *J Biol Chem* **279**: 20889-20897.
- Chen, J., and Harrison, D.E. (2002) Quantitative trait loci regulating relative lymphocyte proportions in mouse peripheral blood. *Blood* **99**: 561-566.

- Chesler, E.J., Lu, L., Shou, S., Qu, Y., Gu, J., Wang, J., Hsu, H.C., *et al.* (2005) Complex trait analysis of gene expression uncovers polygenic and pleiotropic networks that modulate nervous system function. *Nat Genet* **37**: 233-242.
- Chesler, E.J., Miller, D.R., Branstetter, L.R., Galloway, L.D., Jackson, B.L., Philip, V.M., Voy, B.H., *et al.* (2008) The Collaborative Cross at Oak Ridge National Laboratory: developing a powerful resource for systems genetics. *Mamm Genome* **19**: 382-389.
- Churchill, G.A., and Doerge, R.W. (1994) Empirical threshold values for quantitative trait mapping. *Genetics* **138**: 963-971.
- Churchill, G.A., and Airey, D.C., and Allayee, H., and Angel, J.M., and Attie, A.D., and Beatty, J., and Beavis, W.D., *et al.* (2004) The Collaborative Cross, a community resource for the genetic analysis of complex traits. *Nat Genet* **36**: 1133-1137.
- Churchill, G.A. (2007) Recombinant inbred strain panels: a tool for systems genetics. *Physiol Genomics* **31**: 174-175.
- Cohen, J. (2002) The immunopathogenesis of sepsis. *Nature* **420**: 885-891.
- Cole, J.N., McArthur, J.D., McKay, F.C., Sanderson-Smith, M.L., Cork, A.J., Ranson, M., Rohde, M., *et al.* (2006) Trigger for group A streptococcal MIT1 invasive disease. *FASEB J.* **20**: 1745-1747.
- Cortes, G., and Wessels, M.R. (2009) Inhibition of dendritic cell maturation by group A Streptococcus. *J Infect Dis* **200**: 1152-1161.
- Craven, R.R., Gao, X., Allen, I.C., Gris, D., Bubeck Wardenburg, J., McElvania-Tekippe, E., Ting, J.P., *et al.* (2009) Staphylococcus aureus alpha-hemolysin activates the NLRP3-inflammasome in human and mouse monocytic cells. *PLoS One* **4**: e7446.
- Cunningham, M.W. (2000) Pathogenesis of group A streptococcal infections. *Clin Microbiol Rev* **13**: 470-511.
- Cywes Bentley, C., Hakansson, A., Christianson, J., and Wessels, M.R. (2005) Extracellular group A Streptococcus induces keratinocyte apoptosis by dysregulating calcium signalling. *Cell Microbiol* **7**: 945-955.
- Czuprynski, C.J., Brown, J.F., Maroushek, N., Wagner, R.D., and Steinberg, H. (1994) Administration of anti-granulocyte mAb RB6-8C5 impairs the resistance of mice to *Listeria monocytogenes* infection. *J Immunol* **152**: 1836-1846.
- Davies, H.D., McGeer, A., Schwartz, B., Green, K., Cann, D., Simor, A.E., and Low, D.E. (1996) Invasive group A streptococcal infections in Ontario, Canada. Ontario Group A Streptococcal Study Group. *N Engl J Med* **335**: 547-554.

- Deghmane, A.E., Veckerle, C., Giorgini, D., Hong, E., Ruckly, C., and Taha, M.K. (2009) Differential modulation of TNF-alpha-induced apoptosis by *Neisseria meningitidis*. *PLoS Pathog* **5**: e1000405.
- Elgueta, R., Benson, M.J., de Vries, V.C., Wasiuk, A., Guo, Y., and Noelle, R.J. (2009) Molecular mechanism and function of CD40/CD40L engagement in the immune system. *Immunol Rev* **229**: 152-172.
- Ferreira, M.A., Hottenga, J.J., Warrington, N.M., Medland, S.E., Willemsen, G., Lawrence, R.W., Gordon, S., *et al.* (2009) Sequence variants in three loci influence monocyte counts and erythrocyte volume. *Am J Hum Genet* **85**: 745-749.
- Fortin, A., Abel, L., Casanova, J.L., and Gros, P. (2007) Host genetics of mycobacterial diseases in mice and men: forward genetic studies of BCG-osis and tuberculosis. *Annu Rev Genomics Hum Genet* **8**: 163-192.
- Frank, S.A. (2002) *Immunology and Evolution of Infectious Disease*: Princeton (NJ) Princeton University Press.
- Frazer, K.A., and Ballinger, D.G., and Cox, D.R., and Hinds, D.A., and Stuve, L.L., and Gibbs, R.A., and Belmont, J.W., *et al.* (2007) A second generation human haplotype map of over 3.1 million SNPs. *Nature* **449**: 851-861.
- Frick, I.M., Bjorck, L., and Herwald, H. (2007) The dual role of the contact system in bacterial infectious disease. *Thromb Haemost* **98**: 497-502.
- Frodsham, A.J., and Hill, A.V. (2004) Genetics of infectious diseases. *Hum Mol Genet* **13 Spec No 2**: R187-194.
- Garcia-Peydro, M., de Yébenes, V.G., and Toribio, M.L. (2006) Notch1 and IL-7 receptor interplay maintains proliferation of human thymic progenitors while suppressing non-T cell fates. *J Immunol* **177**: 3711-3720.
- Gleich-Theurer, U., Aymanns, S., Haas, G., Mauerer, S., Vogt, J., and Spellerberg, B. (2009) Human serum induces streptococcal c5a peptidase expression. *Infect Immun* **77**: 3817-3825.
- Goldmann, O., Chhatwal, G.S., and Medina, E. (2003) Immune mechanisms underlying host susceptibility to infection with group A streptococci. *J Infect Dis* **187**: 854-861.
- Goldmann, O., Rohde, M., Chhatwal, G.S., and Medina, E. (2004a) Role of macrophages in host resistance to group A streptococci. *Infect Immun* **72**: 2956-2963.
- Goldmann, O., Chhatwal, G.S., and Medina, E. (2004b) Role of host genetic factors in susceptibility to group A streptococcal infections. *Indian J Med Res* **119 Suppl**: 141-143.

Goldmann, O., Lengeling, A., Bose, J., Bloecker, H., Geffers, R., Chhatwal, G.S., and Medina, E. (2005a) The role of the MHC on resistance to group A streptococci in mice. *J Immunol* **175**: 3862-3872.

Goldmann, O., Chhatwal, G.S., and Medina, E. (2005b) Contribution of natural killer cells to the pathogenesis of septic shock induced by *Streptococcus pyogenes* in mice. *J Infect Dis* **191**: 1280-1286.

Goldmann, O., von Kockritz-Blickwede, M., Holtje, C., Chhatwal, G.S., Geffers, R., and Medina, E. (2007) Transcriptome analysis of murine macrophages in response to infection with *Streptococcus pyogenes* reveals an unusual activation program. *Infect Immun* **75**: 4148-4157.

Goldmann, O., Sastalla, I., Wos-Oxley, M., Rohde, M., and Medina, E. (2009) *Streptococcus pyogenes* induces oncosis in macrophages through the activation of an inflammatory programmed cell death pathway. *Cell Microbiol* **11**: 138-155.

Goldmann, O., Lehne, S., and Medina, E. (2010) Age-related susceptibility to *Streptococcus pyogenes* infection in mice: underlying immune dysfunction and strategy to enhance immunity. *J Pathol* **220**: 521-529.

Gomez, C.R., Nomellini, V., Faunce, D.E., and Kovacs, E.J. (2008) Innate immunity and aging. *Exp Gerontol* **43**: 718-728.

Greenhough, A., Smartt, H.J., Moore, A.E., Roberts, H.R., Williams, A.C., Paraskeva, C., and Kaidi, A. (2009) The COX-2/PGE2 pathway: key roles in the hallmarks of cancer and adaptation to the tumour microenvironment. *Carcinogenesis* **30**: 377-386.

Grizzle, W.E., Mountz, J.D., Yang, P.A., Xu, X., Sun, S., Van Zant, G.E., Williams, R.W., *et al.* (2002) BXD recombinant inbred mice represent a novel T cell-mediated immune response tumor model. *Int J Cancer* **101**: 270-279.

Guedez, Y., Kotby, A., El-Demellawy, M., Galal, A., Thomson, G., Zaher, S., Kassem, S., *et al.* (1999) HLA class II associations with rheumatic heart disease are more evident and consistent among clinically homogeneous patients. *Circulation* **99**: 2784-2790.

Harder, J., Franchi, L., Munoz-Planillo, R., Park, J.H., Reimer, T., and Nunez, G. (2009) Activation of the Nlrp3 inflammasome by *Streptococcus pyogenes* requires streptolysin O and NF-kappa B activation but proceeds independently of TLR signaling and P2X7 receptor. *J Immunol* **183**: 5823-5829.

Hardy, C.L., Lu, L., Nguyen, P., Woodland, D.L., Williams, R.W., and Blackman, M.A. (2001) Identification of quantitative trait loci controlling activation of TRBV4 CD8+ T cells during murine gamma-herpesvirus-induced infectious mononucleosis. *Immunogenetics* **53**: 395-400.

Harris, S.G., Padilla, J., Koumas, L., Ray, D., and Phipps, R.P. (2002) Prostaglandins as modulators of immunity. *Trends Immunol* **23**: 144-150.

- Hattori, H., Subramanian, K.K., Sakai, J., Jia, Y., Li, Y., Porter, T.F., Loison, F., *et al.* (2010) Small-molecule screen identifies reactive oxygen species as key regulators of neutrophil chemotaxis. *Proc Natl Acad Sci U S A* **107**: 3546-3551.
- Hauser, A.R., Stevens, D.L., Kaplan, E.L., and Schlievert, P.M. (1991) Molecular analysis of pyrogenic exotoxins from *Streptococcus pyogenes* isolated associated with toxic shock-like syndrome. *J. Clin. Microbiol.* **29**: 1562.
- Heissig, B., Nishida, C., Tashiro, Y., Sato, Y., Ishihara, M., Ohki, M., Gritli, I., *et al.* (2010) Role of neutrophil-derived matrix metalloproteinase-9 in tissue regeneration. *Histol Histopathol* **25**: 765-770.
- Hidalgo-Grass, C., Mishalian, I., Dan-Goor, M., Belotserkovsky, I., Eran, Y., Nizet, V., Peled, A., *et al.* (2006) A streptococcal protease that degrades CXC chemokines and impairs bacterial clearance from infected tissues. *Embo J* **25**: 4628-4637.
- Hoge, C.W., Schwartz, B., Talkington, D.F., Breiman, R.F., MacNeill, E.M., and Englander, S.J. (1993) The changing epidemiology of invasive group A streptococcal infections and the emergence of streptococcal toxic shock-like syndrome. A retrospective population-based study. *JAMA* **269**: 384-389.
- Hormaeche, C.E. (1979a) Natural resistance to *Salmonella typhimurium* in different inbred mouse strains. *Immunology* **37**: 311-318.
- Hormaeche, C.E. (1979b) Genetics of natural resistance to salmonellae in mice. *Immunology* **37**: 319-327.
- Hornef, M.W., Wick, M.J., Rhen, M., and Normark, S. (2002) Bacterial strategies for overcoming host innate and adaptive immune responses. *Nat Immunol* **3**: 1033-1040.
- Huang, S., Wettlaufer, S.H., Hogaboam, C., Aronoff, D.M., and Peters-Golden, M. (2007) Prostaglandin E(2) inhibits collagen expression and proliferation in patient-derived normal lung fibroblasts via E prostanoind 2 receptor and cAMP signaling. *Am J Physiol Lung Cell Mol Physiol* **292**: L405-413.
- Ikebe, T., Hirasawa, K., Suzuki, R., Ohya, H., Isobe, J., Tanaka, D., Katsukawa, C., *et al.* (2007) Distribution of emm genotypes among group A streptococcus isolates from patients with severe invasive streptococcal infections in Japan, 2001-2005. *Epidemiol Infect* **135**: 1227-1229.
- Jackson, I.J. (2001) Mouse genomics: making sense of the sequence. *Curr Biol* **11**: R311-314.
- Jobin, M.C., Gottschalk, M., and Grenier, D. (2006) Upregulation of prostaglandin E2 and matrix metalloproteinase 9 production by human macrophage-like cells: synergistic effect of capsular material and cell wall from *Streptococcus suis*. *Microb Pathog* **40**: 29-34.

- Johansson, L., Thulin, P., Sendi, P., Herten, E., Linder, A., Akesson, P., Low, D.E., *et al.* (2008) Cathelicidin LL-37 in severe *Streptococcus pyogenes* soft tissue infections in humans. *Infect Immun* **76**: 3399-3404.
- Johnson, D.R., Stevens, D.L., and Kaplan, E.L. (1992) Epidemiologic analysis of group A streptococcal serotypes associated with severe systemic infections, rheumatic fever, or uncomplicated pharyngitis. *J Infect Dis* **166**: 374-382.
- Johnson, D.R., Wotton, J.T., Shet, A., and Kaplan, E.L. (2002) A comparison of group A streptococci from invasive and uncomplicated infections: are virulent clones responsible for serious streptococcal infections? *J Infect Dis* **185**: 1586-1595.
- Joo, M., Kwon, M., Sadikot, R.T., Kingsley, P.J., Marnett, L.J., Blackwell, T.S., Peebles, R.S., Jr., *et al.* (2007) Induction and function of lipocalin prostaglandin D synthase in host immunity. *J Immunol* **179**: 2565-2575.
- Kansal, R.G., McGeer, A., Low, D.E., Norrby-Teglund, A., and Kotb, M. (2000) Inverse relation between disease severity and expression of the streptococcal cysteine protease, SpeB, among clonal MIT1 isolates recovered from invasive group A streptococcal infection cases. *Infect Immun* **68**: 6362-6369.
- Kaul, R., McGeer, A., Low, D.E., Green, K., and Schwartz, B. (1997) Population-based surveillance for group A streptococcal necrotizing fasciitis: Clinical features, prognostic indicators, and microbiologic analysis of seventy-seven cases. Ontario Group A Streptococcal Study. *Am J Med* **103**: 18-24.
- Kazmi, S.U., Kansal, R., Aziz, R.K., Hooshdaran, M., Norrby-Teglund, A., Low, D.E., Halim, A.B., *et al.* (2001) Reciprocal, temporal expression of SpeA and SpeB by invasive MIT1 group A streptococcal isolates in vivo. *Infect Immun* **69**: 4988-4995.
- Kiang, J.G., and Tsokos, G.C. (1998) Heat shock protein 70 kDa: molecular biology, biochemistry, and physiology. *Pharmacol Ther* **80**: 183-201.
- Kile, B.T., Mason-Garrison, C.L., and Justice, M.J. (2003) Sex and strain-related differences in the peripheral blood cell values of inbred mouse strains. *Mamm Genome* **14**: 81-85.
- Kim, H.P., Morse, D., and Choi, A.M. (2006) Heat-shock proteins: new keys to the development of cytoprotective therapies. *Expert Opin Ther Targets* **10**: 759-769.
- Klenk, M., Koczan, D., Guthke, R., Nakata, M., Thiesen, H.J., Podbielski, A., and Kreikemeyer, B. (2005) Global epithelial cell transcriptional responses reveal *Streptococcus pyogenes* Fas regulator activity association with bacterial aggressiveness. *Cell Microbiol* **7**: 1237-1250.

- Ko, D.C., Shukla, K.P., Fong, C., Wasnick, M., Brittnacher, M.J., Wurfel, M.M., Holden, T.D., *et al.* (2009) A genome-wide in vitro bacterial-infection screen reveals human variation in the host response associated with inflammatory disease. *Am J Hum Genet* **85**: 214-227.
- Kobayashi, S.D., Braughton, K.R., Whitney, A.R., Voyich, J.M., Schwan, T.G., Musser, J.M., and DeLeo, F.R. (2003) Bacterial pathogens modulate an apoptosis differentiation program in human neutrophils. *Proc Natl Acad Sci U S A* **100**: 10948-10953.
- Kobayashi, T., and Narumiya, S. (2002) Function of prostanoid receptors: studies on knockout mice. *Prostaglandins Other Lipid Mediat* **68-69**: 557-573.
- Kotb, M. (1992) Role of superantigens in the pathogenesis of infectious diseases and their sequelae. *Curr. Opin. Infect. Dis* **5**: 364.
- Kotb, M. (1995) Bacterial pyrogenic exotoxins as superantigens. *Clin Microbiol Rev* **8**: 411-426.
- Kotb, M., Norrby-Teglund, A., McGeer, A., El-Sherbini, H., Dorak, M.T., Khurshid, A., Green, K., *et al.* (2002) An immunogenetic and molecular basis for differences in outcomes of invasive group A streptococcal infections. *Nat Med* **8**: 1398-1404.
- Kotb, M., Norrby-Teglund, A., McGeer, A., Green, K., and Low, D.E. (2003) Association of human leukocyte antigen with outcomes of infectious diseases: the streptococcal experience. *Scand J Infect Dis* **35**: 665-669.
- Kotb, M. (2004) Genetics of susceptibility to infectious diseases. *ASM News* **70 (10)**: 457-463.
- Kustanova, G.A., Murashev, A.N., Guzhova, I.V., Margulis, B.A., Prokhorenko, I.R., Grachev, S.V., and Evgen'ev, M.B. (2006) Protective effect of exogenous 70-kDa heat shock protein during endotoxic shock (sepsis). *Dokl Biol Sci* **411**: 504-507.
- Lamkanfi, M., and Kanneganti, T.D. (2010) Nlrp3: an immune sensor of cellular stress and infection. *Int J Biochem Cell Biol* **42**: 792-795.
- Lappin, E., and Ferguson, A.J. (2009) Gram-positive toxic shock syndromes. *Lancet Infect Dis* **9**: 281-290.
- Leder, L., Llera, A., Lavoie, P.M., Lebedeva, M.I., Li, H., Sekaly, R.P., Bohach, G.A., *et al.* (1998) A mutational analysis of the binding of staphylococcal enterotoxins B and C3 to the T cell receptor beta chain and major histocompatibility complex class II. *J Exp Med* **187**: 823-833.
- Lima, R.G., Moreira, L., Paes-Leme, J., Barreto-de-Souza, V., Castro-Faria-Neto, H.C., Bozza, P.T., and Bou-Habib, D.C. (2006) Interaction of macrophages with apoptotic cells enhances HIV Type 1 replication through PGE2, PAF, and vitronectin receptor. *AIDS Res Hum Retroviruses* **22**: 763-769.

- Lin, A., Loughman, J.A., Zinselmeyer, B.H., Miller, M.J., and Caparon, M.G. (2009) Streptolysin S inhibits neutrophil recruitment during the early stages of *Streptococcus pyogenes* infection. *Infect Immun* **77**: 5190-5201.
- Loof, T.G., Goldmann, O., and Medina, E. (2008) Immune recognition of *Streptococcus pyogenes* by dendritic cells. *Infect Immun* **76**: 2785-2792.
- Low, D.E., Schwartz, B., and McGeer, A. (1997) *The reemergence of severe group A streptococcal disease: an evolutionary perspective*. Washington, D.C: American Society for Microbiology Press.
- Lynch, M., and Walsh, B. (1998) *Genetics and Analysis of Quantitative Traits*. Sinauer Associates, Sunderland, Massachusetts.
- Mahler, M., Janke, C., Wagner, S., and Hedrich, H.J. (2002) Differential susceptibility of inbred mouse strains to *Helicobacter pylori* infection. *Scand J Gastroenterol* **37**: 267-278.
- Maloney, C.G., Thompson, S.D., Hill, H.R., Bohnsack, J.F., McIntyre, T.M., and Zimmerman, G.A. (2000) Induction of cyclooxygenase-2 by human monocytes exposed to group B streptococci. *J Leukoc Biol* **67**: 615-621.
- Marriott, H.M., and Dockrell, D.H. (2006) *Streptococcus pneumoniae*: the role of apoptosis in host defense and pathogenesis. *Int J Biochem Cell Biol* **38**: 1848-1854.
- Mebius, R.E., and Kraal, G. (2005) Structure and function of the spleen. *Nat Rev Immunol* **5**: 606-616.
- Medina, E., Goldmann, O., Rohde, M., Lengeling, A., and Chhatwal, G.S. (2001) Genetic control of susceptibility to group A streptococcal infection in mice. *J Infect Dis* **184**: 846-852.
- Medina, E., Goldmann, O., Toppel, A.W., and Chhatwal, G.S. (2003a) Survival of *Streptococcus pyogenes* within host phagocytic cells: a pathogenic mechanism for persistence and systemic invasion. *J Infect Dis* **187**: 597-603.
- Medina, E., Rohde, M., and Chhatwal, G.S. (2003b) Intracellular survival of *Streptococcus pyogenes* in polymorphonuclear cells results in increased bacterial virulence. *Infect Immun* **71**: 5376-5380.
- Medina, E., and Lengeling, A. (2005) Genetic regulation of host responses to group A streptococcus in mice. *Brief Funct Genomic Proteomic* **4**: 248-257.
- Melvold, R.W., Jokinen, D.M., Miller, S.D., Dal Canto, M.C., and Lipton, H.L. (1990) Identification of a locus on mouse chromosome 3 involved in differential susceptibility to Theiler's murine encephalomyelitis virus-induced demyelinating disease. *J Virol* **64**: 686-690.

- Mestas, J., and Hughes, C.C. (2004) Of mice and not men: differences between mouse and human immunology. *J Immunol* **172**: 2731-2738.
- Miethke, T., Wahl, C., Heeg, K., Echtenacher, B., Krammer, P.H., and Wagner, H. (1992) T cell-mediated lethal shock triggered in mice by the superantigen staphylococcal enterotoxin B: critical role of tumor necrosis factor. *J Exp Med* **175**: 91-98.
- Minami, M., Ohmori, D., Tatsuno, I., Isaka, M., Kawamura, Y., Ohta, M., and Hasegawa, T. (2009) The streptococcal inhibitor of complement (SIC) protects *Streptococcus pyogenes* from bacteriocin-like inhibitory substance (BLIS) from *Streptococcus salivarius*. *FEMS Microbiol Lett* **298**: 67-73.
- Minato, Y., and Yasutomo, K. (2005) Regulation of acquired immune system by notch signaling. *Int J Hematol* **82**: 302-306.
- Mitchell, T.J. (2003) The pathogenesis of streptococcal infections: from tooth decay to meningitis. *Nat Rev Microbiol* **1**: 219-230.
- Mitsos, L.M., Cardon, L.R., Fortin, A., Ryan, L., LaCourse, R., North, R.J., and Gros, P. (2000) Genetic control of susceptibility to infection with *Mycobacterium tuberculosis* in mice. *Genes Immun* **1**: 467-477.
- Mitsos, L.M., Cardon, L.R., Ryan, L., LaCourse, R., North, R.J., and Gros, P. (2003) Susceptibility to tuberculosis: a locus on mouse chromosome 19 (Trl-4) regulates *Mycobacterium tuberculosis* replication in the lungs. *Proc Natl Acad Sci U S A* **100**: 6610-6615.
- Miyairi, I., Tatireddigari, V.R., Mahdi, O.S., Rose, L.A., Belland, R.J., Lu, L., Williams, R.W., *et al.* (2007) The p47 GTPases Iigp2 and Irgb10 regulate innate immunity and inflammation to murine *Chlamydia psittaci* infection. *J Immunol* **179**: 1814-1824.
- Miyoshi-Akiyama, T., Takamatsu, D., Koyanagi, M., Zhao, J., Imanishi, K., and Uchiyama, T. (2005) Cytocidal effect of *Streptococcus pyogenes* on mouse neutrophils in vivo and the critical role of streptolysin S. *J Infect Dis* **192**: 107-116.
- Monsalve, E., Perez, M.A., Rubio, A., Ruiz-Hidalgo, M.J., Baladron, V., Garcia-Ramirez, J.J., Gomez, J.C., *et al.* (2006) Notch-1 up-regulation and signaling following macrophage activation modulates gene expression patterns known to affect antigen-presenting capacity and cytotoxic activity. *J Immunol* **176**: 5362-5373.
- Morahan, G., and Williams, R.W. (2007) Systems genetics: the next generation in genetics research? *Novartis Found Symp* **281**: 181-188; discussion 188-191, 208-189.
- Mosca, M., Polentarutti, N., Mangano, G., Apicella, C., Doni, A., Mancini, F., De Bortoli, M., *et al.* (2007) Regulation of the microsomal prostaglandin E synthase-1 in polarized mononuclear phagocytes and its constitutive expression in neutrophils. *J Leukoc Biol* **82**: 320-326.

- Mountz, J.D., Yang, P., Wu, Q., Zhou, J., Tousson, A., Fitzgerald, A., Allen, J., *et al.* (2005) Genetic segregation of spontaneous erosive arthritis and generalized autoimmune disease in the BXD2 recombinant inbred strain of mice. *Scand J Immunol* **61**: 128-138.
- Muller, M.P., Low, D.E., Green, K.A., Simor, A.E., Loeb, M., Gregson, D., and McGeer, A. (2003) Clinical and epidemiologic features of group A streptococcal pneumonia in Ontario, Canada. *Arch Intern Med* **163**: 467-472.
- Munoz-Planillo, R., Franchi, L., Miller, L.S., and Nunez, G. (2009) A critical role for hemolysins and bacterial lipoproteins in *Staphylococcus aureus*-induced activation of the Nlrp3 inflammasome. *J Immunol* **183**: 3942-3948.
- Nakagawa, I., Nakata, M., Kawabata, S., and Hamada, S. (2004) Transcriptome analysis and gene expression profiles of early apoptosis-related genes in *Streptococcus pyogenes*-infected epithelial cells. *Cell Microbiol* **6**: 939-952.
- Nakayama, T., Mutsuga, N., Yao, L., and Tosato, G. (2006) Prostaglandin E2 promotes degranulation-independent release of MCP-1 from mast cells. *J Leukoc Biol* **79**: 95-104.
- Narumiya, S., Sugimoto, Y., and Ushikubi, F. (1999) Prostanoid receptors: structures, properties, and functions. *Physiol Rev* **79**: 1193-1226.
- Nauseef, W.M. (2007) How human neutrophils kill and degrade microbes: an integrated view. *Immunol Rev* **219**: 88-102.
- Navarini, A.A., Lang, K.S., Verschoor, A., Recher, M., Zinkernagel, A.S., Nizet, V., Odermatt, B., *et al.* (2009) Innate immune-induced depletion of bone marrow neutrophils aggravates systemic bacterial infections. *Proc Natl Acad Sci U S A* **106**: 7107-7112.
- Nilsson, M., Sorensen, O.E., Morgelin, M., Weineisen, M., Sjobring, U., and Herwald, H. (2006) Activation of human polymorphonuclear neutrophils by streptolysin O from *Streptococcus pyogenes* leads to the release of proinflammatory mediators. *Thromb Haemost* **95**: 982-990.
- Nooh, M.M., El-Gengehi, N., Kansal, R., David, C.S., and Kotb, M. (2007) HLA transgenic mice provide evidence for a direct and dominant role of HLA class II variation in modulating the severity of streptococcal sepsis. *J Immunol* **178**: 3076-3083.
- Norrby-Teglund, A., Lustig, R., and Kotb, M. (1997) Differential induction of Th1 versus Th2 cytokines by group A streptococcal toxic shock syndrome isolates. *Infect Immun* **65**: 5209-5215.
- Norrby-Teglund, A., Chatellier, S., Low, D.E., McGeer, A., Green, K., and Kotb, M. (2000) Host variation in cytokine responses to superantigens determine the severity of invasive group A streptococcal infection. *Eur J Immunol* **30**: 3247-3255.
- Norrby-Teglund, A., and Kotb, M. (2000) Host-microbe interactions in the pathogenesis of invasive group A streptococcal infections. *J Med Microbiol* **49**: 849-852.

Norrby-Teglund, A., Thulin, P., Gan, B.S., Kotb, M., McGeer, A., Andersson, J., and Low, D.E. (2001) Evidence for superantigen involvement in severe group a streptococcal tissue infections. *J Infect Dis* **184**: 853-860.

Norrby-Teglund, A., Nepom, G.T., and Kotb, M. (2002) Differential presentation of group A streptococcal superantigens by HLA class II DQ and DR alleles. *Eur J Immunol* **32**: 2570-2577.

Ouburg, S., Bart, A.C.J., Klinkenberg-Knol, E.C., Mulder, C.J., Salvador Pena, A., and Morre, S.A. (2005) A candidate gene approach of immune mediators effecting the susceptibility to and severity of upper gastrointestinal tract diseases in relation to Helicobacter pylori and Epstein-Barr virus infections. *Eur J Gastroenterol Hepatol* **17**: 1213-1224.

Peirce, J.L., Chesler, E.J., Williams, R.W., and Lu, L. (2003) Genetic architecture of the mouse hippocampus: identification of gene loci with selective regional effects. *Genes Brain Behav* **2**: 238-252.

Peirce, J.L., Lu, L., Gu, J., Silver, L.M., and Williams, R.W. (2004) A new set of BXD recombinant inbred lines from advanced intercross populations in mice. *BMC Genet* **5**: 7.

Peirce, J.L., Broman, K.W., Lu, L., Chesler, E.J., Zhou, G., Airey, D.C., Birmingham, A.E., *et al.* (2008) Genome Reshuffling for Advanced Intercross Permutation (GRAIP): simulation and permutation for advanced intercross population analysis. *PLoS One* **3**: e1977.

Peters, L.L., Zhang, W., Lambert, A.J., Brugnara, C., Churchill, G.A., and Platt, O.S. (2005) Quantitative trait loci for baseline white blood cell count, platelet count, and mean platelet volume. *Mamm Genome* **16**: 749-763.

Peters, L.L., Robledo, R.F., Bult, C.J., Churchill, G.A., Paigen, B.J., and Svenson, K.L. (2007) The mouse as a model for human biology: a resource guide for complex trait analysis. *Nat Rev Genet* **8**: 58-69.

Petkova, S.B., Yuan, R., Tsaih, S.W., Schott, W., Roopenian, D.C., and Paigen, B. (2008) Genetic influence on immune phenotype revealed strain-specific variations in peripheral blood lineages. *Physiol Genomics* **34**: 304-314.

Plant, J., and Glynn, A.A. (1976) Genetics of resistance to infection with Salmonella typhimurium in mice. *J Infect Dis* **133**: 72-78.

Proft, T., Sriskandan, S., Yang, L., and Fraser, J.D. (2003) Superantigens and streptococcal toxic shock syndrome. *Emerg Infect Dis* **9**: 1211-1218.

Rittirsch, D., Flierl, M.A., and Ward, P.A. (2008) Harmful molecular mechanisms in sepsis. *Nat Rev Immunol* **8**: 776-787.

- Rolink, A.G., Balciunaite, G., Demoliere, C., and Ceredig, R. (2006) The potential involvement of Notch signaling in NK cell development. *Immunol Lett* **107**: 50-57.
- Roper, R.J., Weis, J.J., McCracken, B.A., Green, C.B., Ma, Y., Weber, K.S., Fairbairn, D., *et al.* (2001) Genetic control of susceptibility to experimental Lyme arthritis is polygenic and exhibits consistent linkage to multiple loci on chromosome 5 in four independent mouse crosses. *Genes Immun* **2**: 388-397.
- Rosen, G.D., and Williams, R.W. (2001) Complex trait analysis of the mouse striatum: independent QTLs modulate volume and neuron number. *BMC Neurosci* **2**: 5.
- Roy, M.F., and Malo, D. (2002) Genetic regulation of host responses to Salmonella infection in mice. *Genes Immun* **3**: 381-393.
- Roy, M.F., Riendeau, N., Loredano-Osti, J.C., and Malo, D. (2006) Complexity in the host response to Salmonella Typhimurium infection in AcB and BcA recombinant congenic strains. *Genes Immun* **7**: 655-666.
- Roy, M.F., Riendeau, N., Bedard, C., Helie, P., Min-Oo, G., Turcotte, K., Gros, P., *et al.* (2007) Pyruvate kinase deficiency confers susceptibility to Salmonella typhimurium infection in mice. *J Exp Med* **204**: 2949-2961.
- Ruiz, N., Wang, B., Pentland, A., and Caparon, M. (1998) Streptolysin O and adherence synergistically modulate proinflammatory responses of keratinocytes to group A streptococci. *Mol Microbiol* **27**: 337-346.
- Sakata, D., Yao, C., and Narumiya, S. (2010) Prostaglandin E(2), an immunoactivator. *J Pharmacol Sci* **112**: 1-5.
- Saraiva, M., and O'Garra, A. (2010) The regulation of IL-10 production by immune cells. *Nat Rev Immunol* **10**: 170-181.
- Serezani, C.H., Chung, J., Ballinger, M.N., Moore, B.B., Aronoff, D.M., and Peters-Golden, M. (2007) Prostaglandin E2 suppresses bacterial killing in alveolar macrophages by inhibiting NADPH oxidase. *Am J Respir Cell Mol Biol* **37**: 562-570.
- Shifman, S., Bell, J.T., Copley, R.R., Taylor, M.S., Williams, R.W., Mott, R., and Flint, J. (2006) A high-resolution single nucleotide polymorphism genetic map of the mouse genome. *PLoS Biol* **4**: e395.
- Sieberts, S.K., and Schadt, E.E. (2007) Moving toward a system genetics view of disease. *Mamm Genome* **18**: 389-401.
- Singleton, K.D., and Wischmeyer, P.E. (2006) Effects of HSP70.1/3 gene knockout on acute respiratory distress syndrome and the inflammatory response following sepsis. *Am J Physiol Lung Cell Mol Physiol* **290**: L956-961.

- Sjolinder, H., Lovkvist, L., Plant, L., Eriksson, J., Aro, H., Jones, A., and Jonsson, A.B. (2008) The ScpC protease of *Streptococcus pyogenes* affects the outcome of sepsis in a murine model. *Infect Immun* **76**: 3959-3966.
- Skamene, E. (1983) Genetic regulation of host resistance to bacterial infection. *Rev Infect Dis* **5 Suppl 4**: S823-832.
- Smith, R.S., Kelly, R., Iglewski, B.H., and Phipps, R.P. (2002) The *Pseudomonas* autoinducer N-(3-oxododecanoyl) homoserine lactone induces cyclooxygenase-2 and prostaglandin E2 production in human lung fibroblasts: implications for inflammation. *J Immunol* **169**: 2636-2642.
- Soehnlein, O., Oehmcke, S., Ma, X., Rothfuchs, A.G., Frithiof, R., van Rooijen, N., Morgelin, M., *et al.* (2008a) Neutrophil degranulation mediates severe lung damage triggered by streptococcal M1 protein. *Eur Respir J* **32**: 405-412.
- Soehnlein, O., Zernecke, A., Eriksson, E.E., Rothfuchs, A.G., Pham, C.T., Herwald, H., Bidzhekov, K., *et al.* (2008b) Neutrophil secretion products pave the way for inflammatory monocytes. *Blood* **112**: 1461-1471.
- Staali, L., Bauer, S., Morgelin, M., Bjorck, L., and Tapper, H. (2006) *Streptococcus pyogenes* bacteria modulate membrane traffic in human neutrophils and selectively inhibit azurophilic granule fusion with phagosomes. *Cell Microbiol* **8**: 690-703.
- Sumby, P., Porcella, S.F., Madrigal, A.G., Barbian, K.D., Virtaneva, K., Ricklefs, S.M., Sturdevant, D.E., *et al.* (2005) Evolutionary origin and emergence of a highly successful clone of serotype M1 group A *Streptococcus* involved multiple horizontal gene transfer events. *J Infect Dis* **192**: 771-782.
- Sumby, P., Zhang, S., Whitney, A.R., Falugi, F., Grandi, G., Graviss, E.A., Deleo, F.R., *et al.* (2008) A Chemokine-Degrading Extracellular Protease Made by Group A *Streptococcus* Alters Pathogenesis by Enhancing Evasion of the Innate Immune Response. *Infect Immun*.
- Sun, H., Ringdahl, U., Homeister, J.W., Fay, W.P., Engleberg, N.C., Yang, A.Y., Rozek, L.S., *et al.* (2004) Plasminogen is a critical host pathogenicity factor for group A streptococcal infection. *Science* **305**: 1283-1286.
- Takahashi, E., Kuranaga, N., Satoh, K., Habu, Y., Shinomiya, N., Asano, T., Seki, S., *et al.* (2007) Induction of CD16+ CD56bright NK cells with antitumour cytotoxicity not only from CD16- CD56bright NK Cells but also from CD16- CD56dim NK cells. *Scand J Immunol* **65**: 126-138.
- Tapper, H., and Herwald, H. (2000) Modulation of hemostatic mechanisms in bacterial infectious diseases. *Blood* **96**: 2329-2337.
- Taylor, B. (1978) *Recombinant inbred strains: Use in gene mapping*. . NY: Academic Press.

- Taylor, B.A., Wnek, C., Kotlus, B.S., Roemer, N., MacTaggart, T., and Phillips, S.J. (1999) Genotyping new BXD recombinant inbred mouse strains and comparison of BXD and consensus maps. *Mamm Genome* **10**: 335-348.
- Thach, D.C., Kleeberger, S.R., Tucker, P.C., and Griffin, D.E. (2001) Genetic control of neuroadapted sindbis virus replication in female mice maps to chromosome 2 and associates with paralysis and mortality. *J Virol* **75**: 8674-8680.
- Thulin, P., Johansson, L., Low, D.E., Gan, B.S., Kotb, M., McGeer, A., and Norrby-Teglund, A. (2006) Viable Group A Streptococci in Macrophages during Acute Soft Tissue Infection. *PLoS Med* **3**: e53.
- Ting, J.P., Lovering, R.C., Alnemri, E.S., Bertin, J., Boss, J.M., Davis, B.K., Flavell, R.A., *et al.* (2008) The NLR gene family: a standard nomenclature. *Immunity* **28**: 285-287.
- Tober, K.L., Thomas-Ahner, J.M., Maruyama, T., and Oberyszyn, T.M. (2007) Possible cross-regulation of the E prostanoïd receptors. *Mol Carcinog* **46**: 711-715.
- Tsaih, S.W., Lu, L., Airey, D.C., Williams, R.W., and Churchill, G.A. (2005) Quantitative trait mapping in a diallel cross of recombinant inbred lines. *Mamm Genome* **16**: 344-355.
- Tuite, A., Mullick, A., and Gros, P. (2004) Genetic analysis of innate immunity in resistance to *Candida albicans*. *Genes Immun* **5**: 576-587.
- Tuite, A., Elias, M., Picard, S., Mullick, A., and Gros, P. (2005) Genetic control of susceptibility to *Candida albicans* in susceptible A/J and resistant C57BL/6J mice. *Genes Immun* **6**: 672-682.
- Turnbull, I.R., Clark, A.T., Stromberg, P.E., Dixon, D.J., Woolsey, C.A., Davis, C.G., Hotchkiss, R.S., *et al.* (2009) Effects of aging on the immunopathologic response to sepsis. *Crit Care Med* **37**: 1018-1023.
- Valdar, W., Flint, J., and Mott, R. (2006) Simulating the collaborative cross: power of quantitative trait loci detection and mapping resolution in large sets of recombinant inbred strains of mice. *Genetics* **172**: 1783-1797.
- van den Brandt, J., Voss, K., Schott, M., Hunig, T., Wolfe, M.S., and Reichardt, H.M. (2004) Inhibition of Notch signaling biases rat thymocyte development towards the NK cell lineage. *Eur J Immunol* **34**: 1405-1413.
- Van Rooijen, N., and Sanders, A. (1994) Liposome mediated depletion of macrophages: mechanism of action, preparation of liposomes and applications. *J Immunol Methods* **174**: 83-93.

Virtaneva, K., Graham, M.R., Porcella, S.F., Hoe, N.P., Su, H., Graviss, E.A., Gardner, T.J., *et al.* (2003) Group A Streptococcus gene expression in humans and cynomolgus macaques with acute pharyngitis. *Infect Immun* **71**: 2199-2207.

Virtaneva, K., Porcella, S.F., Graham, M.R., Ireland, R.M., Johnson, C.A., Ricklefs, S.M., Babar, I., *et al.* (2005) Longitudinal analysis of the group A *Streptococcus* transcriptome in experimental pharyngitis in cynomolgus macaques. *Proc. Natl. Acad. Sci. USA* **102**: 9014-9019.

Vladimirov, V., Badalova, J., Svobodova, M., Havelkova, H., Hart, A.A., Blazkova, H., Demant, P., *et al.* (2003) Different genetic control of cutaneous and visceral disease after *Leishmania major* infection in mice. *Infect Immun* **71**: 2041-2046.

Vogel, G. (2003) Scientists dream of 1001 complex mice. *Science* **301**: 456-458.

Voyich, J.M., Musser, J.M., and DeLeo, F.R. (2004) Streptococcus pyogenes and human neutrophils: a paradigm for evasion of innate host defense by bacterial pathogens. *Microbes Infect* **6**: 1117-1123.

Walker, M.J., Hollands, A., Sanderson-Smith, M.L., Cole, J.N., Kirk, J.K., Henningham, A., McArthur, J.D., *et al.* (2007) DNase Sda1 provides selection pressure for a switch to invasive group A streptococcal infection. *Nat Med* **13**: 981-985.

Wang, J., Williams, R.W., and Manly, K.F. (2003) WebQTL: web-based complex trait analysis. *Neuroinformatics* **1**: 299-308.

Waterston, R.H., and Lindblad-Toh, K., and Birney, E., and Rogers, J., and Abril, J.F., and Agarwal, P., and Agarwala, R., *et al.* (2002) Initial sequencing and comparative analysis of the mouse genome. *Nature* **420**: 520-562.

Watters, J.W., Dewar, K., Lehoczky, J., Boyartchuk, V., and Dietrich, W.F. (2001) Kif1C, a kinesin-like motor protein, mediates mouse macrophage resistance to anthrax lethal factor. *Curr Biol* **11**: 1503-1511.

Welcher, B.C., Carra, J.H., DaSilva, L., Hanson, J., David, C.S., Aman, M.J., and Bavari, S. (2002) Lethal shock induced by streptococcal pyrogenic exotoxin A in mice transgenic for human leukocyte antigen-DQ8 and human CD4 receptors: implications for development of vaccines and therapeutics. *J Infect Dis* **186**: 501-510.

White, E.S., Atrasz, R.G., Dickie, E.G., Aronoff, D.M., Stambolic, V., Mak, T.W., Moore, B.B., *et al.* (2005) Prostaglandin E(2) inhibits fibroblast migration by E-prostanoid 2 receptor-mediated increase in PTEN activity. *Am J Respir Cell Mol Biol* **32**: 135-141.

Williams, R.W., Gu, J., Qi, S., and Lu, L. (2001) The genetic structure of recombinant inbred mice: high-resolution consensus maps for complex trait analysis. *Genome Biol* **2**: RESEARCH0046.

- Williams, R.W. (2006) Expression genetics and the phenotype revolution. *Mamm Genome* **17**: 496-502.
- Woolard, M.D., Wilson, J.E., Hensley, L.L., Jania, L.A., Kawula, T.H., Drake, J.R., and Frelinger, J.A. (2007) Francisella tularensis-infected macrophages release prostaglandin E2 that blocks T cell proliferation and promotes a Th2-like response. *J Immunol* **178**: 2065-2074.
- Yao, C., Sakata, D., Esaki, Y., Li, Y., Matsuoka, T., Kuroiwa, K., Sugimoto, Y., *et al.* (2009) Prostaglandin E2-EP4 signaling promotes immune inflammation through Th1 cell differentiation and Th17 cell expansion. *Nat Med* **15**: 633-640.
- Ye, Z., and Ting, J.P. (2008) NLR, the nucleotide-binding domain leucine-rich repeat containing gene family. *Curr Opin Immunol* **20**: 3-9.
- Yenari, M.A., Liu, J., Zheng, Z., Vexler, Z.S., Lee, J.E., and Giffard, R.G. (2005) Antiapoptotic and anti-inflammatory mechanisms of heat-shock protein protection. *Ann N Y Acad Sci* **1053**: 74-83.
- Yong, M., Mitchell, D., Caudron, A., Toth, I., and Olive, C. (2009) Expression of maturation markers on murine dendritic cells in response to group A streptococcal lipopeptide vaccines. *Vaccine* **27**: 3313-3318.
- Zhang, L., Katz, J.M., Gwinn, M., Dowling, N.F., and Khoury, M.J. (2009a) Systems-based candidate genes for human response to influenza infection. *Infect Genet Evol* **9**: 1148-1157.
- Zhang, W.W., and Matlashewski, G. (2004) In vivo selection for Leishmania donovani miniexon genes that increase virulence in Leishmania major. *Mol Microbiol* **54**: 1051-1062.
- Zhang, X., Majlessi, L., Deriaud, E., Leclerc, C., and Lo-Man, R. (2009b) Coactivation of Syk kinase and MyD88 adaptor protein pathways by bacteria promotes regulatory properties of neutrophils. *Immunity* **31**: 761-771.
- Zhang, Y., Guan, Y., Schneider, A., Brandon, S., Breyer, R.M., and Breyer, M.D. (2000) Characterization of murine vasopressor and vasodepressor prostaglandin E(2) receptors. *Hypertension* **35**: 1129-1134.
- Zinkernagel, A.S., Timmer, A.M., Pence, M.A., Locke, J.B., Buchanan, J.T., Turner, C.E., Mishalian, I., *et al.* (2008) The IL-8 protease SpyCEP/ScpC of group A Streptococcus promotes resistance to neutrophil killing. *Cell Host Microbe* **4**: 170-178.

APPENDIX A. PRIMER SEQUENCES USED FOR QPCR AND THE RELATIVE EXPRESSION LEVELS OF CANDIDATE GENES

This appendix contains two supplementary tables for Chapter 3:

- Table A-1. Primer sequences used in quantitative PCR assays for candidate genes.
- Table A-2. Relative expression levels of candidate gene list expressed as mean fold difference between pre- and post-infection \pm standard deviation (SD) in selected resistant and susceptible strains.

Table A-1. Primer sequences used in quantitative PCR assays for candidate genes.

Gene	Gene Description	Accession Number	Forward 5'	Reverse 3'
<i>Anapc2</i>	Anaphase promoting complex subunit 2	NM_175300	ctcaaggtggcctagagact	agagtgatgatgcacatgtgtg
<i>Asb6</i>	Ankyrin repeat and SOCS box-containing protein 6	NM_133346	aggagcccctggatgatt	cagctccgtgaggaccag
<i>Edf1</i>	Endothelial differentiation-related factor 1	NM_021519	ccgcacaggccaagtcta	aatggaatgctgctgttctg
<i>Entpd2</i>	Ectonucleoside triphosphate diphosphohydrolase 2	NM_009849	cagagaccacctgcaacca	ggctctgtgccgggtact
<i>Fbxw2</i>	F-box and WD-40 domain protein 2	NM_013890	caaagtcaagtctctctgcaca	tccaattggccaaatctt
<i>Garnl3</i>	GTPase activating RANGAP domain-like 3	NM_178888	tccacatgttccatattc	caatgtggcgcttcttt
<i>Gpr107</i>	G protein-coupled receptor 107	NM_178760	cctcgagctctctcaggaag	cacacccgatgtcgtcacta
<i>Hspa5</i>	Heat shock 70kD protein 5 (glucose-regulated protein)	NM_022310	ctgaggcgtattgggaaag	cagcatcttgggttctgtc
<i>Il1α</i>	Interleukin 1 alpha	NM_010554.4	ttggttaatgacctgcaaca	gagcgtcacgaacagttg
<i>Il1rn</i>	Interleukin 1 receptor antagonist	NM_031167	tgtccaagtctgagatga	ttcttgttctgtcagatcagt
<i>Mapkap1</i>	Mitogen-activated protein kinase associated protein 1	NM_177345	acctgccgaggagaagag	gcgtcggactcgaagtacag
<i>Nfatc2</i>	Nfatc2 nuclear factor of activated t-cells, cytoplasmic, calcineurin-dependent 2*	NM_010899	caggaggacacctgtgg	tcatctgctgtccaatgaa
		NM_001037177		
		NM_001037178		
<i>Notch1</i>	Notch gene homolog 1 (Drosophila)	NM_008714	tgcaactgtcctctgccata	gtagcacatgggccaac
<i>Nox1</i>	NADPH oxidase activator 1	NM_172204	atctggagccatggattt	gcgttggctcatcaggaat
<i>Phpt1</i>	Phosphohistidine phosphatase 1	NM_029293	cagagccaggacaggaagata	ttggcttggatcttctcagttg
<i>Phyhd1</i>	Phytanoyl-CoA dioxygenase domain containing 1	NM_172267	gtctggagcccagggaaat	gggcctttagctgtagagtgg
<i>Ppp2r4</i>	Protein phosphatase 2A, regulatory subunit B	NM_138748	ggcagctcacagctcataga	gccttctcatccagaaatg
<i>Psmc5</i>	Proteasome (prosome, macropain) 26S subunit, non-ATPase, 5	NM_080554	gacgggtgaggacgtgta	cgtccgtgatgggtataagc
<i>Ptges</i>	Prostaglandin E synthase	NM_022415	gcacactgctggtcatcaag	acgtttcagcgcacctc
<i>Ptges2</i>	Prostaglandin E synthase 2	NM_133783	cccaggaaggagacagctt	aggtaggctttagggcactaag
<i>Rab14</i>	RAB14, member RAS oncogene family	NM_026697	aggtgctgctcatggtgat	caaccagctgcttaagtggta
<i>Sh2d3c</i>	SH2 domain containing 3C	NM_013781	cagatcccagatctcactca	agcatggactcgggttacag

Table A-1. (Continued).

Gene	Gene Description	Accession Number	Forward 5'	Reverse 3'
<i>Sirpa</i>	Signal-regulatory protein alpha	NM_007547.2	agggagcatgcaaaccttc	tttgatccggaggaggtaga
<i>Traf1</i>	TNF receptor associated factor 1	NM_009421	gagcacatcctgagcttgg	tcttttgagccagggttg
<i>Traf2</i>	TNF receptor associated factor 2	NM_009422	gctccttctgcctgacca	agacacaggcagcacagttc
<i>Tubb2c1</i>	Tubulinbeta 2c	NM_146116.1	gctccttctacagctgtcc	cgctgattacctccagaact
<i>Ubac1</i>	Ubiquitin associated domain containing 1	NM_133835	gaacaacaaccagcagaacg	tccaattcctcaggggatg
<i>Urm1</i>	Ubiquitin related modifier 1 homolog (S. cerevisiae)	NM_026615	gagcgaccagagctgttcat	ggcatcattaatcagcacca

* *Nfatc2* has three transcript variants; we designed a common assay for the three transcripts, and differentiating assays for each isoform. All assays showed similar results, shown are primers sets of common assay for the three transcript variants.

Table A-2. Relative expression levels of candidate gene list expressed as mean fold difference between pre- and post-infection \pm standard deviation (SD) in selected resistant and susceptible strains.

Gene ID	Gene	Resistant	SD	Susceptible	SD
Genes down regulated in resistant group while up regulated in susceptible group					
<i>Anapc2</i>	Anaphase promoting complex subunit 2	0.551	0.022	1.475	0.691
<i>Asb6</i>	Ankyrin repeat and SOCS box-containing protein 6	0.573	0.482	2.300	1.801
<i>Fbxw2</i>	F-box and WD-40 domain protein 2	0.930	0.384	1.159	0.268
<i>Gpr107</i>	G protein-coupled receptor 107	0.866	0.481	2.196	0.758
<i>Il1α</i>	Interleukin 1 alpha	0.739	0.045	54.687	0.011
<i>Il1rn</i>	Interleukin 1 receptor antagonist	0.851	0.384	55.909	0.274
<i>Mapkap1</i>	Mitogen-activated protein kinase associated protein 1	0.732	0.199	1.189	0.460
<i>Nox1</i>	NADPH oxidase activator 1	0.270	0.164	1.086	0.151
<i>Phpt1</i>	Phosphohistidine phosphatase 1	0.229	0.133	0.714	0.155
<i>Ptges</i>	Prostaglandin E synthase	0.417	0.101	5.046	0.679
<i>Ptges2</i>	Prostaglandin E synthase 2	0.913	0.553	1.456	0.122
<i>Rab14</i>	RAB14, member RAS oncogene family	0.704	0.268	1.411	0.711
<i>Sh2d3c</i>	SH2 domain containing 3C	0.162	0.102	1.009	0.389
<i>Phyhd1</i>	Phytanoyl-CoA dioxygenase domain containing 1	0.806	0.727	1.288	0.288
<i>Urm1</i>	Ubiquitin related modifier 1 homolog (S. cerevisiae)	0.834	0.625	1.277	0.309
Genes down regulated in both resistant group and susceptible groups					
<i>pd2</i>	Ectonucleoside triphosphate diphosphohydrolase 2	0.359	0.114	0.654	0.160
<i>Edf1</i>	Endothelial differentiation-related factor 1	0.350	0.375	0.470	0.109
<i>Garnl3</i>	GTPase activating RANGAP domain-like 3	0.601	0.292	0.674	0.158
<i>Nfate2</i>	Nuclear factor of activated t-cells, cytoplasmic, calcineurin-dependent 2	0.178	0.174	0.693	0.147
<i>Psm5</i>	Proteasome (prosome, macropain) 26S subunit, non-ATPase, 5	0.644	0.049	0.963	0.123
<i>Ppp2r4</i>	Protein phosphatase 2A, regulatory subunit B	0.902	0.108	0.734	0.150
<i>Uba1</i>	Ubiquitin associated domain containing 1	0.865	0.960	0.730	0.971
<i>Tubb2c</i>	Tubulin beta 2c	0.846	0.506	0.925	0.477

Table A-2. (Continued).

Gene ID	Gene	Resistant	SD	Susceptible	SD
Genes up regulated in both resistant group and susceptible group					
<i>Hspa5</i>	Heat shock 70kD protein 5 (glucose-regulated protein)	1.717	1.016	4.040	2.587
<i>Notch1</i>	Notch gene homolog 1 (Drosophila)	2.005	1.192	10.424	7.833
<i>Traf1</i>	Tnf receptor-associated factor 1	1.826	0.596	5.995	0.733
<i>Traf2</i>	Tnf receptor-associated factor 2	2.369	2.694	2.421	0.844
<i>Sirpa</i>	Signal-regulatory protein alpha	4.092	6.024	1.607	1.034

APPENDIX B. LIST OF GENES AND TRANSCRIPTS IN THE MAPPED LOCI

This appendix contains lists of genes and transcripts in the mapped quantitative trait loci (QTLs) associated with differential susceptibility to severe group A streptococcal (GAS) sepsis. Public access to an update list of transcripts is available online at www.genenetwork.org under BXD published phenotypes, trait ID 10836. To search for this trait ID, access the search databases page at the above link, use mice as species, BXD as the group, phenotypes as type and BXD published phenotypes as database, and then enter Abdeltawab as the search term and from the retrieved results select trait ID 10836.

This appendix contains three tables:

- Table B-1. Genes and their SNPs in mapped locus on Chr 2 between 22-34 Mb.
- Table B-2. Genes and their SNPs in mapped locus on Chr 2 between 124-150 Mb.
- Table B-3. Genes and their SNPs in mapped locus on Chr X between 50-100 Mb.

Table B-1. Genes and their SNPs in mapped locus on Chr 2 between 22-34 Mb.

Position on Chr 2 (Mb)	Gene symbol	Gene description	NM ID	SNPs	SNP Density
22.1588	Myo3a	myosin IIIA	NM_148413	465	1.49
22.4778	Gad2	glutamic acid decarboxylase 2	NM_008078	211	2.95
22.6115	1700092C17Rik	RIKEN cDNA 1700092C17 gene	AK007039	12	1.91
22.6298	Apbb1ip	amyloid beta (A4) precursor protein-binding, family B, member 1 interacting protein	NM_019456	49	0.48
22.7472	Pdss1	prenyl (solanesyl) diphosphate synthase, subunit 1	NM_019501	0	0.00
22.7500	A130006I12Rik	RIKEN cDNA A130006I12 gene	AK015028	0	0.00
22.7955	Abi1	abl-interactor 1	NM_001077190	17	0.17
22.8470	2210402A03Rik	RIKEN cDNA 2210402A03 gene	AK008796	1	0.51
22.8820	4930534I15Rik	RIKEN cDNA 4930534I15 gene	AK015964	0	0.00
22.9237	Acbd5	acyl-Coenzyme A binding domain containing 5	NM_001102436	4	0.09
22.9736	Mastl	microtubule associated serine/threonine kinase-like	NM_025979	0	0.00
23.0121	Yme1l1	YME1-like 1 (S. cerevisiae)	NM_013771	4	0.10
23.0630	4931423N10Rik	RIKEN cDNA 4931423N10 gene	AK016475	16	0.27
23.1768	Nxph2	neurexophilin 2	NM_008752	7	0.09
23.3485	A330106F07Rik	RIKEN cDNA A330106F07 gene	AK039774	0	0.00
23.3656	Spopl	speckle-type POZ protein-like	NM_029773	5	0.08
23.8584	Hnmt	histamine N-methyltransferase	NM_080462	28	0.60
23.9272	Tbpl2	TATA box binding protein like 2	NM_199059	26	1.05
24.0019	LOC215253	similar to DEAD (Asp-Glu-Ala-Asp) box polypeptide 6	XR_030867	0	0.00
24.0087	Il1f8	interleukin 1 family, member 8	NM_027163	18	2.60
24.0271	2310066D07Rik	RIKEN cDNA 2310066D07 gene	AK010059	0	0.00
24.0420	Il1f9	interleukin 1 family, member 9	NM_153511	0	0.00
24.0709	Il1f6	interleukin 1 family, member 6	NM_019450	1	0.10
24.1325	Il1f5	interleukin 1 family, member 5 (delta)	NM_019451	0	0.00
24.1467	Il1f10	interleukin 1 family, member 10	NM_153077	0	0.00
24.1924	Il1rn	interleukin 1 receptor antagonist	NM_001039701	2	0.14
24.2409	Psd4	pleckstrin and Sec7 domain containing 4	NM_177611	53	2.27
24.2761	Pax8	paired box gene 8	NM_011040	60	1.09
24.4619	Cacna1b	calcium channel, voltage-dependent, N type, alpha 1B subunit	NM_001042528	504	3.21
24.6463	Ehmt1	euchromatic histone methyltransferase 1	NM_001012518	292	2.27
24.7809	Arrec1	arrestin domain containing 1	NM_178408	37	3.77
24.8053	Zmynd19	zinc finger, MYND domain containing 19	NM_026021	27	2.81
24.8179	Wdr85	WD40 repeat domain 85	NM_026044	10	0.90
24.8280	Mrpl41	mitochondrial ribosomal protein L41	NM_001031808	1	0.38
24.8316	Pnpla7	patatin-like phospholipase domain containing 7	NM_146251	11	0.14
24.9099	Nelf	nasal embryonic LHRH factor	NM_001039386	0	0.00
24.9358	Entpd8	ectonucleoside triphosphate diphosphohydrolase 8	NM_028093	11	2.04
24.9412	Noxa1	NADPH oxidase activator 1	NM_172204	20	2.11
24.9973	D530008I23	hypothetical protein D530008I23	AK085201	0	0.00
25.0363	Nrarp	Notch-regulated ankyrin repeat protein	NM_025980	1	0.39
25.0482	A830007P12Rik	RIKEN cDNA A830007P12 gene	NM_146115	2	0.51
25.0552	A730008L03Rik	RIKEN cDNA A730008L03 gene	NM_021393	0	0.00
25.0681	4933433C11Rik	RIKEN cDNA 4933433C11 gene	AK017033	1	0.48
25.0743	BC061039	cDNA sequence BC061039	NM_026624	0	0.00
25.0777	Tubb2c	tubulin, beta 2c	NM_146116	0	0.00
25.0844	Slc34a3	solute carrier family 34 (sodium phosphate), member 3	NM_080854	9	1.69
25.0900	Gm757	gene model 757, (NCBI)	NM_001033410	3	1.30
25.0943	2310002J15Rik	RIKEN cDNA 2310002J15 gene	NM_026415	0	0.00
25.0984	Rnf208	ring finger protein 208	NM_176834	2	1.50
25.1003	Ndor1	NADPH dependent diflavin oxidoreductase 1	NM_001082476	7	0.66
25.1110	C730025P13Rik	RIKEN cDNA C730025P13 gene	NM_177344	0	0.00
25.1181	C430004E15Rik	RIKEN cDNA C430004E15 gene	NM_175286	0	0.00
25.1266	Ssna1	Sjogren's syndrome nuclear autoantigen 1	NM_023464	0	0.00
25.1280	Anapc2	anaphase promoting complex subunit 2	NM_175300	1	0.07
25.1437	4930571C24Rik	RIKEN cDNA 4930571C24 gene	AK019803	1	0.96
25.1455	Lrrc26	leucine rich repeat containing 26	NM_146117	0	0.00
25.1468	E130003G02Rik	RIKEN cDNA E130003G02 gene	AK076389	0	0.00
25.1478	Grin1	glutamate receptor, ionotropic, NMDA1 (zeta 1)	NM_008169	6	0.22
25.1558	2900034K13Rik	RIKEN cDNA 2900034K13 gene	AK019326	0	0.00
25.1883	Man1b1	mannosidase, alpha, class 1B, member 1	NM_001029983	70	3.60
25.2078	Dpp7	dipeptidylpeptidase 7	NM_031843	6	1.48
25.2170	Uap1l1	UDP-N-acetylglucosamine pyrophosphorylase 1-like 1	NM_001033293	6	1.45
25.2278	2010317E24Rik	RIKEN cDNA 2010317E24 gene	NM_001081085	22	3.73
25.2514	Entpd2	ectonucleoside triphosphate diphosphohydrolase 2	NM_009849	12	2.20
25.2586	Npdc1	neural proliferation, differentiation and control gene 1	NM_008721	6	0.94
25.2788	Fut7	fucosyltransferase 7	NM_013524	7	2.27
25.2842	Abca2	ATP-binding cassette, sub-family A (ABC1), member 2	NM_007379	111	5.59
25.3124	Clic3	chloride intracellular channel 3	NM_027085	4	2.07
25.3150	BC029214	cDNA sequence BC029214	NM_153557	9	5.60
25.3222	Ptgds	prostaglandin D2 synthase (brain)	NM_008963	8	2.63
25.3464	Lcn12	lipocalin 12	NM_029958	0	0.00
25.3542	C8g	complement component 8, gamma subunit	NM_027062	0	0.00
25.3563	Fbxw5	F-box and WD-40 domain protein 5	NM_013908	3	0.64
25.3735	Traf2	Tnf receptor-associated factor 2	NM_009422	48	1.66

Table B-1. (Continued).

Position on Chr 2 (Mb)	Gene symbol	Gene description	NM ID	SNPs	SNP Density
25.4134	Edf1	endothelial differentiation-related factor 1	NM_021519	7	1.67
25.4186	Mamdc4	MAM domain containing 4	NM_001081199	21	2.56
25.4290	Phpt1	phosphohistidine phosphatase 1	NM_029293	0	0.00
25.4307	4921530D09Rik	RIKEN cDNA 4921530D09 gene	A1429795	0	0.00
25.4309	Gm996	gene model 996, (NCBI)	NM_001005424	9	1.92
25.4385	B230208H17Rik	RIKEN cDNA B230208H17 gene	NM_001024616	42	1.65
25.4756	Tmem141	transmembrane protein 141	NM_001040130	0	0.00
25.4802	Fcna	ficolin A	NM_007995	2	0.60
25.5086	Lcn8	lipocalin 8	NM_033145	0	0.00
25.5135	Lcn5	lipocalin 5	NM_001042630	2	0.54
25.5323	Lcn6	lipocalin 6	NM_177840	3	0.62
25.5382	Lcn10	lipocalin 10	NM_178036	2	0.60
25.5556	Lcn13	lipocalin 13	NM_153558	0	0.00
25.5612	A230005M16Rik	RIKEN cDNA A230005M16 gene	AK038413	0	0.00
25.5624	Bmyc	brain expressed myelocytomatosis oncogene	NM_023326	0	0.00
25.5925	RP23-225D24.3	novel lipocalin protein	NM_001099301	0	0.00
25.6211	Lcn3	lipocalin 3	NM_010694	0	0.00
25.6325	Lcn11	lipocalin 11	NM_001100455	0	0.00
25.6401	LOC620858	hypothetical protein LOC620858	AK076911	0	0.00
25.6495	Glt6d1	glycosyltransferase 6 domain containing 1	NM_001039095	2	0.09
25.6787	Lcn9	lipocalin 9	NM_029959	4	1.68
25.6985	Sohlh1	spermatogenesis and oogenesis specific basic helix-loop-helix 1	NM_001001714	14	3.29
25.7194	Kcrt1	potassium channel, subfamily T, member 1	NM_175462	46	0.88
25.7580	Camsap1	calmodulin regulated spectrin-associated protein 1	A1642561	0	0.00
25.7789	6230426118Rik	RIKEN cDNA 6230426118 gene	AK018099	1	0.68
25.8392	A230056K03Rik	RIKEN cDNA A230056K03 gene	AK038714	1	1.09
25.8541	Ubac1	ubiquitin associated domain containing 1	NM_133835	89	3.84
25.9111	Btbd14a	BTB (POZ) domain containing 14A	NM_001037098	81	2.20
25.9589	C330006A16Rik	RIKEN cDNA C330006A16 gene	A1551216	0	0.00
25.9941	1810012K08Rik	RIKEN cDNA 1810012K08 gene	AK007459	0	0.00
26.0557	Lhx3	LIM homeobox protein 3	NM_001039653	12	1.89
26.0646	Qsox2	quiescin Q6 sulfhydryl oxidase 2	NM_153559	19	0.67
26.0685	LOC381355	hypothetical LOC381355	XM_923021	0	0.00
26.1011	C030048H21Rik	RIKEN cDNA C030048H21 gene	AK021159	0	0.00
26.1272	4932418E24Rik	RIKEN cDNA 4932418E24 gene	NM_177841	1	0.04
26.1711	Gpsm1	G-protein signalling modulator 1 (AGS3-like, C. elegans)	NM_153410	30	0.92
26.2036	D2Bwg1335e	DNA segment, Chr 2, Brigham & Women's Genetics 1335 expressed	NM_026828	0	0.00
26.2078	Card9	caspace recruitment domain family, member 9	NM_001037747	0	0.00
26.2183	Snapc4	small nuclear RNA activating complex, polypeptide 4	NM_172339	3	0.17
26.2383	Sdccag3	serologically defined colon cancer antigen 3	NM_001085407	4	0.61
26.2397	9430022A06Rik	RIKEN cDNA 9430022A06 gene	AK020431	1	1.05
26.2449	Pmpca	peptidase (mitochondrial processing) alpha	NM_173180	4	0.51
26.2518	Inpp5e	inositol polyphosphate-5-phosphatase E	NM_033134	17	1.31
26.2650	Sec16a	SEC16 homolog A (S. cerevisiae)	NM_153125	29	0.81
26.3015	0610009E02Rik	RIKEN cDNA 0610009E02 gene	AK075572	31	2.31
26.3136	Notch1	Notch gene homolog 1 (Drosophila)	NM_008714	41	0.90
26.4366	Egfl7	EGF-like domain 7	NM_178444	15	1.29
26.4491	Agpat2	1-acylglycerol-3-phosphate O-acyltransferase 2	NM_026212	4	0.38
26.4593	Snhg7	small nucleolar RNA host gene (non-protein coding) 7	A1427062	0	0.00
26.4840	B230317C12Rik	RIKEN cDNA B230317C12 gene	NM_019833	0	0.00
26.4959	5730588L14Rik	RIKEN cDNA 5730588L14 gene	AK030770	1	0.18
26.5232	Lcn4	lipocalin 4	NM_010695	0	0.00
26.6980	Abo	ABO blood group	NM_030718	5	0.22
26.7463	Surf6	surfeit gene 6	NM_009298	0	0.00
26.7608	Med22	mediator complex subunit 22	NM_001033908	0	0.00
26.7663	Rpl7a	ribosomal protein L7a	NM_013721	0	0.00
26.7689	Surf1	surfeit gene 1	NM_013677	2	0.63
26.7719	Surf2	surfeit gene 2	NM_013678	0	0.00
26.7756	Surf4	surfeit gene 4	NM_011512	2	0.14
26.7896	Gm711	gene model 711, (NCBI)	NM_198628	3	0.15
26.8091	Rexo4	REX4, RNA exonuclease 4 homolog (S. cerevisiae)	NM_207234	0	0.00
26.8289	Adamts13	a disintegrin-like and metallopeptidase (reprolysin type) with thrombospondin type 1 motif, 13	NM_001001322	0	0.00
26.8655	5930434B04Rik	RIKEN cDNA 5930434B04 gene	NM_029862	0	0.00
26.8769	Slc2a6	solute carrier family 2 (facilitated glucose transporter), member 6	NM_172659	0	0.00
26.9172	1110002H13Rik	RIKEN cDNA 1110002H13 gene	NM_025376	0	0.00
26.9349	Adamts12	ADAMTS-like 2	NM_029981	0	0.00
26.9675	C630035N08Rik	RIKEN cDNA C630035N08 gene	NM_175427	1	0.03
27.0004	6430548G04	hypothetical protein 6430548G04	AK032445	0	0.00
27.0210	Dbh	dopamine beta hydroxylase	NM_138942	1	0.06
27.0449	Sardh	sarcosine dehydrogenase	NM_138665	2	0.03
27.1192	Vav2	vav 2 oncogene	NM_009500	1	0.01
27.2981	D2Bwg1423e	DNA segment, Chr 2, Brigham & Women's Genetics 1423 expressed	AK038857	0	0.00

Table B-1. (Continued).

Position on Chr 2 (Mb)	Gene symbol	Gene description	NM ID	SNPs	SNP Density
27.3011	Brd3	bromodomain containing 3	NM_001113573	2	0.07
27.3707	Wdr5	WD repeat domain 5	NM_080848	0	0.00
27.5327	Rxra	retinoid X receptor alpha	NM_011305	0	0.00
27.7384	281043011Rik	RIKEN cDNA 281043011 gene	AK019269	0	0.00
27.7419	Col5a1	collagen, type V, alpha 1	NM_015734	7	0.05
27.9320	Fcnb	ficolin B	NM_010190	0	0.00
27.9510	F730016J06Rik	RIKEN cDNA F730016J06 gene	AK036396	1	0.03
28.0486	Olfm1	olfactomedin 1	NM_001038612	0	0.00
28.3035	Gm347	gene model 347, (NCBI)	NM_001005420	0	0.00
28.3175	1700007K13Rik	RIKEN cDNA 1700007K13 gene	NM_027040	0	0.00
28.3236	Mrps2	mitochondrial ribosomal protein S2	NM_080452	0	0.00
28.3533	Gbg1	globoside alpha-1, 3-N-acetylgalactosaminyltransferase 1	NM_139197	0	0.00
28.3687	Ralgds	ral guanine nucleotide dissociation stimulator	NM_009058	3	0.08
28.4113	Cel	carboxyl ester lipase	NM_009885	0	0.00
28.4218	Gtf3c5	general transcription factor IIIC, polypeptide 5	NM_148928	1	0.06
28.4650	Gfi1b	growth factor independent 1B	NM_008114	0	0.00
28.4968	Tsc1	tuberous sclerosis 1	NM_022887	0	0.00
28.5476	1700026L06Rik	RIKEN cDNA 1700026L06 gene	NM_027283	0	0.00
28.5557	1190002A17Rik	RIKEN cDNA 1190002A17 gene	NM_001033874	1	0.01
28.6811	Gtf3c4	general transcription factor IIIC, polypeptide 4	NM_172977	0	0.00
28.6963	Ddx31	DEAD/H (Asp-Glu-Ala-Asp/His) box polypeptide 31	NM_001033294	0	0.00
28.7632	Barh1	BarH-like 1 (Drosophila)	NM_019446	0	0.00
28.9074	1700101E01Rik	RIKEN cDNA 1700101E01 gene	NM_001085514	0	0.00
28.9158	Ttf1	transcription termination factor 1	NM_009442	2	0.07
28.9805	Setx	senataxin	NM_198033	0	0.00
29.0503	Ntng2	netrin G2	NM_133500	1	0.02
29.1064	6530402F18Rik	RIKEN cDNA 6530402F18 gene	AK018312	0	0.00
29.2024	Med27	mediator complex subunit 27	NM_026896	2	0.01
29.4752	Rapgef1	Rap guanine nucleotide exchange factor (GEF) 1	NM_001039086	3	0.02
29.6316	Trub2	TruB pseudouridine (psi) synthase homolog 2 (E. coli)	NM_145520	0	0.00
29.6438	Coq4	coenzyme Q4 homolog (yeast)	NM_178693	1	0.11
29.6582	Slc27a4	solute carrier family 27 (fatty acid transporter), member 4	NM_011989	0	0.00
29.6829	Urm1	ubiquitin related modifier 1 homolog (S. cerevisiae)	NM_026615	0	0.00
29.7242	2600006K01Rik	RIKEN cDNA 2600006K01 gene	AK011165	0	0.00
29.7250	Cercam	cerebral endothelial cell adhesion molecule	NM_207298	1	0.07
29.7452	Odf2	outer dense fiber of sperm tails 2	NM_001113213	0	0.00
29.7909	Gle1	GLE1 RNA export mediator (yeast)	NM_028923	0	0.00
29.8211	Spna2	spectrin alpha 2	NM_001076554	6	0.09
29.8871	Wdr34	WD repeat domain 34	NM_001008498	0	0.00
29.9045	2410198J08Rik	RIKEN cDNA 2410198J08 gene	AK010838	0	0.00
29.9176	Set	SET translocation	NM_023871	0	0.00
29.9343	Pkn3	protein kinase N3	NM_153805	0	0.00
29.9465	Zdhc12	zinc finger, DHHC domain containing 12	NM_001037762	1	0.37
29.9528	Zer1	zer-1 homolog (C. elegans)	NM_178694	1	0.04
29.9894	Tbc1d13	TBC1 domain family, member 13	NM_146252	2	0.11
30.0270	Endog	endonuclease G	NM_007931	0	0.00
30.0290	D2Wsu81e	DNA segment, Chr 2, Wayne State University 81, expressed	NM_172660	0	0.00
30.0407	Ccb1	cysteine conjugate-beta lyase 1	NM_172404	0	0.00
30.0927	1700084E18Rik	RIKEN cDNA 1700084E18 gene	AK006990	0	0.00
30.0933	Lrrc8a	leucine rich repeat containing 8A	NM_177725	0	0.00
30.1221	Phyhd1	phytanoyl-CoA dioxygenase domain containing 1	NM_172267	0	0.00
30.1397	Dolk	dolichol kinase	NM_177648	0	0.00
30.1420	Nup188	nucleoporin 188	NM_198304	1	0.02
30.2003	Sh3glb2	SH3-domain GRB2-like endophilin B2	NM_139302	0	0.00
30.2199	5730472N09Rik	RIKEN cDNA 5730472N09 gene	NM_175392	5	0.24
30.2479	Dolpp1	dolichyl pyrophosphate phosphatase 1	NM_020329	11	1.36
30.2560	Crat	carmitine acetyltransferase	NM_007760	91	5.96
30.2716	Ppp2r4	protein phosphatase 2A, regulatory subunit B (PR 53)	NM_138748	16	0.50
30.3282	Ier5l	immediate early response 5-like	NM_030244	0	0.00
30.4506	Cstad	CSA-conditional, T cell activation-dependent protein	NM_030137	2	0.14
30.4852	9330198N18Rik	RIKEN cDNA 9330198N18 gene	AK020395	14	0.24
30.6511	1700001O22Rik	RIKEN cDNA 1700001O22 gene	NM_198000	0	0.00
30.6593	4930527E20Rik	RIKEN cDNA 4930527E20 gene	AK019703	0	0.00
30.6635	2610205E22Rik	RIKEN cDNA 2610205E22 gene	NM_170592	1	0.07
30.6786	Asb6	ankyrin repeat and SOCS box-containing protein 6	NM_133346	0	0.00
30.7009	Prrx2	paired related homeobox 2	NM_009116	15	0.42
30.7450	Ptges	prostaglandin E synthase	NM_022415	1	0.07
30.8085	Tor1b	torsin family 1, member B	NM_133673	1	0.17
30.8161	Tor1a	torsin family 1, member A (torsin A)	NM_144884	1	0.14
30.8284	BC005624	cDNA sequence BC005624	NM_144885	6	0.66
30.8294	Prdm12	PR domain containing 12	XM_355325	0	0.00
30.8516	Usp20	ubiquitin specific peptidase 20	NM_028846	6	0.22

Table B-1. (Continued).

Position on Chr 2 (Mb)	Gene symbol	Gene description	NM ID	SNPs	SNP Density
30.8817	Fnbp1	formin binding protein 1	NM_001038700	81	0.70
31.0066	D330023K18Rik	RIKEN cDNA D330023K18 gene	AK043516	0	0.00
31.0079	Gpr107	G protein-coupled receptor 107	NM_178760	124	1.93
31.0079	9930033D15Rik	RIKEN cDNA 9930033D15 gene	AK036987	12	3.69
31.1014	Freq	frequenin homolog (Drosophila)	NM_019681	42	0.85
31.1699	Hmcn2	hemiceptin 2	NM_177649	369	2.53
31.3258	Ass1	argininosuccinate synthetase 1	NM_007494	6	0.12
31.4282	Fubp3	far upstream element (FUSE) binding protein 3	NM_001033389	3	0.07
31.5263	Exosc2	exosome component 2	NM_144886	0	0.00
31.5441	Abl1	v-abl Abelson murine leukemia oncogene 1	NM_001112703	15	0.13
31.6617	Qrfp	pyroglutamylated RFamide peptide	NM_183424	0	0.00
31.6688	Fibcd1	fibrinogen C domain containing 1	NM_178887	11	0.34
31.7428	Lamc3	laminin gamma 3	NM_011836	10	0.17
31.8041	1110064A23Rik	RIKEN cDNA 1110064A23 gene	AK004365	0	0.00
31.8058	2810003C17Rik	RIKEN cDNA 2810003C17 gene	NM_145144	0	0.00
31.8300	Nup214	nucleoporin 214	NM_172268	3	0.04
31.9224	A130092J06Rik	RIKEN cDNA A130092J06 gene	NM_175511	2	0.12
31.9379	1700020L05Rik	RIKEN cDNA 1700020L05 gene	AK006171	0	0.00
31.9512	Ppapdc3	phosphatidic acid phosphatase lype 2 domain containing 3	NM_145521	2	0.13
32.0067	5830434P21Rik	RIKEN cDNA 5830434P21 gene	NM_172661	7	0.08
32.0828	E030004H24Rik	RIKEN cDNA E030004H24 gene	AK086846	2	1.67
32.0922	Pomt1	protein-O-mannosyltransferase 1	NM_145145	2	0.11
32.1105	Uck1	uridine-cytidine kinase 1	NM_011675	0	0.00
32.1343	2900010J23Rik	RIKEN cDNA 2900010J23 gene	NM_175190	3	0.33
32.1438	Golga2	golgi autoantigen, golgin subfamily a, 2	NM_001080968	1	0.05
32.1640	Dnm1	dynamins 1	NM_010065	5	0.11
32.2188	Ciz1	CDKN1A interacting zinc finger protein 1	NM_028412	2	0.13
32.2346	1110008P14Rik	RIKEN cDNA 1110008P14 gene	NM_198001	0	0.00
32.2402	Lcn2	lipocalin 2	NM_008491	0	0.00
32.2518	Ptges2	prostaglandin E synthase 2	NM_133783	0	0.00
32.2700	Slc25a25	solute carrier family 25 (mitochondrial carrier, phosphate carrier), member 25	NM_146118	2	0.05
32.3060	4933440H19Rik	RIKEN cDNA 4933440H19 gene	NM_194335	0	0.00
32.3909	C230093N12Rik	RIKEN cDNA C230093N12 gene	NM_153560	13	0.38
32.4264	Dpm2	dolichol-phosphate (beta-D) mannosyltransferase 2	NM_010073	3	1.11
32.4297	9430097D07Rik	RIKEN cDNA 9430097D07 gene	AK035182	0	0.00
32.4313	Pip5k1l	phosphatidylinositol-4-phosphate 5-kinase-like 1	NM_198191	33	4.15
32.4430	ST6galnac4	ST6 (alpha-N-acetyl-neuraminy-2,3-beta-galactosyl-1,3)-N-acetylgalactosaminide alpha-2,6-sialyltransferase 4	NM_011373	15	1.16
32.4552	ST6galnac6	ST6 (alpha-N-acetyl-neuraminy-2,3-beta-galactosyl-1,3)-N-acetylgalactosaminide alpha-2,6-sialyltransferase 6	NM_001025310	8	0.38
32.4850	Ak1	adenylate kinase 1	NM_021515	0	0.00
32.5021	Eng	endoglin	NM_007932	2	0.06
32.5381	Fpgs	folypolyglutamyl synthetase	NM_010236	0	0.00
32.5549	6330409D20Rik	RIKEN cDNA 6330409D20 gene	AA517851	0	0.00
32.5613	Cdk9	cyclin-dependent kinase 9 (CDC2-related kinase)	NM_130860	0	0.00
32.5766	Sh2d3c	SH2 domain containing 3C	NM_013781	0	0.00
32.6128	Tor2a	torsins family 2, member A	NM_152800	2	0.40
32.6177	Ttc16	tetratricopeptide repeat domain 16	NM_177384	3	0.23
32.6313	Pth1	peptidyl-tRNA hydrolase 1 homolog (S. cerevisiae)	NM_178595	1	0.56
32.6329	1700019L03Rik	RIKEN cDNA 1700019L03 gene	NM_025619	5	0.72
32.6431	Stxbp1	syntaxin binding protein 1	NM_00113569	8	0.13
32.7317	9130404D14Rik	RIKEN cDNA 9130404D14 gene	NM_146119	11	0.22
32.7411	D130056L21Rik	RIKEN cDNA D130056L21 gene	AK051447	0	0.00
32.7807	Lrsam1	leucine rich repeat and sterile alpha motif containing 1	NM_199302	9	0.25
32.7853	Snora65	small nucleolar RNA, HIACA box 65	NR_002898	0	0.00
32.8172	Rpl12	ribosomal protein L12	NM_009076	0	0.00
32.8285	Slc2a8	solute carrier family 2, (facilitated glucose transporter), member 8	NM_019488	0	0.00
32.8419	Garnl3	GTPase activating RANGAP domain-like 3	NM_178888	12	0.12
32.9925	Ralgps1	Ral GEF with PH domain and SH3 binding motif 1	NM_175211	70	0.30
33.0715	Angptl2	angiopoietin-like 2	NM_011923	14	0.44
33.2616	Zbtb34	zinc finger and BTB domain containing 34	NM_001085507	11	0.44
33.3058	Zbtb43	zinc finger and BTB domain containing 43	NM_001025594	43	2.36
33.4202	Lmx1b	LIM homeobox transcription factor 1 beta	NM_010725	64	0.84
33.4969	C130021I20Rik	Riken cDNA C130021I20 gene	AK081497	27	5.38
33.5719	9430024E24Rik	RIKEN cDNA 9430024E24 gene	AK020435	0	0.00
33.5855	2610528K11Rik	RIKEN cDNA 2610528K11 gene	NM_175184	266	1.68
33.6355	A630071L07Rik	RIKEN cDNA A630071L07 gene	AA874387	0	0.00
33.8738	C230014O12Rik	RIKEN cDNA C230014O12 gene	AK048710	151	1.69
34.0274	Pbx3	pre B-cell leukemia transcription factor 3	NM_016768	17	0.08
34.1433	C79798	expressed sequence C79798	AK138624	1	0.06
34.1940	B930068K11Rik	RIKEN cDNA B930068K11 gene	AK081020	0	0.00
34.2713	5830434F19Rik	RIKEN cDNA 5830434F19 gene	AK017969	0	0.00
34.2875	Mapkap1	mitogen-activated protein kinase associated protein 1	NM_177345	386	2.00
34.3581	4930414H07Rik	RIKEN cDNA 4930414H07 gene	AK015137	1	1.23
34.4640	1700007J24Rik	RIKEN cDNA 1700007J24 gene	AK005727	0	0.00
34.5325	Gapvd1	GTPase activating protein and VPS9 domains 1	NM_025709	3	0.04
34.6276	Hspa5	heat shock protein 5	NM_022310	1	0.23
34.6342	Rabepk	Rab9 effector protein with kelch motifs	NM_145522	4	0.19
34.6578	4930550L05Rik	RIKEN cDNA 4930550L05 gene	AK019757	2	0.21
34.6607	Fbxw2	F-box and WD-40 domain protein 2	NM_013890	3	0.14
34.7076	Psm5	proteasome (prosome, macropain) 26S subunit, non-ATPase, 5	NM_080554	1	0.05
34.7266	5730407M17Rik	RIKEN cDNA 5730407M17 gene	AK017517	0	0.00
34.7300	D730039F16Rik	RIKEN cDNA D730039F16 gene	NM_030021	0	0.00
34.7493	Phf19	PHD finger protein 19	NM_028716	16	0.79
34.7988	Traf1	Tnf receptor-associated factor 1	NM_009421	24	1.30
34.8389	Hc	hemolytic complement	NM_010406	62	0.79
34.9396	AI182371	expressed sequence AI182371	NM_178885	1	0.06

Table B-2. Genes and their SNPs in mapped locus on Chr 2 between 124-150 Mb.

Position on Chr 2 (Mb)	Gene symbol	Gene description	NM ID	SNPs	SNP Density
124.9783	Slc12a1	solute carrier family 12, member 1	NM_001079690	224	2.89
125.0730	Dut	deoxyuridine triphosphatase	NM_023595	79	6.69
125.1003	A530010F05Rik	RIKEN cDNA A530010F05 gene	AK079928	0	0.00
125.1263	Fbn1	fibrillin 1	NM_007993	706	3.43
125.3888	Cep152	centrosomal protein 152	NM_001081091	232	3.74
125.4532	Shc4	SHC (Src homology 2 domain containing) family, member 4	NM_199022	353	3.65
125.4988	Eid1	EP300 interacting inhibitor of differentiation 1	NM_025613	13	5.11
125.5627	3110001I20Rik	RIKEN cDNA 3110001I20 gene	NM_177608	138	3.01
125.6560	Cops2	COP9 (constitutive photomorphogenic) homolog, subunit 2 (<i>Arabidopsis thaliana</i>)	NM_009939	172	5.99
125.6850	Galk2	galactokinase 2	NM_175154	359	2.87
125.8094	4930525F21Rik	RIKEN cDNA 4930525F21 gene	NM_029455	373	2.29
125.8605	Fgf7	fibroblast growth factor 7	NM_008008	139	2.49
125.9779	Dtwd1	DTW domain containing 1	NM_026981	76	5.79
126.1467	Atp8b4	ATPase, class I, type 8B, member 4	NM_001080944	593	3.48
126.3617	A630026N12Rik	RIKEN cDNA A630026N12 gene	AI021452	0	0.00
126.3788	Slc27a2	solute carrier family 27 (fatty acid transporter), member 2	NM_011978	116	3.29
126.4194	Hdc	histidine decarboxylase	NM_008230	190	7.60
126.4546	Gabpb1	GA repeat binding protein, beta 1	NM_010249	136	2.92
126.5331	Usp8	ubiquitin specific peptidase 8	NM_019729	130	2.50
126.5349	Polr2l	polymerase (RNA) II (DNA directed) polypeptide L	AK011021	0	0.00
126.5872	Usp50	ubiquitin specific peptidase 50	NM_029163	57	2.59
126.6173	Trpm7	transient receptor potential cation channel, subfamily M, member 7	NM_021450	209	2.47
126.6692	B930086H10Rik	RIKEN cDNA B930086H10 gene	AK047541	12	7.27
126.7199	2010106G01Rik	RIKEN cDNA 2010106G01 gene	NM_023220	132	3.38
126.8344	Ap4e1	adaptor-related protein complex AP-4, epsilon 1	NM_175550	159	2.60
126.8964	Blvr4	biliverdin reductase A	NM_026678	106	4.01
126.9296	Ncaph	non-SMC condensin I complex, subunit H	NM_144818	151	5.02
126.9663	1700041B20Rik	RIKEN cDNA 1700041B20 gene	AK006667	8	3.88
127.0303	1810024B03Rik	RIKEN cDNA 1810024B03 gene	AK019023	7	1.92
127.0341	Ascc3l1	activating signal cointegrator 1 complex subunit 3-like 1	NM_177214	158	4.93
127.0667	Ciao1	cytosolic iron-sulfur protein assembly 1 homolog (<i>S. cerevisiae</i>)	NM_025296	16	2.33
127.0737	Tmem127	transmembrane protein 127	NM_175145	35	2.74
127.0960	Stard7	START domain containing 7	NM_139308	100	3.48
127.1619	Dusp2	dual specificity phosphatase 2	NM_010090	9	4.06
127.1644	AstI	astacin-like metalloendopeptidase (M12 family)	NM_172539	73	3.84
127.1890	Adra2b	adrenergic receptor, alpha 2b	NM_009633	15	3.81
127.2509	A530057A03Rik	RIKEN cDNA A530057A03 gene	NM_001081089	36	3.30
127.2620	Fahd2a	fumarylacetoacetate hydrolase domain containing 2A	NM_029629	41	4.95
127.2822	Kcnp3	Kv channel interacting protein 3, calsenuin	NM_001111331	158	6.08
127.3527	Prom2	prominin 2	NM_138750	29	2.00
127.4013	Zfp661	zinc finger protein 661	NM_001111029	12	1.31
127.4132	Mrps5	mitochondrial ribosomal protein S5	NM_029963	40	2.42
127.4590	Mal	myelin and lymphocyte protein, T-cell differentiation protein	NM_010762	87	3.71
127.4837	1500011K16Rik	RIKEN cDNA 1500011K16 gene	AA738625	0	0.00
127.5301	Mall	mal, T-cell differentiation protein-like	NM_145532	91	3.57
127.5665	Nphp1	nephronophthisis 1 (juvenile) homolog (human)	NM_016902	157	3.26
127.6259	Bub1	budding uninhibited by benzimidazoles 1 homolog (<i>S. cerevisiae</i>)	NM_001113179	119	3.76
127.6804	Acox1	acyl-Coenzyme A oxidase-like	NM_028765	1228	4.56
127.7460	0610042E11Rik	RIKEN cDNA 0610042E11 gene	AK002906	11	4.31
127.9518	Bcl2l11	BCL2-like 11 (apoptosis facilitator)	NM_009754	193	5.29
128.1244	LOC100043424	hypothetical protein LOC100043424	AK144927	416	3.18
128.2881	Gm355	gene model 355, (NCBI)	XM_001003757	0	0.00
128.4358	Anapc1	anaphase promoting complex subunit 1	NM_008569	305	3.95
128.5247	Mertk	c-mer proto-oncogene tyrosine kinase	NM_008587	543	5.26
128.6440	Tmem87b	transmembrane protein 87B	NM_028248	83	2.31
128.6897	Fbln7	fibulin 7	NM_024237	114	3.44
128.7165	LOC215539	similar to CG3299-PA	XM_917820	0	0.00
128.7520	Zc3h8	zinc finger CCCH type containing 8	NM_020594	74	4.17
128.7814	4933427J07Rik	RIKEN cDNA 4933427J07 gene	AK016956	7	3.19
128.7931	Zc3h6	zinc finger CCCH type containing 6	NM_178404	197	3.85
128.8643	4930402C16Rik	RIKEN cDNA 4930402C16 gene	AK015044	0	0.00
128.8917	Tli	tubulin tyrosine ligase	NM_027192	90	3.24
128.9268	Rpo1-2	RNA polymerase 1-2	NM_009086	69	2.70
128.9556	Chchd5	coiled-coil-helix-coiled-coil-helix domain containing 5	NM_025395	20	4.67
129.0245	Slc20a1	solute carrier family 20, member 1	NM_015747	0	0.00
129.0317	9830144P21Rik	RIKEN cDNA 9830144P21 gene	AK036644	0	0.00
129.0447	A730036I17Rik	RIKEN cDNA A730036I17 gene	AK042900	0	0.00
129.0946	Ckap2l	cytoskeleton associated protein 2-like	NM_181589	0	0.00
129.1253	Il1a	interleukin 1 alpha	NM_010554	1	0.10
129.1903	Il1b	interleukin 1 beta	NM_008361	0	0.00
129.2841	F830045P16Rik	RIKEN cDNA F830045P16 gene	NM_177653	3	0.04
129.4193	Sirpa	signal-regulatory protein alpha	NM_007547	1	0.03
129.4221	2900076A13Rik	RIKEN cDNA 2900076A13 gene	AK013795	0	0.00
129.5137	Pdyn	prodynorphin	NM_018863	1	0.54

Table B-2. (Continued).

Position on Chr 2 (Mb)	Gene symbol	Gene description	NM ID	SNPs	SNP Density
129.6253	4932416H05Rik	RIKEN cDNA 4932416H05 gene	AB041802	0	0.00
129.6263	Stk35	serine/threonine kinase 35	NM_001038635	2	0.06
129.8381	Tgm3	transglutaminase 3, E polypeptide	NM_009374	1	0.03
129.9261	AU015228	expressed sequence AU015228	NM_001033197	0	0.00
129.9490	Tgm6	transglutaminase 6	NM_177726	0	0.00
129.9974	Snrpb	small nuclear ribonucleoprotein B	NM_009225	0	0.00
130.0209	Tmc2	transmembrane channel-like gene family 2	NM_138655	4	0.06
130.0995	2810036E18Rik	RIKEN cDNA 2810036E18 gene	AK012862	0	0.00
130.1001	Nol5a	nucleolar protein 5A	NM_024193	0	0.00
130.1050	ldh3b	isocitrate dehydrogenase 3 (NAD+) beta	NM_130884	0	0.00
130.1105	A930025D01Rik	RIKEN cDNA A930025D01 gene	NM_001114541	0	0.00
130.1217	Ebf4	early B-cell factor 4	NM_001110513	2	0.03
130.2138	C130063K03Rik	RIKEN cDNA C130063K03 gene	AK048471	1	0.60
130.2165	Cpxm1	carboxypeptidase X 1 (M14 family)	NM_019696	0	0.00
130.2246	C230006B20	hypothetical LOC403344	AK082093	0	0.00
130.2312	1700020A23Rik	RIKEN cDNA 1700020A23 gene	AK006141	0	0.00
130.2323	4933425O20Rik	RIKEN cDNA 4933425O20 gene	NM_025753	0	0.00
130.2501	Vps16	vacuolar protein sorting 16 (yeast)	NM_030559	0	0.00
130.2763	Ptpra	protein tyrosine phosphatase, receptor type, A	NM_008980	3	0.03
130.2812	1700012O15Rik	RIKEN cDNA 1700012O15 gene	A1449821	0	0.00
130.3497	9530056E24Rik	RIKEN cDNA 9530056E24 gene	AK035489	0	0.00
130.3695	4930473A02Rik	RIKEN cDNA 4930473A02 gene	AK015562	0	0.00
130.3895	Mrps26	mitochondrial ribosomal protein S26	NM_207207	0	0.00
130.4019	Oxt	oxytocin	NM_011025	0	0.00
130.4064	Avp	arginine vasopressin	NM_009732	0	0.00
130.4157	Ubox5	U box domain containing 5	NM_080562	2	0.05
130.4396	Fastkd5	FAST kinase domains 5	NM_198176	0	0.00
130.4586	RP23-100C5.8	ProSAPiP1 protein	NM_197945	0	0.00
130.4798	2600009E05Rik	RIKEN cDNA 2600009E05 gene	NM_029832	0	0.00
130.4936	Itpa	inosine triphosphatase (nucleoside triphosphate pyrophosphatase)	NM_025922	1	0.07
130.5098	Slc4a11	solute carrier family 4, sodium bicarbonate transporter-like, member 11	NM_001081162	0	0.00
130.5336	4930402H24Rik	RIKEN cDNA 4930402H24 gene	NM_029432	5	0.04
130.6659	C030014O09Rik	RIKEN cDNA C030014O09 gene	AK021082	0	0.00
130.6952	6330526H18Rik	RIKEN cDNA 6330526H18 gene	AK018221	0	0.00
130.7054	A730017L22Rik	RIKEN cDNA A730017L22 gene	AK042707	0	0.00
130.7322	Atrn	atractin	NM_009730	361	2.92
130.8659	Gfra4	glial cell line derived neurotrophic factor family receptor alpha 4	NM_020014	15	5.98
130.8768	Adam33	a disintegrin and metalloproteinase domain 33	NM_033615	45	3.54
130.8950	Siglec1	sialic acid binding Ig-like lectin 1, sialoadhesin	NM_011426	63	3.59
130.9531	Hspa12b	heat shock protein 12B	NM_028306	40	2.15
130.9721	1700037H04Rik	RIKEN cDNA 1700037H04 gene	NM_026091	52	3.80
130.9960	Spef1	sperm flagellar 1	NM_027641	15	3.30
131.0030	Cenpb	centromere protein B	NM_007682	14	5.14
131.0127	Cdc25b	cell division cycle 25 homolog B (S. pombe)	NM_001111075	63	5.46
131.0362	2310035K24Rik	RIKEN cDNA 2310035K24 gene	NM_027129	2	0.65
131.0599	D430028G21Rik	RIKEN cDNA D430028G21 gene	NM_144888	30	2.16
131.0882	Pank2	pantothenate kinase 2 (Hallervorden-Spatz syndrome)	NM_153501	125	3.41
131.1242	Rnf24	ring finger protein 24	NM_178607	141	2.59
131.3177	Smox	spermine oxidase	NM_145533	116	3.49
131.3711	Adra1d	adrenergic receptor, alpha 1d	NM_013460	34	2.01
131.4736	4930425F17Rik	RIKEN cDNA 4930425F17 gene	AK019583	0	0.00
131.5470	Erv3	endogenous retroviral sequence 3	AA087213	0	0.00
131.6457	5330413P13Rik	RIKEN cDNA 5330413P13 gene	AK030453	72	2.60
131.7357	Prnp	prion protein	NM_011170	2	0.07
131.7766	Prnd	prion protein dublet	NM_023043	0	0.00
131.8186	Rassf2	Ras association (RalGDS/AF-6) domain family 2	NM_175445	3	0.08
131.8782	Slc23a2	solute carrier family 23 (nucleobase transporters), member 2	NM_018824	12	0.13
131.9064	EG329521	predicted gene, EG329521	XM_001480655	0	0.00
132.0652	5730494N06Rik	RIKEN cDNA 5730494N06 gene	NM_027478	0	0.00
132.0750	Pcna	proliferating cell nuclear antigen	NM_011045	0	0.00
132.0890	Cds2	CDP-diacylglycerol synthase (phosphatidate cytidylyltransferase) 2	NM_138651	2	0.04
132.1969	Prokr2	prokineticin receptor 2	NM_144944	0	0.00
132.2505	4921508D12Rik	RIKEN cDNA 4921508D12 gene	AK014842	3	0.11
132.3154	1700058J15Rik	RIKEN cDNA 1700058J15 gene	AK006832	0	0.00
132.3165	1700026D11Rik	RIKEN cDNA 1700026D11 gene	AK006376	2	0.06
132.3548	Prei4	preimplantation protein 4	NM_001042671	1	0.02
132.3847	E030016H06Rik	RIKEN cDNA E030016H06 gene	AK086966	0	0.00
132.4239	AU019990	expressed sequence AU019990	AK135901	1	0.02
132.5160	1110034G24Rik	RIKEN cDNA 1110034G24 gene	AK004090	2	0.03
132.6070	Chgb	chromogranin B	NM_007694	2	0.14
132.6300	Trmt6	tRNA methyltransferase 6 homolog (S. cerevisiae)	NM_175113	1	0.08
132.6421	Mcm8	minichromosome maintenance deficient 8 (S. cerevisiae)	NM_025676	0	0.00
132.6735	Cris1	cardiolipin synthase 1	NM_001024385	6	0.32
132.6943	B430119L13Rik	RIKEN cDNA B430119L13 gene	NM_177303	0	0.00

Table B-2. (Continued).

Position on Chr 2 (Mb)	Gene symbol	Gene description	NM ID	SNPs	SNP Density
132.7299	5830467P10Rik	RIKEN cDNA 5830467P10 gene	NM_198029	3	0.07
132.7770	2900022B07Rik	RIKEN cDNA 2900022B07 gene	AK013567	0	0.00
133.2578	A430048G15Rik	RIKEN cDNA A430048G15 gene	AK040035	0	0.00
133.3789	Bmp2	bone morphogenetic protein 2	NM_007553	1	0.10
134.3231	Hao1	hydroxyacid oxidase 1, liver	NM_010403	5	0.09
134.4202	Txndc13	thioredoxin domain containing 13	NM_029148	18	0.36
134.6119	Plcb1	phospholipase C, beta 1	NM_019677	1440	2.09
134.9953	4930545L23Rik	RIKEN cDNA 4930545L23 gene	AK019742	81	1.76
135.4063	9630028H03Rik	RIKEN cDNA 9630028H03 gene	AK036032	0	0.00
135.5676	Plcb4	phospholipase C, beta 4	NM_013829	106	0.39
135.8837	6330527O06Rik	RIKEN cDNA 6330527O06 gene	NM_029530	1	0.08
135.9068	Pak7	p21 (CDKN1A)-activated kinase 7	NM_172858	105	0.34
135.9460	2900018K06Rik	RIKEN cDNA 2900018K06 gene	AK013551	0	0.00
136.3276	BC034902	cDNA sequence BC034902	AK040732	1	0.07
136.3581	Ankrd5	ankyrin repeat domain 5	NM_175667	0	0.00
136.5392	Snap25	synaptosomal-associated protein 25	NM_011428	2	0.03
136.6995	Mkks	McKusick-Kaufman syndrome protein	NM_021527	1	0.06
136.7170	2210009G21Rik	RIKEN cDNA 2210009G21 gene	NM_001038641	5	0.03
136.9072	Jag1	jagged 1	NM_013822	1	0.03
138.0823	Btb3	BTB (POZ) domain containing 3	NM_001025431	2	0.06
139.0826	LOC545466	hypothetical LOC545466	AK090153	516	1.23
139.3197	Sptc3	serine palmitoyltransferase, long chain base subunit 3	NM_175467	336	2.34
139.4499	5430433G21Rik	RIKEN cDNA 5430433G21 gene	A1849658	0	0.00
139.4991	3021401L19Rik	RIKEN cDNA 3021401L19 gene	AK013907	3	3.05
139.6592	Tasp1	taspase, threonine aspartase 1	NM_175225	753	3.23
139.7646	LOC269365	similar to ribosomal protein S19	XM_001005575	2	40.00
139.8899	LOC672103	hypothetical LOC672103	AK139706	18	6.80
139.9456	Esf1	ESF1, nucleolar pre-rRNA processing protein, homolog (S. cerevisiae)	NM_001081090	224	4.42
139.9964	2310003L22Rik	RIKEN cDNA 2310003L22 gene	NM_027093	124	3.58
140.0556	Sel12	sel-1 suppressor of lin-12-like 2 (C. elegans)	NM_001033296	549	3.43
140.2212	MacroD2	MACRO domain containing 2	NM_001013802	7771	3.90
140.4839	Flrt3	fibronectin leucine rich transmembrane protein 3	NM_178382	25	1.88
141.0008	2900060K15Rik	RIKEN cDNA 2900060K15 gene	AK013735	18	13.55
142.4441	Kif16b	kinesin family member 16B	NM_001081133	1268	4.48
142.7287	4930511F01Rik	RIKEN cDNA 4930511F01 gene	AK015749	0	0.00
142.8888	Snrpb2	U2 small nuclear ribonucleoprotein B	NM_021335	5	0.56
142.9042	Otor	otoraplin	NM_020595	25	7.79
143.3619	C630020P19Rik	RIKEN cDNA C630020P19 gene	AK035754	37	3.17
143.3719	Pcsk2	proprotein convertase subtilisin/kexin type 2	NM_008792	985	3.65
143.5733	9430032N09Rik	RIKEN cDNA 9430032N09 gene	AK034766	225	5.41
143.6523	Bfsp1	beaded filament structural protein in lens-CP94	NM_009751	162	4.42
143.7411	Dstn	destrin	NM_019771	69	2.46
143.7731	Rrbp1	ribosome binding protein 1	NM_024281	213	3.33
143.8588	Banf2	barrier to autointegration factor 2	NM_001044750	95	2.32
143.9989	EG433481	predicted gene, EG433481	AK144672	101	6.26
144.0690	4930444E06Rik	RIKEN cDNA 4930444E06 gene	AK015377	0	0.00
144.0759	Snx5	sorting nexin 5	NM_024225	57	2.79
144.0968	8430406I07Rik	RIKEN cDNA 8430406I07 gene	NM_028984	33	3.24
144.1309	Ovol2	ovo-like 2 (Drosophila)	NM_026924	47	1.75
144.1575	1700108N11Rik	RIKEN cDNA 1700108N11 gene	AK007144	10	11.76
144.1948	Csrp2bp	cysteine and glycine-rich protein 2 binding protein	NM_181417	120	3.11
144.2851	LOC668917	similar to Zinc finger protein 133	AK137157	32	3.78
144.2909	Zfp133	zinc finger protein 133	AF332089	7	4.51
144.2963	6330439K17Rik	RIKEN cDNA 6330439K17 gene	NM_172859	210	3.69
144.3535	Polr3f	polymerase (RNA) III (DNA directed) polypeptide F	NM_029763	71	5.06
144.3680	Rbbp9	retinoblastoma binding protein 9	NM_015754	29	3.37
144.3820	Sec23b	SEC23B (S. cerevisiae)	NM_019787	154	4.47
144.4198	Gm561	gene model 561, (NCBI)	NM_001033297	5	3.84
144.4257	Dtd1	D-tyrosyl-tRNA deacylase 1 homolog (S. cerevisiae)	NM_025314	535	3.17
144.6494	1700010M22Rik	RIKEN cDNA 1700010M22 gene	NM_025490	1	1.33
145.0683	Slc24a3	solute carrier family 24 (sodium/potassium/calcium exchanger), member 3	NM_053195	1482	3.71
145.5013	BC039771	cDNA sequence BC039771	AK031463	127	3.22
145.5013	LOC433482	hypothetical gene supported by BC028556	BC028556	4	4.37
145.6119	Rin2	Ras and Rab interactor 2	NM_028724	2	0.02
145.7290	Nat5	N-acetyltransferase 5 (ARD1 homolog, S. cerevisiae)	NM_026425	0	0.00
145.7319	AU022840	expressed sequence AU022840	AK079038	0	0.00
145.7432	Crnk1	Crn, crooked neck-like 1 (Drosophila)	NM_025820	0	0.00
145.7605	4930529M08Rik	RIKEN cDNA 4930529M08 gene	NM_175280	1	0.03
146.0477	Insm1	insulinoma-associated 1	NM_016889	0	0.00
146.0670	A230067G21Rik	RIKEN cDNA A230067G21 gene	NM_001033348	8	0.03
146.0850	A930019D19Rik	RIKEN cDNA A930019D19 gene	AK020875	0	0.00
146.0958	B130033B12Rik	RIKEN cDNA B130033B12 gene	AK045105	0	0.00
146.2274	9630019E01Rik	RIKEN cDNA 9630019E01 gene	AK035937	0	0.00
146.3687	4933406D12Rik	RIKEN cDNA 4933406D12 gene	AK016684	1	0.31

Table B-2. (Continued).

Position on Chr 2 (Mb)	Gene symbol	Gene description	NM ID	SNPs	SNP Density
146.6816	Gm114	gene model 114, (NCBI)	NM_001033298	1	0.01
146.8388	Xrn2	5'-3' exonuclease 2	NM_011917	0	0.00
146.9096	Nkx2-4	NK2 transcription factor related, locus 4 (Drosophila)	NM_023504	0	0.00
147.0089	Nkx2-2	NK2 transcription factor related, locus 2 (Drosophila)	NM_001077632	0	0.00
147.0132	6430503K07Rik	RIKEN cDNA 6430503K07 gene	AK020097	0	0.00
147.1873	Al646519	expressed sequence Al646519	AB080658	0	0.00
147.1907	Pax1	paired box gene 1	NM_008780	0	0.00
147.5364	A530006G24Rik	RIKEN cDNA A530006G24 gene	AK079921	65	9.37
147.7705	9030622O22Rik	RIKEN cDNA 9030622O22 gene	AK018565	157	5.00
147.8686	Foxa2	forkhead box A2	NM_010446	4	0.98
148.1062	2310021N16Rik	RIKEN cDNA 2310021N16 gene	AK009452	0	0.00
148.2211	Sstr4	somatostatin receptor 4	NM_009219	5	3.60
148.2302	Thbd	thrombomodulin	NM_009378	13	3.50
148.2546	4833411I10Rik	RIKEN cDNA 4833411I10 gene	AK014679	2	1.28
148.2624	Cd93	CD93 antigen	NM_010740	0	0.00
148.4847	Cst12	cystatin 12	AA208646	0	0.00
148.4984	Nxt1	NTF2-related export protein 1	NM_001110159	10	2.93
148.5069	Gzf1	GDNF-inducible zinc finger protein 1	NM_028986	26	2.20
148.5204	Napb	N-ethylmaleimide sensitive fusion protein attachment protein beta	NM_019632	95	2.52
148.5761	Cst11	cystatin-like 1	NM_177655	2	0.40
148.5944	Cst11	cystatin 11	NM_030059	0	0.00
148.6077	8030411F24Rik	RIKEN cDNA 8030411F24 gene	NM_030135	2	0.51
148.6246	Cst8	cystatin 8 (cystatin-related epididymal spermatogenic)	NM_009978	12	1.78
148.6458	Cst13	cystatin 13	NM_027024	40	3.88
148.6609	Cst9	cystatin 9	NM_009979	7	1.95
148.6724	9230104L09Rik	RIKEN cDNA 9230104L09 gene	NM_029960	1	0.24
148.6907	Gm1330	gene model 1330, (NCBI)	BN000358	0	0.00
148.6975	Cst3	cystatin C	NM_009976	12	3.21
149.0482	LOC241715	similar to chloride channel, nucleotide-sensitive, 1A	XR_034975	2	51.28
149.2310	Cst10	cystatin 10 (chondrocytes)	NM_021405	0	0.00
149.6553	C530025M09Rik	RIKEN cDNA C530025M09 gene	AK035608	0	0.00
149.7086	LOC279056	similar to XPMC2 prevents mitotic catastrophe 2 homolog	XR_034724	0	0.00
149.9321	2010315B03Rik	RIKEN cDNA 2010315B03 gene	AA155546	0	0.00
149.9401	Zfp120	zinc finger protein 120	NM_023266	2	0.09

Table B-3. Genes and their SNPs in mapped locus on Chr X between 50-100Mb.

Position on Chr X (Mb)	Gene symbol	Gene description	NM ID	SNPs	SNP Density
50.1444	6330534C20Rik	RIKEN cDNA 6330534C20 gene	NM_001034059	7	0.85
50.2654	Phf6	PHD finger protein 6	NM_027642	8	0.18
50.3413	Hprt1	hypoxanthine guanine phosphoribosyl transferase 1	NM_013556	8	0.24
50.4063	9430052C07Rik	RIKEN cDNA 9430052C07 gene	AK020467	0	0.00
50.4094	C430049B03Rik	RIKEN cDNA C430049B03 gene	AK012483	0	0.00
50.4232	Plac1	placental specific protein 1	NM_019538	1	0.02
50.5966	4632404H22Rik	RIKEN cDNA 4632404H22 gene	NM_030167	0	0.00
50.6266	4930432H15Rik	RIKEN cDNA 4930432H15 gene	NM_028671	0	0.00
50.6982	Mospd1	motile sperm domain containing 1	NM_027409	0	0.00
50.7881	Etd	embryonic testis differentiation	NM_175147	0	0.00
50.9111	Cxx1c	CAAX box 1 homolog C (human)	NM_028375	0	0.00
50.9457	Cxx1a	CAAX box 1 homolog A (human)	NM_024170	0	0.00
50.9724	Cxx1b	CAAX box 1 homolog B (human)	NM_001018063	0	0.00
50.9897	4933416I08Rik	RIKEN cDNA 4933416I08 gene	AK016833	0	0.00
50.9990	AW822252	expressed sequence AW822252	AK045939	0	0.00
51.0280	4930502E18Rik	RIKEN cDNA 4930502E18 gene	NM_029142	0	0.00
51.0461	1700013H16Rik	RIKEN cDNA 1700013H16 gene	AK005953	0	0.00
51.0759	Zfp363	zinc finger protein 36, C3H type-like 3	NM_001009549	0	0.00
51.0869	Xlr	X-linked lymphocyte-regulated complex	NM_011725	0	0.00
51.2726	LOC100040271	hypothetical protein LOC100040271	AK142406	0	0.00
51.6523	4930527E24Rik	RIKEN cDNA 4930527E24 gene	AK015913	2	0.01
52.6671	1600025M17Rik	RIKEN cDNA 1600025M17 gene	AA693115	0	0.00
52.7250	6330419J24Rik	RIKEN cDNA 6330419J24 gene	AI846914	0	0.00
53.3897	3830403N18Rik	RIKEN cDNA 3830403N18 gene	NM_027510	0	0.00
53.4430	Gm773	gene model 773, (NCBI)	NM_001033423	3	0.13
53.5996	Zfp449	zinc finger protein 449	NM_030139	5	0.26
53.6344	6530403M18Rik	RIKEN cDNA 6530403M18 gene	AK018320	0	0.00
53.7081	Ddx26b	DEAD/H (Asp-Glu-Ala-Asp/His) box polypeptide 26B	NM_172779	13	0.25
53.7971	Gm648	gene model 648, (NCBI)	NM_001033372	0	0.00
53.8099	Gm364	gene model 364, (NCBI)	XM_141763	0	0.00
53.8387	Tmem32	transmembrane protein 32	NM_146234	1	0.08
53.8630	Slc9a6	solute carrier family 9 (sodium/hydrogen exchanger), isoform 6	NM_172780	12	0.23
53.9850	Fhl1	four and a half LIM domains 1	NM_001077361	5	0.08
54.0511	Mtap7d3	MAP7 domain containing 3	NM_177293	3	0.12
54.2166	Gpr112	G protein-coupled receptor 112	NM_001110790	18	1.06
54.2963	Brs3	bombesin-like receptor 3	NM_009766	3	0.53
54.3068	Htatsf1	HIV TAT specific factor 1	NM_028242	2	0.15
54.3413	Vgll1	vestigial like 1 homolog (Drosophila)	NM_133251	8	0.46
54.4653	Cd40lg	CD40 ligand	NM_011616	25	2.10
54.4847	Arhgef6	Rac/Cdc42 guanine nucleotide exchange factor (GEF) 6	NM_152801	70	0.65
54.6316	4732460I02Rik	RIKEN cDNA 4732460I02 gene	AK028836	0	0.00
54.6395	Rbmx	RNA binding motif protein, X chromosome	NM_011252	1	0.15
54.7498	Gpr101	G protein-coupled receptor 101	NM_001033360	0	0.00
55.2152	AY339874	cDNA sequence AY339874	AY339874	0	0.00
55.2838	Zic3	zinc finger protein of the cerebellum 3	NM_009575	1	0.17
56.1646	4930550L24Rik	RIKEN cDNA 4930550L24 gene	NM_023774	0	0.00
56.3153	Fgf13	fibroblast growth factor 13	NM_010200	2	0.03
56.3458	9430082L08Rik	RIKEN cDNA 9430082L08 gene	AK020501	0	0.00
56.8093	Gm715	gene model 715, (NCBI)	XM_205232	0	0.00
56.8377	EG245436	predicted gene, EG245436	XM_891715	0	0.00
57.2526	F9	coagulation factor IX	NM_007979	1	0.03
57.3091	Mcf2	mcf.2 transforming sequence	NM_133197	21	0.23
57.3954	C230004F18Rik	RIKEN cDNA C230004F18 gene	AI851532	0	0.00
57.4540	C030023E24Rik	RIKEN cDNA C030023E24 gene	AI853519	0	0.00
57.4765	Atp11c	ATPase, class VI, type 11C	NM_001001798	2	0.01
57.5527	EG245440	predicted gene, EG245440	XM_001473465	0	0.00
58.1445	Sox3	SRY-box containing gene 3	NM_009237	0	0.00
58.3696	LOC627159	similar to Steroid hormone receptor ERR2 (Estrogen-related receptor, beta)	AK158351	0	0.00
58.9628	Ldoc1	leucine zipper, down-regulated in cancer 1	NM_001018087	0	0.00
59.5403	4933402E13Rik	RIKEN cDNA 4933402E13 gene	AK016614	0	0.00
59.7212	4931400O07Rik	RIKEN cDNA 4931400O07 gene	AK016421	0	0.00
59.7637	1700019B21Rik	RIKEN cDNA 1700019B21 gene	AK006108	0	0.00
61.3096	Ctag2	cancer/testis antigen 2	AI503560	0	0.00
61.4046	EG627470	predicted gene, EG627470	BC048649	0	0.00
61.4267	3830417A13Rik	RIKEN cDNA 3830417A13 gene	NM_027512	2	0.38
61.5226	Slitrk4	SLIT and NTRK-like family, member 4	NM_178740	1	0.13
63.5565	4930447F04Rik	RIKEN cDNA 4930447F04 gene	AK015402	0	0.00
63.9025	Slitrk2	SLIT and NTRK-like family, member 2	NM_198863	0	0.00
63.9515	Gm1140	gene model 1140, (NCBI)	XM_001474142	0	0.00
64.7114	1700036O09Rik	RIKEN cDNA 1700036O09 gene	AK006615	0	0.00
65.1730	4933436I01Rik	RIKEN cDNA 4933436I01 gene	NM_025763	0	0.00
65.9317	Fmr1	fragile X mental retardation syndrome 1 homolog	NM_008031	48	1.22
66.0151	Fmr1nb	fragile X mental retardation 1 neighbor	NM_174993	82	1.93
66.1455	EG627927	predicted gene, EG627927	NM_001098842	0	0.00
66.6135	Af2	AF4/FMR2 family, member 2	NM_008032	166	0.33

Table B-3. (Continued).

Position on Chr X (Mb)	Gene symbol	Gene description	NM ID	SNPs	SNP Density
66.6624	2610007B07Rik	RIKEN cDNA 2610007B07 gene	AK011331	0	0.00
66.8250	Hsfy2-ps	heat shock transcription factor, Y linked 2 pseudogene	XM_290025	0	0.00
67.1824	1700111N16Rik	RIKEN cDNA 1700111N16 gene	AK007172	208	0.97
67.1985	1700020N15Rik	RIKEN cDNA 1700020N15 gene	AK006180	0	0.00
67.5962	lds	iduronate 2-sulfatase	NM_001038990	2	0.09
67.6391	1110012L19Rik	RIKEN cDNA 1110012L19 gene	NM_026787	1	0.29
67.6471	4930567H17Rik	RIKEN cDNA 4930567H17 gene	NM_001033807	0	0.00
67.7132	BC023829	cDNA sequence BC023829	NM_001033328	24	1.41
67.7987	LOC628053	hypothetical LOC628053	NM_001081476	0	0.00
68.2417	Fate1	fetal and adult testis expressed 1	NR_003243	0	0.00
68.3034	Mamld1	mastermind-like domain containing 1	NM_001081354	36	0.34
68.4683	Mtm1	X-linked myotubular myopathy gene 1	NM_019926	102	1.02
68.6179	Mtmr1	myotubularin related protein 1	NM_016985	3	0.06
68.6732	Cd99l2	Cd99 antigen-like 2	NM_138309	1	0.01
68.8092	Hmgb3	high mobility group box 3	NM_008253	0	0.00
68.9169	Gpr50	G-protein-coupled receptor 50	NM_010340	0	0.00
69.0621	2610030H06Rik	RIKEN cDNA 2610030H06 gene	NM_001081356	1	0.13
69.1778	Gm1141	gene model 1141, (NCBI)	AK133067	8	0.95
69.2084	Prrg3	proline rich Gla (G-carboxyglutamic acid) 3 (transmembrane)	NM_001081135	26	2.68
69.2372	Cnga2	cyclic nucleotide gated channel alpha 2	NM_007724	38	2.07
69.4674	Magea4	melanoma antigen, family A, 4	NM_020280	0	0.00
69.5028	Gabre	gamma-aminobutyric acid (GABA-A) receptor, subunit epsilon	NM_017369	8	0.46
69.6272	Magea10	melanoma antigen family A, 10	NM_001085506	0	0.00
69.6792	Gabra3	gamma-aminobutyric acid (GABA-A) receptor, subunit alpha 3	NM_008067	31	0.14
70.0708	Gabrq	gamma-aminobutyric acid (GABA-A) receptor, subunit theta	NM_020488	0	0.00
70.1147	Magea9	melanoma antigen, family A, 9	NM_181855	0	0.00
70.1589	Cetn2	centrin 2	NM_019405	0	0.00
70.1639	Nsdhl	NAD(P) dependent steroid dehydrogenase-like	NM_010941	6	0.15
70.2327	Zfp185	zinc finger protein 185	NM_001109043	3	0.07
70.2793	Pnma5	paraneoplastic antigen family 5	NM_001100461	0	0.00
70.3101	Pnma3	paraneoplastic antigen MA3	NM_153169	0	0.00
70.3197	Xlr4a	X-linked lymphocyte-regulated 4A	NM_001081642	0	0.00
70.3316	Xlr3a	X-linked lymphocyte-regulated 3A	NM_001110784	3	0.28
70.3530	Xlr5a	X-linked lymphocyte-regulated 5A	NM_001045539	11	1.09
70.3826	DXBay18	DNA segment, Chr X, Baylor 18	NM_001025384	19	1.55
70.3942	Xlr5b	X-linked lymphocyte-regulated 5B	NM_001111293	21	2.20
70.4141	Tex28	testis expressed 28	XM_358216	0	0.00
70.4206	4930408F14Rik	RIKEN cDNA 4930408F14 gene	AK015110	0	0.00
70.4375	Xlr3b	X-linked lymphocyte-regulated 3B	NM_001081643	9	0.84
70.4597	Xlr4b	X-linked lymphocyte-regulated 4B	NM_021365	13	1.61
70.4736	F8a	factor 8-associated gene A	NM_007978	4	1.61
70.4794	Xlr4c	X-linked lymphocyte-regulated 4C	NM_183094	10	1.10
70.4999	Xlr3c	X-linked lymphocyte-regulated 3C	NM_011727	8	0.74
70.5252	Snora70	small nucleolar RNA, H/ACA box 70	NR_002899	0	0.00
70.5305	Xlr5c	X-linked lymphocyte-regulated 5C	NM_031493	3	0.56
70.5880	Zfp275	zinc finger protein 275	NM_031494	1	0.06
70.6564	Zfp92	zinc finger protein 92	NM_009566	0	0.00
70.6790	Trex2	three prime repair exonuclease 2	NM_011907	0	0.00
70.6827	Uchl5ip	UCHL5 interacting protein	NM_028633	2	0.09
70.7290	Bgn	biglycan	NM_007542	10	0.81
70.7484	Atp2b3	ATPase, Ca++ transporting, plasma membrane 3	NM_177236	4	0.06
70.8204	EG245472	predicted gene, EG245472	XM_141845	0	0.00
70.8848	Dusp9	dual specificity phosphatase 9	NM_029352	3	0.74
70.9013	Pnck	pregnancy upregulated non-ubiquitously expressed CaM kinase	NM_012040	0	0.00
70.9185	Slc6a8	solute carrier family 6 (neurotransmitter transporter, creatine), member 8	NM_133987	0	0.00
70.9315	Bcap31	B-cell receptor-associated protein 31	NM_012060	10	0.33
70.9619	Abcd1	ATP-binding cassette, sub-family D (ALD), member 1	NM_007435	3	0.14
71.0024	Plxnb3	plexin B3	NM_019587	0	0.00
71.0198	Srpk3	serine/arginine-rich protein specific kinase 3	NM_019684	2	0.44
71.0243	ldh3g	isocitrate dehydrogenase 3 (NAD+), gamma	NM_008323	0	0.00
71.0324	Ssr4	signal sequence receptor, delta	NM_009279	0	0.00
71.0387	Pdzd4	PDZ domain containing 4	NM_001029868	7	0.22
71.0991	L1cam	L1 cell adhesion molecule	NM_008478	12	0.44
71.1374	Avpr2	arginine vasopressin receptor 2	NM_019404	0	0.00
71.1397	Arhgap4	Rho GTPase activating protein 4	NM_138630	1	0.06
71.1622	Ard1	N-acetyltransferase ARD1 homolog (S. cerevisiae)	NM_019870	0	0.00
71.1675	Renbp	renin binding protein	NM_023132	0	0.00
71.1881	Hcfc1	host cell factor C1	NM_008224	6	0.26
71.2593	Irak1	interleukin-1 receptor-associated kinase 1	NM_008363	0	0.00
71.2722	Mecp2	methyl CpG binding protein 2	NM_001081979	1	0.02
71.3728	Opn1mw	opsin 1 (cone pigments), medium-wave-sensitive (color blindness, deutan)	NM_008106	4	0.17
71.4226	Tktl1	transketolase-like 1	NM_031379	1	0.03
71.4688	Flna	filamin, alpha	NM_010227	3	0.13
71.5002	Emd	emerin	NM_007927	0	0.00
71.5162	Rpl10	ribosomal protein 10	NM_052835	0	0.00

Table B-3. (Continued).

Position on Chr X (Mb)	Gene symbol	Gene description	NM ID	SNPs	SNP Density
71.5186	Dnase1l1	deoxyribonuclease 1-like 1	NM_027109	0	0.00
71.5281	Taz	tafazzin	NM_181516	0	0.00
71.5364	B230340J04Rik	RIKEN cDNA B230340J04 gene	AK032075	0	0.00
71.5425	Atp6ap1	ATPase, H+ transporting, lysosomal accessory protein 1	NM_018794	1	0.13
71.5506	Gdi1	guanosine diphosphate (GDP) dissociation inhibitor 1	NM_010273	0	0.00
71.5584	D0HXS9928E	DNA segment, human DXS9928E	NM_138607	0	0.00
71.5744	Plxn3	plexin A3	NM_008883	2	0.13
71.5975	Lage3	L antigen family, member 3	NM_025410	0	0.00
71.6127	Ubl4	ubiquitin-like 4	NM_145405	0	0.00
71.6146	Slc10a3	solute carrier family 10 (sodium/bile acid cotransporter family), member 3	NM_145406	0	0.00
71.6301	1810037C20Rik	RIKEN cDNA 1810037C20 gene	NM_025473	1	0.12
71.6548	G6pdx	glucose-6-phosphate dehydrogenase X-linked	NM_008062	1	0.05
71.6700	Ikbkg	inhibitor of kappaB kinase gamma	NM_010547	1	0.04
71.7256	EG628456	predicted gene, EG628456	NM_001099305	0	0.00
71.8397	Olfrl325	olfactory receptor 1325	NM_146398	0	0.00
71.8845	EG434797	predicted gene, EG434797	NM_001099302	0	0.00
71.9863	EG628518	predicted gene, EG628518	NM_001099306	0	0.00
72.0825	EG546325	predicted gene, EG546325	NM_001081670	0	0.00
72.2339	Gab3	growth factor receptor bound protein 2-associated protein 3	NM_153073	59	0.61
72.3413	Dkc1	dyskeratosis congenita 1, dyskerin homolog (human)	NM_001030307	19	1.37
72.3551	Mpp1	membrane protein, palmitoylated	NM_008621	23	1.08
72.3914	4930428E23Rik	RIKEN cDNA 4930428E23 gene	AK132828	21	1.19
72.4181	F8	coagulation factor VIII	NM_007977	312	1.50
72.6278	Fundc2	FUN14 domain containing 2	NM_026126	10	0.73
72.6502	Mtcp1	mature T-cell proliferation 1	NM_001039373	15	1.28
72.6620	Brcc3	BRCA1/BRCA2-containing complex, subunit 3	NM_145956	39	1.05
72.7596	Vbp1	von Hippel-Lindau binding protein 1	NM_011892	27	1.31
72.8174	Rab39b	RAB39B, member RAS oncogene family	NM_175122	15	2.44
72.9717	4933407K13Rik	RIKEN cDNA 4933407K13 gene	AK016728	60	2.05
73.0310	Pls3	plastin 3 (T-isoform)	NM_145629	87	0.98
73.5096	EG238829	predicted gene, EG238829	NM_001013760	0	0.00
73.5927	Magea7	melanoma antigen, family A, 7	BC107020	0	0.00
73.6387	4930428D18Rik	RIKEN cDNA 4930428D18 gene	NM_001033799	0	0.00
73.8279	4930468A15Rik	RIKEN cDNA 4930468A15 gene	AK015525	6	0.30
74.4969	LOC236874	similar to odorant binding protein la	XM_135951	0	0.00
74.5877	5830424K16Rik	RIKEN cDNA 5830424K16 gene	AK017945	0	0.00
74.7566	Tbl1x	transducin (beta)-like 1 X-linked	NM_020601	14	0.09
75.0074	Prkx	protein kinase, X-linked	NM_016979	12	0.35
75.0832	Pbsn	probasin	NM_017471	2	0.13
75.1101	OTTMUSG00000017	predicted gene, OTTMUSG00000017677	NM_001025383	0	0.00
75.1101	OTTMUSG00000017	predicted gene, OTTMUSG00000017407	XM_621007	0	0.00
75.1101	OTTMUSG00000017	predicted gene, OTTMUSG00000017866	NM_001085544	0	0.00
75.1101	OTTMUSG00000017	predicted gene, OTTMUSG00000017976	XM_204404	0	0.00
75.1101	OTTMUSG00000017	predicted gene, OTTMUSG00000017155	NM_001085351	0	0.00
75.1101	OTTMUSG00000017	predicted gene, OTTMUSG00000017728	XM_972942	0	0.00
75.1101	OTTMUSG00000017	predicted gene, OTTMUSG00000017608	AY512909	0	0.00
75.1101	OTTMUSG00000017	predicted gene, OTTMUSG00000017540	AK170409	0	0.00
75.2336	5430402E10Rik	RIKEN cDNA 5430402E10 gene	NM_027768	0	0.00
75.3308	Obp1a	odorant binding protein la	NM_008754	0	0.00
75.3708	EG546335	predicted gene, EG546335	NM_001085534	0	0.00
75.6150	4930480E11Rik	RIKEN cDNA 4930480E11 gene	AK015598	0	0.00
75.7153	Prrg1	proline rich Gla (G-carboxyglutamic acid) 1	AK008151	19	0.17
75.8206	B930042K01Rik	RIKEN cDNA B930042K01 gene	AK040303	0	0.00
75.9831	4921509A18Rik	RIKEN cDNA 4921509A18 gene	AK014848	0	0.00
76.3137	LOC211705	similar to prohibitin	XR_032681	0	0.00
76.5759	EG667736	predicted gene, EG667736	NM_001099310	59	2.14
76.7279	EG636104	predicted gene, EG636104	NM_001099307	57	1.64
76.8686	2410003J06Rik	RIKEN cDNA 2410003J06 gene	NM_001113734	10	0.81
78.3160	Tmem47	transmembrane protein 47	NM_138751	1	0.04
78.6649	4930595M18Rik	RIKEN cDNA 4930595M18 gene	NM_173435	13	0.34
80.1942	Dmd	dystrophin, muscular dystrophy	NM_007868	1317	0.58
80.7320	Tsga8	testis specific gene A8	AB032764	0	0.00
81.5228	1600014K23Rik	RIKEN cDNA 1600014K23 gene	A1324104	0	0.00
82.1414	5430427O19Rik	RIKEN cDNA 5430427O19 gene	AA175893	0	0.00
82.6512	Gm41	gene model 41, (NCBI)	XM_111935	0	0.00
82.8194	Map3k7ip3	mitogen-activated protein kinase kinase kinase 7 interacting protein 3	NM_025729	85	1.41
82.9473	Gyk	glycerol kinase	NM_008194	53	0.71
82.9792	E130114A11Rik	RIKEN cDNA E130114A11 gene	AK021388	5	5.36
83.0720	LOC100041562	hypothetical protein LOC100041562	AK035200	4	0.41
83.2895	1700072E05Rik	RIKEN cDNA 1700072E05 gene	NM_028554	0	0.00
83.4371	Nr0b1	nuclear receptor subfamily 0, group B, member 1	NM_007430	0	0.00
83.4956	CN716893	expressed sequence CN716893	NM_001033492	3	0.50
83.9863	6330532G10Rik	RIKEN cDNA 6330532G10 gene	AK018225	0	0.00
83.9926	Il1rap1	interleukin 1 receptor accessory protein-like 1	AK081272	39	0.03
84.9261	2900005I04Rik	RIKEN cDNA 2900005I04 gene	AK013482	0	0.00

Table B-3. (Continued).

Position on Chr X (Mb)	Gene symbol	Gene description	NM ID	SNPs	SNP Density
86.1818	4930415L06Rik	RIKEN cDNA 4930415L06 gene	NR_003621	0	0.00
86.4519	Gm370	gene model 370, (NCBI)	XM_141921	0	0.00
86.6492	Pet2	plasmacytoma expressed transcript 2	NM_008821	0	0.00
86.9976	4932429P05Rik	RIKEN cDNA 4932429P05 gene	NM_001085511	0	0.00
87.7338	EG278167	predicted gene, EG278167	XM_205261	0	0.00
88.3464	EG236893	predicted gene, EG236893	XM_141935	0	0.00
88.5771	Mageb1	melanoma antigen, family B, 1	NM_010759	0	0.00
88.5772	Mageb2	melanoma antigen, family B, 2	NM_031171	0	0.00
88.8206	1700084M14Rik	RIKEN cDNA 1700084M14 gene	AK006997	0	0.00
88.8775	Mageb5	melanoma antigen, family B, 5	AK006807	0	0.00
89.1773	EG278087	predicted gene, EG278087	NM_001083629	0	0.00
89.3642	Mageb18	melanoma antigen family B, 18	NM_173783	60	0.12
89.7353	EG546347	predicted gene, EG546347	NM_001034103	0	0.00
90.2356	EG245516	predicted gene, EG245516	XM_001472506	0	0.00
90.4015	RP23-438H3.2	hypothetical protein LOC69357	NM_183280	0	0.00
90.4016	1700003E24Rik	RIKEN cDNA 1700003E24 gene	AK005630	0	0.00
90.5320	Arx	aristaless related homeobox gene (Drosophila)	NM_007492	0	0.00
90.5501	Pola1	polymerase (DNA directed), alpha 1	NM_008892	5	0.02
90.9002	Pcyt1b	phosphate cytidylyltransferase 1, choline, beta isoform	NM_177546	14	0.15
91.0100	Pdk3	pyruvate dehydrogenase kinase, isoenzyme 3	NM_145630	0	0.00
91.2001	Gm371	gene model 371, (NCBI)	XM_141955	0	0.00
91.2140	AU015836	expressed sequence AU015836	AK145358	0	0.00
91.3200	Zfx	zinc finger protein X-linked	NM_001044386	0	0.00
91.4340	Eif2s3x	eukaryotic translation initiation factor 2, subunit 3, structural gene X-linked	NM_012010	1	0.04
91.4803	Kih15	kelch-like 15 (Drosophila)	NM_001039059	0	0.00
91.6004	4932442L08Rik	RIKEN cDNA 4932442L08 gene	AK016569	0	0.00
91.6124	Apoo	apolipoprotein O	NM_026673	0	0.00
91.7808	Maged1	melanoma antigen, family D, 1	NM_019791	0	0.00
91.8814	Gsp12	G1 to S phase transition 2	NM_008179	0	0.00
91.9699	Zxdb	zinc finger, X-linked, duplicated B	NM_001081473	0	0.00
92.2178	Spin4	spindlin family, member 4	NM_178753	1	0.24
92.2443	Arhgef9	Cdc42 guanine nucleotide exchange factor (GEF) 9	NM_001033329	1	0.01
92.3544	5730407O05Rik	RIKEN cDNA 5730407O05 gene	AK017518	0	0.00
92.6157	2810002O09Rik	RIKEN cDNA 2810002O09 gene	NM_175179	0	0.00
92.6655	Asb12	ankyrin repeat and SOCS box-containing protein 12	NM_008058	0	0.00
92.8345	AK129302	cDNA sequence AK129302	NM_001003916	0	0.00
92.9070	Zc3h12b	zinc finger CCCH-type containing 12B	NM_001034907	2	0.01
92.9279	1700010D01Rik	RIKEN cDNA 1700010D01 gene	NM_029590	0	0.00
93.1307	Las1l	LAS1-like (S. cerevisiae)	NM_152822	0	0.00
93.2914	Msn	moesin	NM_010833	2	0.03
93.4353	ENSMUSG000000065	predicted gene, ENSMUSG000000065522	AK170206	1	0.27
93.4353	ENSMUSG000000065	predicted gene, ENSMUSG000000065996	AK086046	1	0.27
93.4425	Vsig4	V-set and immunoglobulin domain containing 4	NM_177789	0	0.00
93.5022	B230358A15Rik	RIKEN cDNA B230358A15 gene	NM_172931	1	0.02
93.6508	Heph	hephaestin	NM_010417	0	0.00
93.9089	Gpr165	G protein-coupled receptor 165	NM_029536	0	0.00
94.1294	1700125M20Rik	RIKEN cDNA 1700125M20 gene	AK007284	0	0.00
94.2679	Pgr15l	G protein-coupled receptor 15-like	NM_001033361	1	0.11
94.5292	Eda2r	ectodysplasin A2 isoform receptor	NM_175540	0	0.00
95.3451	Ar	androgen receptor	NM_013476	5	0.03
95.7529	Ophn1	oligophrenin 1	NM_052976	2	0.01
96.1331	Yip6	Yip1 domain family, member 6	NM_207633	1	0.09
96.2380	Stard8	START domain containing 8	NM_199018	0	0.00
96.3315	Efnb1	ephrin B1	NM_010110	1	0.08
96.6007	OTTMUSG000000018	predicted gene, OTTMUSG00000018981	XM_001473979	0	0.00
96.6007	OTTMUSG000000018	predicted gene, OTTMUSG00000018988	XM_486794	0	0.00
96.6007	OTTMUSG000000018	predicted gene, OTTMUSG00000018964	XM_982089	0	0.00
96.6007	OTTMUSG000000018	predicted gene, OTTMUSG00000018973	XM_982748	0	0.00
96.6007	OTTMUSG000000018	predicted gene, OTTMUSG00000018874	AK033508	0	0.00
96.6007	OTTMUSG000000018	predicted gene, OTTMUSG00000018617	AK045662	0	0.00
96.6007	OTTMUSG000000018	predicted gene, OTTMUSG00000018077	AK132930	0	0.00
96.6007	OTTMUSG000000018	predicted gene, OTTMUSG00000018931	AK147193	0	0.00
96.6007	OTTMUSG000000018	predicted gene, OTTMUSG00000018066	AK135730	0	0.00
96.6007	OTTMUSG000000018	predicted gene, OTTMUSG00000018358	AK076701	0	0.00
96.6611	Pja1	praja1, RING-H2 motif containing	NM_001083110	0	0.00
97.0164	Tnen28	transmembrane protein 28	NM_001081283	0	0.00
97.1709	Eda	ectodysplasin-A	NM_010099	11	0.03
97.4047	D030036P13Rik	RIKEN cDNA D030036P13 gene	A853652	0	0.00
97.5976	Dgat2l4	diacylglycerol O-acyltransferase 2-like 4	NM_177746	1	0.10
97.6244	Otud6a	OTU domain containing 6A	BC153817	0	0.00
97.6897	Igfbp1	immunoglobulin (CD79A) binding protein 1	NM_008784	0	0.00
97.7202	Dgat2l6	diacylglycerol O-acyltransferase 2-like 6	NM_001114084	0	0.00
97.7676	Dgat2l3	diacylglycerol O-acyltransferase 2-like 3	NM_001081136	0	0.00
97.7855	P2ry4	pyrimidineric receptor P2Y, G-protein coupled, 4	NM_020621	0	0.00
97.8009	Arr3	arrestin 3, retinal	NM_133205	0	0.00

Table B-3. (Continued).

Position on Chr X (Mb)	Gene symbol	Gene description	NM ID	SNPs	SNP Density
97.8182	Pdzd11	PDZ domain containing 11	NM_028303	0	0.00
97.8214	Kif4	kinesin family member 4	NM_008446	0	0.00
97.9252	Gdpd2	glycerophosphodiester phosphodiesterase domain containing 2	NM_023608	0	0.00
97.9631	Dlg3	discs, large homolog 3 (Drosophila)	NM_016747	1	0.02
97.9943	EG212753	predicted gene, EG212753	XM_001478790	0	0.00
98.0219	Gm1717	gene model 1717, (NCBI)	AI449690	0	0.00
98.0340	Tex11	testis expressed gene 11	NM_031384	12	0.05
98.2746	Slc7a3	solute carrier family 7 (cationic amino acid transporter, y+ system), member 3	NM_007515	0	0.00
98.2931	Snx12	sorting nexin 12	NM_001110310	4	0.03
98.2945	1110062M06Rik	RIKEN cDNA 1110062M06 gene	AI225852	0	0.00
98.3095	LOC331476	similar to SUMO-1-specific protease	XM_001474143	0	0.00
98.3269	E130102C15Rik	RIKEN cDNA E130102C15 gene	AK021367	0	0.00
98.4499	Foxo4	forkhead box O4	NM_018789	0	0.00
98.4567	Gm614	gene model 614, (NCBI)	NM_001033362	0	0.00
98.4597	Il2rg	interleukin 2 receptor, gamma chain	NM_013563	0	0.00
98.4694	Med12	mediator of RNA polymerase II transcription, subunit 12 homolog (yeast)	NM_021521	0	0.00
98.4945	Nlgn3	neuroligin 3	NM_172932	0	0.00
98.5180	2900075N08Rik	RIKEN cDNA 2900075N08 gene	AK013791	0	0.00
98.5727	Gjb1	gap junction protein, beta 1	NM_008124	0	0.00
98.5997	Zmym3	zinc finger, MYM-type 3	NM_019831	0	0.00
98.6251	Nono	non-POU-domain-containing, octamer binding protein	NM_023144	5	0.26
98.6444	Itgb1bp2	integrin beta 1 binding protein 2	NM_013712	2	0.45
98.7281	Taf1	TAF1 RNA polymerase II, TATA box binding protein (TBP)-associated factor	NM_001081008	5	0.07
98.8354	Ogt	O-linked N-acetylglucosamine (GlcNAc) transferase	NM_139144	10	0.23
98.8399	8430425A16Rik	RIKEN cDNA 8430425A16 gene	AK018439	0	0.00
98.9269	Cxcr3	chemokine (C-X-C motif) receptor 3	NM_009910	0	0.00
98.9900	8030474K03Rik	RIKEN cDNA 8030474K03 gene	AK033245	2	0.50
99.0447	EG621083	predicted gene, EG621083	AK142977	21	0.21
99.2619	Rgag4	retrotransposon gag domain containing 4	NM_183318	0	0.00
99.2697	Pabpc12a	poly(A) binding protein, cytoplasmic 1-like 2A	XM_141989	0	0.00
99.2799	6430511F03	hypothetical protein 6430511F03	AK032250	0	0.00
99.3148	Pin4	protein (peptidyl-prolyl cis/trans isomerase) NIMA-interacting, 4 (parvulin)	NM_027181	1	0.12
99.3383	Ercc6l	excision repair cross-complementing rodent repair deficiency complementation group 6 - like	NM_146235	3	0.21
99.3803	Rps4x	ribosomal protein S4, X-linked	NM_009094	3	0.87
99.4428	Cited1	Cbp/p300-interacting transactivator with Glu/Asp-rich carboxy-terminal domain 1	NM_007709	3	0.69
99.4480	LOC434825	hypothetical gene supported by AK090266	AK090266	1	0.20
99.4800	Hdac8	histone deacetylase 8	NM_027382	36	0.16
99.5106	4732468M13Rik	RIKEN cDNA 4732468M13 gene	AK041832	0	0.00
99.6663	Xist	inactive X specific transcripts	NR_001463	0	0.00
99.6874	Tsix	X (inactive)-specific transcript, antisense	NR_002844	0	0.00
99.7093	Phka1	phosphorylase kinase alpha 1	NM_008832	43	0.33
99.9032	Dmrtc1b	DMRT-like family C1b	NM_001039116	1	0.14
99.9865	EG382233	predicted gene, EG382233	BC049655	3	0.42

APPENDIX C. POLYMORPHISM ANALYSIS OF GENES AND TRANSCRIPTS IN THE MAPPED LOCI

This appendix contains lists of single nucleotide polymorphism (SNPs) of genes and transcripts in the mapped quantitative trait loci (QTLs) associated with differential susceptibility to severe group A streptococcal (GAS) sepsis. The analysis was done on selected highly susceptible and highly resistant strains, namely, BXD77, 97, 100 and 75 as highly susceptible strains. In contrast, BXD69, 73, 48 and 87 are highly resistant strains, in addition, both parental strains B6 and D2 were included in this analysis. I performed the analysis on May 1, 2010 using mouse phenome database (MPD) employing the SNP wizard online tool at <http://phenome.jax.org/SNP>. The retrieved data was based on several databases including; national center for biotechnology information (NCBI) Mouse Build 37 (known as mm9), NCBI SNP database (dbSNP) build 128 and the joint project of the European Molecular Biology Laboratory (EMBL), European Bioinformatics Institute (EBI) and the Wellcome Trust Sanger Institute, (Ensembl) build 48. SNPs among BXD strains were based on Wellcome-CTC Mouse Strain SNP Genotype Set (Shifman *et al.*, 2006).

There are three tables in this appendix:

- Table C-1. SNP analysis of genes in mapped locus on Chr 2 between 22-34 Mb.
- Table C-2. SNP analysis of genes in mapped locus on Chr 2 between 125-150 Mb.
- Table C-3. SNP analysis of genes in mapped locus on Chr X between 50-100 Mb.

The tables in this appendix contain the following abbreviations for SNP functional classes retrieved:

Cn	Coding non-synonymous; SNP changes the amino acid/peptide,
Cs	Coding synonymous; SNP does not change the amino acid/peptide,
UTR	Untranslated region, SNP is in non-coding interval of mRNA,
S	SNP is in a splice-site; first two or last two bases of intron (few),
I	SNP is in an intron, except first 2 and last 2 bases (see above splice-site SNP), and
L	Locus region; not assigned to a gene; can be in region of gene but not in transcribed region; or may be in regulatory region.

Table C-1. SNP analysis of genes in mapped locus on Chr 2 between 22-34 Mb.

Position (Chr Mb)	NCBI gene annotation	Ensembl 48 gene annotation	dbSNP 128 SNP annotation	DBA12J	BXD77	BXD97/RwwJ	BXD100	BXD75	BXD69/RwwJ	BXD73/RwwJ	BXD48/RwwJ	BXD87/RwwJ	C57BL/6J	dbSNP	Observed
02 22.074031				A	A	A	A	A	G	G	G	G	G	rs13476377	A/G
02 22.317950	Myo3a exon16	agrees	Cs I625	G	G	G	G	G	A	A	A	A	A	rs13476378	C/T
02 22.421338	Myo3a intron7	... intron25	I	G	G	G	G	G	A	A	A	A	A	rs6369767	A/G
02 22.676436	Apbb1ip intron3	agrees	I	A	A	A	A	A	G	G	G	G	G	rs13476379	C/T
02 23.199301	Nxph2 intron1	agrees	I	G	G	G	G	G	A	A	A	A	A	rs6193345	A/G
02 23.347108				G	G	G	G	G	G	G	G	G	G	rs6404309	C/T
02 23.743224				C	C	C	C	C	A	A	A	A	A	rs33142586	A/C
02 23.949161	Tbpl2 intron3	agrees	I	T	T	T	T	T	A	A	A	A	A	rs52428815	A/T
02 24.064725				G	G	G	G	G	A	A	A	A	A	rs6301542	C/T
02 24.390673				A	A	A	A	A	G	G	G	G	G	rs6286688	A/G
02 24.827274	Wdr85 exon9	agrees	Wdr85 Cn N392S	G	G	G	G	G	A	A	A	A	A	rs13476386	A/G
02 25.322635	Ptgd5 intron6	... intron7	I	G	G	G	G	G	A	A	A	A	A	rs8250941	C/T
02 25.395303	Traf2 intron1	agrees	I	G	G	G	G	G	A	A	A	A	A	rs6164049	A/G
02 25.726697				G	G	G	G	G	A	A	A	A	A	rs13476390	A/G
02 25.951041	Btbd14a intron1	agrees	I	G	G	G	G	G	A	A	A	A	A	rs13476391	C/T
02 26.129101	4932418E24Rik intron9	... intron10	I	G	G	G	G	G	G	G	G	G	G	rs6360080	A/G
02 26.204246	D2Bwg1335e UTR	... exon3,UTR	Gpsm1 L	C	C	C	C	C	C	C	C	C	C	rs29960390	C/G
02 26.223875	Snopc4 exon17	agrees	Cs R675	A	A	A	A	A	C	C	C	C	C	rs3681655	G/T
02 26.733409				G	G	G	G	G	C	C	C	C	C	rs32966594	C/G
02 27.145189	Vav2 intron11	agrees	I	A	A	A	A	A	A	A	A	A	A	rs3718405	A/C
02 27.501061				A	A	A	A	A	A	A	A	A	A	rs13476396	A/G
02 27.743096	Col5a1 intron1	agrees	I	G	G	G	G	G	G	G	G	G	G	rs6181760	A/G
02 27.996831				A	A	A	A	A	A	A	A	A	A	rs13476398	C/T
02 28.144658				A	A	A	A	A	A	A	A	A	A	rs13476399	C/T
02 28.325100	Mrps2 exon4	agrees	Cn H149Y	G	G	G	G	G	G	G	G	G	G	rs13476400	C/T
02 28.401712	Ralgds intron9	agrees	I	A	A	A	A	A	A	A	A	A	A	rs6308258	A/G
02 28.735055	Ddx31 intron16	agrees	I	C	C	C	C	C	C	C	C	C	C	rs13476402	A/C
02 28.942336	Ttf1 UTR	agrees	U	G	G	G	G	G	G	G	G	G	G	rs3023797	A/G
02 29.101203	Ntng2 intron1	6530402F18Rik intron1	Ntng2 I	A	A	A	A	A	A	A	A	A	A	rs13476403	C/T
02 29.356230	Crsp8 intron5	Med27 intron5	Med27 I	G	G	G	G	G	G	G	G	G	G	rs13476404	A/G
02 29.463489				G	G	G	G	G	G	G	G	G	G	rs13476405	A/G
02 29.634380	Trub2 exon7	agrees	Cn N180S	A	A	A	A	A	A	A	A	A	A	rs13476406	C/T
02 29.756922	Odf2 intron5	agrees	I	G	G	G	G	G	G	G	G	G	G	rs13476407	A/G
02 30.043342	Ccbl1 intron6	... intron3	I	G	G	G	G	G	G	G	G	G	G	rs3154953	A/G
02 30.268356	Crat intron2	... intron3	I	C	C	C	C	C	C	C	C	C	C	rs3689602	G/T
02 30.296487	Ppp2r4 intron8	agrees	I	A	A	A	A	A	G	G	G	G	G	rs13476408	C/T
02 30.302966	Ppp2r4 UTR	... exon10,UTR	U	G	G	G	G	G	A	A	A	A	A	rs33748336	C/T
02 30.541430				A	A	A	A	A	G	G	G	G	G	rs13476409	A/G
02 31.027542	Gpr107 exon5	agrees	Cn Q153R	G	G	G	G	G	A	A	A	A	A	rs13459062	A/G
02 31.135514	Freq intron2	agrees	I	A	A	A	A	A	C	C	C	C	C	rs27193194	A/C
02 31.290124	LOC665700 intron57	Hmcn2 intron82	Hmcn2 I	C	C	C	C	C	G	G	G	G	G	rs27208772	C/G
02 31.555725				G	G	G	G	G	G	G	G	G	G	rs6186876	A/G
02 31.678179	Fibcd1 intron4	agrees	I	G	G	G	G	G	A	A	A	A	A	rs13476413	A/G
02 32.089220	5830434P21Rik UTR	... exon32,UTR	U	A	A	A	A	A	G	G	G	G	G	rs13459063	C/T
02 32.470462	St6galnac6 exon6	... exon5	Cs F152	A	A	A	A	A	G	G	G	G	G	rs13459060	C/T
02 32.647961	Stxbp1 intron18		I	A	A	A	A	A	G	G	G	G	G	rs27207848	C/T
02 32.877472	Garnl3 intron14	... intron15		A	A	A	A	A	G	G	G	G	G	(no-rs)	?/?
02 33.073858	Angptl2 intron1	agrees	Angptl2 I	T	T	T	T	T	A	A	A	A	A	rs13476418	A/T
02 33.305487			Zbtb43 L	C	C	C	C	C	A	A	A	A	A	rs13476419	A/C
02 33.798339				G	G	G	G	G	A	A	A	A	A	rs27222258	A/G
02 33.850139				C	C	C	C	C	A	A	A	A	A	rs13476442	G/T
02 33.990290				C	C	C	C	C	G	G	G	G	G	rs13476423	C/G
02 34.478981	Mapkap1 exon4	... exon12,UTR	Cs R493	C	C	C	C	C	A	A	A	A	A	rs13476425	A/C
02 34.748653			Phf19 L	A	A	A	A	A	G	G	G	G	G	rs13476426	A/G
02 34.869157	Hc exon24	agrees	Cn N1001D	G	G	G	G	G	A	A	A	A	A	rs13476427	C/T

Table C-2. SNP analysis of genes in mapped locus on Chr 2 between 125-150 Mb.

Position (Chr Mb)	NCBI gene annotation	Ensembl 48 gene annotation	dbSNP 128 SNP annotation	DBA12J	BXD77	BXD97/RwwJ	BXD100	BXD75	BXD69/RwwJ	BXD73/RwwJ	BXD48/RwwJ	BXD87/RwwJ	C57BL/6J	dbSNP	Observed
02.125.123509				A	A	A	A	A	A	A	A	A	A	rs6401493	C/T
02.125.127623	Fbn1 exon66	agrees	Cn N2773S	A	A	A	A	A	A	A	A	A	A	rs8251635	C/T
02.125.304785	Fbn1 intron3	agrees	I	A	G	A	G	A	G	G	G	G	G	rs6374387	C/T
02.125.364688				G	G	G	G	G	G	G	G	G	G	rs3697020	C/T
02.125.564678	3110001120Rik UTR	... exon18,UTR	U	A	C	A	C	A	C	C	C	C	C	rs3725315	G/T
02.125.704535	Galk2 intron2	agrees	I	C	A	C	A	C	A	A	A	A	A	rs3708635	G/T
02.125.866915	Fgf7 intron2	agrees	I	G	A	G	A	G	A	A	A	A	A	rs3667348	A/G
02.126.005696				G	A	G	A	G	A	A	A	A	A	rs3704471	C/T
02.126.259800		Atp8b4 intron6		A	G	A	G	A	G	G	G	G	G	rs6369977	A/G
02.126.470820	Gabpb1 intron7	agrees	I	G	C	G	C	G	C	C	C	C	C	rs3720259	C/G
02.126.557730	Usp8 intron4	... intron5	I	G	C	G	C	G	C	C	C	C	C	rs13476758	C/G
02.126.929174			Ncaph L	A	G	A	G	A	G	G	G	G	G	rs4223448	C/T
02.126.967277	1700041B20Rik exon2	... exon3,UTR	Cs G259	G	A	G	A	G	A	A	A	A	A	rs13476760	C/T
02.127.292727	Kcnp3 intron2	agrees	I	G	G	G	G	G	G	G	G	G	G	rs13476761	C/T
02.127.522306				A	G	A	G	A	G	G	G	G	G	rs3680660	C/T
02.127.787332	Acox1 intron9	agrees	I	C	G	C	G	C	G	G	G	G	G	rs13476763	C/G
02.127.840969	Acox1 intron12	agrees	I	A	G	A	G	A	G	G	G	G	G	rs6280404	C/T
02.127.974055	Bcl2l11 intron3	... intron4	I	G	A	G	A	G	G	A	A	A	A	rs13476764	C/T
02.128.199227		OTTMUSG00000015351 intron1	LOC100043424 I	G	A	G	A	G	A	A	A	A	A	rs6411422	A/G
02.128.300336				G	A	G	A	G	A	A	A	A	A	rs13476765	C/T
02.128.383738				G	A	G	A	G	A	A	A	A	A	rs6325084	C/T
02.128.617919	Mertk intron16	agrees	I	G	A	G	A	G	A	A	A	A	A	rs13476766	A/G
02.128.877858				G	A	G	A	G	A	A	A	A	A	rs3671147	C/T
02.128.959466	Chchd5 UTR	... exon4,UTR	U	G	A	G	A	G	A	A	A	A	A	rs13459165	C/T
02.128.959490	Chchd5 UTR	... exon4,UTR	U	T	A	T	A	T	A	A	A	A	A	rs13469412	A/T
02.129.049210	A730036117Rik intron1	agrees	I	G	A	G	A	G	A	A	A	A	A	rs3662407	A/G
02.129.089790	LOC671466 intron2		I	G	G	G	G	G	G	G	G	G	G	rs6318992	A/G
02.129.125489	Il1a UTR	... exon7,UTR	U	A	T	A	T	A	T	T	T	T	T	rs3022902	A/T
02.129.383337				T	T	T	T	T	T	T	T	T	T	rs13476768	A/T
02.129.457556	Sirpa UTR	... exon9,UTR	U	A	A	A	A	A	A	A	A	A	A	rs27257479	G/T
02.129.542808				A	A	A	A	A	A	A	A	A	A	rs6161193	A/C
02.129.928492	AU015228 UTR		U	G	G	G	G	G	G	G	G	G	G	rs4223491	A/G
02.129.970551	Tgm6 intron9	agrees	I	A	A	A	A	A	A	A	A	A	A	rs3661596	C/T
02.130.216766	Cpxm1 exon14	agrees	Cs G680	G	G	G	G	G	G	G	G	G	G	rs4223497	C/T
02.130.367115	Ptpra exon13	... exon14	Cs Y497	G	G	G	G	G	G	G	G	G	G	rs13459166	C/T
02.130.507288	ltpa UTR	... exon8,UTR	U	A	A	A	A	A	A	A	A	A	A	rs13465151	A/T
02.130.534029	4930402H24Rik UTR	... exon37,UTR	U	A	A	A	A	A	A	A	A	A	A	rs4223500	A/G
02.130.777824	Atrn intron6	agrees	I	A	A	A	A	A	A	A	A	A	A	rs13476772	C/T
02.130.839645	Atrn intron6	... intron25	I	G	G	G	G	G	G	G	G	G	G	rs3665528	A/G
02.130.877524	Adam33 intron19	agrees	I	C	C	C	C	C	C	C	C	C	C	rs8264979	G/T
02.130.881869	Adam33 intron6	agrees	I	A	G	A	G	A	G	G	G	G	G	rs8264884	A/G
02.131.240779				G	A	G	A	G	A	A	A	A	A	rs13476774	A/G
02.131.352413				A	G	A	A	G	G	G	G	G	G	rs3690254	A/G
02.131.372744	Adra1d intron1	agrees	I	A	G	A	G	A	G	G	G	G	G	rs6206689	A/G
02.131.487026				A	G	A	G	A	G	G	G	G	G	rs27288211	C/T
02.131.679416				A	G	A	G	A	G	G	G	G	G	rs4223510	C/T
02.131.819271	Rassf2 UTR	... exon11,UTR	U	A	G	A	G	A	G	G	G	G	G	rs4223511	C/T
02.132.094113	Cds2 intron1		I	G	G	G	G	G	G	G	G	G	G	rs3701463	C/T
02.132.181539				A	A	A	A	A	A	A	A	A	A	rs3699051	A/G
02.132.268510		4921508D12Rik intron1		C	C	C	C	C	C	C	C	C	C	rs13476777	A/C
02.132.423204				A	A	A	A	A	A	A	A	A	A	rs13476778	C/T
02.132.588030				G	G	G	G	G	G	G	G	G	G	rs3722210	A/G
02.132.631319	3300001M20Rik exon11	Trmt6 exon11	Trmt6 Cs L260	A	A	A	A	A	A	A	A	A	A	rs6288723	C/T
02.132.770061	5830467P10Rik intron1	agrees	I	A	A	A	A	A	A	A	A	A	A	rs13476779	A/G
02.132.944863				G	G	G	G	G	G	G	G	G	G	rs27240387	C/T

Table C-2. (Continued).

Position (Chr Mb)	NCBI gene annotation	Ensembl 48 gene annotation	dbSNP 128 SNP annotation	DBA1ZJ	BXD77	BXD97/RwwJ	BXD100	BXD75	BXD69/RwwJ	BXD73/RwwJ	BXD48/RwwJ	BXD87/RwwJ	C57BL/6J	dbSNP	Observed
02 133.346268				G	G	G	G	G	G	G	G	G	G	rs3676388	A/G
02 133.388963			Bmp2L	A	A	A	A	A	A	A	A	A	A	rs3022934	C/T
02 133.535082				G	G	G	G	G	G	G	G	G	G	rs3684247	A/G
02 133.686867				G	G	G	G	G	G	G	G	G	G	rs13476783	C/T
02 133.748173				A	A	A	A	A	A	A	A	A	A	rs6397401	A/T
02 134.133774				A	A	A	A	A	A	A	A	A	A	rs6234650	A/G
02 134.345047	Hao1 intron4	agrees	I	A	C	A	C	A	C	C	C	C	C	rs13476784	A/C
02 134.586818				G	A	G	A	G	A	A	A	A	A	rs13476785	C/T
02 134.712881	Plcb1 intron2	agrees	I	C	A	C	A	C	A	A	A	A	A	rs13476786	A/C
02 134.965497	Plcb1 intron3	agrees	I	A	G	A	G	A	G	G	G	G	G	rs13476787	C/T
02 135.137988	Plcb1 intron11	... intron8	I	G	A	G	A	G	A	A	A	A	A	rs13476788	C/T
02 135.360002				G	A	G	A	G	A	A	A	A	A	rs13476789	C/T
02 135.469719				A	C	A	C	A	C	C	C	C	C	rs13476790	A/C
02 135.592555	Plcb4 intron1		I	G	A	G	A	G	A	A	A	A	A	rs6345820	A/G
02 135.758395	Plcb4 intron8	... intron7	I	C	G	C	G	C	G	G	G	G	G	rs29716787	C/G
02 135.953692	Pak7 intron3	... intron4	I	A	G	A	G	A	G	G	G	G	G	rs27237140	C/T
02 136.253017				C	A	C	A	C	A	A	A	A	A	rs13476793	G/T
02 136.567700	Snap25 intron1	agrees	I	A	A	A	A	A	A	A	A	A	A	rs13476794	G/T
02 136.704189	Mkks intron3	agrees	I	G	G	G	G	G	G	G	G	G	G	rs8246404	A/G
02 137.050704				G	G	G	G	G	G	G	G	G	G	rs3710324	C/T
02 137.281348				A	A	A	A	A	A	A	A	A	A	rs13476797	C/T
02 137.513613				A	A	A	A	A	A	A	A	A	A	rs13476798	A/C
02 137.618159				A	A	A	A	A	A	A	A	A	A	rs6249968	A/G
02 137.970245				A	A	A	A	A	A	A	A	A	A	rs3653457	A/C
02 138.305756				G	A	G	A	G	A	G	A	G	A	rs13476801	C/T
02 138.596276				C	C	C	C	C	C	C	C	C	C	rs13476802	A/C
02 138.749442				A	A	A	A	A	A	A	A	A	A	rs6362243	C/T
02 138.895273				A	A	A	A	A	A	A	A	A	A	rs6200333	A/G
02 139.005406				C	C	C	C	C	C	C	C	C	C	rs6158085	A/C
02 139.322068	C130053K05Rik intron2	Sptic3 intron2	Sptic3I	C	G	C	G	C	G	C	G	C	G	rs13476804	C/G
02 139.549796	5430433G21Rik intron1		I	G	A	G	A	G	A	G	A	G	A	rs13476805	C/T
02 139.558446	5430433G21Rik intron2		I	G	A	G	A	G	A	G	A	G	A	rs6282055	C/T
02 139.745898	Tasp1 intron9	... intron10	I	A	G	A	G	A	G	G	A	G	G	rs6251185	A/G
02 140.191732	Self12 intron1	agrees	I	G	A	G	A	G	A	G	A	G	A	rs6238987	A/G
02 140.632270				G	A	G	A	G	A	G	A	G	A	rs13476807	A/G
02 140.949623				A	G	A	G	A	G	G	A	G	G	rs6188553	C/T
02 140.949863				C	A	C	A	C	A	A	C	A	A	rs6187777	G/T
02 141.269051				G	A	G	A	G	A	G	A	G	A	rs6303304	C/T
02 141.506452		MacroD2 intron6		C	A	C	A	C	A	A	C	A	A	rs6346451	G/T
02 141.778076		MacroD2 intron8		G	A	G	A	G	A	G	A	G	A	rs6397890	C/T
02 142.006271		MacroD2 intron2		G	A	G	A	G	A	G	A	G	A	rs6360457	A/G
02 142.226462				A	G	A	G	A	G	G	A	G	G	rs13476810	A/G
02 142.529801	Kif16b intron20	... intron21	I	A	G	A	G	A	G	G	A	G	G	rs6331493	C/T
02 142.540462	Kif16b exon18	agrees	Cs E596	A	G	A	G	A	G	A	G	G	G	rs13476811	C/T
02 142.725202	Kif16b intron1	agrees	I	C	G	C	G	C	G	C	G	C	G	rs13476812	C/G
02 142.911592				A	C	A	C	A	C	C	A	C	C	rs13476813	G/T
02 143.215177				G	A	G	A	G	A	G	A	G	A	rs13476814	C/T
02 143.420472	Pcsk2 intron2	agrees	I	G	A	G	A	G	A	G	A	G	A	rs6195594	A/G
02 143.748895	Dstn intron1	agrees	I	A	G	A	G	A	G	G	A	G	G	rs3687229	C/T
02 143.770431				G	A	G	A	G	A	G	A	G	A	rs33511869	C/T
02 143.786839	Rrbp1 intron11	... intron10	I	C	A	C	A	C	A	C	A	C	A	rs3707946	A/C
02 144.199389	Csrp2bp exon2	agrees	Cs T18	A	G	A	G	A	G	G	A	G	G	rs13476817	A/G
02 144.359114	Poir3f intron4	agrees	I	G	A	G	A	G	A	G	A	G	A	rs3655895	A/G
02 144.582696	Dtd1 intron5	agrees	I	G	A	G	A	G	A	G	A	G	A	rs13476818	C/T
02 144.594327	Dtd1 UTR	agrees	U	A	G	A	G	A	G	G	A	G	G	rs3023694	A/G
02 144.636566				G	A	G	A	G	A	G	A	G	A	rs3661718	A/G

Table C-2. (Continued).

Position (Chr Mb)	NCBI gene annotation	Ensembl 48 gene annotation	dbSNP 128 SNP annotation	DBA2J	BXD77	BXD97/RwwwJ	BXD100	BXD75	BXD69/RwwwJ	BXD73/RwwwJ	BXD48/RwwwJ	BXD87/RwwwJ	C57BL6J	dbSNP	Observed
02 144.810573				A	G	A	G	A	G	G	A	G	G	rs6170159	C/T
02 145.107384	Slc24a3 intron2	agrees	I	G	A	G	A	G	A	A	G	A	A	rs3022909	A/G
02 145.433591	Slc24a3 intron6	... intron12	I	G	A	G	A	G	A	A	G	A	A	rs3679762	A/G
02 145.712336	Rin2 UTR	... exon13,UTR	U	A	A	A	A	A	A	A	A	A	A	rs27272367	A/G
02 145.858075		4930529M08Rik intron14		A	A	A	A	A	A	A	A	A	A	rs6363071	A/G
02 145.996022				A	A	A	A	A	A	A	A	A	A	rs13476820	C/T
02 146.117744		A230067G21Rik intron38		A	A	A	A	A	A	A	A	A	A	rs3676491	G/T
02 146.464837				A	A	A	A	A	A	A	A	A	A	rs3668423	A/G
02 146.524475				A	A	A	A	A	A	A	A	A	A	rs6254019	A/G
02 146.880833	Xrn2 intron24	agrees	I	A	A	A	A	A	A	A	A	A	A	rs3724835	A/G
02 147.204386				A	A	A	A	A	A	A	A	A	A	rs13476822	A/G
02 147.254465				A	A	A	A	A	A	A	A	A	A	rs3701696	C/T
02 147.477700	LOC640914 intron1			A	G	A	G	A	G	G	A	G	G	rs3698870	A/G
02 147.607368				T	T	T	T	T	T	T	T	T	T	rs3683143	A/T
02 147.753900				G	A	G	A	G	A	A	G	A	A	rs13476825	C/T
02 147.881059				G	A	G	A	A	A	A	G	A	A	rs6209325	C/T
02 147.932881				A	G	A	G	G	G	G	A	G	G	rs6332517	C/T
02 148.222019	Sstr4 exon1	agrees	Cs P270	C	A	C	A	A	A	A	C	A	A	rs29556174	G/T
02 148.230161			Thbd L	A	G	A	G	G	G	A	G	G		rs4223558	A/G
02 148.230256	Thbd UTR	... exon1,UTR	U	C	C	C	C	C	C	C	C	C	C	rs4223557	A/C
02 148.232342	Thbd exon1	agrees	Cs G446	A	G	A	G	G	G	G	A	G	G	rs13476826	A/G
02 148.357423				G	A	G	A	A	A	A	G	A	A	rs13476827	A/G
02 148.573862				C	G	C	G	G	G	G	C	G	G	rs6288803	C/G
02 148.697668	Cst3 UTR	... exon3,UTR	U	A	G	A	G	G	G	G	A	G	G	rs8256617	A/G
02 148.975537				A	G	A	G	G	G	G	A	G	G	rs13476830	A/G
02 149.070623				G	A	G	A	A	A	A	G	A	A	rs3723883	C/T
02 149.271015				T	A	T	A	A	A	A	T	A	A	rs3676033	A/T
02 149.491613				A	G	A	G	G	G	G	A	G	G	rs6206791	A/G
02 149.561210	EG667048 intron1			C	A	C	A	A	A	A	C	A	A	rs13476832	A/C
02 149.688083			OTTMUSG000000157501	A	A	A	A	A	A	A	A	A	A	rs6246342	A/G
02 149.750008	OTTMUSG00000015750 intron1		I	A	A	A	A	A	A	A	A	A	A	rs6176485	A/G
02 149.804749	OTTMUSG00000015750 intron2		I	A	G	A	G	G	G	G	A	G	G	rs13476833	A/G

Table C-3. SNP analysis of genes in mapped locus on Chr X between 50-100 Mb.

Position (Chr Mb)	NCBI gene annotation	Ensembl 48 gene annotation	dbSNP 128 SNP annotation	DBA2J	BXD77	BXD97/RwwJ	BXD100	BXD75	BXD69/RwwJ	BXD73/RwwJ	BXD48/RwwJ	BXD87/RwwJ	C57BL/6J	dbSNP	Observed
X 50.304196	Phf6 intron8	... intron11		A	A	C	C	C	C	A	C	A	C	rs13483756	G/T
X 50.441456	Plac1 intron2	agrees		A	A	G	G	G	G	A	G	A	G	rs13483757	C/T
X 50.688138				A	A	G	G	G	G	A	G	A	G	rs13483758	C/T
X 51.078618	Zfp36l3 exon1	agrees	Cn M268V	G	G	A	A	A	A	G	A	G	A	rs13483759	C/T
X 53.469071				A	A	A	A	A	A	A	A	A	A	rs13483761	A/G
X 53.755235	Ddx26b intron14	agrees		A	A	A	A	A	A	A	A	A	A	rs6202026	A/G
X 54.012901	Fhl1 intron3	... intron2		A	A	A	A	A	A	A	A	A	A	rs13483763	C/T
X 54.787689				A	A	A	C	C	C	A	C	A	C	rs13483765	A/C
X 55.021542				A	A	A	G	G	G	A	G	A	G	rs13483766	C/T
X 55.119516				A	A	A	T	T	T	A	T	A	T	rs13483767	A/T
X 55.423039				G	G	A	A	A	A	G	A	G	A	rs13483768	C/T
X 55.907643				A	A	T	T	T	T	A	T	A	T	rs13483769	A/T
X 56.198835				A	A	G	G	G	G	A	G	A	G	rs29057816	C/T
X 56.322051	Fgf13 intron3	agrees		G	G	G	G	G	G	G	G	G	G	rs6361318	C/T
X 56.488675				G	G	A	G	A	A	G	A	G	A	rs13483770	A/G
X 56.638971				A	A	A	A	A	A	A	A	A	A	rs13483771	A/G
X 56.786516				G	G	G	G	G	G	G	G	G	G	rs31736534	C/T
X 57.174959				G	G	G	G	G	G	G	G	G	G	rs6172548	A/G
X 58.428522		C230004F18Rik exon7		G	G	G	G	G	G	G	G	G	G	rs13483777	C/T
X 58.726530				A	A	A	A	A	A	A	A	A	A	rs13483778	A/G
X 59.012359				A	A	A	A	A	A	A	A	A	A	rs6156066	A/G
X 59.629009				A	A	A	A	A	A	A	A	A	A	rs13483781	A/G
X 59.725144				A	A	A	A	A	A	A	A	A	A	rs6315050	A/G
X 60.353111				G	G	G	G	G	G	G	G	G	G	rs6273297	A/G
X 60.678266				G	G	G	G	G	G	G	G	G	G	rs6371771	C/T
X 60.897610				A	A	A	A	A	A	A	A	A	A	rs13483783	C/T
X 61.595306				A	A	G	A	G	G	A	G	A	G	rs13483785	A/G
X 61.868817				C	C	A	C	A	C	A	C	A	C	rs13483786	A/C
X 62.557333				T	T	T	T	T	T	T	T	T	T	rs13483790	A/T
X 62.802036				G	G	G	G	G	G	G	G	G	G	rs3695410	A/G
X 62.871894				A	A	A	A	A	A	A	A	A	A	rs13483791	G/T
X 63.211829				C	C	C	C	C	C	C	C	C	C	rs6317266	A/C
X 63.548433				A	A	A	A	A	A	A	A	A	A	rs13483793	A/T
X 63.963690				G	G	G	G	G	G	G	G	G	G	rs31231784	A/G
X 64.133911				G	G	G	G	G	G	G	G	G	G	rs29048726	C/T
X 64.489187				A	A	A	A	A	A	A	A	A	A	rs29049502	G/T
X 64.565854				G	G	G	G	G	G	G	G	G	G	rs31212020	C/T
X 64.717310				A	A	A	A	A	A	A	A	A	A	rs33870777	C/T
X 64.860968				G	G	G	G	G	G	G	G	G	G	rs31306210	C/T
X 65.033446				C	C	C	C	C	C	C	C	C	C	rs29048228	A/C
X 65.202453				A	A	A	A	A	A	A	A	A	A	rs29051320	G/T
X 65.262708				G	G	G	G	G	G	G	G	G	G	rs6296283	C/T
X 65.406453				G	G	G	G	G	G	G	G	G	G	rs13483797	A/G
X 65.868220				G	G	G	G	G	G	G	G	G	G	rs29049652	A/G
X 66.262536				C	C	C	C	C	C	C	C	C	C	rs13483808	G/T
X 66.607415				A	A	C	A	C	C	A	C	A	C	rs13483810	G/T
X 66.798088	Aff2 exon3	agrees	Cn T228A	G	G	A	G	A	A	G	A	G	A	rs13483811	A/G
X 66.915814		Aff2 intron3		G	G	A	G	A	A	G	A	G	A	rs3089604	C/T
X 67.347285				C	C	A	C	A	A	C	A	C	A	rs13483813	A/C
X 68.020243				A	A	G	A	G	G	A	G	A	G	rs13483814	A/G
X 68.130578				G	G	A	G	A	A	G	A	G	A	rs13483815	A/G
X 68.621588	Mttr1 intron1	agrees		A	A	A	A	A	A	A	A	A	A	rs6159220	A/T
X 68.694215	Cd99l2 intron3	... intron4		G	G	A	A	A	A	G	A	G	A	rs3157124	C/T
X 69.187248				A	A	G	G	G	G	A	G	A	G	rs13483818	A/G
X 69.924084				G	G	C	C	C	C	G	C	G	C	rs13483821	C/G
X 70.261115	Zfp185 exon11	agrees	Cn I211V	G	G	A	A	A	A	G	A	G	A	rs13483822	A/G

Table C-3. (Continued).

Position (Chr Mb)	NCBI gene annotation	Ensembl 48 gene annotation	dbSNP 128 SNP annotation	DBA2J	BXD77	BXD97/RwwJ	BXD100	BXD75	BXD69/RwwJ	BXD73/RwwJ	BXD48/RwwJ	BXD87/RwwJ	C57BL/6J	dbSNP	Observed
X 70.591777	Zfp275 intron2	agrees		A	A	G	G	G	G	A	G	A	G	rs13483823	C/T
X 70.862405				G	G	G	G	G	G	G	G	G	G	rs6291099	C/T
X 71.121919	L1cam intron1	agrees		A	A	G	G	G	A	A	G	A	G	rs13483824	A/G
X 71.452881	Tktl1 intron12	agrees		A	A	G	G	G	A	A	G	A	G	rs13483825	A/G
X 71.578525	Plxna3 intron4	agrees		G	G	A	A	A	G	G	A	G	A	rs29036935	A/G
X 71.702281				A	A	A	A	A	A	A	A	A	A	rs13483826	C/T
X 72.973693				A	A	A	A	A	A	A	A	A	A	rs13483831	A/G
X 73.568953				A	A	G	G	G	A	A	G	A	G	rs13483834	C/T
X 73.669338				C	C	A	A	A	C	C	A	C	A	rs29032402	A/C
X 73.867519				G	G	A	A	A	G	G	A	G	A	rs29034080	A/G
X 73.994756				C	C	A	A	A	C	C	A	C	A	rs29033159	A/C
X 74.333567				G	G	C	C	C	G	G	C	G	C	rs29031390	C/G
X 74.437611				A	A	G	G	G	A	A	G	A	G	rs13483838	A/G
X 76.270169				A	A	A	A	A	A	A	A	A	A	rs6232687	A/G
X 76.642086	LOC100041373 intron13			G	G	G	G	G	G	G	G	G	G	rs6400558	C/T
X 76.792464				G	G	A	A	A	G	G	A	G	A	rs29033641	C/T
X 76.974502				C	C	C	C	C	C	C	C	C	C	rs6358828	G/T
X 77.128597				A	A	G	G	G	A	A	G	A	G	rs31114399	C/T
X 77.442176				C	C	A	A	A	C	C	A	C	A	rs13483849	G/T
X 77.596981				T	T	A	A	A	T	T	A	T	A	rs29030057	A/T
X 77.758255				A	A	G	G	G	A	A	G	A	G	rs33872327	C/T
X 77.964147				C	C	G	G	G	C	C	G	C	G	rs13483852	C/G
X 78.316989	Tmem47 intron1	agrees		A	A	G	G	G	A	A	G	A	G	rs13483853	A/G
X 78.387471				A	A	C	C	C	A	A	C	A	C	rs29122940	G/T
X 78.565195				C	C	A	A	A	C	C	A	C	A	rs29122347	A/C
X 78.716893				G	G	C	C	C	G	G	C	G	C	rs29124734	C/G
X 79.175607				A	A	C	C	C	A	A	C	A	C	rs13483857	G/T
X 79.446294				G	G	A	A	A	G	G	A	G	A	rs13483858	C/T
X 79.763566				G	G	A	A	A	G	G	A	G	A	rs29121137	A/G
X 79.962339				A	A	G	G	G	A	A	G	A	G	rs29120700	A/G
X 80.269841	Dmd intron1	agrees		A	A	G	G	G	A	A	G	A	G	rs13483862	A/G
X 80.517265	Dmd intron2	agrees		A	A	G	G	G	A	A	G	A	G	rs13483863	C/T
X 80.674835			Dmd I	G	G	A	A	A	G	G	A	G	A	rs31396732	C/T
X 80.819498	Dmd intron1	... intron7		A	A	T	T	T	A	A	T	A	T	rs29063388	A/T
X 81.021583	Dmd intron13	... intron19		G	G	G	G	G	G	G	G	G	G	rs6389792	C/G
X 81.087944	Dmd intron23	... intron29		G	G	A	A	A	G	G	A	G	A	rs13483864	C/T
X 81.485465	Dmd intron38	... intron44		C	C	C	C	C	C	C	C	C	C	rs6276382	G/T
X 81.842456	Dmd intron6	... intron53		A	A	G	G	G	A	A	G	A	G	rs13483868	A/G
X 82.043294	Dmd intron10	... intron57		A	A	G	G	G	A	A	G	A	G	rs13483869	A/G
X 82.133393	Dmd intron13	... intron60		C	C	A	A	A	C	C	A	C	A	rs3675552	A/C
X 82.563944				G	G	A	A	A	G	G	A	G	A	rs13483870	C/T
X 82.743905				G	G	A	A	A	G	G	A	G	A	rs3725966	C/T
X 83.044868				G	G	C	C	C	G	G	C	G	C	rs31117642	C/G
X 83.314902				A	A	G	G	G	A	A	G	A	G	rs13483873	A/G
X 83.474831				G	G	A	A	A	G	G	A	G	A	rs33867225	C/T
X 83.632157				A	A	G	G	G	A	A	G	A	G	rs31319847	A/G
X 83.754274				G	G	A	A	A	G	G	A	G	A	rs3696812	A/G
X 84.193868	Il1rap1 intron5	... intron6		G	G	A	A	A	G	G	A	G	A	rs13483877	A/G
X 84.490778	Il1rap1 intron4	... intron5		T	T	A	A	A	T	T	A	T	A	rs13483878	A/T
X 84.635263	Il1rap1 intron2	... intron3		A	A	A	A	A	A	A	A	A	A	rs6380311	G/T
X 84.917154		Il1rap1 intron2		A	A	A	A	A	A	A	A	A	A	rs6228331	A/G
X 85.166458		Il1rap1 intron1		G	G	G	G	G	G	G	G	G	G	rs6179920	A/G
X 85.700670				G	G	G	G	G	G	G	G	G	G	rs6212120	C/T
X 86.920572				A	A	G	G	G	A	A	G	A	G	rs13483803	C/T
X 87.440160				G	G	A	A	A	G	G	A	G	A	rs13483805	A/G
X 87.724390				A	A	A	A	A	A	A	A	A	A	rs6211131	C/T

Table C-3. (Continued).

Position (Chr Mb)	NCBI gene annotation	Ensembl 48 gene annotation	dbSNP 128 SNP annotation	DBA2J	BXD77	BXD97/RwwJ	BXD100	BXD75	BXD69/RwwJ	BXD73/RwwJ	BXD48/RwwJ	BXD87/RwwJ	C57BL/6J	dbSNP	Observed
X 87.943903				A	A	A	A	A	A	A	A	A	A	rs6221067	A/G
X 88.357437				A	A	A	A	A	A	A	A	A	A	rs6259276	A/T
X 88.466052				G	G	G	G	G	G	G	G	G	G	rs6162389	C/T
X 89.326263	EG236892 intron1		I	G	G	G	G	G	G	G	G	G	G	rs6224816	A/G
X 89.566020				G	G	G	G	G	G	G	G	G	G	(no-rs)	?/?
X 89.920839				C	C	A	A	A	C	C	A	C	A	rs13483880	G/T
X 90.058794				C	C	G	G	G	C	C	G	C	G	rs29070461	C/G
X 90.183658				A	A	C	C	C	A	A	C	A	C	rs29072783	A/C
X 90.523800				A	A	G	G	G	A	A	G	A	G	rs13483881	A/G
X 91.150210	EG668103 intron1		I	A	A	A	A	A	A	A	A	A	A	rs13483884	C/T
X 91.583744			LOC631145 L	A	A	A	A	A	A	A	A	A	A	rs13483885	C/T
X 91.781474	Maged1 exon12	agrees	Cs A686	G	G	G	G	G	G	G	G	G	G	rs13459181	A/G
X 92.246917	Arhgef9 UTR	... intron10	U	A	A	A	A	A	A	A	A	A	A	rs13483887	A/G
X 92.516668				G	G	G	G	G	G	G	G	G	G	rs13483888	C/T
X 92.842774	AK129302 intron1	agrees	I	G	G	G	G	G	G	G	G	G	G	rs13483890	C/T
X 93.098708	A130028J20Rik intron4	Zc3h12b intron5	Zc3h12b I	A	A	A	A	A	A	A	A	A	A	rs13483891	A/C
X 93.378516				G	G	G	G	G	G	G	G	G	G	rs13483892	A/G
X 93.694393	Heph exon12	agrees	Cn N592S	A	A	A	A	A	A	A	A	A	A	rs13483894	A/G
X 94.171734				T	T	T	T	T	T	T	T	T	T	rs6182892	A/T
X 94.404878				G	G	G	G	G	G	G	G	G	G	rs6309772	C/T
X 94.532103	Eda2r UTR	agrees	U	A	A	A	A	A	A	A	A	A	A	rs6367841	G/T
X 95.119353				A	A	A	A	A	A	A	A	A	A	rs13483898	A/G
X 95.472455	Ar intron2	agrees	I	A	A	A	A	A	A	A	A	A	A	rs3672400	C/T
X 95.543918				G	G	G	G	G	G	G	G	G	G	rs29086868	C/G
X 95.727753				A	A	A	A	A	A	A	A	A	A	rs13483899	A/C
X 95.921452	Ophn1 exon7	agrees	Cs A162	A	A	A	A	A	A	A	A	A	A	rs13483900	C/T
X 96.090321				A	A	A	A	A	A	A	A	A	A	rs3680829	A/T
X 96.259400	Stard8 intron3	agrees	I	A	A	A	A	A	A	A	A	A	A	rs13483902	C/T
X 96.844849				A	A	A	A	A	A	A	A	A	A	rs29081061	C/T
X 97.014720			EG620592 L	G	G	G	G	G	G	G	G	G	G	rs31142709	A/G
X 97.191531	Eda intron1	agrees	I	G	G	G	G	G	G	G	G	G	G	rs29083820	A/G
X 97.614860				G	G	G	G	G	G	G	G	G	G	rs13483909	A/G
X 97.921890	Kif4 exon30	agrees	Cs A1195	G	G	G	G	G	G	G	G	G	G	rs13483910	A/G
X 97.922028	Kif4 UTR	... exon30,UTR	U	C	C	C	C	C	C	C	C	C	C	rs4232594	C/G
X 97.961994			Dlg3 L	A	A	A	A	A	A	A	A	A	A	rs3714964	C/T
X 98.027382				G	G	G	G	G	G	G	G	G	G	rs13483911	C/T
X 98.333835		Snx12 intron4		C	C	C	C	C	C	C	C	C	C	rs29079390	G/T
X 98.847444	Ogt intron3	agrees	I	G	G	G	G	G	G	G	G	G	G	rs6171419	C/T
X 99.620143	Hdac8 intron7	agrees	I	A	A	A	A	G	A	H	G	H	G	rs29080049	A/G
X 99.935066				C	C	C	C	C	C	C	C	C	C	rs31253166	G/T

**APPENDIX D. LIST OF PUBLISHED LOCI AND GENES ON CHROMOSOME 2
THAT ARE ASSOCIATED WITH DIFFERENTIAL SUSCEPTIBILITY TO
INFECTIOUS DISEASES**

This appendix contains a list of quantitative trait loci (QTLs) and genes on Chr 2 that were found by published studies investigating susceptibility to infectious diseases other than GAS sepsis, based on literature search on May 3, 2010. From the list below, only one study used recombinant inbred (RI) mice strains (CXB-RI strains) (Thach *et al.*, 2001). Other retrieved studies used either F2 crosses or backcrossed of some strains of interest.

Table D-1. Diseases and mouse models associated with quantitative trait loci and genes located at Chromosome 2 loci mapped in current study.

Disease	Model and Strain Used	Candidate Genes/Loci	References
Neuroadapted Sindbis virus (NSV)	C57Bl/6J and Balb/cBy, CXB inbred mice	QTL on Chr 2 near D2Mit447 (60cM)	(Thach <i>et al.</i> , 2001)
Chlamydia trachomatis	C57Bl/6J and C3H/HeJ and F2 crosses and congenic	QTLs on Chr 2, 3 and 11	(Bernstein-Hanley <i>et al.</i> , 2006)
Borrelia burgdorferi (lyme disease)	C57BL/6N X C3H/HeN (C57BL/6N X C3H/HeN) F1 X C3H/HeN and (C57BL/6N X C3H/HeN) F1 X C57BL/6N backcrosses	Bbaa15 locus and proximity of markers D2Mit278 and D2Mit224	(Roper <i>et al.</i> , 2001)
Leishmania major	F2 crosses of (CcS-16 x BALB/c)	Lmr14	(Havelkova <i>et al.</i> , 2006) (Zhang and Matlashewski, 2004) (Vladimirov <i>et al.</i> , 2003)
Leishmania donovani	B10.LP-H-3 b and B10.CE(30NX) and (B10.LP-H-3 b x B10)F1	Immune response locus 2 (Ir2)	DeTolla 1980
Candida albicans.	[A/J x C57BL/6J] F2 crosses	Hemolytic complement (Hc or C5)	(Tuite <i>et al.</i> , 2004; Tuite <i>et al.</i> , 2005)
Salmonella typhimurium	(AcB61 x 129S6) F2 crosses	Hemolytic complement (Hc or C5)	(Roy <i>et al.</i> , 2007)
Listeria monocytogenes	A/J and B6	Hemolytic complement (Hc or C5)	(Czuprynski <i>et al.</i> , 2003)

VITA

Nourtan Fathy Abdeltawab, a Cairo, Egypt native, was born on June 14, 1979. She graduated from the English high school, Education Home School, Dokki, Giza, in 1997. She received her Bachelor's degree, Excellent with highest honors, in Pharmaceutical Sciences, College of Pharmacy, Cairo University 2002. She was then appointed as a teaching assistant at Department of Microbiology and Immunology, College of Pharmacy, Cairo University where she worked on studies towards her M.Sc. degree. In August 2004, Nourtan joined The University of Tennessee Health Science Center in Memphis, for her PhD studies. Summer of 2005, Nourtan joined the research team of Dr. Malak Kotb laboratory, where she worked on her dissertation project. In September 2008, Nourtan relocated with Dr. Kotb to University of Cincinnati, Ohio, where she finished her dissertation work. She is expected to graduate in May 2010 from University of Tennessee Health Science Center.